Synthesis of Arborescent Copolymers Based on Poly(γ-benzyl L-glutamate)

by

Gregory Whitton

A thesis
presented to the University of Waterloo
in fulfillment of the
thesis requirement for the degree of
Doctor of Philosophy
in
Chemistry

Waterloo, Ontario, Canada, 2013

AUTHOR'S DECLARATION

I hereby declare that I am the sole author of this thesis. This is a true copy of the thesis, including any required final revisions, as accepted by my examiners.

I understand that my thesis may be made electronically available to the public.

Abstract

The synthesis of arborescent poly(γ-benzyl L-glutamate) (PBG) molecules was achieved through successive grafting reactions of linear PBG chains. These linear PBG building blocks were obtained by the ring-opening polymerization of γ-benzyl L-glutamic acid N-carboxyanhydride initiated with *n*-hexylamine. Cleavage of a fraction of the benzyl ester groups on a linear PBG substrate, followed by coupling with linear PBG side chains via standard peptide coupling techniques, yielded a comb-branched or generation zero (G0) arborescent PBG. Further cycles of partial deprotection and grafting reactions led to arborescent PBG molecules of the subsequent generations (G1-G3). Molecular weights reaching over 10^6 were obtained for G3 arborescent PBG, while maintaining narrow molecular weight distributions ($M_w/M_n \leq 1.06$) for each generation. The arborescent PBG molecules displayed α-helix to randomly coiled chain conformation changes from N,N-dimethylformamide to dimethylsulfoxide.

Amphiphilic copolymers were obtained by grafting the arborescent PBG substrates randomly with side chains of either poly(glycidol acetal), poly(ethylene oxide), or poly(γ-*tert*-butyl L-glutamate) via the same peptide coupling techniques used to generate arborescent PBG. Copolymers were also synthesized by a chain end grafting method, whereby the linear chain segments were coupled exclusively with the chain termini of the arborescent PBG substrates. Water-soluble species were obtained by removal of the acetal and *tert*-butyl protecting groups from the poly(glycidol acetal) and poly(γ-*tert*-butyl L-glutamate) side chains, respectively, while the copolymers with poly(ethylene oxide) side chains did not require further modifications. Dynamic light scattering (DLS) measurements on the

arborescent copolymers in aqueous solutions revealed that unimolecular micelles were the dominant species for the chain end grafted arborescent copolymers, whereas the randomly grafted arborescent copolymers were either insoluble or displayed significant aggregation.

The synthesis of arborescent copolymers with PBG cores was also achieved through "click" chemistry, using the copper-catalyzed azide-alkyne Huisgen cycloaddition (CuAAC) reaction. To that end, polyglycidol, poly(ethylene oxide), and poly(2-trimethylsilylethyl acrylate) chains terminally functionalized with azide groups were grafted onto either randomly or chain end alkyne-functionalized arborescent PBG substrates. DLS analysis revealed solubility trends similar to the arborescent copolymers obtained by the peptide coupling method. The CuAAC reaction enables the incorporation of a broader range of polymers into arborescent copolymer structures derived from PBG substrates.

Acknowledgements

Firstly, I gratefully acknowledge the support, guidance, knowledge, expertise, and wisdom of Prof. Dr. Mario Gauthier during the course of this work; he was vital to the success of this research and the development and advancement of my skills. I would also like to acknowledge my family and friends, especially Laura Sardone, for their positive support and encouragement throughout my graduate studies.

In addition, I would like to thank the following individuals who provided valuable support and influence regarding my research:

Mr. Toufic Aridi
Dr. Jason Dockendorff
Mr. Timothy Hall
Dr. Mark Ingratta
Mr. Olivier Nguon
Prof. Pu Chen
Prof. Jean Duhamel
Prof. John Honek
Dr. Firmin Moingeon
Mrs. Jan Venne

Finally I wish to thank the following groups and agencies for financial support: The Natural Sciences and Engineering Research Council (NSERC), the University of Waterloo, and The Institute for Polymer Research.

Dedication

I dedicate this work to my loving mother and late father, who have provided me with the opportunity to pursue my goals through their unwavering support, guidance, and encouragement.

"Learn from yesterday, live for today, hope for tomorrow. The important thing is to not stop questioning."

Albert Einstein

Table of Contents

List of Figures

List of Tables

List of Abbreviations and Symbols

2VP	2-Vinylpyridine
α	Extent of reaction
AA	α-Amino acid
AM	Activated monomer
ATRP	Atom transfer radical polymerization
b	Block
BA	*tert*-Butyl acrylate
bipy	2,2-Bipyridyl
Boc	*tert*-Butyloxycarbonyl
Boc-Lys	N^{ε}-(*tert*-Butyloxycarbonyl)-L-lysine
b.p.	Boiling point
BTF	Benzotrifluoride
BTFBA	3,5-bis-(Trifluoromethyl)benzaldehyde
Bz-Glu	γ-Benzyl L-glutamic acid
Bz	Benzyl
c	Click graft
CDMSS	4-(Chlorodimethylsilyl)styrene
C_e	Coupling efficiency
CMC	Critical micelle concentration
CMM	Couple-monomer methodology
COD	1,5-Cyclooctadiene
CuAAC	Copper(I)-catalyzed azide-alkyne Huisgen cycloaddition
CuBr	Copper bromide
$CuSO_4$	Copper(II) sulfate pentahydrate
D	Dendritic branching units
d	Deuterated
D(t)	Autocorrelation function
DB	Degree of branching

DCM	Dichloromethane
d_{h1}	Hydrodynamic diameter from 1st-order analysis of the correlation function
d_{h2}	Hydrodynamic diameter from 2nd-order analysis of the correlation function
DIC	N,N'-Diisopropylcarbodiimide
DLS	Dynamic light scattering
DMA	*N*,*N*-Dimethylacetamide
DMF	*N*,*N*-Dimethylformamide
DMM	Double-monomer methodology
DMSO	Dimethylsulfoxide
dn/dc	Refractive index increment
DPE	1,1-Diphenylethylene
DPMK	Diphenylmethylpotassium
DRI	Differential refractometer index
DVB	Divinylbenzene
eg	Chain end-graft
EO	Ethylene oxide
EtOAc	Ethyl acetate
eq	Equivalents
f_{ABn}	Functionality of the AB_n monomer
Fmoc	9-Fluorenylmethyloxycarbonyl
f_n	Number-average branching functionality
f_{NH2}	Primary amine functionality level
FPT	Freeze-pump-thaw
f_{tBu}	Mole fraction of *tert*-butyl ester protecting groups
G	Generation
g	Graft
$\|g_1(\tau)\|$	First-order correlation function
$\|g_2(\tau)\|$	Second-order correlation function

Glu-NCA	γ-Benzyl L-glutamic acid N-carboxyanhydride
$(OtBu)_2$-PBG	Glu$(OtBu)_2$-Poly(γ-benzyl L-glutamate)
GTP	Group transfer polymerizations
G_y	Grafting yield
h	Hour(s)
HBr	Hydrogen bromide
HCl	Hydrogen chloride or hydrochloric acid
HEA	2-Hydroxyethyl acrylate
HEA-TMS	2-(Trimethylsilyloxy)ethyl acrylate
HF	Hydrofluoric acid
HOAt	1-Hydroxy-7-azabenzotriazole
HOBt	1-Hydroxybenzotriazole
HOXt	N-Hydroxy derivative
HVT	High-vacuum techniques
IR	Infrared
L	Linear chain segment
LHAA	(6-Lithiohexyl)acetaldehyde acetal
LiCl	Lithium chloride
$LiAlH_4$	Lithium aluminum hydride
KNaph	Potassium naphthalene
MAA	Methacrylic acid
MALDI	Matrix-assisted laser desorption ionization
MALLS	Multi-angle laser light scattering
M_0	Number-average molecular weight of the primary chains
M_B	Number-average molecular weight of structural unit derived from the coupling agent
M/I	Monomer to initiator molar concentration ratio
M_G	Number-average molecular weight of graft polymer
M_n^{br}	Number-average molecular weight of branch
M_n	Number-average molecular weight

MW	Molecular weight
M_w	Weight-average molecular weight
MWCO	Molecular weight cutoff
MWD	Molecular weight distribution
n	Refractive index
N_A	Avogadro's number
NA	Normal amine
NaAsc	Sodium ascorbate
$NaHCO_3$	Sodium hydrogen carbonate
NaN_3	Sodium azide
n-BuLi	*n*-Butyllithium
N_c	Core multiplicities
NCA	α-Amino acid N-carboxyanhydride
NMR	Nuclear magnetic resonance
NOXt	N-Hydroxy derivative
N^{α},N^{ε}-diFmoc-Lys	N^{α},N^{ε}-Di(9-fluorenylmethoxycarbonyl)-L-lysine
P2VP	Poly(2-vinylpyridine)
PAH	Polycyclic aromatic hydrocarbon
PAMAM	Polyamidoamine
PB	Polybutadiene
PBG	Poly(γ-benzyl L-glutamate)
PBS	Phosphate buffer solution
PDI	Polydispersity index
PEG	Poly(ethylene glycol)
PEI	Polyethyleneimines
PEO	Poly(ethylene oxide)
PGA	Poly(L-glutamic acid)
PGly	Polyglycidol
PGlyAc	Poly(glycidol acetal)
PHEA	Poly(2-hydroxyethyl acrylate)

P(HEA-TMS)	Poly(2-trimethylsilylethyl acrylate)
PhMgCl	Phenylmagnesium chloride
PMDETA	*N,N,N',N'',N''*-Pentamethyldiethylenetriamine
PMMA	Poly(methacrylic acid)
PPLG	Poly(γ-propargyl L-glutamate)
PS	Polystyrene
PS-*d*	Deuterated polystyrene
P*t*BMA	Poly(*tert*-butyl methacrylate)
PtBuGlu	Poly(γ-*tert*-butyl L-glutamate)
PTP	Proton-transfer polymerization
RBF	Round-bottomed flask
ROMBP	Ring-opening multi-branching polymerization
ROP	Ring-opening polymerization
SANS	Small-angle neutron scattering
SCROP	Self-condensing ring-opening polymerization
SCVP	Self-condensing vinyl polymerization
SEC	Size exclusion chromatography
sec-BuLi	*sec*-Butyllithium
SMM	Single-monomer methodology
SPPS	Solid phase peptide synthesis
T	Terminal branching units
tBu	*tert*-Butyl
tBuGlu	γ-*tert*-Butyl L-Glutamic Acid
TEA	Triethylamine
TFA	Trifluoroacetic acid
TFA-Lys	ε-Trifluoroacetyl-L-lysine
TFBA	4-Trifluorobenzaldehyde
THF	Tetrahydrofuran
TMS	Trimethylsilyl
TMSCl	Chlorotrimethylsilane

TOF	Time of flight
$(TPP)_3$-CuBr	Bromotris(triphenylphosphine) copper(I) bromide
UV	Ultraviolet
VBC	Vinylbenzyl chloride
X	Degree of polymerization
X_n	Number-average degree of polymerization
Z	Number of surface groups
Z-Lys	ε-Benzyloxycarbonyl-L-lysine

Chapter 1

Foreword

1.1 Opening Remarks

Dendritic polymers are the most recently discovered class of branched macromolecules and offer an increasingly wide range of architectures with unique properties. Arborescent polymers are a sub-class of the dendritic polymer family, and are synthesized using a generation-based growth scheme employing repetitive cycles of functionalization and grafting reactions. Anionic polymerization and grafting techniques have been used to synthesize different arborescent homopolymers[1-3] and copolymers.[4,5] Numerous studies have confirmed that these methods provide extensive control over the architecture and the physical properties of these materials.[6] It has also been shown that arborescent copolymers with amphiphilic properties can behave like water-soluble unimolecular micelles, and are capable of the microencapsulation and the controlled release of small molecules.[7,8] Unfortunately, due to their non-biocompatible components, these arborescent copolymers did not meet the biocompatibility requirements for biomedical applications. An investigation to produce biocompatible arborescent copolymers for microencapsulation and the controlled release of small molecules is thus of considerable interest to the field of nanomedicine.

1.2 Research Objectives and Thesis Outline

The synthesis of arborescent homopolymers and copolymers has been so far restricted to monomers that are suitable for anionic polymerization. The research presented in this Thesis focuses on the synthesis of well-defined arborescent polymers of poly(γ-benzyl L-glutamate) (PBG), as well as the synthesis of amphiphilic arborescent copolymers incorporating an arborescent PBG hydrophobic core, that may be suitable for the microencapsulation and the controlled release of small molecules. The polymerization and grafting techniques required

for the synthesis of these molecules were investigated, along with their solution properties, to better understand these novel arborescent polymer systems.

Background information on the various synthetic techniques for generating linear polypeptides and dendritic polymers is provided in Chapter 2. Chapter 3 reports on the preparation of arborescent PBG, starting from the synthesis of linear PBG and successive grafting reactions by standard peptide coupling techniques. Chapter 4 describes the synthesis of amphiphilic arborescent copolymers from arborescent PBG substrates randomly functionalized with carboxylic acid groups, and either amine-functionalized polyglycidol, poly(ethylene oxide), or poly(L-glutamic acid) side chains to form a hydrophilic shell. The solution properties of the copolymers were investigated using dynamic light scattering measurements. Chapter 5 describes the synthesis and the characterization of amphiphilic arborescent copolymers using the same shell components as in Chapter 4, but by terminal grafting onto carboxylic acid functionalities located at the chain ends of the PBG substrates, so as to produce better defined core-shell morphologies for the copolymers and potentially enhanced water solubility. The grafting methods employed in Chapters 3, 4, and 5 are based on traditional carbodiimide-type peptide coupling techniques, but a new grafting method based on the copper-catalyzed azide-alkyne Huisgen cycloaddition (CuAAC) reaction is explored in Chapter 6 to generate both randomly and chain end grafted arborescent copolymers. Various azide-functionalized side chains were grafted onto alkyne-functionalized PBG substrates by that method. The CuAAC grafting reaction is interesting because it broadens the range of polymer components that can be used to construct arborescent homopolymers and copolymers through a generation-based growth scheme.

Lastly, Chapter 7 provides an overall summary of the work completed, original contributions to knowledge, and suggestions for future work.

Each chapter of this thesis is organized in a manuscript format, where each chapter includes an introductory section providing background material related to the specific topic considered, followed by experimental methods, results and discussion, and conclusions sections. In accordance with the University of Waterloo Thesis Regulations, this Thesis includes an abstract in the preliminary pages, but each research chapter (Chapters 3-6) also includes an analogous Overview section. Further abiding by the Thesis Regulations, a single list of references is provided at the very end of the document, but it is organized and numbered according to each individual chapter.

Chapter 2

Introduction: Synthesis of Linear Polypeptides, Dendritic Polymers, and Amphiphilic Arborescent Micelles

2.1 Introduction

In recent years there has been growing interest in the design and use of synthetic polypeptides.[1-3] A polypeptide can be defined as a polymer of amino acids linked via amide bonds. Many amino acids have been used to generate homopolypeptides and copolypeptides, giving rise to interesting characteristics.[2,4] The strategies commonly used for the synthesis of linear polypeptides will be discussed in Section 2.2. The main attraction of polypeptides lies in their potential biocompatibility, i.e. as a material that is compatible with living cells, tissues, organs, or biological systems, and poses little risks of injury, toxicity, or rejection by the immune system. It has been known for several decades that many synthetic polypeptides based on L-amino acids can be recognized and digested by enzymes.[5] This provides an opportunity for using polypeptides as biodegradable components in biomedical applications.[6] Beyond the synthesis of linear polypeptides, these materials may also be used to generate more complex macromolecular architectures.[2,7,8]

Dendritic polymers, as the newest class of branched polymers, have attracted much interest due to their unique properties in comparison to linear polymers. Dendritic polymers can be generated through different pathways, and are classified under three main categories: dendrimers, hyperbranched polymers, and dendrigraft (arborescent) polymers. The synthetic strategies used for these dendritic structures will be discussed in Section 2.3.

Polymeric micelles typically have a core-shell morphology and are often obtained by the self-assembly of amphiphilic block or graft copolymers in a selective solvent, where the soluble component forms a shell around the core containing the insoluble component. One of the applications of a micellar structure is to solubilize materials in media where they would normally be insoluble. Micellar species derived from block copolymers, dendritic,

hyperbranched, and arborescent copolymers have all been studied. Due to their ease of synthesis, amphiphilic block copolymers have received the most attention in the past.[9,10] A newer class of polymer micelles that shows promise in the field of microencapsulation is the dendritic polymer micelles.[11-14] The synthesis of dendrigraft (arborescent) micelles will be discussed in Section 2.4.

2.2 Synthesis of Linear Polypeptides

Polypeptides can be synthesized by different strategies that are typically selected depending on the characteristics desired for the product. The two dominant strategies being used today are the solid phase peptide synthesis (SPPS) pioneered by Merrifield in 1963,[15] and the ring-opening polymerization (ROP) of α-amino acid N-carboxyanhydrides (NCAs), first introduced in the early 1900's.[16] A third method, protein engineering, used to produce peptides with desired amino acid sequences (using the 20 natural amino acids), is considered more of a biosynthesis path than a chemical synthesis route and will not be considered here. Synthesis using SPPS and the ROP of NCAs will be discussed in detail in this chapter. A number of non-natural amino acids can also be used in these techniques; however the focus will remain on polypeptides based on the natural α-amino acids (AA) or their derivatives.

2.2.1 Solid Phase Peptide Synthesis

The introduction of SPPS revolutionized peptide synthesis methodology, as it greatly simplified the tedious purification steps that are necessary when synthesizing peptides in solution. SPPS allows the growth of peptide chains anchored to a solid substrate, which allows the easy elimination of excess reagents and by-products at each step of the synthesis. SPPS also enabled the automation of peptide synthesis. Figure 2.1 shows the step-wise

automated process used in SPPS. After defining a synthetic strategy and programming a specific AA sequence, the machine automatically performs the multistep synthesis to obtain the desired peptide sequence. The coupling and deprotection reactions are repeated as required for each AA.

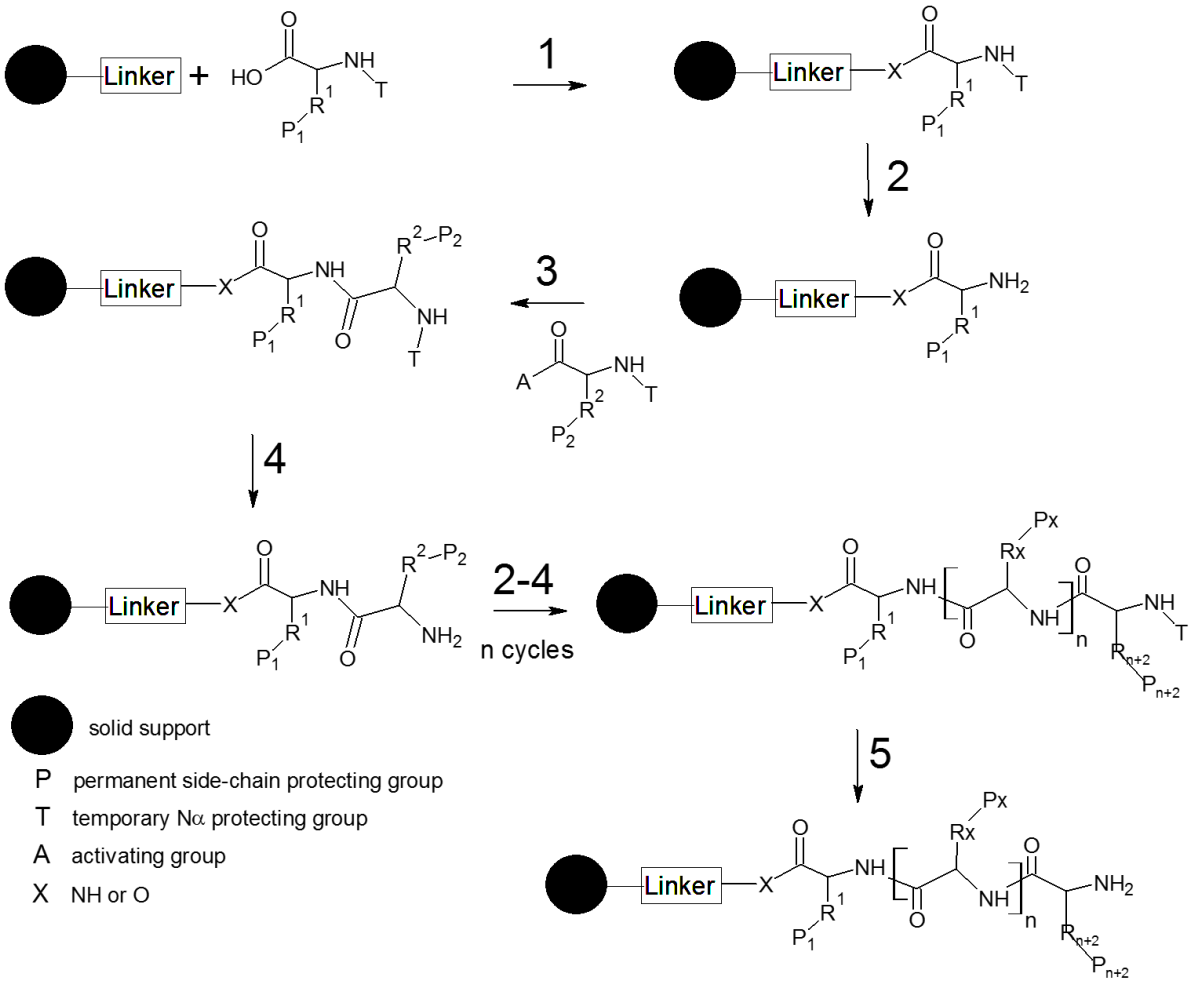

Figure 2.1 Step-wise solid phase peptide synthesis.

2.2.1.1 Solid Supports

The peptide synthesis begins with a solid support where the first peptide in the sequence is anchored for the entire duration of the synthesis. This solid support is the main characteristic distinguishing the SPPS from solution phase peptide synthesis, since it allows easy purification after each step. This also enables the use of large excesses of reagents, which in turn provide a much higher overall yield of the desired polypeptide. Prior to SPPS, this was one of the major factors limiting the size of polypeptides that could be synthesized in solution while maintaining a high purity. For instance, if the desired peptide contains five AAs, then five coupling steps (Figure 2.1, step 3) must be performed. If each step has a 90% yield for the AA additions, the final polypeptide would contain only 59% (0.90^5) of the desired polypeptide and 41% of a mixture of undesired AA sequences (this is assuming 100% efficiency for the deprotection steps 2 and 4 in Figure 2.1. If the sequence were increased to 20 AAs then the overall yield would drop to 12% (0.90^{20}), corresponding to 88% of undesired AA sequences. The purity of the peptide therefore relies heavily on the efficiency of each coupling step. To increase the yield of each step, and consequently the overall yield and purity, it is helpful to introduce an excess of reagents (up to 10 molar equivalents). A solid support allows excess reagents to be used and subsequently removed, and can increase the coupling yield up to 99-100%. In turn, these higher yields allow the production of larger polypeptides of high purity.

A solid support consists of a polymer matrix and a linker molecule. Literally hundreds of different solid supports are commercially available, but the most widely used polymer matrix today is still the one originally introduced by Merrifield,[15] namely cross-linked beads of a styrene-divinylbenzene copolymer. Cross-linked polyamide-based matrices

and polystyrene (PS)-poly(ethylene glycol) (PEG) composites also exist but are not as commonly used. These polymer matrices are designed to swell, but not dissolve, in a given solvent such as N,N-dimethylformamide (DMF) or dichloromethane (DCM). Once swollen, the linker functionalities on the support can be accessed by the reagents in solution and couple with the C-terminus of the starting AA. After a coupling or deprotection step is completed the solid support is washed thoroughly to remove excess reagents and by-products, leaving only the desired material linked to the solid support.

2.2.1.2 α-Amino Acid Protecting Groups

Some AAs contain a side chain functional group that may react during amide bond formation (Figure 2.1, step 3). For this reason it is necessary to protect these functional groups during polypeptide synthesis. There are two types of protecting groups used in SPPS, "temporary" and "permanent", as shown in Figure 2.1. Temporary protecting groups are relatively easy to cleave, and are used at the N-terminus to ensure that only one AA becomes attached to the peptide chains in each coupling cycle. Permanent protecting groups, that are stable under the reaction conditions used in the SPPS process, serve to protect the side chains of the AA, to ensure that they do not participate in any reactions during polypeptide growth.

The two main types of temporary/permanent protecting groups, displayed in Figure 2.2, are the *tert*-butyloxycarbonyl (Boc)/benzyl (Bz) (Figure 2.2, Strategy 1), and the 9-fluorenylmethyloxycarbonyl (Fmoc)/*tert*-butyl (tBu) (Figure 2.2, Strategy 2) protecting groups. Strategy 1 is the older method, which is based on differences in acid lability between the temporary and permanent protecting groups. For instance, the Boc group is easily removed by neat trifluoroacetic acid (TFA), but to remove the Bz protecting group and to

cleave the polypeptide from the solid support, stronger acidic conditions are necessary. In the past this has been done with anhydrous hydrofluoric acid (HF), but due to its high toxicity and the need for special equipment (lined with polytetrafluoroethylene), a new approach using a hydrogen bromide (HBr) solution in acetic acid was also developed with TFA as the reaction medium. Unfortunately Strategy 1 has the potential to be harmful to the structural integrity of polypeptide chains, especially for polypeptides containing "sensitive" sequences.

A newer approach is Strategy 2 in Figure 2.2, using the Fmoc/tBu protecting groups. The N-Fmoc group is base-labile, whereas the protecting groups for the side chains and the C-terminus linkers are acid-labile. The advantage of this approach is that since the temporary and permanent protecting groups are removed by different mechanisms, they allow milder acidic conditions for the final deprotection step and the cleavage of the peptide chain from the solid support.

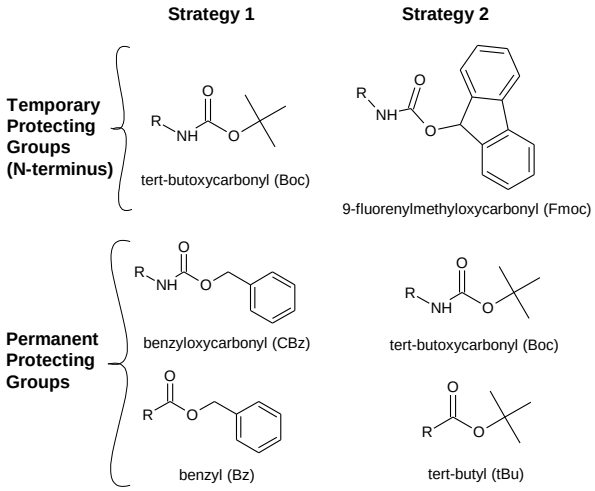

Figure 2.2 Temporary and permanent protecting groups for SPPS.

2.2.1.3 Coupling Reaction

Peptide bond formation requires the activation of a carboxyl group, followed by aminolysis of the activated carbonyl. For the efficient coupling of AAs, a promoting reagent is necessary. Studies have been performed to help determine which coupling agents work best under specific reaction conditions, as well as the advantages and disadvantages of different coupling reagents.[17- 19] The types of coupling reagents commonly used include phosphonium, uronium, immonium, carbodiimide, imidazolium, and organophosphorus compounds, as well as other coupling reagents.[19] This review will focus on the carbodiimide coupling method, as it was used in the research reported in Chapters 3, 4 and 5.

Activation of the carboxyl groups is necessary for the coupling reaction to proceed at a reasonable rate. The carbonyl activation and coupling reactions are displayed in Figure 2.3. Unfortunately this activation step, along with the coupling reaction, can lead to the loss of chirality for the AA undergoing activation. This can occur according to two different paths, both being base-catalyzed and displayed in Figure 2.4.[17,19] Path A in Figure 2.4 results from proton abstraction at the chiral carbon, leading to enolate formation. Path B depends on proton abstraction from the nitrogen atom and rearrangement, resulting in the formation of an oxazolone ring. While both paths result in the loss of chirality, the coupling reaction can still proceed.

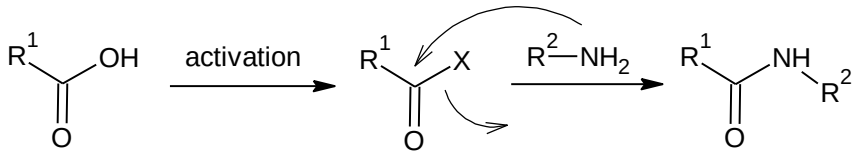

Figure 2.3 Peptide coupling with carboxylic acid activation.

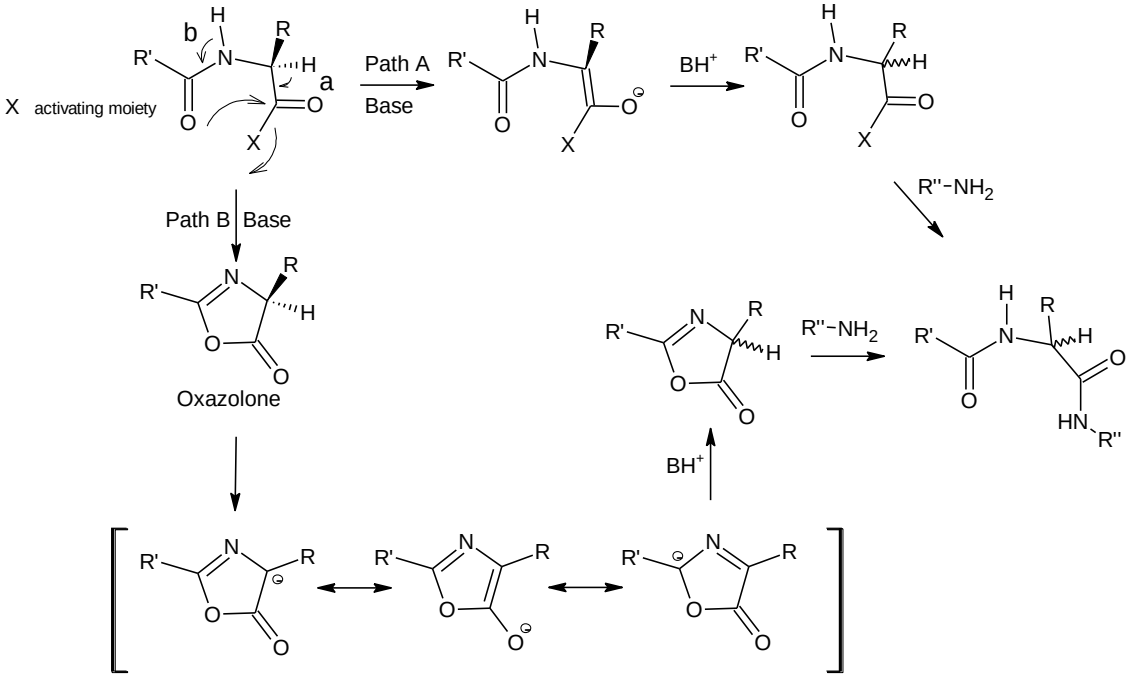

Figure 2.4 Racemization at the C-terminal of an amino acid during peptide coupling.

Beyond the loss of chirality, there are a few side reactions that can occur specifically with carbodiimide-activated systems. Figure 2.5 depicts a few common side reactions involving the O-acylisourea intermediate.[17] Path A in Figure 2.5 shows the desired reaction with a carbodiimide activator. Path B is followed when an additive, such as an N-hydroxy derivative (HOXt), is used to help promote the correct coupling pathway. Commonly used N-hydroxy derivatives are 1-hydroxy-7-azabenzotriazole (HOAt) and 1-hydroxybenzotriazole (HOBt). The advantage of using such additives in the coupling reaction is that the intermediate containing the HOXt is less reactive than the O-acylisourea, which suppresses the formation of an N-acylurea (Figure 2.5, Path D), a stable species that will prevent the coupling reaction from proceeding. The HOXt works by protonating the O-acylisourea, thus

preventing the intramolecular reaction from occurring. This protonation can also decrease the degree of racemization, as it disfavors rearrangement. Path C in Figure 2.5 can occur if there is an excess of carboxylic acid present. This will still result in the coupling reaction proceeding, but can be avoided by using an excess of coupling reagents to ensure there are no unactivated carboxyl groups.

After the desired number of peptide coupling reactions has been achieved, the last step in SPPS involves the removal of the side chain protecting groups and the cleavage of the peptide from the solid support. This can usually be done in a single step. For instance, when using the Fmoc/tBu protecting method (Figure 2.2, Strategy 2), the tBu and Boc protecting groups as well as the linker to the solid support can be removed by neat TFA. The polypeptide is then isolated from the solid support by filtration.

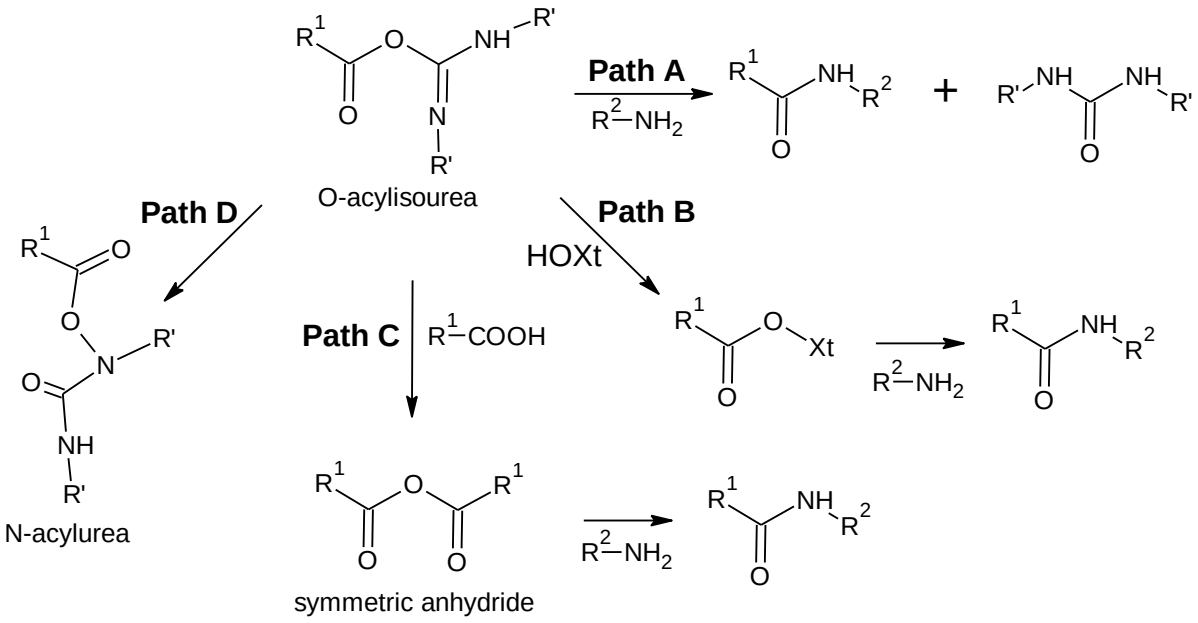

Figure 2.5 Carbodiimide activation and side reactions.

2.2.2 Ring-opening Polymerization of α-Amino Acid N-Carboxyanhydrides

In recent years, the synthesis of polypeptides using the ring-opening polymerization of NCAs has been thoroughly discussed in review papers.[2,3] There are well-established procedures for the synthesis of the NCA monomers, as well as for their polymerization to generate polypeptides. This section will discuss the different approaches used in the ring-opening polymerization (ROP) of NCAs, as well as side reactions associated with these methods. There is great interest behind the ROP of NCAs due to the large variety of polypeptides that can be produced, and the capability of producing high molecular weight polypeptides.

2.2.2.1 Monomer Synthesis

The first cyclic anhydride of an AA (known as Leuchs' anhydride) was reported in 1906 by Leuchs et al. for glycine.[16] More recent developments in this area have allowed the synthesis of NCAs in high purity and yield.[20] The modern approach to the synthesis of NCAs is a phosgenation reaction, using phosgene or a suitable substitute.[21] The synthesis of an NCA with triphosgene is illustrated in Figure 2.6. The reaction must be performed under anhydrous conditions due to the ease of hydrolysis of the cyclic anhydride, which will regenerate the starting AA. Phosgene-free synthesis has also been performed for a few different amino acids,[22,23] but it is still relatively new and not as reliable for other AAs.

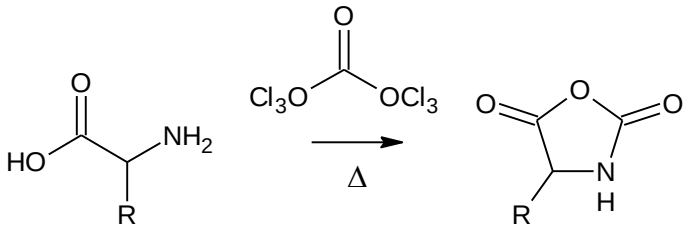

Figure 2.6 Synthesis of an NCA by phosgenation with triphosgene.

The purification of the NCA monomer is important, since purity is crucial for controlled ROP. It is known that impurities such as hydrogen chloride (HCl), the salts produced in the monomer synthesis, as well as unreacted triphosgene can affect the polymerization.[20] Poché et al. proposed that the synthesis be performed in ethyl acetate (EtOAc) instead of tetrahydrofuran (THF), and that aqueous washes at 0º C be subsequently performed to remove HCl and other impurities. This is done by first washing with deionized water, and then with a 0.5% aqueous sodium hydrogen carbonate solution. Along with HCl, unreacted amino acid hydrochloride salts are also removed by the aqueous washes.

Long term storage of the NCA monomers can be problematic, even at low temperatures, because even a small amount of water on the NCA crystals can slowly start the polymerization in the solid state. For this reason, NCAs should be stored at low temperatures ($T \leq -20$ ºC) and used as soon as possible after their synthesis.

2.2.2.2 Polymerization Strategies

The ROP reactions of NCAs are not as sensitive to impurities as anionic or cationic polymerizations. Nonetheless, NCA polymerizations require the use of purified monomers and are sensitive to impurities that are nucleophilic enough to initiate the reaction. Traditionally a primary amine (e.g. *n*-hexylamine) is used to initiate the ROP of NCAs (Figure 2.7). This mechanism is applicable to the N-unsubstituted NCA monomers. When there is a protecting group on the amine, the reaction becomes a step-wise addition similar to the SPPS reactions. In that case the protecting group on the nitrogen must be removed to produce the primary amine, which is necessary to continue the polymerization process. This modified approach allows control over the sequence of amino acids, but is much less

efficient at producing high molecular weight polypeptides. For this reason, N-substituted monomers are not as widely used as the N-unsubstituted monomers for the ROP of NCAs.

Primary amines are ideal candidates for the normal amine (NA) initiation mechanism, since they possess strong nucleophilic character relatively to their basicity. Secondary and tertiary amines are poor initiators by the NA mechanism due to their lower nucleophilic character; they still induce the polymerization of NCAs, however, but by another path called the activated monomer (AM) mechanism. The AM mechanism is provided in Figure 2.8 also for an *n*-hexylamine initiator, but secondary and tertiary amines are much more likely to induce the AM mechanism due to their increased basicity.

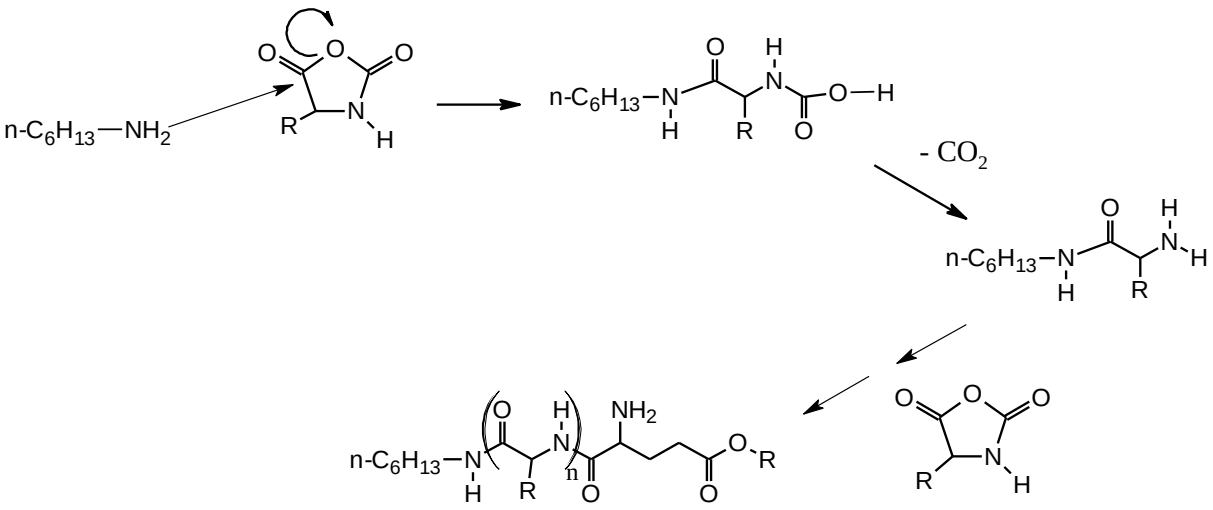

Figure 2.7 Normal amine polymerization mechanism for *n*-hexylamine in the ROP of NCAs.

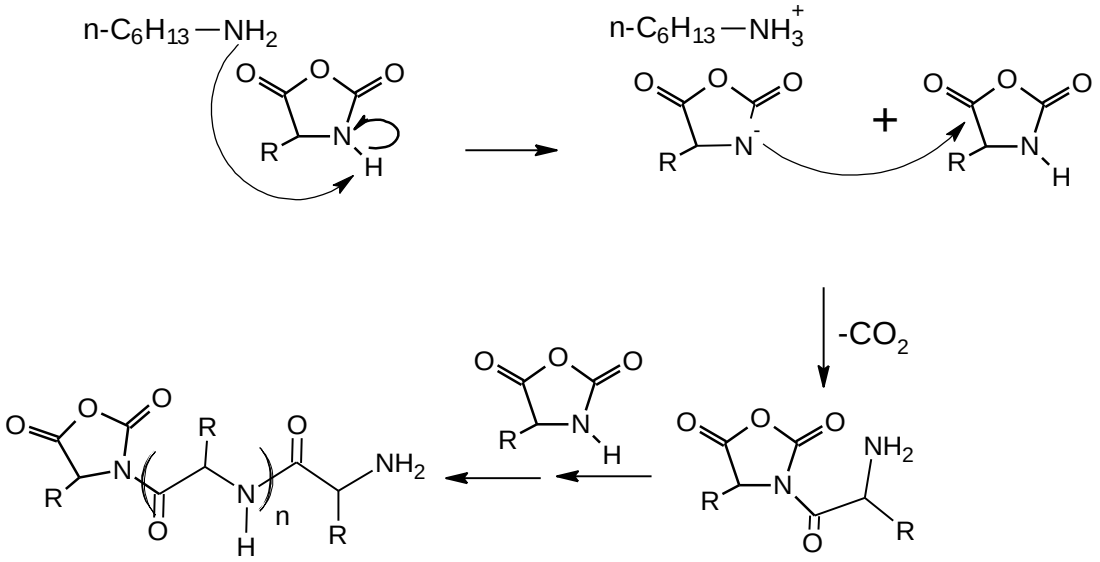

Figure 2.8 Activated monomer polymerization mechanism for *n*-hexylamine in the ROP of NCAs.

The goals in the ROP of NCAs are to maintain chirality, to achieve a narrow molecular weight distribution (MWD) or a low polydispersity index (PDI = M_w/M_n), and to be able to predict the molecular weight based on the monomer to initiator stoichiometric ratio (M/I). As compared with SPPS, a major concern with the ROP of NCAs is the molecular weight distribution of the polypeptides thus obtained. In SPPS, essentially monodispersed polypeptides are often obtained. The ROP method has the same characteristics as most living polymerization reactions, in that it is susceptible to MWD broadening due to the relative rates of initiation and propagation as well as side reactions. Polymerization strategies have been explored to reduce side reactions such as the occurrence of the AM mechanism. The use of transition metal complex[24,25] and primary amine hydrochloride[26] initiators for the ROP of NCAs has thus been investigated. The reaction conditions have also been modified by using high vacuum techniques,[27] or by decreasing the reaction temperature.[28] The loss of chirality

is usually not a concern in the ROP of NCAs since the α-hydrogen is not removed during the polymerization, so the chirality present in the original AA is maintained in the polypeptide.

To produce high molecular weight polypeptides, Deming first proposed to use nickel (Ni) complexes with 2,2-bipyridyl (bipy) and 1,5-cyclooctadiene (COD) as ROP mediators.[24] Shortly thereafter, Deming et al. also performed the Ni(0)- and cobalt(0)-mediated ROP of NCAs and demonstrated that the outcome of these reactions was strongly dependent on the reaction conditions used.[25] The initiation of the NCA polymerization by transition metal complexes is illustrated in Figure 2.9, while Figure 2.10 shows how the metal complex participates in chain growth. Propagation results from the attack of the nucleophilic amido group on the electrophilic C_5 carbonyl of the NCA monomer. This proposed mechanism shows how the metal is able to migrate along the growing polymer chain and is held by a stable chelate at the chain ends. Block copolypeptides were also synthesized by the Ni(0)-mediated ROP of NCAs, with molecular weights predictable from the monomer to catalyst (initiator) ratio, and high molecular weights (M_n > 200,000) could be achieved while maintaining a narrow MWD (M_w/M_n < 1.2).[24]

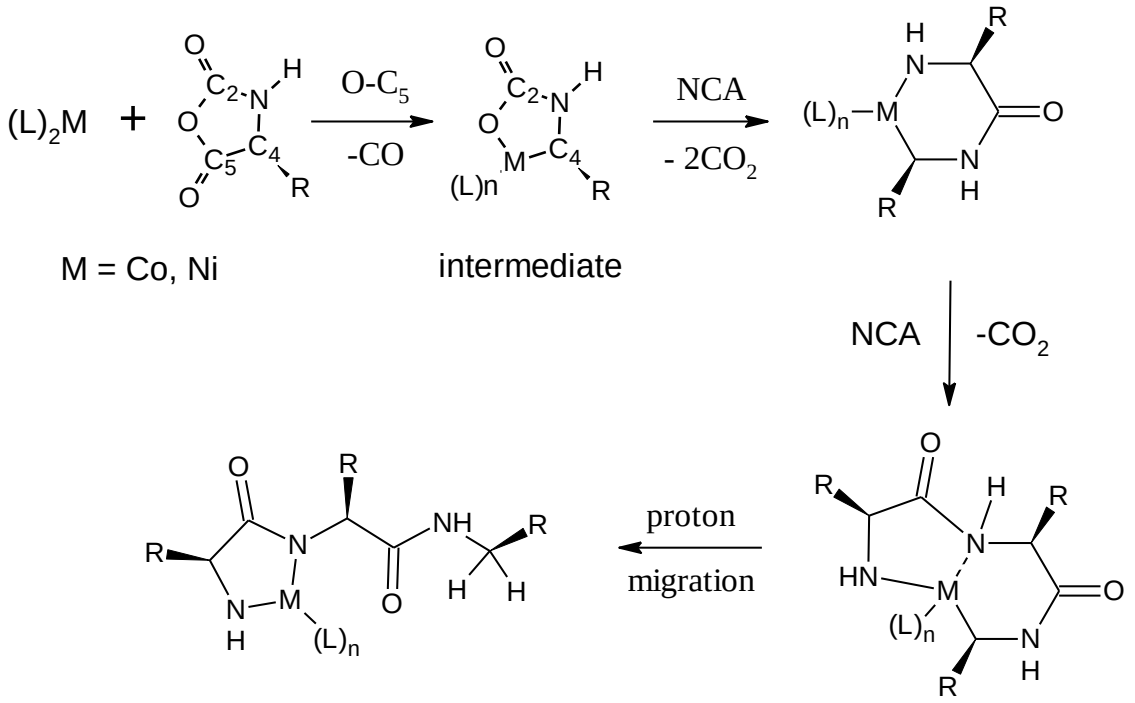

Figure 2.9 Initiation of the ROP of NCAs by transition metal complexes.

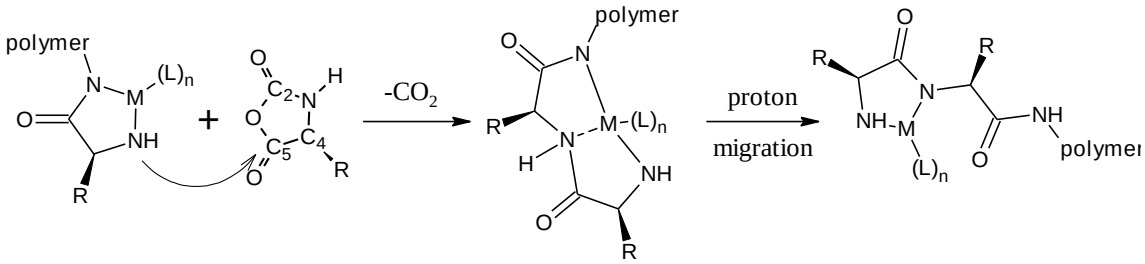

Figure 2.10 Participation of the transition metal complexes in the propagation step of the ROP of NCAs.

Primary amine hydrochloride salts have a mechanism similar to their respective primary amine analogues in the initiation and propagation steps of the NCA ROP. Unfortunately, their reactivity is also considerably lower since an equilibrium exits between the free primary amine and its hydrochloride salt as shown in Figure 2.11. The equilibrium

lies predominantly towards the hydrochloride salt form, which leads to slower initiation and propagation rates, but also reduces the occurrence of the undesired AM mechanism. Dimitrov and Schlaad thus used polystyrene macroinitiators (M_n = 5500) with a hydrochloride salt primary amine terminus to produce block copolymers containing a polypeptide block.[26] The polymerizations, carried out in DMF between 40-80 ºC, produced larger polypeptide blocks than expected ($M_n \approx$ 13,000 for a target M_n = 8200) due to traces of impurities in the NCAs that deactivated a portion of the macroinitiator; a narrow MWD (M_w/M_n <1.03) was nevertheless maintained for the copolymers. Lutz et al. applied a similar procedure to a poly(ethylene oxide) macroinitiator ($M_n \approx$ 5000) with a primary amine hydrochloride salt terminus.[29] Short polypeptide segments (6-8 units, $M_n \leq$ 2000) were thus grown from the macroinitiator while maintaining a narrow MWD (M_w/M_n < 1.05). In this case however, the relatively short polypeptide segment attached to the poly(ethylene oxide) macroinitiator would have limited impact on the MWD due to its low weight fraction (~30%) in the copolymer. Using small molecule hydrochloride salt initiators would provide a better assessment of how these hydrochloride salt initiators affect the MWD in the ROP of NCAs.

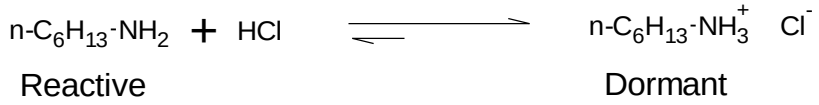

Figure 2.11 Equilibrium between the free *n*-hexylamine and *n*-hexylamine hydrochloride salt forms.

The ROP of NCAs is susceptible to side reactions, among others due to impurities present in the reaction. These impurities can originate from the monomer, the solvent or the

initiator, depending on the purification steps used prior to polymerization. It is known that NCA monomers may contain trace amounts of impurities such as HCl, HCl salts, AA hydrochlorides, and triphosgene. N,N-Dimethylformamide (DMF), a solvent commonly used for these reactions, can also contain impurities such as dimethylamine.[30] It was proposed that high vacuum techniques (HVT) could be useful to remove these impurities,[27] and were thus used with custom glassware to distil the DMF and to recrystallize the NCA monomer immediately before polymerization. Hadjichristidis and co-workers postulated that in the absence of impurities, there occurrence of the AM mechanism and chain end termination could be minimized during the reaction. This was confirmed by the synthesis of poly(γ-benzyl L-glutamate) (PBG) and block copolypeptides containing PBG with different sequences, having high molecular weights ($M_n \leq 100{,}000$) and narrow MWDs ($M_w/M_n < 1.2$), easily controlled by the monomer to initiator ratio.

Another method suggested to decrease side reactions in the ROP of NCAs is to simply decrease the reaction temperature. Since rate constants are related to temperature through the Arrhenius equation, a decrease in reaction temperature should reduce the rate of side reactions more than the rate of propagation if their activation energies are higher than for the propagation step. Vayaboury et al. have indeed shown that chain termination was minimized at 0º C in the polymerization of the N_ε-trifluoroacetyl L-lysine NCA.[28] Based on non-aqueous capillary electrophoresis analysis, it was reported that 99% of the chain end functionality was maintained when the polymerization was performed at 0 ºC, as compared to only 22% when it was performed at room temperature. Unfortunately no PDI values were reported for the products, so it is unknown how the temperature decrease affects the MWD.

The strategies developed to produce linear polypeptides by the ROP of NCA monomers are quite versatile. Different strategies can be used depending on the requirements for the final polypeptide. Random and block copolymers may also be synthesized by the ROP method, which provides a wide range of copolypeptides with tailored properties that can serve as building blocks to construct more complex architectures. The next section will discuss different methods for the synthesis of branched polymer systems, some of which show promise for the synthesis of branched polypeptides.

2.3 Synthesis of Dendritic Polymers

Dendritic polymers are highly branched macromolecules with a tree-like structure. These systems can be divided into three main categories, based on the architecture and the degree of structural perfection of each system: Dendrimers, hyperbranched polymers, and dendrigraft polymers. Dendrimers ideally have a perfectly branched structure that contains a defined number of branching points and have a strictly controlled growth sequence. Hyperbranched polymers have a highly imperfect structure relying on statistical branching that provides little control over the growth of the chains. The dendrigraft polymers are somewhere between dendrimers and hyperbranched polymers with respect to the control of growth and structural perfection. The synthesis of dendrimers requires distinct protection, condensation, and deprotection steps for each generation. This step-wise synthesis provides a highly controlled synthesis and produces almost monodispersed macromolecules ($M_w/M_n < 1.01$). The synthesis of hyperbranched polymers is much simpler in practice and uses unprotected polyfunctional monomers, which generate random branching sites during the continuous growth of the macromolecules. These poorly defined structures have a broad molecular

weight distribution ($M_w/M_n > 2$) in most cases. Dendrigraft polymers are synthesized by a step-wise approach similar to dendrimers; however, polymeric building blocks are used instead of small molecules. Under appropriate conditions during the polymerization and grafting steps, very large macromolecules can be generated quickly while still maintaining a relatively narrow MWD ($M_w/M_n < 1.1$-1.2).

A graphical comparison of the structure of the three classes of dendritic polymers is shown in Figure 2.12. The different concentric circles in Figure 2.12 represent branching levels introduced in successive generations. At each level of branching (generation) the dendrimer (Figure 2.12A) shows a perfect structural growth, whereas the hyperbranched polymer (Figure 2.12B) has multiple imperfections due to less controlled reactions. Depending on the size of the polymeric units used for the dendrigraft polymers (Figure 2.12C), large macromolecules can be constructed in only a few branching cycles.

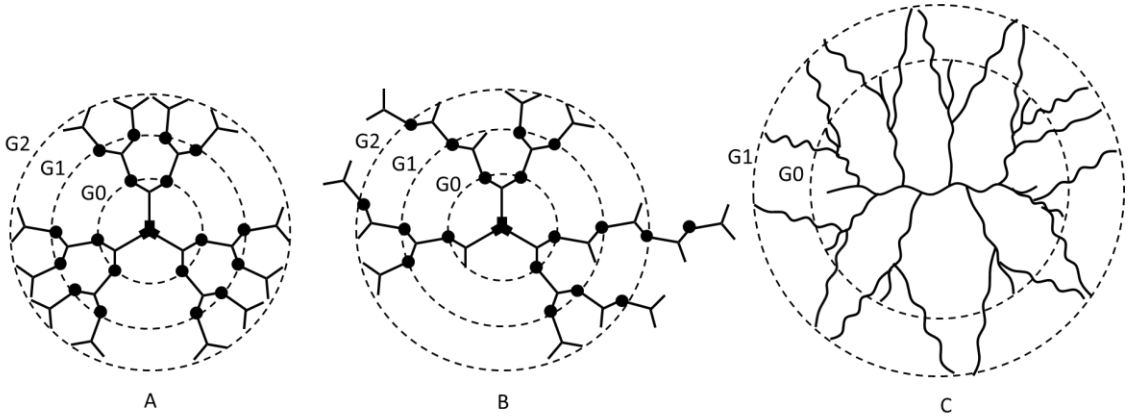

Figure 2.12 Structure of dendritic polymers: (A) Dendrimer, (B) hyperbranched polymer, and (C) dendrigraft polymer.

2.3.1 Dendrimers

The synthesis of tree-like structures on the molecular level was widely promoted by Donald A. Tomalia, but the first syntheses of dendritic molecules actually go back to the late 1970s.[31] The Tomalia group published their first paper on the divergent synthesis of dendrimers, the poly(amido amine) (PAMAM) dendrimers, in 1985.[32] In the same year work by Newkome et al. was published on the divergent synthesis of dendritic structures called arborols.[33] A few years later Hawker and Fréchet described the convergent synthesis of dendrimers using 3,5-dihydroxybenzyl alcohol.[34] Divergent and convergent synthetic strategies for the synthesis of dendrimers are compared in Figure 2.13, where this synthesis of a generation 2 (G2) dendrimer from AB_n-type monomers is depicted by both strategies. The black dots in the figure represent the branching points in the structures, generated by coupling functionalities A with B. In both strategies there is the same number of branching points in the G2 dendrimer, but the starting material and intermediate products are different. Ideally both approaches produce the same final structure, but this is not always the case due to side reactions and purification issues.

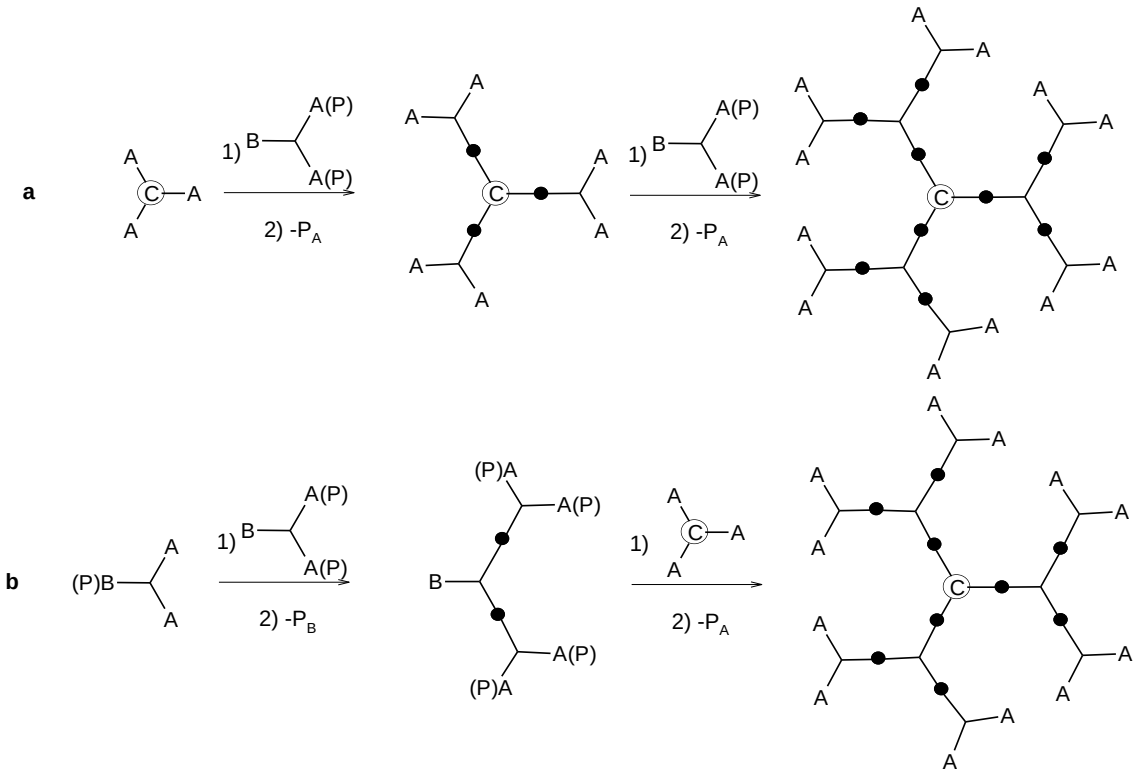

Figure 2.13 Synthesis of a G2 Dendrimer by (a) divergent and (b) convergent strategies.

Dendrimers have unique characteristics that make them useful for many applications, including the encapsulation of small molecules. Each dendrimer molecule contains a core, an interior branched region, and a shell or superficial region. The void space of the interior is determined by the branching functionality, while the interior composition controls guest-host interactions for a given dendrimer. The surface region contains terminal groups that can control the entry and exit of guest molecules to/from the dendrimer interior. The interior and surface properties can be manipulated by selecting specific monomeric units and synthetic strategies.

2.3.1.1 Divergent Strategy

The construction of dendrimers by the divergent method begins from a core molecule, with monomer addition proceeding outward toward the surface of the macromolecule. The core represents the generation zero (G0) and contains one or more reactive sites. Covalently connecting a layer of monomeric units to the core produces a G1 dendrimer. The number of monomeric units that can be added depends on the number of reactive sites on the core. A key feature of the divergent method is the exponentially increasing number of reactions that are required for the attachment of each subsequent generation. With the increasing number of reactions required for each generation, growth occurs with increased potential for side reactions. A perfect dendrimer structure will result only when all the available reaction sites have reacted as intended. If incomplete reactions occur, the dendrimer structure is flawed; the earlier in the growth process these flaws occur, the more impact they will have on the dendrimer properties.

Branching within dendrimers is an attribute that can be strictly controlled. Controlling the branching density is important since dendrimers can serve for many applications that require varying degrees of density for the macromolecule. Branching in a dendrimer is dependent on the monomer valency. A monomer (similar to the one shown in Figure 2.13) that contains one B functionality and a number X of A functionalities can be referred to as a $1 \rightarrow X$ branching monomer. If there are two or three A functionalities on the monomer, they are therefore referred to as $1 \rightarrow 2$ and $1 \rightarrow 3$ branching monomers, respectively. In a divergent construction with a core molecule containing 3 reactive sites (as in Figure 2.13a), the progression of the growth would correspond to $3 \rightarrow 3*X \rightarrow 3*(X)^2 \rightarrow 3*(X)^3 \rightarrow \ldots$ and so on. The total number of added monomer units at each generation is therefore dependent on the

branching functionality *X* of a given monomer. For example, using 1→2 and 1→3 type monomers in combination with a core functionality of three, the branching patterns are 3→6→12→24→48→**96**, and 3→9→27→81→243→**729,** respectively. Even by only G5 there is large molecular weight difference between the 1→2 and 1→3 branching dendrimers, since the total branching functionality is more than seven times greater in the 1→3 branched system. Regardless of the monomer valency, both G5 dendrimers should have comparable hydrodynamic diameters, which means that the 1→3 dendrimer is much denser.

Many functional groups and monomeric units have been used to produce dendrimers by a divergent strategy. Probably the best known dendrimer family synthesized by a divergent strategy is the poly(amido amine) (PAMAM) dendrimers. These were first produced by Tomalia et al.,[32] beginning with a core of either ammonia or ethylenediamine as shown in Figure 2.14. Ammonia and ethylenediamine have core multiplicities (N_c) of 3 and 4, respectively, due to the number of protons in their structure that can be abstracted by a base. Michael addition occurs between ammonia and acrylate ester that is followed by amidation of the ester groups with a large excess of ethylenediamine to produce primary amine terminal groups. Half generations can also be produced in these systems by halting the synthesis after the Michael addition with the acrylate. Monodispersed PAMAM dendrimers of up to G10 have been synthesized by this approach, with molecular weights up to 934,000, and containing close to 5,000 surface groups.

The classification of dendrimers can be done by defining three of their characteristics: The number of branching points (2, 3, etc.), the branching structure (N, C, aryl, etc.), and the connectivity of the structure (containing N, amide, ester, etc.). PAMAM is known as a 1→2 N-branched dendrimer with *amide* connectivity, as it contains 2 branching points produced at

the site of the primary amine (N-branched) and contains an *amide* bond after a monomer addition.

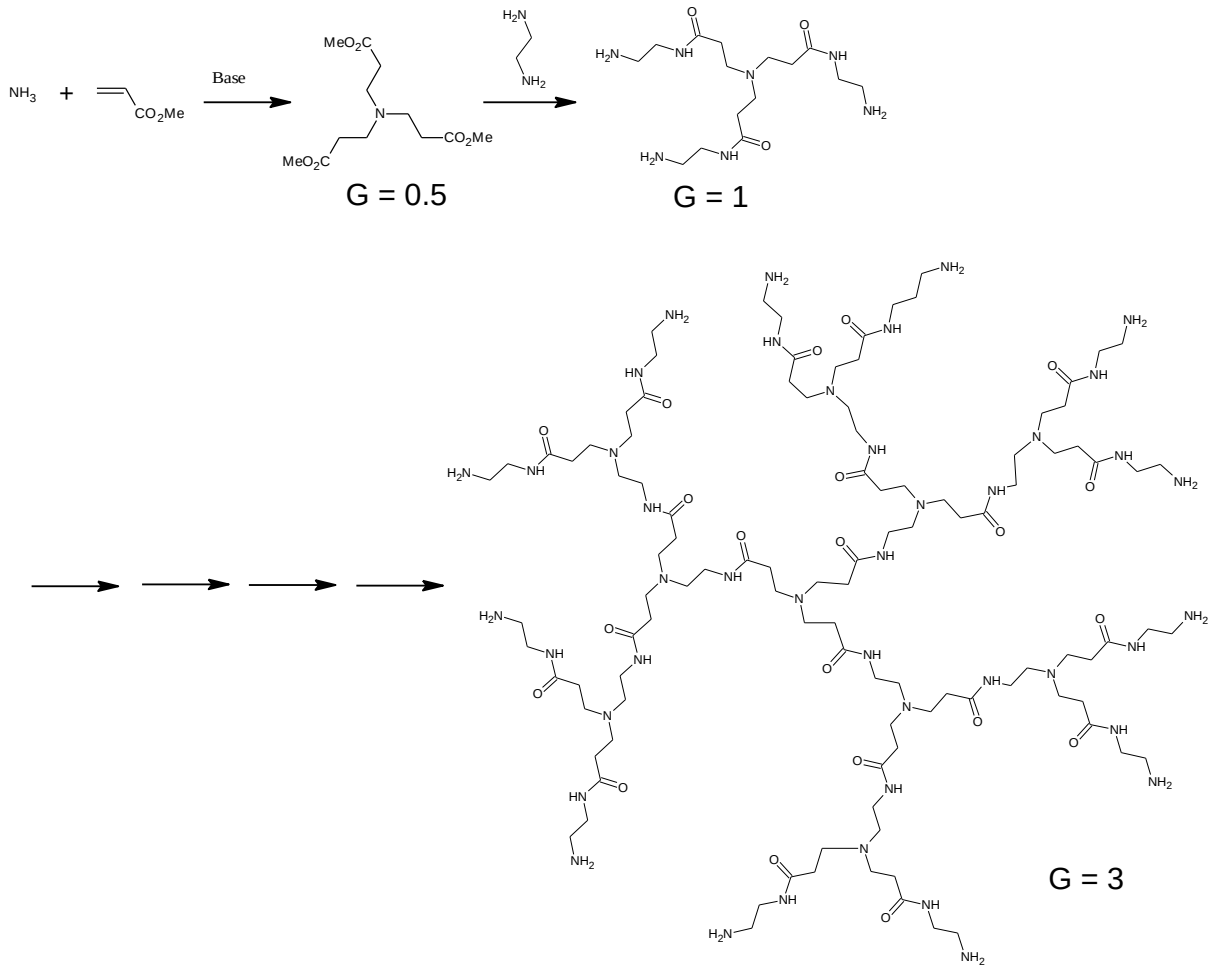

Figure 2.14 Synthesis of PAMAM using ammonia as a core.

Between 1979 and 1981, Denkewalter et al.[35,36] reported the first divergent preparation of dendritic polypeptides utilizing the protected amino acid N,N'-*bis*(*tert*-butyloxycarbonyl)-L-lysine as monomeric building block. The synthesis for a G1 lysine dendrimer is shown in Figure 2.15. This dendrimer is an example of a 1→2 C-branched

dendrimer with *amide* connectivity. The deprotection in neat TFA removed the protecting groups easily. The process could be repeated to produce higher generations of lysine dendrimers.

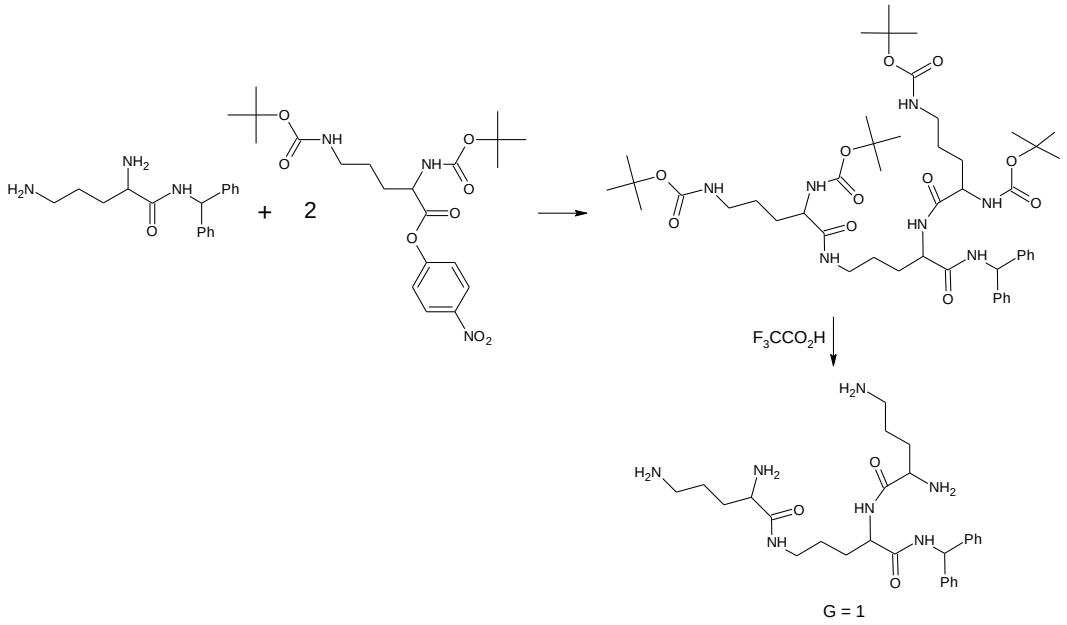

Figure 2.15 Synthesis of a G1 polylysine dendrimer.

2.3.1.2 Convergent Strategy

In a convergent synthetic scheme, a dendrimer is synthesized from the "outside-in". This concept was initially described by Hawker and Fréchet,[34] and shortly thereafter by Miller and Neenan.[37] The concept is shown in Figure 2.13b. Similarly to the divergent growth strategy, the convergent strategy requires iterative sequences of activation and coupling for the continued growth of successive generations. However in the convergent strategy, the number of reactive sites involved in the coupling reaction remains constant for each generation. This is advantageous as it makes it easier to maintain control over the purity of the product. It also

allows a reduction in the amount of reagents required for complete coupling, and provides freedom to use a variety of different functional groups at the focal point. The reaction begins with what will eventually become the periphery of the dendrimer and proceeds inwards, towards the so-called focal point. Another advantage of this method over the divergent strategy is that there is a larger difference in molecular weight between the starting material and by-products with incompletely reacted functional groups (e.g. the AB_2 monomers), enabling easier separation of the different components.

Hawker and Fréchet[34] thus described the synthesis of polyether dendrimers from the monomer 3,5-dihydroxybenzyl alcohol. The two-step repetitive synthesis of dendritic fragments (dendrons) containing one bromide functionality at the focal point is described in Figure 2.16. Dendrons ranging from G1-Br to G6-Br were synthesized and used in the reaction with a polyfunctional core to generate a dendrimer as demonstrated in Figure 2.17. The convergent strategy carries a nomenclature similar to the one described for the divergent strategy, where the polyethers in Figure 2.16 and Figure 2.17 can be described as 1→2 aryl-branched dendrimers with *ether* connectivity. A unique benefit of the convergent strategy is the ability to synthesize asymmetric dendrimers containing different structural elements.[38] In this case two or more different dendrons can be attached to a core molecule to produce a segmented dendrimer. The convergent strategy, like the divergent strategy, can be successful in producing dendrimers with a nearly perfect structure from a wide range of materials; however the convergent strategy still requires tedious step-wise reactions with multiple iterations to generate high molecular weight dendrimers.

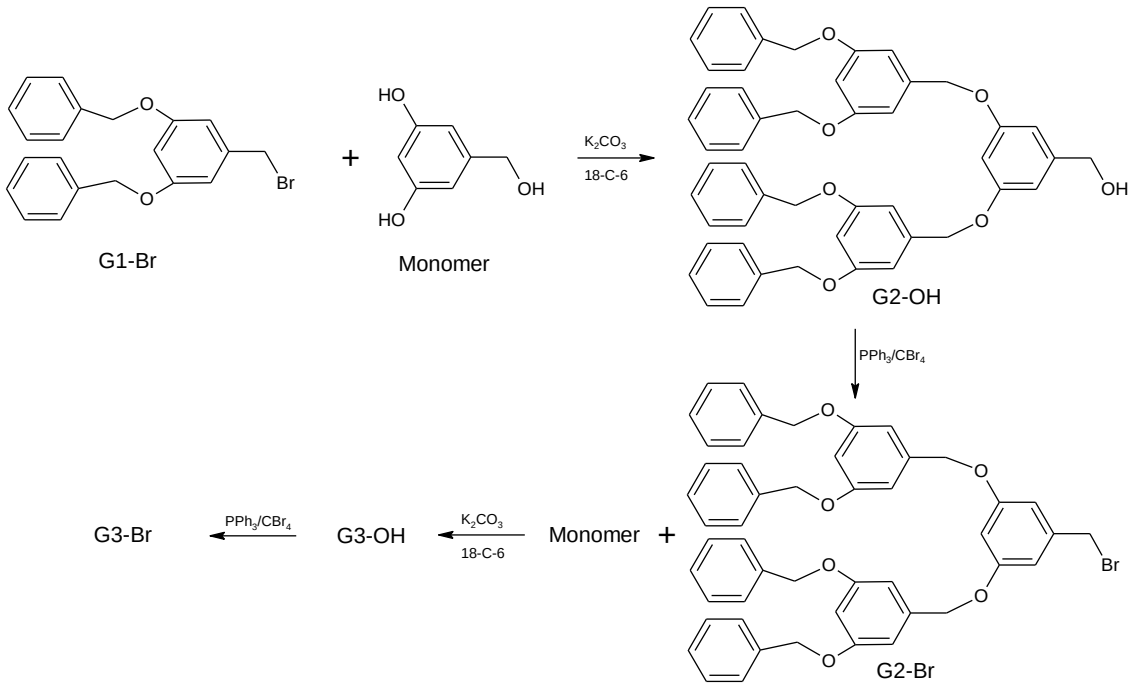

Figure 2.16 Synthesis of G3 polyether macromolecules with a bromobenzyl functionality at the focal point.

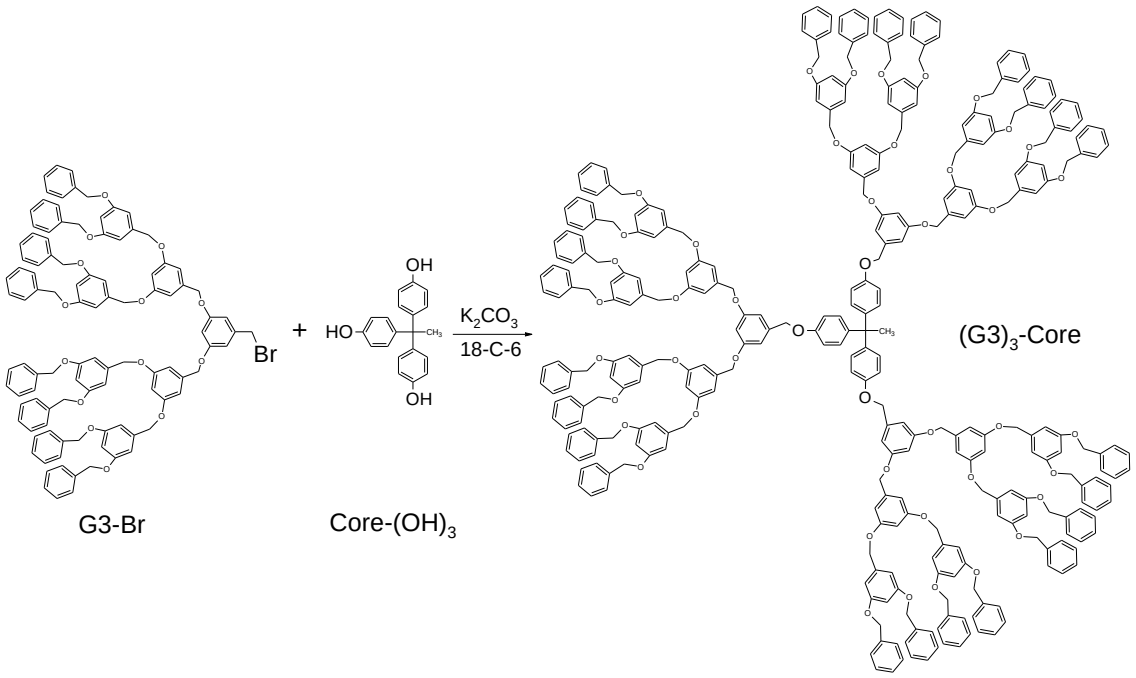

Figure 2.17 Reaction of G3 bromine-functional dendrons with a polyfunctional core to generate a polyether dendrimer.

2.3.2 Hyperbranched Polymers

Hyperbranched polymers have a dendritic architecture with random branching points. The synthesis of hyperbranched polymers is simpler than for dendrimers in that AB_n-type monomers are still utilized but they do not contain protecting groups, which results in uncontrolled random growth. The simpler synthetic methods used for hyperbranched polymers provide cheaper alternatives to dendrimers when optimal properties are not required. The synthesis of hyperbranched polymers was first reported in 1988 by Gunatillake et al.,[39] and shortly thereafter by Kim and Webster who coined the term "hyperbranched polymers".[40] In 1991, Hawker and Fréchet produced hyperbranched polyesters with polystyrene-equivalent weight-average molecular weights of up to 200,000 and relatively

large polydispersity indices ($M_w/M_n > 2$).[41] A statistical model for the growth of hyperbranched polymers from AB_n-type monomers was actually first proposed by Flory in 1952.[42] This model was able to relate the branching level to the extent of reaction, but was unable to quantify the level of structural imperfection of hyperbranched polymers obtained from AB_2-type monomers. Hawker et al. defined the degree of branching (DB) in terms of the different monomer units present within a given hyperbranched polymer.[41] The terminal branching (T) units, where no B functional groups have reacted, the dendritic branching (D) units, where both B functional groups have reacted, and linear (L) chain segments, where only one of the B functional groups has reacted, are displayed on the dendrimer and hyperbranched polymers of Figure 2.18. A structurally perfect dendrimer only contains terminal and dendrimer units, whereas hyperbranched polymers also contain linear segments. The degree of branching for a given hyperbranched polymer as defined by Hawker et al.[41] is expressed in Equation 2.1, by dividing the number of fully branched units (D and T) by the total number of monomer units within the polymer (D, T, and L).

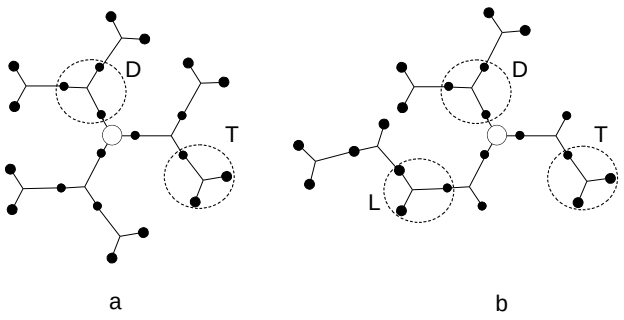

Figure 2.18 Structural units in a dendrimer (a, DB = 1) and a hyperbranched polymer (b, DB = 0.56): Dendritic (D), terminal (T), and linear (L).

$$DB = \frac{D + T}{D + T + L} \tag{2.1}$$

The dendrimer in Figure 2.18a corresponds to a DB of 1, whereas the hyperbranched polymer in Figure 2.18b corresponds to a DB of 0.56. According to Equation 2.1, a linear polymer would have a DB of 0 if the end-units were neglected. To account for this problem, a modified form of Equation 2.1 was proposed by two different groups in 1997 as expressed in Equation 2.2.[43,44] Applying this equation to the dendrimer and the hyperbranched polymer in Figure 2.18 provides DB' values of 1 and 0.33, respectively.

$$DB' = \frac{2D}{2D + L} \tag{2.2}$$

The uncontrolled growth of hyperbranched polymers leads to asymmetrical growth within each individual molecule, as well as non-uniform growth among individual molecules, producing a broad MWD ($M_w/M_n > 2$). Flory was able to predict the polydispersity of a hyperbranched polymer derived from AB_n-type monomers in terms of the weight-average degree of polymerization, X_w, and the number-average degree of polymerization, X_n, as seen in Equation 2.3. Flory also related the degree of polymerization to the extent of reaction (α) and the overall functionality of the AB_n monomer (*f*). For an AB_2 monomer *f* has a value of 3, and the extent of reaction is measured as the ratio of a reacted B functional group versus the total number of B functional groups within the hyperbranched polymer. The value of α may approach but never reach 0.5, since every B functionality that reacts brings two more unreacted B functionalities into the hyperbranched polymer. According to Equation 2.3, at low conversion the polydispersity corresponds to a Flory distribution ($M_w/M_n \approx 2$) and increases as the reactions proceeds (increasing α). It should be noted that the degree of

branching is not related to the polydispersity. Some hyperbranched polymer systems may produce low polydispersities but not lead to high degrees of branching, as the DB is controlled by statistics.[44]

$$PDI = \frac{X_{\mathrm{w}}}{X_{\mathrm{n}}} = \frac{1 - \alpha^2(f-1)}{1 - \alpha(f-1)} \tag{2.3}$$

Unprotected and high functionality monomers can lead to side reactions, including gelation. Intramolecular backbiting does not cause gelation but terminates molecular growth. One way to reduce intramolecular backbiting is to slowly add monomer by a 'concurrent slow addition' method introduced by Frey and co-workers.[45] This concept was applied to the synthesis of hyperbranched polymers with controlled molecular weights, high degrees of branching, and relatively narrow MWD ($M_w/M_n < 1.5$).[46-49]

The methods for generating hyperbranched polymers fall in two main categories: The single-monomer methodology (SMM), where AB_n-type monomers are used, and the double-monomer methodology (DMM), where reactions of A_2 + B_3 monomer pairs are employed. Gelation was difficult to avoid with classic A_2 + B_3 reactions until a couple-monomer methodology (CMM) was introduced, whereby the reactivity of the functional groups within the monomer pairs is carefully selected (AA' + B'B_n), thus producing AB_n-type intermediates for which reactions can proceed similarly to the SMM mechanism and gelation can be avoided.[50,51]

2.3.2.1 Single-monomer Methodology

Several polymerization mechanisms can be applied to the SMM to produce hyperbranched polymers, including among others polycondensation, self-condensing vinyl polymerization,

and self-condensing ring-opening polymerization. The first example of a single monomer polycondensation was reported by Kim and Webster using 3,5-dibromophenylboronic acid in the presence of a Pd catalyst to produce a hyperbranched polyphenylene, where the unreacted bromide functionalities were then converted to carboxylate salts to make the polymer water-soluble. A general scheme depicting this reaction is shown in Figure 2.19. Higher branching functionality monomers such as AB_3, AB_4, and AB_6, have also been used to prepare hyperbranched polyesters[52] and polysiloxanes[53] by polycondensation.

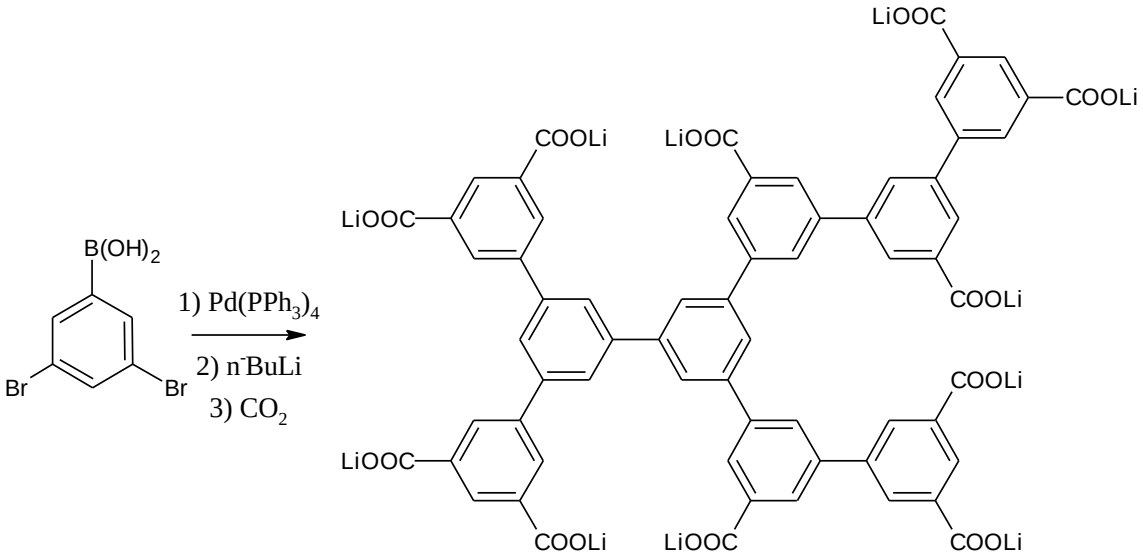

Figure 2.19 Synthesis of hyperbranched water-soluble polyphenylene-carboxylate by the single-monomer polycondensation method.

Self-condensing vinyl polymerization (SCVP) was introduced by Fréchet et al.[54] for the synthesis of hyperbranched polystyrene from a styrene derivative, 3-(1-chloroethyl)ethenylbenzene. This species was called an '*inimer*' for its capacity to act as both initiator and monomer under specific conditions. In these reactions, external activation is

necessary to convert an *inimer* (AB monomer) into an activated *inimer* (AB^* monomer) containing an anionic, cationic, or radical species. Fréchet et al. developed both cationic[54] and radical[55] SCVP methods for the synthesis of hyperbranched polystyrene. A general reaction scheme for the synthesis of hyperbranched polystyrene through SCVP using a cationic activated species is shown in Figure 2.20. Ideally, in SCVP, new propagating and initiating centers are generated by each monomer addition, leading to hyperbranched polymers. SCVP is susceptible to cross-linking, and improvements can be made by applying controlled polymerizations methods such as atom transfer radical polymerization (ATRP)[56,57] or group transfer polymerization (GTP).[58,59]

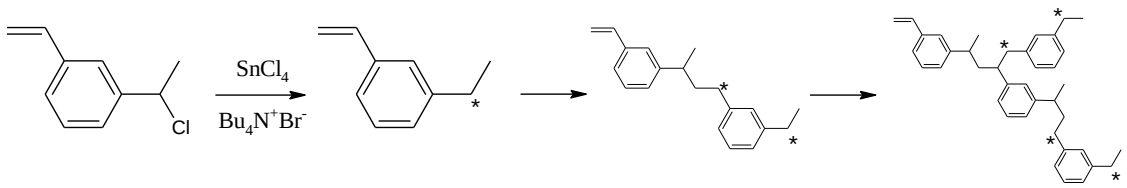

Figure 2.20 Synthesis of hyperbranched polystyrene by self-condensing vinyl polymerization (SCVP) using the *inimer* 3-(1-chloroethyl)ethenylbenzene.

Self-condensing ring-opening polymerization (SCROP) or ring-opening multi-branching polymerization (ROMBP) relies on principles similar to SCVP, where new initiating sites are created by the propagation reaction. The first ROMBP reaction was reported by Suzuki et al., using cyclic carbamates to generate low molecular weight (M_n < 3,000) hyperbranched polyamines with the help of a palladium catalyst.[60] These low molecular weight hyperbranched polyamines had a relatively narrow MWD ($M_w/M_n \approx$ 1.3-1.5) for hyperbranched polymer systems. Another example of this approach is the work of

Dworak et al., who produced low molecular weight (M_n < 6000) hyperbranched polyglycidol with M_w/M_n = 1.2-1.6 by cationic polymerization of unprotected glycidol.[61] A few years later, Sunder et al. demonstrated the synthesis of hyperbranched polyglycidol by anionic polymerization of unprotected glycidol, with comparable molecular weights and slightly narrower MWD (M_w/M_n = 1.13-1.47).[62] A schematic representation of the anionic polymerization of hyperbranched polyglycidol is shown in Figure 2.21. Vandenberg first pointed out that intra- as well as intermolecular proton transfers are possible after the ring-opening reaction when polymerizing unprotected glycidol,[63] which can lead to the formation of primary alkoxide active sites. Frey and co-workers controlled the concentration of active sites present in the polymerization by partial (10%) deprotonation of the initiator system, leading to simultaneous growth of all the chain ends and ultimately control over the molecular weight and the MWD of the hyperbranched polyglycidol. It can be seen from Figure 2.21 that the number of active sites per hydroxyl group decreases as the reaction proceeds, since each monomer addition produces two new hydroxyl groups while the number of active sites remains constant.

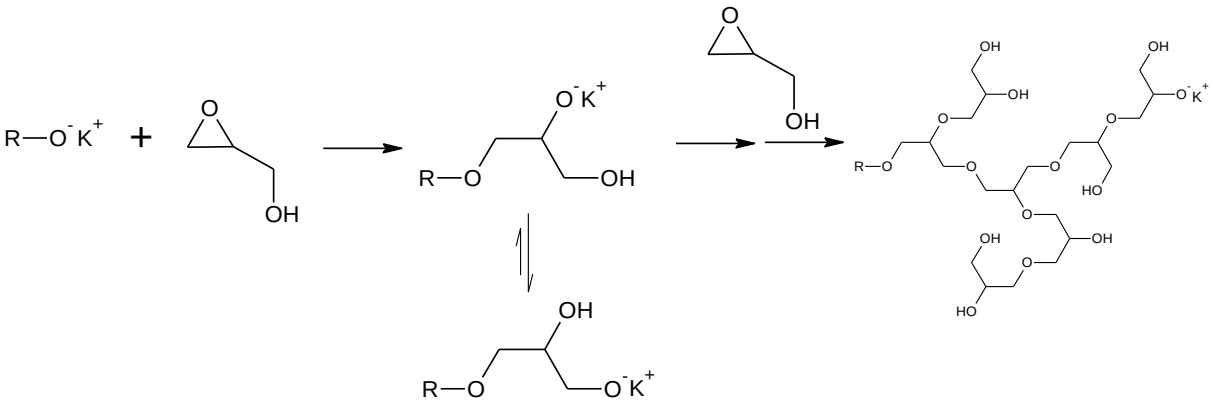

Figure 2.21 Schematic representation of the anionic polymerization of glycidol.

Proton transfer polymerization (PTP) was first introduced by Chang and Fréchet.[64] PTP has similarities to the ROMBP of glycidol, but the monomers are of the H-AB_2-type where only a catalytic amount of initiator (sodium hydroxide) is needed to abstract the proton from the monomer. A general reaction scheme for this approach is shown in Figure 2.22. The activated monomer can then react with another monomer, followed by proton transfer to generate a new activated monomer, and so on.

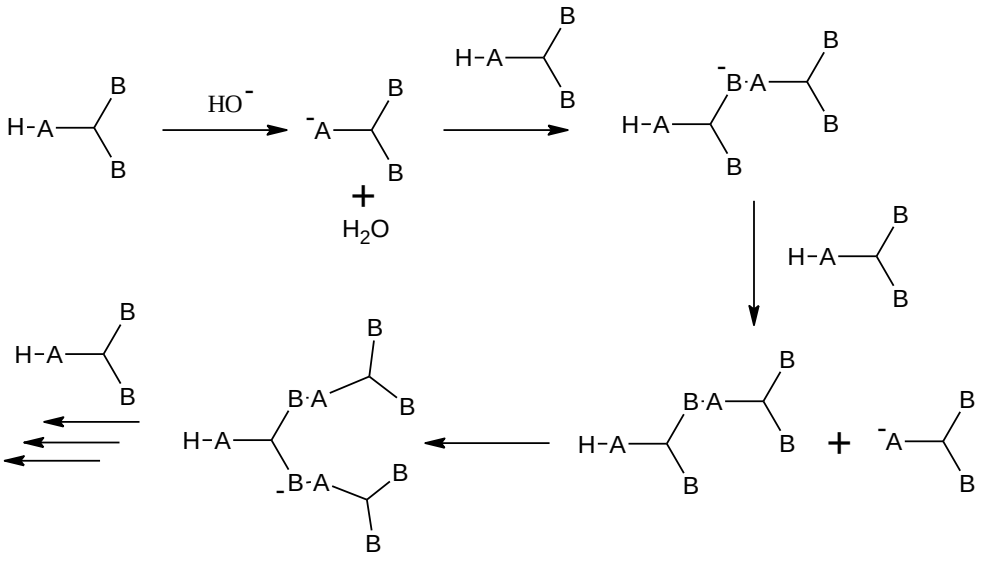

Figure 2.22 Proton transfer polymerization of an H-AB_2-type monomer.

2.3.2.2 Couple-monomer Methodology

The couple-monomer methodology (CMM) was introduced to avoid gelation that occurs for traditional A_2 + B_3 double-monomer methodology (DMM) reactions, and is now the most widely used approach when the DMM is applied. Selecting matched monomer pairs is the most important factor in CMM. If the functional groups in an A_2 monomer have different levels of reactivity, A and A', and two different levels of reactivity are also present in a B_3

monomer, such as $B'B_2$, ideally a new AB_2 monomer is produced in situ by a fast reaction between A' and B'. The newly formed AB_2 monomer can undergo SMM reactions to produce hyperbranched polymers. The CMM is still a one-pot synthesis, but by altering the reactivity of A and B functionalities, as well as the monomer feed ratio, the development of hyperbranched polymers with unique architectures is possible by that method. A detailed review of the CMM approach by Gao and Yan demonstrated the versatility of the CMM in producing hyperbranched polymers.[65]

2.3.3 Dendrigraft Polymers

Dendrigraft (arborescent) polymers combine features of dendrimers and hyperbranched polymers. Dendrigraft polymers can reach much higher molecular weights than dendrimers or hyperbranched polymers, while still maintaining narrow MWD ($M_w/M_n < 1.1$), which justifies designating them as semi-controlled dendritic structures.[66] These macromolecules can be synthesized by three distinct methodologies, consisting of *grafting onto* (divergent), *grafting from* (divergent), and *grafting through* (convergent) techniques. The advantage of these techniques is the use of *polymeric* building blocks. The divergent strategies rely on successive grafting reactions starting from a linear polymer substrate. In the *grafting onto* technique, side chains synthesized in a separate reaction are coupled with a linear substrate, whereas the *grafting from* technique uses initiating sites on a linear substrate to grow the side chains. The *grafting through* technique is analogous to hyperbranched polymer syntheses, whereby self-branching condensation reactions produce dendrigraft molecules in a one-pot reaction. For all three strategies the branching points are randomly distributed in most cases,

and the branching density can be varied by adjusting the functionalization level of the substrate.

2.3.3.1 Divergent *Grafting Onto* Strategy

The *grafting onto* strategy is most commonly used to produce macromolecules with tailored characteristics, since successive grafting reaction cycles provide control over the molecular structure, the length of the side chains used, and the branching density. The first dendrigraft systems, obtained by a *grafting onto* approach, were reported simultaneously by two groups in 1991: Tomalia et al. described the synthesis of Comb-burst® polyethyleneimine (PEI) using cationic polymerization techniques,[67] while Gauthier and Möller used anionic techniques to generate polystyrene (PS) dendrigraft polymers, denominated *arborescent* polymers.[68] Both ionic grafting techniques began with a polymer substrate that was functionalized to contain the desired number of reactive sites, that were then coupled with 'living' polymer chains. The newly formed comb-branched polymers were further functionalized to serve as substrates for a new grafting reaction of 'living' polymer chains. A schematic representation of the *grafting onto* strategy is provided in Figure 2.23, where the comb-branched polymer first synthesized is denoted as a generation zero (G0) graft polymer. This divergent *grafting onto* scheme leads to a geometric increase in molecular weight over successive reactions. Since the substrate, the side chains, and the graft polymer can be characterized individually, the number of side chains attached in a grafting reaction can be quantified, as well as the average spacing between the side chains. As seen in Figure 2.23, repeating the cycles of substrate functionalization and grafting leads to the subsequent generations (G1, G2, etc.) of dendrigraft polymers.

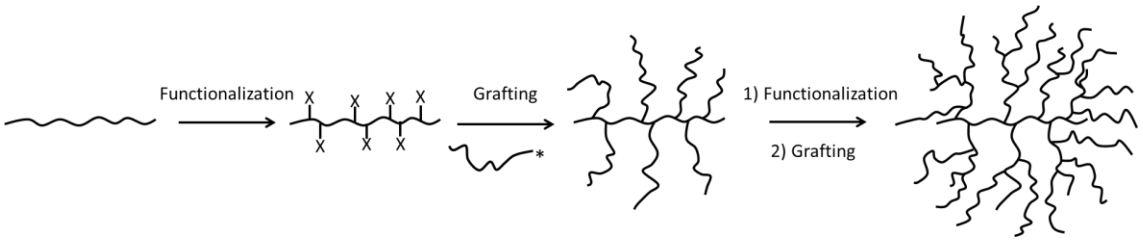

Figure 2.23 Schematic representation of the generation-based *grafting onto* synthetic strategy for dendrigraft polymers.

A number of requirements must be met to obtain well-defined dendrigraft polymers by the *grafting onto* strategy. First, it must be possible to modify the linear substrate and the graft polymers of the subsequent generations with functionalities capable of reacting with the 'living' polymer side chains without cross-linking. Both the substrate and the 'living' side chains must also be devoid of side reactions in the grafting process. Ionic polymerization techniques are well-suited to the synthesis of dendrigraft polymers, as they maintain good 'living' characteristics under inert environments that provide control over their molecular weight and MWD, leading to well-defined structures. The success of the grafting reactions can be quantified with three characteristics: The grafting yield (G_y), defined as the fraction of side chains used in the grafting reaction that become attached to the substrate; the number-average branching functionality (f_n), corresponding to the number of side chains added to the substrate in the grafting reaction; and the coupling efficiency (C_e), defined as the fraction of sites on the substrate that have coupled with side chains. The value of f_n can be determined using Equation 2.4:

$$f_n = \frac{M_n(G) - M_n(G-1)}{M_n^{br}} \tag{2.4}$$

where $M_n(G)$, $M_n(G-1)$, and M_n^{br} are the number-average molecular weight of graft polymers of generation G, of the preceding generation, and of the side chains, respectively. The grafting yield can be estimated by size exclusion chromatography (SEC) analysis using a differential refractometer index (DRI) detector, from the peak areas for the graft polymer and the unreacted side chains according to the following equation:

$$G_y = \frac{\text{Graft Polymer Area}}{\text{Total Peak Area}} \tag{2.5}$$

The grafting yield can be determined from Equation 2.5 as long as the DRI response is identical for both the graft polymer and the unreacted side chains. The coupling efficiency, C_e, is determined by dividing the number of side chains added to the substrate in the grafting reaction (f_n) by the total number of coupling sites available on the substrate. If a 1:1 molar ratio of coupling sites to side chains is used in a grafting reaction then G_y and C_e should be identical, since the coupling site and the side chains react in the same stoichiometry.

The first arborescent polystyrene (PS) structures where synthesized using chloromethyl coupling sites randomly distributed on the phenyl pendants of PS substrates, coupled with 'living' polystyryl anions.[68] Due to the potential for cross-linking in the chloromethylation reaction used to introduce coupling sites on the PS substrates, and the use chloromethyl methyl ether, a potent carcinogen, a different coupling method was subsequently developed by Li and Gauthier, using acetyl coupling sites to produce results comparable to the chloromethyl sites.[69] A comparison of the synthesis of arborescent PS using both coupling methods is provided in Figure 2.24. The 'living' polystyryl anions are capped with a single 1,1-diphenylethylene unit before coupling with the chloromethyl groups (Figure 2.24a), to avoid side reactions of the highly reactive polystyryl anions. A similar

approach was used for the 'living' polystyryl anions that were coupled with the acetyl groups (Figure 2.24b), by capping with a few units of 2-vinylpyridine.[69] When using acetylation levels of 20-30 mol% for linear PS substrates and short side chains (M_n = 5000), grafting yields of up to 95% were reached; however the grafting yield decreased as the generation number increased, due to steric effects (structure crowding) and the inability of the side chains to diffuse to coupling sites located deeper inside the substrate. This effect was compounded when longer PS side chains (M_n = 30,000) were used, and lower grafting yields were observed for each generation as compared to the analogous reactions with short side chains, further confirming that the grafting reaction was diffusion-controlled and that steric hindrance was the main driving force for these lower grafting yields. Despite the decreases in grafting yield observed for the higher generations, arborescent polystyrenes with $M_n >> 10^6$ and narrow MWD ($M_w/M_n < 1.10$) were obtained.

The strategy initially developed for arborescent PS was subsequently modified for the synthesis of different arborescent homopolymers such as arborescent polybutadiene[70,71] and polyisoprene.[72] Arborescent copolymers have also been obtained by the *grafting onto* strategy, and will be discussed in Section 2.4.

The synthesis of Comb-burst® polymers by a divergent *grafting onto* strategy was developed by Tomalia et al. using cationic polymerization techniques, and provided structures similar to the arborescent polymers.[67] While the number of investigations on dendrigraft polymer synthesis by cationic polymerization and grafting is more limited than for anionic polymerization, this technique expands the potential of the *grafting onto* approach to include polymers that are synthesized by cationic polymerization techniques.

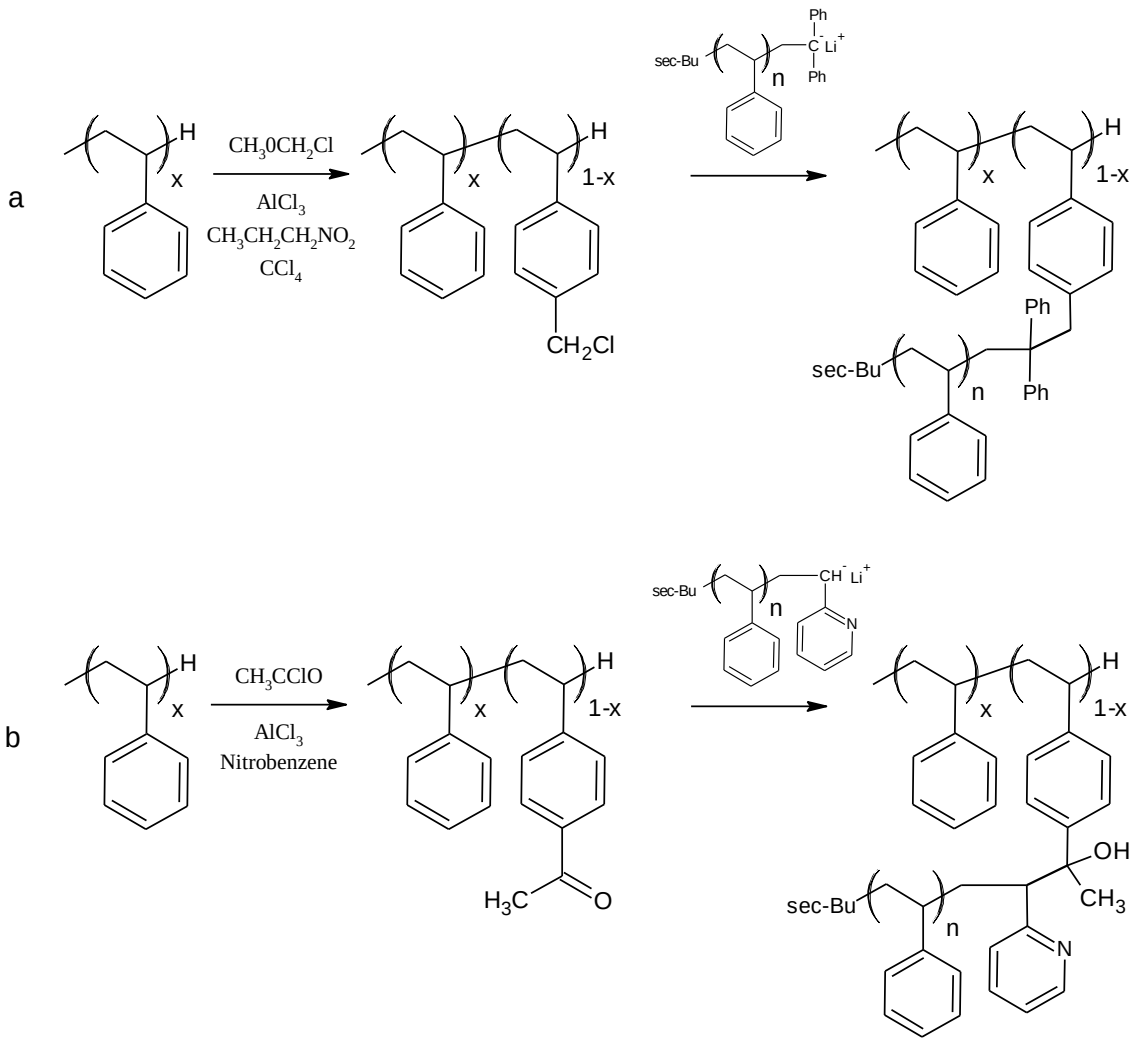

Figure 2.24 Schematic representation of the synthesis of arborescent PS using (a) chloromethyl functionalities and (b) acetyl functionalities on the substrates.

2.3.3.2 Divergent *Grafting From* Strategy

The divergent *grafting from* method typically begins with a linear substrate containing randomly distributed initiating sites, from which polymer chains are grown. This approach has received less attention than the *grafting onto* approach: The dendrigraft polymers obtained are more difficult to characterize, since the uniformity of the polymer chains grown

from the substrates cannot be determined unless cleavable linkages are present that allow the removal and analysis of the side chains.[73] The benefit of using the *grafting from* approach is that the purification is often simpler, since either full monomer conversion is achieved or the removal of unreacted monomer is easier than for unreacted side chains in the *grafting onto* approach.

Two types of branching processes have been used in the *grafting from* approach: terminal branching from the chain ends, or randomly distributed branching points along the substrate. The synthesis of dendrigraft polymers according to a *grafting from* scheme was introduced by Six and Gnanou, who prepared dendritic poly(ethylene oxide) (PEO) starting from a trifunctional core and branching points limited to the ends of the PEO chains grown in the previous generation.[74] The application of the *grafting from* strategy to the synthesis of dendrigraft PEO and other related structures has been reviewed in detail by Teertstra and Gauthier.[73] It is also worth mentioning the work of Klok and co-workers that used terminal branching for the synthesis of dendrigraft poly (L-lysine).[75] In that case the ring-opening polymerization (ROP) of either ε-benzyloxycarbonyl-L-lysine N-carboxyanhydride (Z-Lys NCA) or ε-trifluoroacetyl-L-lysine N-carboxyanhydride (TFA-Lys NCA) was initiated by mono- or bifunctional initiators to produce linear poly(Z-Lys) or poly(TFA-Lys) segments, followed by end functionalization with N^{α},N^{ε}-di(9-fluorenylmethoxycarbonyl)-L-lysine (N^{α},N^{ε}-diFmoc-Lys), which was then selectively deprotected to produce two new primary amine initiating sites. Highly branched poly(L-lysine) of generations up to G2 (4 polymerization cycles), with number-average molecular weights of over 80,000 and polydispersities ranging from 1.2-1.5, were obtained after removal of all the protecting groups.

The *grafting from* strategy using a polymer substrate with randomly distributed initiating sites can be applied by introducing reactive sites either through chemical modification or copolymerization. This strategy produces structures similar to the Comb-burst® and arborescent polymers, due to the random distribution of branching points. Klok and Rodriguez-Hernández thus generated dendritic graft poly(L-lysine) by the ROP of orthogonally protected N^{ε}-(*tert*-butyloxycarbonyl)-L-lysine N-carboxyanhydride (Boc-Lys NCA) and Z-Lys NCA initiated by *n*-hexylamine.[76] Selective deprotection of the randomly distributed N^{ε}-(*tert*-butyloxycarbonyl) protecting groups produced free primary amines capable of initiating a new ROP reaction of Boc-Lys NCA and Z-Lys NCA. After reaching the desired generation number deprotection of all the lysine protecting groups was achieved, to obtain the corresponding dendritic-graft poly(L-lysine). A schematic representation of the synthesis of dendritic-graft poly(L-lysine) is illustrated in Figure 2.25. The G0, G1, and G2 dendrigraft poly(L-lysine) generated had number-average molecular weights of 7000, 23,000, and 29,000, with corresponding polydispersity indices of 1.6, 1.4 and 1.5, respectively.

Previously to the work done by Klok and Rodriguez-Hernández, Dworak and co-workers also synthesized arborescent polyglycidol from 2,3-epoxypropyl-1-ethoxyethyl ether (glycidol acetal).[77] The anionic ring-opening polymerization of glycidol acetal is controlled and produces well-defined linear poly(glycidol acetal). After the polymerization, removal of the acetal protecting groups generated linear polyglycidol, where the free hydroxyl groups on each repeat unit could be deprotonated to initiate the polymerization of glycidol acetal. Arborescent polyglycidol of generations up to G2 (four polymerization cycles) were thus synthesized with number-average molecular weights up to 1.8×10^6 and polydispersities of 1.25-1.43. The limitation in this procedure lies in the uncontrolled number of branching

points produced during the polymerization, since each monomer unit of polyglycidol is potentially capable of initiation. This also produces a large number of alcoholate functionalities in close proximity, leading to poor solubility of the macroinitiator substrates in solvents commonly used for anionic polymerization. Solubilization was improved by deprotonating less than 10% of the hydroxyl groups; however due to fast proton exchange between the alcoholate anions and the free hydroxyl groups, this did not alleviate the issue of the uncontrolled number of branching points.

More recently, a similar approach was used for the synthesis of poly(L-lysine) by Collet et al.[78] The spontaneous aqueous polycondensation reaction of ε-trifluoroacetyl-L-lysine N-carboxyanhydride (TFA-Lys NCA) followed by full deprotection of the ε-trifluoroacetyl group produced low molecular weight linear poly(L-lysine). Further polycondensation could be initiated by the linear poly(L-lysine) substrate to generate a comb-branched poly(L-lysine), and so on. Poly(L-lysine) of generations up to G5 (5 polycondensation cycles), with number-average molecular weights up to 172,000 and polydispersities of 1.4-1.5 were produced by that method.

Other divergent *grafting from* strategies using random branching have been applied to the synthesis of dendrigraft poly(ε-caprolactone) using ROP,[79] and dendrigraft PS using anionic polymerization in a one-pot synthesis with mixed monomer additions.[80]

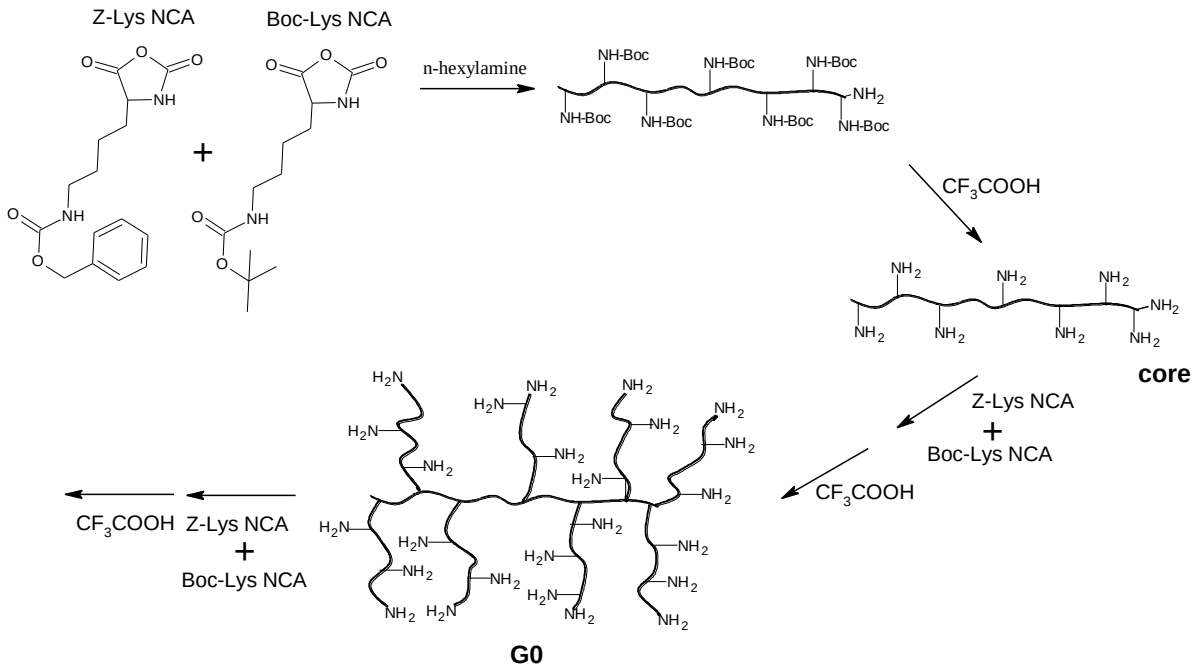

Figure 2.25 Schematic representation of the synthesis of dendrigraft poly(L-lysine) by a *grafting from* strategy.

2.3.3.3 Convergent *Grafting Through* Strategy

The convergent *grafting through* method can be performed as a one-pot reaction and therefore demands less time and resources as compared to the *grafting onto* and *grafting from* strategies. Structures analogous to the dendrigraft polymers are obtained by self-branching condensation reactions of macroanions. This occurs when a bifunctional vinyl monomer (also containing a coupling site) is incorporated into a polymerization reaction, such that the vinyl group participates in the propagation reaction while the second functional group can couple *in situ* with the living macroanions. The divergent grafting through approach was developed by Knauss et al. for the synthesis of dendritic PS, by incorporating either 4-(chlorodimethylsilyl)styrene (CDMSS)[81] or vinylbenzyl chloride (VBC)[82] as bifunctional

monomers also containing coupling sites. A portion of the living polystyryllithium chains can react with the chlorosilyl or chloromethyl sites by nucleophilic substitution, due to their higher reactivity, before propagation takes place via the vinyl group.[83,84] This coupling reaction produces a macromonomer that can react with the remaining living polystyryllithium chains and produce a branched structure. Through the slow addition of coupling agent and styrene, multi-branched macromonomers are generated that can continue to propagate with the living polystyryllithium chains left in the mixture until the point where the macromonomers become too sterically hindered, which limits the attainable molecular weight. A schematic representation of the *grafting through* method using VBC and styrene to synthesize dendrigraft polystyrene is displayed in Figure 2.26. When only the coupling agent is used, highly branched structures similar to star polymers are produced. When styrene and the coupling agent are used simultaneously, the growth and branching density of the molecules is controlled by the ratio of styrene to coupling agent. Knauss et al. varied the molar ratio of CDMSS to styrene and found that as this ratio was lowered (less CDMSS was used), higher molecular weight polymers were obtained. Number-average molecular weights of up to 600,000 and polydispersities of 1.1-1.5 were thus obtained.[81] Attempts to use VBC in the same manner as CDMSS were less successful, as number-average molecular weights of only up to 41,000 and polydispersity indices of 1.2-1.9 were obtained.

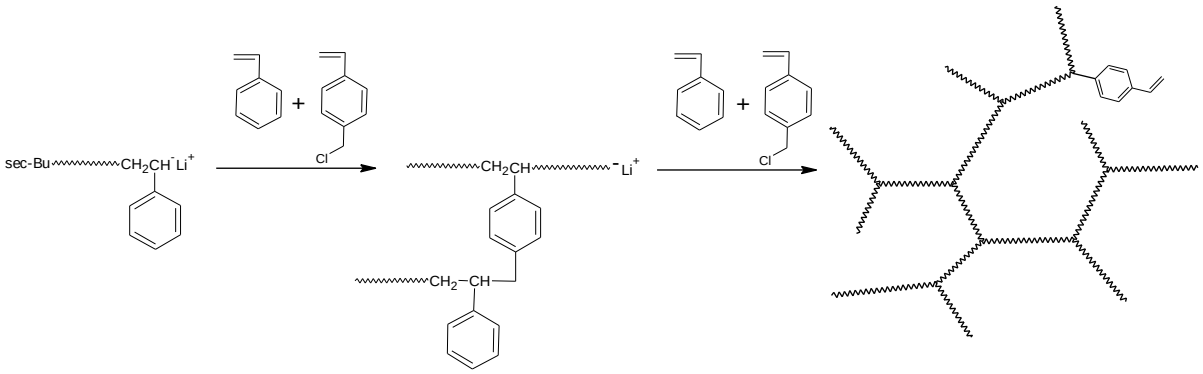

Figure 2.26 One-pot *grafting through* method for the synthesis of dendrigraft polystyrene.

The generation number of the molecules is not as clearly defined in these one-pot reactions as in the divergent syntheses, due to the continuous growth of the branched structures. It was nevertheless suggested that an average generation number (G) could be calculated for these materials using Equation 2.6, where M_G and M_0 correspond to the M_n of the graft polymer and the primary chains (before addition of the coupling agent), respectively, and M_B is the molecular weight of the structural unit derived from the coupling agent. The average generation number (G) of the polymers produced by Knauss et al. as defined by Equation 2.6, when using varying ratios of coupling agent (CDMSS) and styrene, varied between 4.5 and 5.6.[81]

$$G = \frac{\log(M_G) - \log(M_0 - M_B)}{\log 2} \tag{2.6}$$

The convergent *grafting through* method, with continuous monomer and coupling agent additions, is analogous to the hyperbranched polymer syntheses by the *inimer* approach in self-condensing polymerization. The structures obtained by both methods are difficult to characterize, but the polymers can be synthesized with minimal time and resources. The

convergent *grafting through* method produces relatively narrow MWD, but it is limited in terms of the molecular weight range that can be obtained.[81,82]

2.4 Synthesis of Amphiphilic Arborescent Micelles

The synthesis of water-soluble polymeric micelles has attracted considerable attention over the past 20 years as their applications in various areas are promising. The self-assembly of amphiphilic block copolymers is a widely used method to generate water-soluble micelles since their synthesis is relatively simple, and their self-assembly in selective solvents is well-understood.[85-87] Dendritic polymers can also display amphiphilic properties, but with the advantage of having a fully covalent, branched structure that disfavors self-assembly. Consequently, they often behave like unimolecular micelles. The first example of dendritic structure with a potential for micellar behavior was the "arborol" systems of Newkome et al.,[33] whereby a relatively non-polar dendritic core structure was functionalized with a polyol surface making the dendrimer water-soluble, but their unimolecular character was not investigated. Due to their ability to form clear-cut core-shell morphologies, along with other unique features, dendrimers have been extensively studied over the past decade for the purpose of microencapsulation.[12,88,89] Hyperbranched polymers may also be useful as micelles and are much easier to synthesize than dendrimers, but they are typically polydispersed. As well, their one-pot synthesis does not provide the opportunity to generate clear-cut core-shell morphologies, which typically leads to their self-assembly into multimolecular micelles.[90,91]

The synthesis of amphiphilic dendrigraft (arborescent) polymers provides a compromise between the nearly structurally perfect dendrimers obtained by tedious synthetic

methods and the polydispersed, structurally imperfect hyperbranched polymers derived from simple one-pot syntheses. Arborescent polymers synthesized by variations of the *grafting onto* approach originally developed by Gauthier and Möller[68] can generate well-defined ($M_w/M_n < 1.1$) branched structures with high molecular weights ($M_n >> 10^6$) in only a few reaction cycles. The generation-based *grafting onto* synthetic strategy depicted in Figure 2.23 can be easily adapted to generate amphiphilic copolymer structures, by using side chains with a different composition in the last grafting cycle, i.e. a hydrophilic polymer. The following sections will provide an overview of various types of amphiphilic arborescent micelles synthesized to date, using either the divergent *grafting onto* or divergent *grafting from* methodologies.

2.4.1 Arborescent Polystyrene-*graft*-Poly(2-Vinylpyridine)

The synthesis of arborescent polystyrene-*graft*-poly(2-vinylpyridine) (PS-*g*-P2VP) was achieved by the same *grafting onto* technique developed for the synthesis of arborescent PS, using either randomly distributed chloromethyl[92] or acetyl[93] coupling sites (Figure 2.24). In this case however, either short ($M_w \approx 5000$) or long ($M_w \approx 30{,}000$) living poly(2-vinylpyridinyl)lithium side chains were grafted instead of polystyryllithium in the last reaction cycle. Linear PS, and arborescent G0, G1, and G2 PS were used as substrates and led to grafting yields ranging from 26-95%, lower grafting yields being obtained when using longer poly(2-vinylpyridine) (P2VP) side chains or for larger PS substrates. The variations in grafting yields observed for arborescent copolymers were consistent with those observed for the homopolymers, as they likewise primarily depend on the accessibility of the coupling sites. When using acetyl coupling sites, weight-average molecular weights reaching up to 2.5

$\times 10^7$ and 6.1×10^7 were achieved when using short and long P2VP side chains, respectively, while maintaining narrow molecular weight distributions ($M_w/M_n \leq 1.08$).

The arborescent PS-*g*-P2VP systems are the most thoroughly investigated amphiphilic arborescent copolymers to date and have yielded interesting information about their unique characteristics. Upon ionization of the P2VP side chains, arborescent PS-*g*-P2VP can form unimolecular micelles in aqueous media, as determined from dynamic light scattering (DLS) measurements.[92,93] Furthermore, the dissolution protocol used to generate the micelles was found to affect their overall size and size distribution: Direct dissolution of the copolymers into aqueous HCl produced slightly larger hydrodynamic diameters (due to a minor amount of aggregation) as compared to dissolution in THF followed by dilution with aqueous HCl.[93] In view of the minor differences found, both protocols were nevertheless considered to yield unimolecular micelles as the dominant species in solution.

To further understand the solution behavior of arborescent copolymers, small-angle neutron scattering (SANS) measurements were used to characterize the morphology of arborescent PS-*g*-P2VP copolymers with short P2VP side chains in deuterated methanol (CD_3OD).[94] The results indicated that the PS cores were not in a fully collapsed state, presumably due to a relatively diffuse interface between the PS core and the P2VP shell resulting from the random distribution of coupling sites on the PS substrates. It was also determined that as the size of the arborescent copolymers increased, so did the overall density, which is opposite to the behavior normally observed for coiled linear polymer chains. The arborescent copolymers behaved increasingly like hard spheres as their size increased. Similar trends were observed in SANS experiments with arborescent polystyrene-

graft-deuterated polystyrene, when attaching short ($M_w \approx 5000$) deuterated PS (PS-*d*) chains to form a shell onto G2 and G3 arborescent PS cores.[95] It was also observed that the core-shell morphology was better defined for the higher generation G3PS-*graft*-PS-*d* copolymer than for the lower generation G2PS-*graft*-PS-*d* sample, due to the denser G3 core not allowing the PS-*d* shell chains to diffuse to the coupling sites located deeper into the core in the grafting reaction.

Arborescent PS-*g*-P2VP copolymers with different structures were investigated as unimolecular micelles, to determine their solubilization capacities and kinetics for various polycyclic aromatic hydrocarbon (PAH) hydrophobic probes in aqueous solutions by ultraviolet (UV) and fluorescence spectroscopies.[13] The solubilization capacity and rate of the probes were found to depend on both the micelle structure and the nature of the probes used. Thus for 1-pyrenemethanol, the solubilization capacity of the copolymers increased with the PS content as well as the overall molecular weight (generation number) of the copolymers. However the *rate* of 1-pyrenemethanol solubilization decreased as the PS content and the overall molecular weight (generation number) for the copolymers increased. It was suggested, in agreement with previous studies on block copolymer micelles, that three regions exist in the PS-*g*-P2VP micelles in which the PAH probes could be located, namely the hydrophobic core, the hydrophilic shell, and the interfacial region between the core and the shell. Depending on the hydrophobicity of the probes, they could be located in one or more of these regions.

The kinetics of release from arborescent PS-*g*-P2VP copolymers in dilute HCl solutions were also examined for model drugs using fluorescence and UV spectroscopies.[14] Several important characteristics of arborescent PS-*g*-P2VP were revealed in this study,

when using indomethacin and lidocaine in the *in vitro* release studies, but most importantly that these unimolecular micelles displayed sustained release characteristics due mainly to a diffusion-controlled release mechanism.

2.4.2 Arborescent Polystyrene-*graft*-Poly(Ethylene Oxide)

Arborescent polystyrene-*graft*-poly(ethylene oxide) PS-*g*-PEO copolymers were synthesized by a divergent *grafting from* strategy, through the polymerization of ethylene oxide (EO) in a chain extension reaction from hydroxyl groups located at the chain ends of arborescent PS substrates.[96] A schematic representation of the synthesis of a G1PS-*g*-PEO arborescent copolymer is provided in Figure 2.27 as an example. A generation 0 arborescent PS (G0PS) substrate was synthesized by the same anionic grafting technique shown in Figure 2.24a, but subsequently functionalized and coupled with polystyryllithium anions that were obtained by initiation with (6-lithiohexyl)acetaldehyde acetal (LHAA), to yield a generation 1 arborescent PS (G1PS) with acetal chain ends on the outside of the molecule. Cleavage of the acetal protecting groups at the chain ends through hydrolysis yielded a hydroxyl-functionalized G1PS core, which was deprotonated with potassium naphthalide (KNaph) to initiate the polymerization of EO. The "thickness" of the hydrophilic layer was controlled by the amount of EO added during the shell growth process in these reactions. Arborescent G1PS-g-PEO copolymers containing 19 and 66% of PEO by weight were thus synthesized with polydispersity indices of 1.21 and 1.07, respectively. An arborescent G4PS-g-PEO copolymer containing 36% of PEO by weight was also obtained.

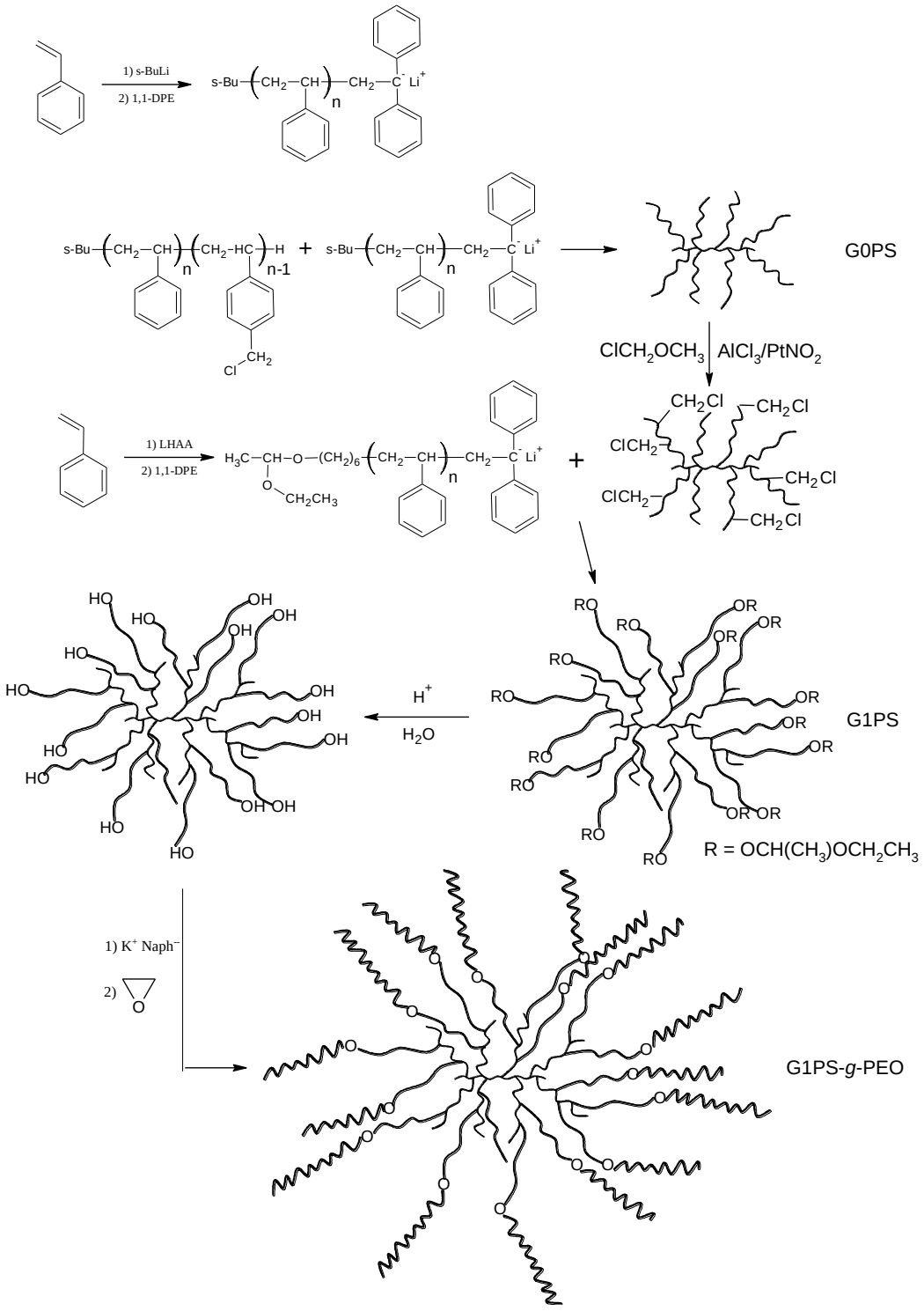

Figure 2.27 Synthesis of arborescent PS-*g*-PEO copolymers by a divergent *grafting from* method.

The weight fraction of PEO in the arborescent PS-*g*-PEO copolymers synthesized by the *grafting from* strategy was significantly lower than the weight fraction of P2VP (> 80%) in the arborescent PS-*g*-P2VP copolymers obtained by the *grafting onto* approach. Due to their significantly lower weight fraction of hydrophilic shell component, the arborescent PS-*g*-PEO copolymers would be expected to display significantly different solubility characteristics from their P2VP counterparts. Dispersion of the samples in water by sonication led to turbid solutions for both the G1PS-*g*-PEO and G4PS-*g*-PEO samples. However when these samples were first dissolved in THF and then added drop-wise to water, both G1PS-*g*-PEO samples produced transparent solutions while the G4PS-*g*-PEO sample still produced a slightly opalescent solution. Since DLS measurements were not performed on the PS-*g*-PEO samples in water, it is unfortunately not clear whether aggregation was present under these conditions. These results nevertheless suggest that the weight fraction of the hydrophilic component is not the only factor influencing micelle stability: The degree of definition of the core-shell morphology must also be considered. For the arborescent PS-*g*-PEO copolymers, the PEO chain segments were grown near the periphery (from the chain ends) of the arborescent PS core, which is expected to enhance core-shell phase separation due to the greater mobility of the shell segments. Enhanced phase separation was recently confirmed in SANS contrast matching experiments for a G1PS-*g-deuterated*-PEO sample.[97] The interfacial region is therefore expected to be much thinner for these systems relatively to the arborescent PS-*g*-P2VP copolymers, where the P2VP chain segments are randomly grafted on the PS substrates. A better-defined core-shell morphology may allow the hydrophilic shell to shield the core from intermolecular hydrophobic interactions more

efficiently, leading to unimolecular micellar behavior even for arborescent copolymers with lower hydrophilic shell weight fractions.

2.4.3 Arborescent Polystyrene-*graft*-Poly(*tert*-Butyl Methacrylate)

The synthesis of arborescent polystyrene-*graft*-poly(*tert*-butyl methacrylate) (PS-*g*-PtBMA) was achieved by a *grafting onto* technique similar to the one used for the synthesis of arborescent PS from chloromethyl sites, but using bromomethylated PS substrates to couple with 'living' poly(*tert*-butyl methacrylate) (PtBMA) anions.[98] The synthesis of arborescent PS-*g*-PtBMA copolymers is illustrated in Figure 2.28. Copolymers with either short ($M_w \approx$ 5,000) or long ($M_w \approx$ 30,000) PtBMA side chains were prepared by grafting onto linear, G0, G1, and G2 bromomethylated arborescent polystyrenes. Weight-average molecular weights ranging from 8.8×10^4 to 6.3×10^7 were obtained for the copolymers, with relatively low apparent polydispersity indices ($M_w/M_n \approx$ 1.14-1.25). A reaction using a chloromethylated G0PS substrate and short PtBMA chains was initially attempted and led to a disappointing 45% grafting yield. Since 'living' PtBMA macroanions are not as reactive as 'living' P2VP, the chloromethyl sites were replaced with more reactive bromomethyl groups on the PS substrates to achieve a grafting yield of 67%. The grafting yield was also affected by the molecular weight of the PtBMA side chain, in analogy to the other systems discussed previously. A 25-200% excess of PtBMA side chains was ultimately used in the grafting reactions with respect to the bromomethyl groups, depending on the substrate generation number and the length of the side chains used. An excess of side chains ultimately led to lower grafting yields, due to the large excess of side chains present in the reactions, but maximized the number of PtBMA side chains grafted onto the substrate.

To obtain amphiphilic arborescent structures, the PS-*g*-PtBMA copolymers were treated with trimethylsilyl iodide and HCl to cleave the *tert*-butyl ester group and produce arborescent polystyrene-*graft*-poly(methacrylic acid) (PS-*g*-PMAA) copolymers. Measurements were performed with DLS for the copolymers in 95:5 methanol:water mixtures containing 0.05 N NaCl, as well as a 95:5 methanol:water mixtures containing 0.01 N NaOH and 0.05 N NaCl, to investigate the increase in hydrodynamic radius of the molecules upon ionization of the side chains. The copolymers derived from G0PS and G1PS cores produced clear solutions, while those containing the G2PS core produced opalescent solutions. Upon ionization using NaOH enhanced molecular expansion was observed for the arborescent systems, due to the polyelectrolyte effect, in comparison to linear PMAA samples with comparable hydrodynamic radii in the non-ionized state. These results demonstrated that the arborescent PS-*g*-PMAA copolymers behaved similarly to the P2VP copolymers upon ionization the PMAA side chains, to produce water-soluble unimolecular micelles.

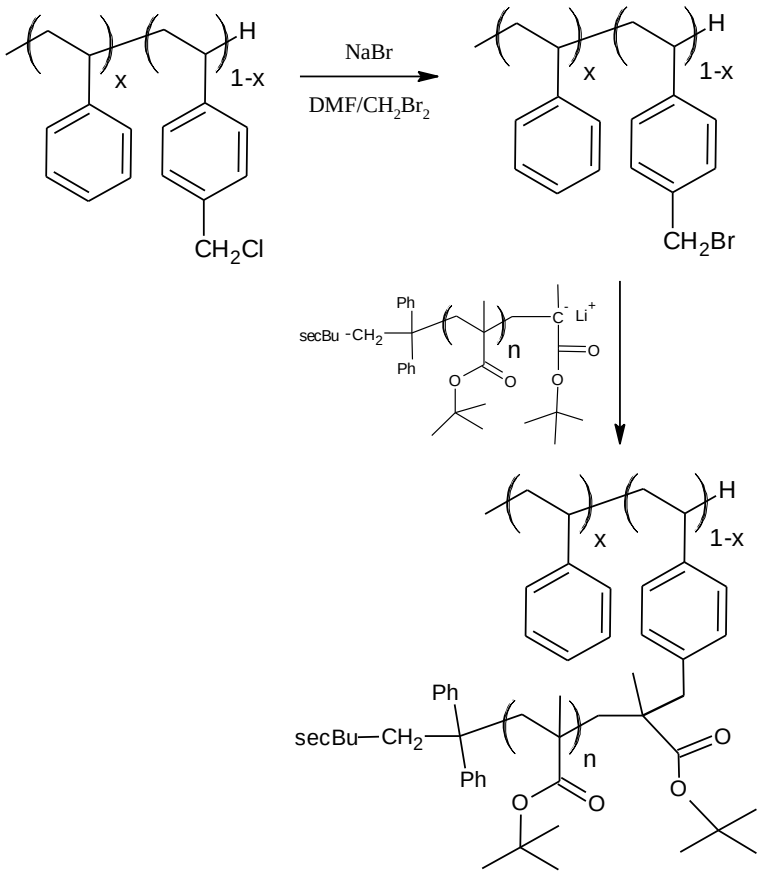

Figure 2.28 Synthesis of arborescent PS-*g*-PtBMA copolymers by a divergent *grafting onto* method.

2.5 Concluding Remarks

The synthesis of linear polypeptides has steadily improved over the past 50 years, with the development and perfection of solid phase peptide synthesis (SPPS), as well as the ring-opening polymerization (ROP) of α-amino acid N-carboxyanhydrides (NCA). Today these techniques both provide relatively simple methods to produce polypeptides with predictable structures and functions, which have potential for a variety of biomedical applications.[99] A wide range of natural α-amino acids can be used in either the SPPS or ROP methods. Copolypeptides with controlled characteristics in terms of sequence and composition and

narrow MWD can now also be prepared even through the ROP of NCA. The use of polypeptides in self-assembly and higher order structures is an expanding research field further increasing the number of potential applications of synthetic polypeptides.[100,101]

The synthesis of dendritic polymers reviewed here likewise provides evidence of a rapidly growing field for a class of branched polymers with unique properties. The three sub-classes of dendritic polymers (dendrimers, hyperbranched polymers, and dendrigraft polymers) can be obtained by various synthetic pathways providing polymers with tailored properties. Dendrigraft polymers represent a compromise between monodispersed dendrimers, requiring exhaustive synthetic work, and highly polydispersed hyperbranched polymers generated from one-pot reactions. Dendrigraft (arborescent) polymers, obtained by a generation-based synthetic scheme analogous to dendrimers, have well-defined structures ($M_w/M_n < 1.1$) and high molecular weights ($M_n >> 10^6$) obtained in a few grafting cycles.

Amphiphilic arborescent copolymers have proven to be useful as water-soluble unimolecular micelles. The solution properties of arborescent PS-*g*-P2VP copolymers have been most thoroughly investigated, and it was demonstrated that arborescent copolymers can be tailored for specific requirements by adjusting their composition, branching functionality, and the overall size (generation number). The synthesis of arborescent polymers and copolymers based on polypeptides would provide new structures with high potential for biomedical applications, and more specifically as sustained-release drug delivery systems.

Chapter 3

Arborescent Polypeptides from γ-Benzyl L-Glutamic Acid

3.1 Overview

The synthesis of arborescent polymers with poly(γ-benzyl L-glutamate) (PBG) side chains was achieved through successive grafting reactions. The linear PBG building blocks were produced by the ring-opening polymerization of γ-benzyl L-glutamic acid N-carboxyanhydride initiated with *n*-hexylamine. It was necessary to optimize the polymerization conditions to minimize the loss of amino chain termini in the reaction. Cleavage of a fraction of the benzyl groups on a linear PBG substrate and coupling with linear PBG using a carbodiimide promoter yielded a comb-branched or generation zero (G0) arborescent PBG. Further partial deprotection and grafting cycles led to arborescent PBG of generations G1–G3. The solvent used in the coupling reaction had a dramatic influence on the yield of graft polymers of generations G1 and above, dimethylsulfoxide being preferable to N,N-dimethylformamide. The *grafting onto* scheme yielded well-defined ($M_w/M_n \leq 1.06$), high molecular weight arborescent PBG in a few reaction cycles, with number-average molecular weights and branching functionalities reaching over 10^6 and 290, respectively, for the G3 polymer. α-Helix to coiled conformation transitions were observed from N,N-dimethylformamide to dimethylsulfoxide solutions even for the branched polymers.

3.2 Introduction

Dendritic polymers have attracted much attention due to their intriguing structure and unusual properties. Many methods have been suggested to synthesize different families of dendritic macromolecules including dendrimers, hyperbranched polymers, and dendrigraft (arborescent) polymers from a wide range of monomers.[1-5] This allows tailoring of the properties of these materials to optimize their performance in different applications, of which

the biomedical field certainly represents a major area of interest.[6-8] A primary concern for most biomedical applications is biocompatibility, typically requiring a lack of toxicity, immunological response, or other physiological reactions.

The earliest examples of dendritic structures reported included dendrimers derived from L-lysine building blocks, analogous to globular polypeptides.[9-11] The concept of dendrimers with amide-like structures was considerably expanded by Tomalia, who reported the synthesis of polyamidoamine (PAMAM) dendrimers, now commercially available and being investigated in a number of biomedical applications.[8] Other examples of potentially biocompatible dendrimers reported in the literature include triazine (melamine) dendrimers,[12] oligosaccharide–polypeptide dendrimers,[13] glycodendrimers,[14] and PAMAM–poly(L-glutamic acid) dendrimers.[15] Hyperbranched dendritic systems in that category have also been reported including hyperbranched polyglycerols,[16] polyesters,[17] and polylysines.[18] The number of examples of possibly biocompatible dendrigraft polymers, and particularly those with peptide-like structures, nevertheless remains limited.

A distinct characteristic of dendrigraft polymers is the attainment of large (10–100 nm) molecular dimensions in a few synthetic cycles (generations), while maintaining low polydispersity indices (PDI = M_w/M_n ~ 1.1 typically).[19] A convenient *grafting from* technique was reported by Klok et al. using L-lysine derivatives to synthesize dendrigraft polypeptides.[18] This synthetic scheme involved the polymerization of protected L-lysine N-carboxyanhydride (NCA) to produce a linear substrate that was subsequently deprotected to generate primary amine moieties serving as initiating sites for the next generation of side chains. The method of Klok et al. yielded large (up to generation G2) dendrigraft structures, but suffered from significant molecular weight distribution (MWD) broadening over

successive cycles due to side reactions. A variation of the same technique used the copolymerization of a protected L-lysine NCA with another amino acid NCA.[18,20] Selective deprotection of the L-lysine units provided control over the branching density of the molecules in this scheme, but the MWD broadening issue remained unsolved. The *grafting from* technique developed by Klok was subsequently modified recently by Collet et al., using trifluoroacetyl-protected L-lysine NCA.[21] In this case the polymerization was carried out in mildly acidic (pH 6.5) water and the polypeptide was deprotected with ammonia, to afford short linear poly(L-lysine trifluoroacetate) segments with a number-average degree of polymerization X_n = 8. The fully deprotected linear substrate served as a polyfunctional initiator for the growth of protected poly(L-lysine) side chains, in analogy to the Klok procedure. Subsequent cycles of deprotection and side chain growth led to dendrigraft polymer structures of generations up to G3, with $M_n \leq 1.72\times10^5$ and M_w/M_n values of 1.36–1.46.

Beyond dendritic architectures, it should be pointed out that other techniques have yielded star-branched polypeptides of low branching functionalities (f = 3) having a high molecular weight and narrow MWDs. Thus Aliferis et al. obtained 3-arm star-block copolypeptides with molecular weights up to 1.8 x 10^5 and M_w/M_n = 1.08.[22] This was done using amine-initiated polypeptides of γ-benzyl L-glutamate-NCA and ε-benzyloxycarbonyl L-lysine NCA. These homopolypeptides and block copolypeptides were coupled using a triphenylmethane-4,4',4''-triisocyante linker.

We now report on the synthesis of well-defined (M_w/M_n < 1.1) arborescent polymers from poly(γ-benzyl L-glutamate) (PBG) building blocks. The approach used is a *grafting*

onto scheme analogous to those reported previously for the synthesis of arborescent polymers from different vinyl monomers.[1,19] This method is distinct from the ones described above for protected L-lysine NCA, in that side chains synthesized in a separate reaction are *grafted onto* the substrate. This enables full structural characterization of the branched polymers (side chain and overall molecular weight, branching functionality), while maintaining a narrow molecular weight distribution over successive grafting cycles. The approach proposed for the preparation of arborescent polypeptides is summarized in Figure 3.1. Linear PBG chains are obtained by ring-opening polymerization of γ-benzyl L-glutamic acid N-carboxyanhydride (Glu-NCA) with a primary amine initiator. Partial deprotection of the linear PBG provides a grafting substrate with carboxylic acid moieties, that can be coupled with the primary amine terminus of PBG by standard peptide coupling techniques to create a generation zero (G0) or comb-branched polypeptide. Subsequent generations of arborescent polypeptides are obtained by successive cycles of partial deprotection and grafting reactions. The PBG arborescent polypeptides obtained are interesting as model compounds for globular proteins, and can serve as intermediates in the preparation of unimolecular micelles potentially useful for controlled drug delivery applications.

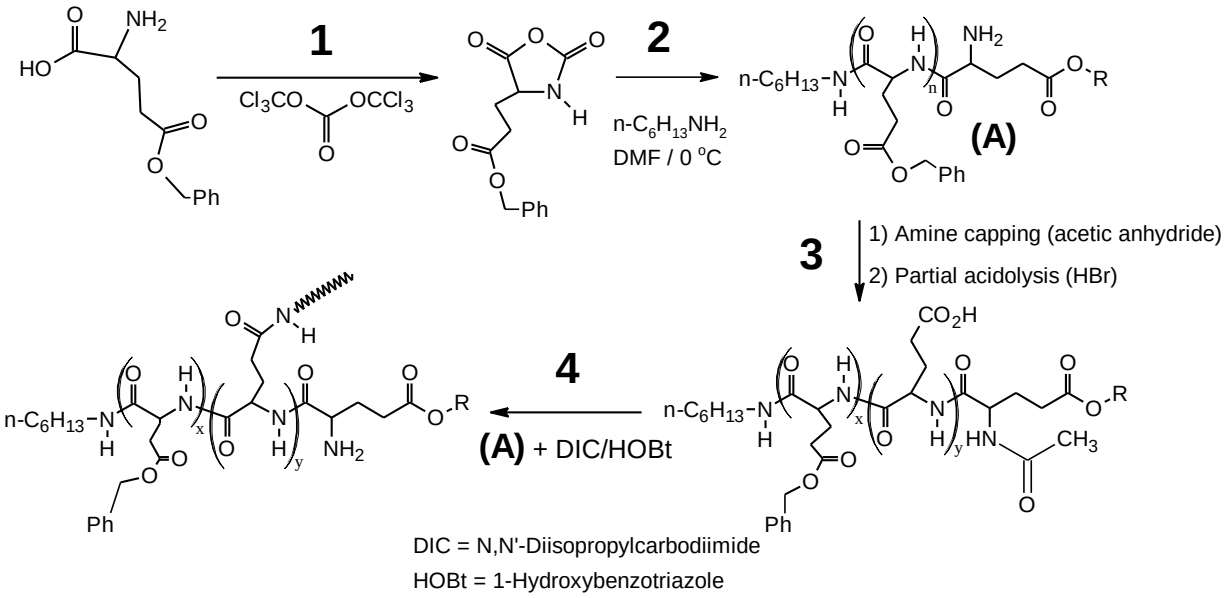

Figure 3.1 Synthesis of G0 arborescent PBG with a comb-branched structure. G1–G3 dendritic structures are obtained by repetition of the partial acidolysis and grafting steps.

3.3 Experimental Procedures

3.3.1 Characterization and Sample Preparation

Analytical SEC measurements were done on a system consisting of a Waters 510 HPLC pump, a 50 μL injection loop, and a Waters 2410 differential refractometer (DRI) detector. A Wyatt MiniDAWN laser light scattering detector operating at a wavelength of 690 nm served to determine the absolute molecular weight of the graft polymers. The column used was a 500 mm × 10 mm Jordi Gel DVB Mixed Bed model with a linear polystyrene molecular weight range of 10^2–10^7. N,N-Dimethylacetamide (DMA) with LiCl (1 g/L, added to minimize adsorption of the polymer on the column) at a flow rate of 1.0 mL/min served as the mobile phase at room temperature.

Preparative SEC was carried out on a system consisting of a Waters M45 HPLC pump, a 2-mL sample injection loop, a Waters R401 differential refractometer detector, and a Jordi Gel DVB 1000 Å 250 mm × 22 mm preparative SEC column. N,N-Dimethylacetamide with 0.2 g/L LiCl served as the mobile phase. The crude polymer was injected as a 30 mg/mL solution and the SEC system was operated at room temperature at a flow rate of 3.0 mL/min.

^{1}H NMR spectroscopy served to determine the degree of polymerization of the linear polymers, to monitor the deprotection level of the substrates, and to analyze the conformation of the polypeptide chains. The instruments used were Bruker 300 MHz and 500 MHz spectrometers. The 500 MHz instrument was employed only in conformation analysis. The concentration of all the samples was 20 mg/mL and 16 scans were averaged on both instruments.

Titrations were performed for selected linear and arborescent partially deprotected substrates to confirm the deprotection levels determined from ^{1}H NMR analysis. The substrate (50 mg) was added to a mixture of DMF (10 mL) and water (5 mL) with 3 drops of phenolphthalein indicator (0.5% w/v in methanol). The solution was quickly titrated to a pink coloration (stable over 30 s) with a 0.1 N NaOH solution in methanol, to minimize interference from atmospheric CO_2.

Matrix-assisted laser desorption ionization time of flight (MALDI–TOF) mass spectrometry was used to investigate side reactions in the ring-opening polymerization of Glu-NCA and to optimize the polymerization conditions. The MALDI–TOF measurements were performed on a Bruker Reflex III instrument equipped with a 337 nm nitrogen laser.

Positive ion spectra from 1000–10000 m/z were acquired in the linear mode with a 20 kV acceleration voltage. Aliquots of the sample solution and a saturated solution of sinapinic acid matrix in 1:1 H_2O/ACN with 0.1 % TFA (4 μl each) were mixed and air-dried on a stainless steel MALDI plate. The instrument was externally calibrated with adrenocorticotropic hormone fragment 18–39 (Sigma) and equine Cytochrome C (Sigma). The samples were spotted in duplicate, 100 scans were accumulated and then processed manually using the XTOF software (Bruker).

Dynamic light scattering (DLS) measurements were carried out to determine the hydrodynamic diameter of the arborescent PBG molecules in DMF and in DMSO. The concentration of the samples ranged from 0.5–2% w/v (depending on the generation number) and LiCl (0.05% w/v) was added to prevent aggregation. The measurements were done on a Brookhaven BI-200 SM instrument at a temperature of 25 ºC and a scattering angle of 90º. The 256-channel correlator was operated in the exponential sampling mode, the last 4 data acquisition channels being used for the baseline measurements. The translational diffusion coefficients used for the hydrodynamic diameter calculations were determined from first- and second-order analysis of the normalized electric field correlation function.

3.3.2 Solvent and Reagent Purification

N,N'-Dimethylformamide (DMF; Aldrich, peptide synthesis grade) was purified by distillation under reduced pressure and was stored in the dark to prevent degradation due to photochemical reactions. Dimethylsulfoxide and *n*-hexylamine were purified by stirring overnight with CaH_2 and distillation under reduced pressure. The DMF, DMSO, and *n*-hexylamine were stored under nitrogen in round-bottomed flasks (RBF) over 3 Å molecular

sieves (EMD). Ethyl acetate (Fisher, 99.9%) was distilled from $LiAlH_4$ under nitrogen. The purified compounds were stored in round-bottomed flasks over 3A molecular sieves (EMD). γ-Benzyl L-glutamic acid (Bz-Glu; Bachem, >99%), HBr solution (Aldrich, 33% in acetic acid), N,N'-diisopropylcarbodiimide (DIC; Aldrich, 99%), 1-hydroxybenzotriazole (HOBt; Fluka, water content ca. 15% w/w), trifluroroacetic acid (TFA, Caledon), methanol (Omnisolv), diethyl ether (Omnisolv), triethylamine (TEA, EMD), acetic anhydride (Caledon), tetrahydrofuran (THF, Omnisolv), triphosgene (Aldrich, 98%), and $LiAlH_4$ (Aldrich, 95%), deuterated DMF (d_7-DMF, Cambridge isotopes, D, 99.9%), and deuterated DMSO (d_6-DMSO, Cambridge isotopes, D, 99.9%) were used as received from the suppliers.

3.3.3 Synthesis of γ-Benzyl L-Glutamic Acid N-Carboxyanhydride (Glu-NCA)

The procedure used was adapted from the method of Poché et al.[23] Bz-Glu (10.0 g; 42.0 mmol) was suspended in 300 mL of dry ethyl acetate in a 1-L round-bottomed flask fitted with a refluxing condenser and a gas bubbler. The flask was purged with N_2 and heated to reflux. Triphosgene (4.8 g, 16 mmol) was then added and refluxing was continued for 3 h. **Caution:** Triphosgene is highly toxic, so the whole procedure should be carried out in a well-vented fume hood. The flask was then removed, stoppered, and cooled in a freezer (–10 °C) for 1 h. The solution was transferred to a cold separatory funnel and quickly washed successively with 100 mL of ice-cold water and 100 mL of chilled 0.5% aqueous $NaHCO_3$ solution. The organic phase was dried over anhydrous $MgSO_4$, filtered, and concentrated to 100–120 mL on a rotary evaporator. An equal volume of cold hexane was then added to induce crystallization of the product. The mixture was left in the freezer overnight and the solid product was recovered by filtration in a Schlenk funnel under N_2. It was then dried

overnight under vacuum, and stored under N_2 in a refrigerator (4 °C). Yield = 10.2 g (92 %); ^{1}H NMR (300 MHz, $CDCl_3$): 7.58–7.24 (s, 5H), 6.75 (s, 1H), 5.11 (s, 2H), 4.38–4.33 (t, 1H), 2.59–2.53 (t, 2H), 2.35–2.21 (m, 1H), 2.21–2.02 (m, 1H).

3.3.4 Synthesis of Poly(γ-benzyl L-glutamate)

A linear polymer serving as side chain material (sample PBG-41) was synthesized by dissolving Glu-NCA (8.00 g, 30.4 mmol) in dry DMF (20 mL) in a 50-mL round-bottomed flask at 0 °C. After the monomer was dissolved *n*-hexylamine (200 μL, 1.52 mmol, for a target X_n = 20) was added with rapid stirring. The evolution of CO_2 was noticeable at the beginning, and the reaction was allowed to proceed for 2.5–3 d at 0 °C. The linear polymer was recovered by precipitation in methanol and suction filtration, and dried under vacuum overnight. Yield = 80%, M_w/M_n = 1.10. ^{1}H NMR (300 MHz, d_6-DMSO): X_n = 26.0, δ: 8.04 (b, 26H), 7.48–7.20 (s, 130H), 5.02–4.89 (s, 52H), 4.10–3.88 (b, 26H), 2.34–1.91 (b, 104H), 1.33–1.18 (b, 10H), 0.78–0.76 (s, 3H).

3.3.5 Synthesis of PBG Precursor for Grafting Substrate

A linear PBG sample (PBG-34) serving as substrate for the preparation of a G0 (comb-branched) polypeptide was synthesized as described above with minor modifications: The target X_n was 50, the reaction was performed at room temperature, and it was quenched with acetic anhydride to deactivate the terminal amine moiety.

The PBG sample was synthesized from Glu-NCA (2.0 g, 7.6 mmol) in 5.0 mL of DMF and *n*-hexylamine (20 μL, 0.15 mmol) at room temperature. After 4 h acetic anhydride (290 μL, 3.1 mmol) was added and the reaction was stirred for 1 h before sample recovery.

Yield = 1.5 g (90%), ^{1}H NMR (300 MHz, d_6-DMSO): X_n = 51.0, δ: 8.04 (b, 51H), 7.48–7.20 (s, 255H), 5.02–4.89 (s, 102H), 4.10–3.88 (b, 51H), 2.34–1.91 (b, 204H), 1.33–1.18 (b, 10H), 0.78–0.76 (s, 3H), SEC: M_w/M_n = 1.19.

3.3.6 Partial Deprotection of Linear PBG Substrate

PBG-34 (X_n = 51, 1.46 g, 6.66 mmol Bz-Glu units) was dissolved in TFA (15 mL) and 0.35 mL of 33% (w/w) HBr solution in acetic acid (0.14 g HBr, 0.25 equiv HBr per Bz-Glu residue) was added with stirring. After 3 h the polymer was precipitated in diethyl ether and recovered by suction filtration to give an orange solid. After drying the polymer was dispersed in 10–12 mL of THF and enough DMF (ca. 1–2 mL) was added to obtain a clear solution. The polymer was precipitated again in diethyl ether to yield a white product. Yield = 0.92 g (72%), 31 mol% of free glutamic acid moieties.

3.3.7 Synthesis of G0 Arborescent PBG

The partially deprotected polymer serving as substrate [PBG-34-CO_2H, 0.141 g, 0.220 mmol –CO_2H] and the polymer serving as side chains [PBG-64, 1.10 g, 0.275 mmol chains] were dissolved in 6 mL of dry DMF in a 25-mL round-bottomed flask. The peptide coupling reagents DIC (1.72 mL of 10% v/v solution in DMF, 1.10 mmol) and HOBt (0.149 g, 1.10 mmol) were then added to the reaction with TEA (0.8 mL, 5.5 mmol). The reaction was allowed to proceed for 24 h at room temperature before adding *n*-hexylamine (0.50 mL, 4.94 mmol) to deactivate residual carboxylic acid sites. After 1 h the product was precipitated in methanol and recovered by suction filtration. Linear PBG contaminant was removed from the G0 crude polymer by preparative size exclusion chromatography (SEC). The purified G0

polymer was recovered by evaporation to dryness under high vacuum, dissolution in TFA, and precipitation in methanol.

3.3.8 Synthesis of Upper Generation (G1–G3) Arborescent PBG

The purified G0 polymer (G0-52, 0.400 g, 1.82 mmol Bz-Glu units) was first partially deprotected by dissolution in TFA (4 mL), and 0.13 mL of 33% (w/w) HBr solution in acetic acid (0.044 g HBr, 0.30 equiv HBr per Bz-Glu residue) was added with stirring. After 3 h the polymer was recovered and further purified as described for the linear sample. Yield = 0.240 g, (68%), 32 mol% glutamic acid moieties. The deprotected G0 polymer (G0-52-CO_2H, 0.212 g, 0.356 mmol –CO_2H) was coupled with linear side chains [PBG-64, 1.90 g, 0.445 mmol chains] by the same method described for the G0 reaction, but using DMSO (8 mL) rather than DMF as solvent. The crude G1 polypeptide was purified by preparative size exclusion chromatography (SEC) as described for the G0 polymer. The G2 and G3 arborescent PBG samples were synthesized and purified as described for the G1 sample.

3.4 Results and Discussion

3.4.1 Synthesis of Linear PBG

Several methods reported in the literature for the synthesis of PBG have led to different results in terms of yield and their ability to minimize side reactions. Ideally the PBG building blocks serving in the synthesis of arborescent polypeptides should be obtained in high yield, have a narrow MWD and a predictable X_n, and preserve their primary amine group at the chain end. Beyond the influence of monomer purity and the activated monomer polymerization mechanism (Figure 3.2), cyclization of the amino terminus into a lactam

structure (Figure 3.3) during storage is the dominant side reaction known to affect PBG chains.[24] The activated monomer polymerization mechanism is a well-known problem in the polymerization of NCA monomers.[25] The monomer activated via proton abstraction by the initiator (Figure 3.2, Path 1) can subsequently initiate chain growth. Propagation of the activated monomer-initiated chain can proceed by ring opening of NCA monomers. One issue with the activated monomer mechanism is that since the amine is not consumed in the initiation reaction, the additional polypeptide chains produced by that mechanism may lead to a degree of polymerization lower than expected. Another potential side reaction related to the activated monomer mechanism is due to the fact that the chain derived from the activated monomer still contains a cyclic anhydride moiety, which is susceptible to attack by other nucleophiles. Attack of the cyclic anhydride moiety by the initiator (*n*-hexylamine in this case) has no net effect beyond compensating for the under-consumption of initiator. If the attack involves another polypeptide chain, however, dimerization will take place through amide bond formation as shown in Figure 3.3. These side reactions therefore mainly lead to broadening of the molecular weight distribution, but have little influence on the reactivity of the amine chain end. The normal amine-initiated polymerization mechanism (Figure 3.2, Path 2) is typically the dominant path in NCA polymerization initiated by primary amines. Regardless of the exact propagation method involved, a primary amine should subsist at the chain end once all NCA monomer is consumed unless chain termination (amine end deactivation) takes place.

According to Mitchell et al.[24] the cyclization reaction of PBG depicted in Figure 3.4 can occur at higher reaction temperatures, but also after the polymerization is complete or during sample storage. Cyclization at the amine terminus can be minimized by maintaining

the PBG samples at low temperatures during isolation and storage. Preservation of the primary amine terminus is essential for the grafting reaction: Deactivation of this moiety yields linear PBG chains incapable of coupling with the substrate.

Since the main concern with the grafting reactions is to preserve the primary amine chain end in linear PBG, the activated monomer polymerization mechanism should not be a main concern. It will be shown that the mass spectra provided in Figure 3.5 for the linear PBG samples give no hint of the presence of polymer chains containing an activated monomer initiator (*vide infra*).

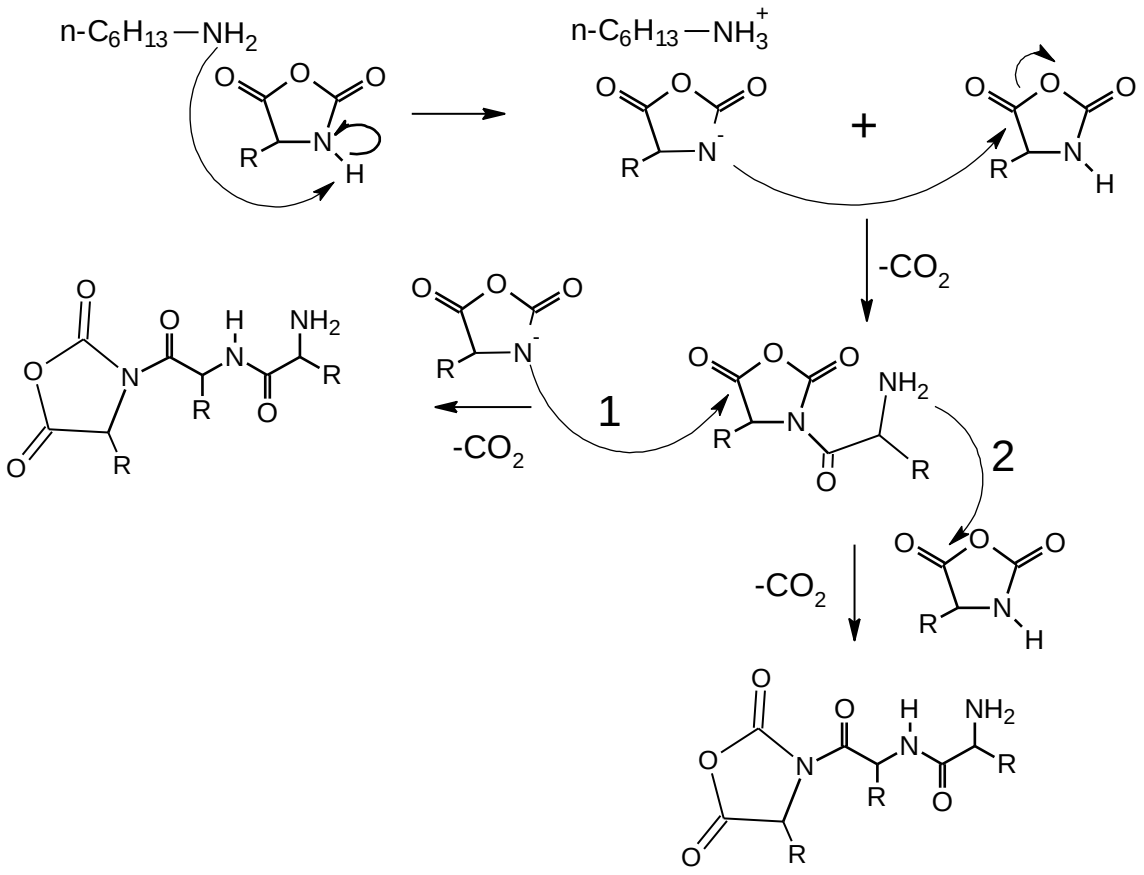

Figure 3.2 Activated NCA monomer polymerization mechanism.[25]

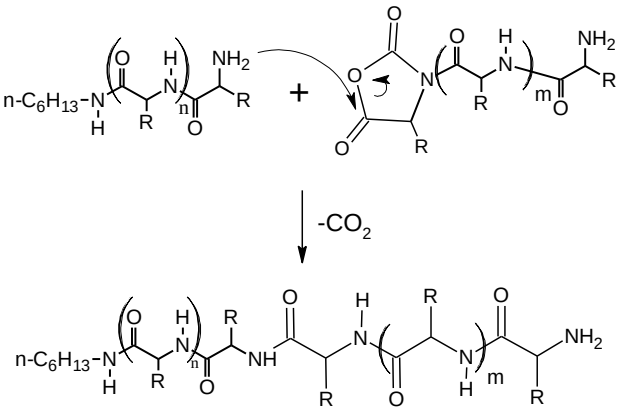

Figure 3.3 Attack of primary amine chain end on activated monomer oligomer.[25]

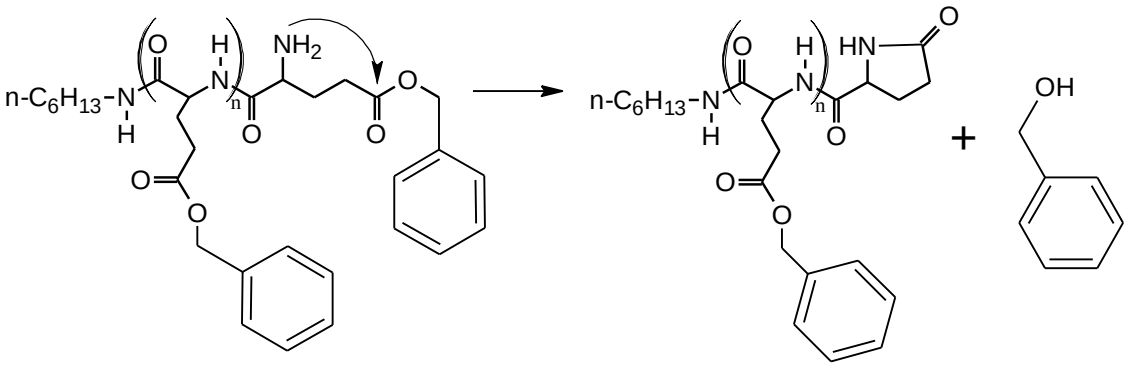

Figure 3.4 Deactivation of primary amines on linear PBG by chain end cyclization.

One method suggested to minimize side reactions during the polymerization is to use the hydrochloride salt form of amine initiators, to decrease the reactivity of the primary amine propagating center.[26,27] The growth of short PBG segments (X_n ~ 8, M_n = 2000) from a poly(ethylene oxide) macroinitiator (X_n ~ 110, M_n = 5000) terminated with a primary amine in the hydrochloride form was thus reported in DMF at 40–60 ºC. Values of M_w/M_n < 1.05 were obtained,[26] but it is clear that the short PBG segment extending the PEO chain would have little influence on the overall M_w/M_n of the block copolymers obtained under

these conditions. Block copolymers with poly(ε-benzyl carbamate L-lysine) contents of 66-70% by weight were also synthesized at 40–80 ºC from an amine-terminated polystyrene macroinitiator in the hydrochloride form (PS-NH_2·HCl, X_n = 52), M_w/M_n < 1.03 being also reported in this case.[25] Hadjichristidis and coworkers rather relied on high-vacuum break-seal techniques to create a strictly anhydrous environment and eliminate impurities causing side reactions.[28] This approach yielded high molecular weight PBG (M_n ~ 10^5) with M_w/M_n < 1.20.

The preferred method to generate the linear PBG building blocks, used in the current investigation, was the polymerization of Glu-NCA at 0 ºC as suggested by Vayaboury et al.[29] This method was deemed (on the basis of the MALDI–TOF analysis results discussed below, and the ^{19}F NMR results discussed in the grafting reaction section) to yield a satisfactory fraction of primary amine end groups, while being also experimentally less demanding than reactions involving the hydrochloride salt initiators[25,26] or the high-vacuum break-seal techniques.[27] MALDI–TOF mass spectrometry analysis of linear PBG samples (Figure 3.5) clearly confirms the presence of two chain populations, since end-group cyclization leads to a mass loss of 108.2 Da. In Figures 3.5a and 3.5b, the mass spectra obtained respectively for linear samples PBG-39-NH_2 and PBG-41-NH_2 have a higher intensity ladder, corresponding to the chains with a primary amine terminus. The inset of Figure 3.5a shows an example for a peak from this ladder at 4508.0 Da, corresponding to the sum of molar masses for the initiator (*n*-hexylamine, 101.2 Da), a polypeptide chain segment with a degree of polymerization X = 20, (× repeating unit mass of 219.2 Da = 4384.0 Da), and the mass of the salt cations used in the analysis, Na (23 Da) or K (39 Da). Therefore the total molecular weight of a PBG chain with X = 20, associated with sodium or potassium ions, is either

4508.0 Da or 4524.0 Da, respectively. The less intense ladder in the spectra of Figure 3.5a and 3.5b corresponds to the end-cyclized component of the linear PBG samples. For the same component with X = 20 discussed above, peaks are expected for the end-cyclized polymer at 4399.8 Da and 4415.8 Da, as observed in the inset of Figure 3.5a. This difference corresponds to the loss of benzyl alcohol (108.2 Da) during chain end cyclization. To confirm that cyclization did not occur during the MALDI-TOF experiment, samples PBG-39 and PBG-41 were also reacted in DMF with an excess of acetic anhydride to end-cap the primary amines as shown in Figure 3.6. The corresponding mass spectra obtained for PBG-39-NH-$COCH_3$ and PBG-41-NH-$COCH_3$ are provided in Figures 3.5c and 3.5d. The signal to noise ratio of the mass spectra for both end-capped PBG samples is decreased, presumably due to decreased ionizability of the capped PBG chains as compared to the chains containing the primary amine. When comparing Figures 3.5a and 3.5c, an increase in molecular weight is observed for the more intense polymer ladder (e.g., peak at 4550.0 Da for X = 20); however the lower intensity ladder in Figure 3.5c still matches the result found in Figure 3.5a (4399.8 Da for X = 20). It can also be seen that the MWD is narrower when the polymerization was performed at 0 °C (sample PBG-41, Figures 3.5b and 3.5d), which is consistent with enhanced living character of the amine termini throughout the polymerization. It is further worth mentioning that there is no evidence for a polymer ladder relating to PBG chains initiated by the activated monomer polymerization mechanism. This polymer ladder would correspond to a mass increase of 162.0 Da relatively to the most intense ladder (mass of activated monomer, 263.2 Da - mass of *n*-hexylamine, 101.2 Da), which is absent in the mass spectra.

Unfortunately MALDI analysis cannot serve to quantify the fraction of chains carrying a primary amine terminus, because the signal intensity for the species in the mixture is not only proportional to their concentration but also depends on their propensity to become ionized. Nevertheless the ratio of average peak intensities (I_{cycl}/I_{NH2}) for the cyclized and the amine-terminated species, respectively, can serve as a basis for comparison of the success of the reaction.

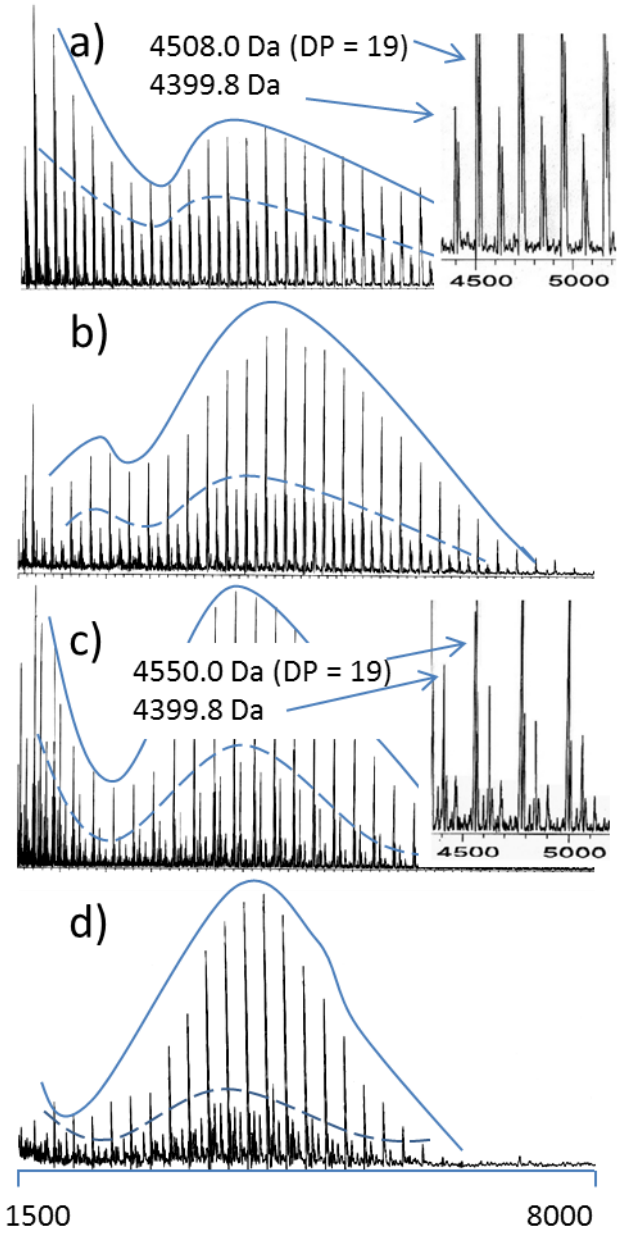

Figure 3.5 MALDI–TOF mass spectra for linear PBG samples in Table 1: a) PBG-39, b) PBG-41, c) PBG-39- NH-$COCH_3$, and d) PBG-41- NH-$COCH_3$.

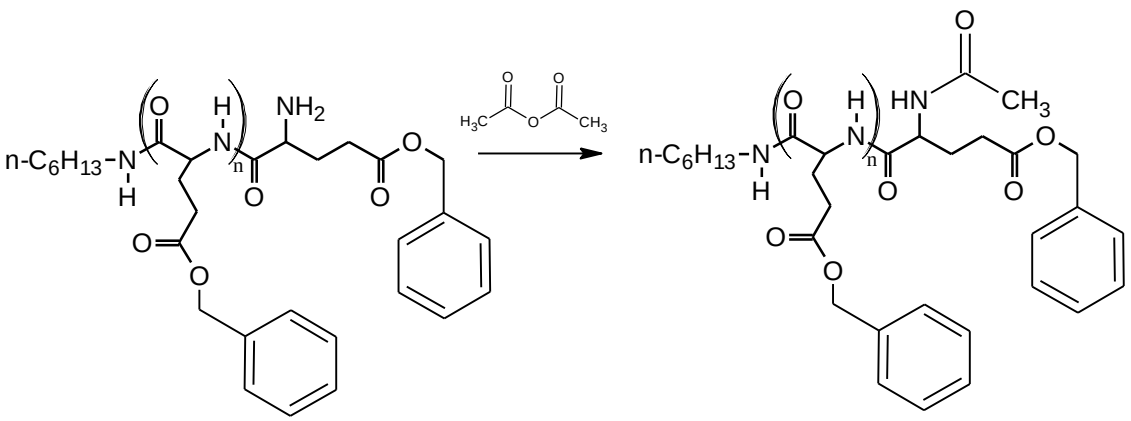

Figure 3.6 Capping of the amine terminus on linear PBG with acetic anhydride.

The characterization results obtained for the polymerization of Glu-NCA under different conditions are compared in Table 3.1. Only apparent (polystyrene-equivalent) molecular weights and M_w/M_n values could be obtained by SEC analysis of these linear samples because of the very weak and noisy signal obtained from the SEC-MALLS detector. Absolute values of X_n and M_n were rather estimated from ^{1}H NMR analysis of the samples, by comparing the integrated intensities for the benzylic methylene protons in the ester pendant of the structural units (δ ~ 5.0–4.8 ppm) and the terminal methyl group signal from the *n*-hexylamine initiator fragment (δ ~ 0.74–0.78 ppm). A monomer to initiator ratio (M/I) or target X_n = 50 was employed for the polymers used as linear substrates (corresponding to M_n ~ 11,000), while an M/I ratio = 23 (M_n ~ 5000) was targeted for the polymers used as side chains in the grafting reactions. The experimental X_n values were close to the theoretical values, with the exception of sample PBG-64. Recovery yields of 60–90% and narrow MWD were obtained for the linear homopolymer samples. The MALDI–TOF peak ratio (I_{cycl}/I_{NH2}) observed for two of the PBG samples synthesized at room temperature (PGB-39 and PBG-40 in Table 3.1) was ca. 4/10. When the polymerization was performed at 0 ºC (PGB-41 and

PGB-42 in Table 3.1), this ratio decreased to 3/10. Using side chains obtained by each polymerization method (PGB-39 and PGB-41) in grafting reactions for the preparation of G0 samples, the side chains synthesized at 0 ºC gave a grafting yield (defined as the fraction of side chains becoming attached to the substrate) of 65%, as compared to 58% for the sample synthesized at room temperature. These experimental results confirm that the fraction of chains carrying a reactive primary amine group at their chain end was higher for the side chains synthesized at 0 ºC, as expected from the semi-quantitative MALDI-TOF analysis results.

It should also be noted that the M_w/M_n values obtained are lower for the samples prepared at low temperature (ca. 1.09-1.11 at 0 ºC vs. 1.17–1.20 at room temperature), which is again consistent with minimized chain termination. Furthermore, the 0 ºC reactions were stopped after 3 d in the current investigation, in an attempt to minimize the loss of the primary amine chain ends through side reactions, while Vayaboury et al. allowed their reactions to proceed for 7 d. On the basis of the results from MALDI–TOF analysis, the narrower MWD, and the higher grafting yields obtained, all subsequent polymerizations were carried out at 0 ºC rather than at room temperature. Analysis of the derivatized chain ends by ^{19}F NMR spectroscopy, discussed in the grafting reaction section, will further demonstrate the benefits of performing the polymerizations at 0 °C.

Table 3.1 Synthesis of Linear PBG

			^{1}H NMR		SEC[a]
sample	reaction temp	M/I	X_n	M_n	M_w/M_n
PBG-19	RT	50	50.0	11100	1.20
PBG-34	RT	50	51.3	11400	1.19
PBG-39	RT	23	25.7	5800	1.18
PBG-40	RT	23	24.8	5600	1.17
PBG-41	0	23	26.0	5800	1.10
PBG-42	0	23	22.8	5100	1.10
PBG-64	0	23	16.0	3900	1.09
PBG-75	0	23	26.4	5900	1.09
PBG-A	0	23	23.6	5300	1.11

[a] Apparent values from SEC analysis with a DRI detector and a linear polystyrene standards calibration curve.

3.4.2 Deprotection of Linear PBG Substrate

The treatment of PBG with HBr allowed the cleavage of a controlled fraction (ca. 25–30%) of benzyl ester protecting groups to generate coupling sites, in analogy to other arborescent polymer syntheses.[1,19] The extent of deprotection was monitored by ^{1}H NMR spectroscopy analysis. The most reliable analysis method found used the peak area ratio for the methylene protons (2H at 4.9-5.0 ppm), that are only present on repeat units with the benzyl ester protecting group, and the methine protons (1H at 3.7-4.4 ppm), that are in each repeat unit and are not affected by deprotection. An example is provided in Figure 3.7 for PBG-34-CO_2H, where the integration of the methylene protons (1.38/2H, protected units only) is divided by the integrated peak area of the methine protons (1.00/1H in each repeating unit) to give the fraction of repeat units still protected (0.69, or 69%). The corresponding level of deprotection is therefore 0.31 or 31%.

For arborescent polypeptides (G0–G2) the benzylic/methine proton ratio was not exactly 2:1 as for the linear substrate but rather 1.8:1, due to the deprotection steps carried out in the previous grafting cycles. This decreased ratio was taken into account when comparing spectra before and after deprotection for the G0–G2 substrates. Typical results for the partial deprotection of linear and branched substrates by acidolysis are provided in Table 3.2. Analysis of the deprotection level by ^{1}H NMR spectroscopy and by titration was completed for selected samples and yielded comparable results for the linear polypeptides. The graft polymers were more difficult to titrate due to their decreased solubility, leading to precipitation during the titration procedure. The results obtained for sample G0-62 nevertheless demonstrate that ^{1}H NMR analysis and the titration procedure yielded consistent deprotection levels even for the branched substrates. It has been reported that deprotection with HBr/HOAc-TFA can result in peptide chain cleavage, especially if the reactions are not performed under strictly anhydrous conditions.[30] For the procedures used in the current investigation, with only partial deprotection (0.30 equivalent HBR added with respect to benzyl ester moieties), all the HBr was consumed over the 3 h reaction period, while maintaining anhydrous conditions. This should ensure that no chain cleavage occurred during the deprotection step. To confirm this SEC analysis of the branched polypeptides was again performed following deprotection, to detect the occurrence of any degradation or chain cleavage reactions. For example, the deprotection of sample G0-52 (Table 3.2) led to a decrease in molecular weight from M_n = 54,000 to 47,000, which corresponds to 32% deprotection of the benzyl ester moieties. The deprotection level determined by ^{1}H NMR analysis of G0-52 was also 32%. The SEC traces for G0-52 and G0-52-CO_2H are compared in Figure 3.8 and have a similar shape. The corresponding M_w/M_n values for G0-52 and

partially deprotected G0-52-CO_2H are 1.04 and 1.05, respectively. It is therefore clear that no significant degradation occurred under the conditions used for the partial deprotection of the arborescent PBG samples.

Table 3.2 Partial Deprotection of PBG Substrates

sample	mole ratio HBr:benzyl ester units	mol% deprotection	
		^{1}H NMR	titration
PBG-19-CO_2H	0.25:1	34	31
PBG-34-CO_2H	0.25:1	31	30
G0-52-CO_2H	0.3:1	32	-
G0-53-CO_2H	0.3:1	32	-
G0-62-CO_2H	0.3:1	41	38
G1-2-CO_2H	0.2:1	16	-
G2-3-CO_2H	0.3:1	26	-

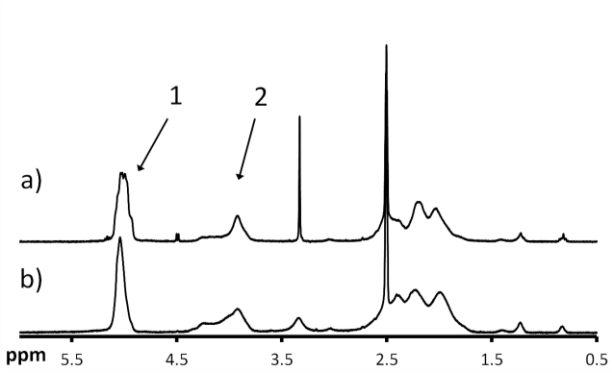

Figure 3.7 ^{1}H NMR spectra for PBG-34 (a) before and (b) after partial deprotection with HBr. The peaks labelled as 1 and 2 correspond to the benzylic methylene and the backbone methine protons, respectively.

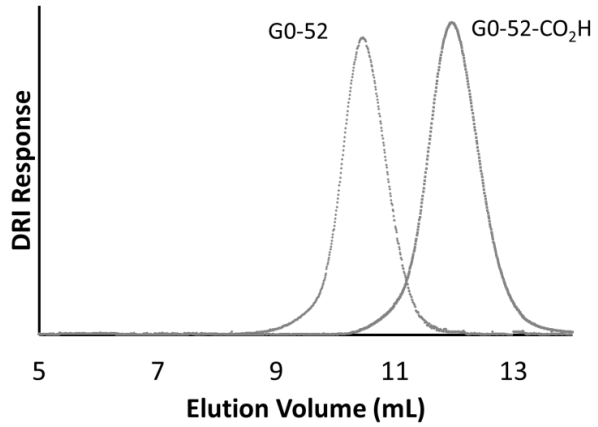

Figure 3.8 SEC Analysis of a G0 arborescent PBG polymer before and after partial acidolysis of the benzylic protecting groups.

3.4.3 Grafting Reaction

Coupling of the HOBt-activated substrate with the side chains is illustrated in Figure 3.9; the details of the activation of the carboxylic acid groups by DIC and HOBt are not shown. The diisopropylurea formed in the reaction is relatively soluble and easily eliminated during precipitation of the graft polymers.

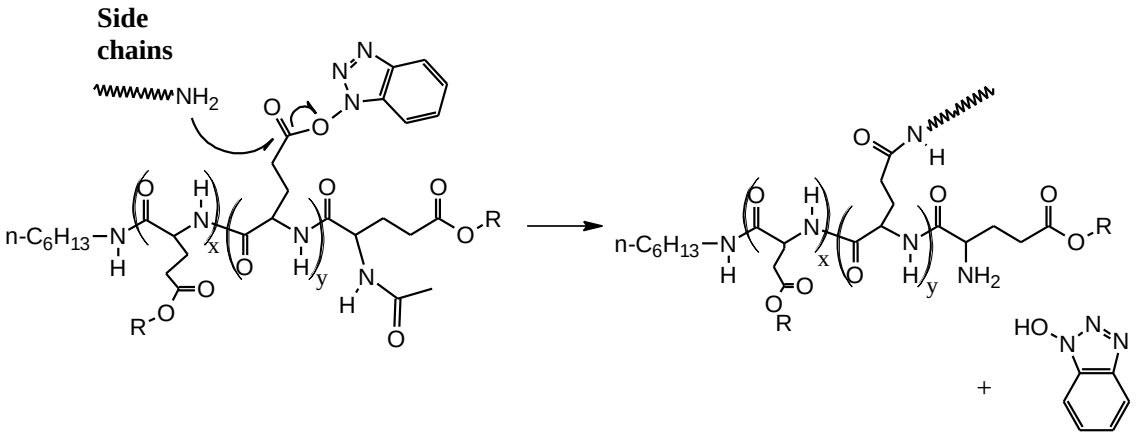

Figure 3.9 Coupling reaction of the activated substrate with the side chains.

The success of the grafting reaction can be quantified in terms of the grafting yield and the coupling efficiency. The grafting yield, defined as the fraction of the side chains added to the reaction becoming attached to the substrate, can be estimated from the relative areas of the peaks for the graft polymer and the side chains in the SEC analysis of the crude product. Taking as an example sample G0-40, generated from substrate PBG-34-CO_2H (M_n ~ 11,000, 31 mol% -CO_2H functionalities) and side chains PBG-38 (M_n ~ 6600, not shown in Table 3.1), the peaks on the left and the right of the SEC trace on Figure 3.10, corresponding to the graft polymer and the linear contaminant, have respective areas (in arbitrary units) of 71,500 and 38,800. Taking into account the weight fraction of the substrate in the graft polymer (10.7%), the peak area for the graft polymer can be corrected as 71,500 × 0.893 = 63,800. A grafting yield of 63,800 / (63,800 + 38,800) = 0.622 (62%) is thus calculated. The coupling efficiency, defined as the fraction of active sites on the substrate consumed in the grafting reaction, corresponds to the ratio of the number of side chains grafted and the number of coupling sites available on the substrate. This requires knowledge of the absolute molecular weight of both components. Consequently the absolute M_n of the graft polymers was determined on a SEC system equipped with a MALLS detector, while the M_n of the side chains was determined by ^1H NMR analysis (since the SEC-MALLS signal was too noisy). Thus sample G0-40 had M_n = 53000, while M_n = 11,000 and 6600 for the substrate and the side chains, respectively. This gives a number-average branching functionality f_n = (53,000 – 11,000) / 6600 = 6.4 chains per graft polymer. Since the linear substrate had X_n = 51 and a deprotection level of 31 mol%, corresponding to 51 × 0.31 = 15.8 coupling sites on average, a coupling efficiency of 6.4 / 15.8 = 0.405 (41%) was achieved for sample G0-40. The grafting yield observed in the reactions is obviously determined in part by the loss of the

primary amine termini on the side chains. To compensate for the presence of unreactive chain ends, a 25% excess of side chains was used in all the reactions (*vide infra*). Unfortunately, this excess also contributes to decreasing the grafting yield. The coupling yield (and indirectly also the grafting yield) depends on the accessibility of the coupling sites on the substrate during the grafting reaction. The remaining coupling sites on the substrate necessarily become more hindered as the grafting reaction proceeds, making further grafting reactions more difficult. Another limiting factor could be the presence of impurities in the solvent serving in the grafting reaction. This issue will be considered below.

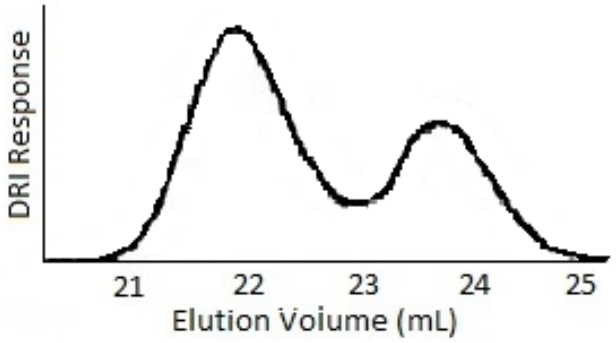

Figure 3.10 SEC Analysis of crude G0-40 sample of Table 3 (62% grafting yield).

The grafting procedures purposely used a 25% molar excess of side chains in the reactions, in order to maximize the coupling efficiency at the expense of the grafting yield. The coupling agents (DIC and HOBt) were also used in 5-fold excess, to guarantee the activation of all the carboxylic acid coupling sites. Furthermore, triethylamine was added as a proton scavenger to ensure that the amino termini of the side chains remained in their primary amine (non-protonated) form throughout the reaction. Excess *n*-hexylamine was added at the end of the grafting reaction (24 h) and allowed to react for 1 h, to ensure that all

the activated coupling sites were reacted (deactivated), so they were not available in subsequent grafting reactions. This effectively prevented side chains used in the subsequent grafting reactions from reacting with the coupling sites activated in the previous reaction cycles. During deprotection of each generation of arborescent PBG substrate, there is also potential for the removal of the benzyl ester groups located on the repeat units of side chains grafted early on in the procedure. Due to increased steric crowding near the core, these grafting sites are much less accessible relatively to the grafting sites at the periphery however, so the occurrence of structural imperfections due to coupling sites located deeper inside the substrate should be limited.

The synthesis of the upper generation (G1–G3) arborescent polymers was carried out by the same method used for the G0 materials, but it was preferable to substitute DMSO for DMF as solvent in the reaction. Initial attempts to synthesize the G1 polymer in DMF were unsuccessful, the grafting yield being limited to 8–15%. It was first hypothesized that the failed reactions were linked to the formation of α-helices by the partially deprotected PBG substrate in DMF, since this phenomenon is known to occur for PBG in both its protected[31] and fully deprotected [poly(glutamic acid)] forms in DMF.[32,33] The formation of α-helices by the G0 arborescent polymer substrate and/or the side chain material could hinder the diffusion of the side chains to the coupling sites, potentially limiting the grafting yield attained. Conversely, a non-helicogenic solvent such as DMSO, by inducing a random coil conformation for the substrate and side chains, could enhance the accessibility of the coupling sites. In agreement with this hypothesis, it was initially verified (Figure 3.11) that higher grafting yields could be achieved in DMSO (53%) than in DMF (8%).

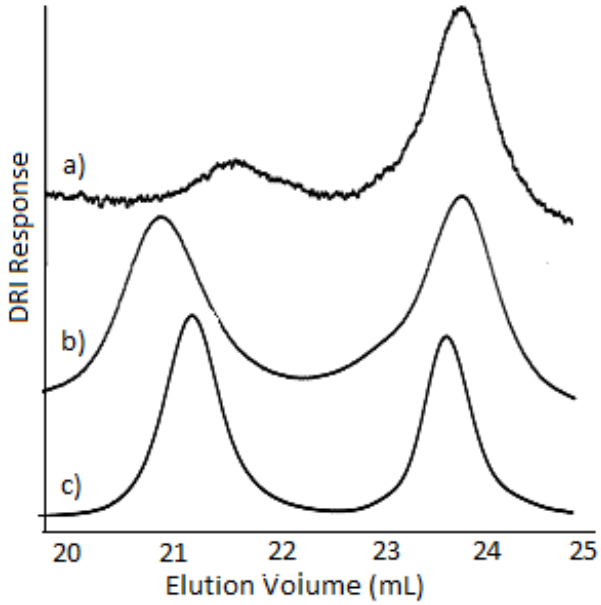

Figure 3.11 SEC traces for G1 samples synthesized in (a) DMF, (b) DMSO, and (c) DMF purified and stored in the dark.

The conformation of the G0 substrate and the side chains was investigated by ^{1}H NMR analysis in both solvents, since distinct signals are expected for the benzyl glutamate units[30,34] when the chains adopt either α-helical or random coil conformations. A study of PBG by Maeda et al. also confirmed the formation of random coils in DMSO for linear chains with X_n = 11 and 26,[31] i.e. with a size range comparable to the polymers serving as side chains in the current investigation. ^{1}H NMR spectra for G0 and G3 arborescent PBG polymers, recorded in DMF and in DMSO, are compared in Figure 3.12; the G1 and G2 polymers yielded similar results (not shown). The arborescent PBG samples behave the same way as the linear polymers, α-helices being formed predominantly in DMF while random coils are observed in DMSO. The different conformations in the two solvents could thus explain the grafting yield variations observed, as discussed above.

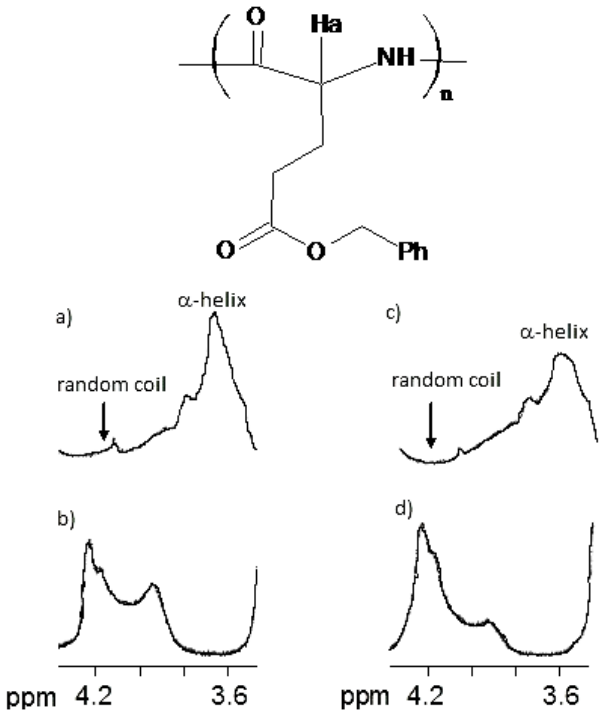

Figure 3.12 ^{1}H NMR spectra for the methine protons of G0 and G3 arborescent PBG in d_7-DMF (a, c) and in d_6-DMSO (b, d).

Beyond the potential influence of chain conformation an alternate explanation for the low grafting yields observed, unrelated to α-helix formation, was brought to our attention.[35] It has indeed been shown that DMF is susceptible to contamination by traces of cyanide ions forming quickly after its purification, due to the occurrence of a photochemical reaction.[36,37] Careful purification without exposure to light was determined to be the best method to avoid this contamination.[35] To verify this second hypothesis, DMF was purified by distillation under reduced pressure *in the dark*. The purified solvent was then used immediately in the synthesis of a G1 arborescent polymer, and the grafting reaction was also carried out in the dark. The grafting yield achieved under these conditions (Figure 3.11c) was 57%, i.e.

comparable to the other G1 synthesis performed in DMSO (Figure 3.11b). It therefore appears that the low grafting yields observed initially in DMF purified by the standard procedure (without shielding from light) are linked predominantly to the photochemical formation of cyanide impurities rather than to the α-helix conformation of the polymers. The lack of influence of DMF contamination in the synthesis of the G0 polymers can be explained by the rate of the coupling reaction being faster for the linear than for the G0 substrate, which leads to insignificant competition between the rate of photogeneration of the impurities and the coupling reaction. While DMF and DMSO appear equally suitable as solvents for the coupling reaction, the purification of DMSO is much less problematic than DMF from a practical viewpoint. For that reason, subsequent grafting reactions were carried out exclusively in DMSO.

The grafting yields for the arborescent PBG system are relatively low in comparison to other arborescent systems obtained by comparable grafting onto strategies.[19] One obvious reason for this could be the limited "living" character of the amine termini on the side chains, which would limit the coupling reaction. To determine whether this was the main factor coming into play a grafting reaction was performed, after which the unreacted side chains were isolated by preparative SEC and analyzed to determine their active amine content. If the limiting factor in the grafting reaction under the conditions used (25% excess of side chains) were indeed the living character of the amine termini, the unreacted side chains isolated after the grafting reaction should contain no active primary amine groups. Once isolated from the graft polymer, a technique developed by Ji et al.[38] was used to determine the concentration of active primary amines in the PBG side chains. This technique uses the reaction of either 3,5-bis-(trifluoromethyl)benzaldehyde (BTFBA) or 4-trifluorobenzaldehyde (TFBA) with

primary amines, to produce imine functionalities at the chain end of the polymer. ^{19}F NMR analysis may then be used to observe the chemical shift of the fluorine atoms when the imine is formed. It was suggested to employ benzotrifluoride (BTF) in 3-fold excess, to serve as internal standard and yield quantitative results. The 3-fold excess of aldehyde is also useful to force the reaction to completion in less than 2 h. In the case of PBG analysis, TFBA was preferred due to overlap of the signals for BTFBA and the PBG-imine. Figure 3.13a shows the ^{19}F NMR spectrum obtained for linear sample PBG-A (Table 3.1), synthesized at 0° C. An amine functionality level $f_{NH2} > 98\%$ was obtained by that method. The ^{19}F NMR analysis was repeated for this sample 4 weeks later, following storage in the powder form and under nitrogen, either in the refrigerator (5° C) or at room temperature. The f_{NH2} determined for these samples had decreased to 90 and 78%, respectively (^{19}F NMR spectra not shown). This confirms the original observation made by Mitchell et al. about chain end cyclization occurring after the polymerization was completed.[24] The linear side chains PBG-A (Table 3.1) with $f_{NH2} = 90\%$ were used in the actual grafting reaction to prepare an arborescent G1PBG using a G0 substrate (30% deprotection level), so that the isolation of the side chains could be achieved without contamination by the G1PBG polymer in preparative SEC. After 24 h reaction, a grafting yield of 52% was achieved at which point the unreacted side chains were isolated from the G1PBG polymer. The ^{19}F NMR spectrum obtained for the isolated unreacted side chains, shown in Figure 3.13b, corresponds to $f_{NH2} = 16\%$. It is relatively low as expected, since the side chains with active amine were partly grafted onto the substrate, and some chains were presumably deactivated during the grafting reaction. Most importantly, since amine chain ends are still present in a portion of the recovered side chains, this result

clearly demonstrates that the 'living' character of the amine chains ends is likely not the limiting factor in these grafting reactions but rather steric hindrance on the substrates.

Aliferis et al. also performed coupling reactions to generate 3-arm star copolypeptides from linear PBG. Their technique used isocyanate functionalities, that are highly reactive towards primary amines, but they still employed a 30% excess of linear PBG and 4 weeks for complete reaction.[22] This suggests that steric hindrance was a limiting factor even in the synthesis of these simple 3-arm star copolypeptides structures. It is therefore not surprising that steric hindrance was likewise a limiting factor in the current investigation.

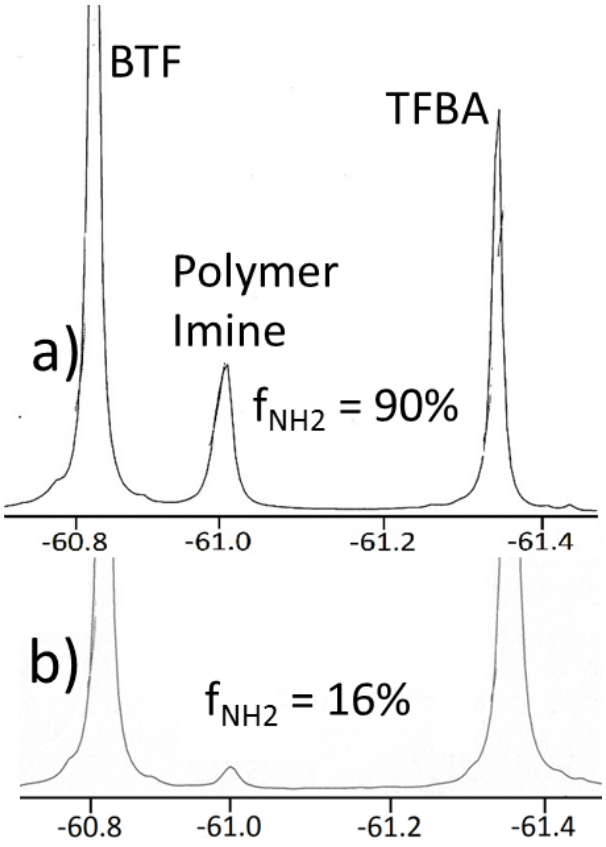

Figure 3.13 ^{19}F NMR analysis of (a) PBG-A synthesized at 0° C, (b) unreacted PBG-A side chains isolated from the G1 grafting reaction.

The synthesis of a series of arborescent PBG samples of generations up to G3 is illustrated with their SEC elution curves in Figure 3.14. It is clear that the elution volume of the graft polymers decreases over successive generations, while the breadth of the peaks remains relatively constant. The corresponding characterization data are summarized in Table 3.3. Polydispersity indices $M_w/M_n < 1.06$ were obtained for all the samples, which highlights the success of the *grafting onto* technique developed for the synthesis of arborescent polypeptides: Polymers with M_n values reaching over 10^6 were obtained in only four grafting cycles, while a narrow MWD was maintained over successive generations. This contrasts with the situation encountered when arborescent polylysines were synthesized from their NCA derivatives according to a *grafting from* scheme (branches grown from the substrate).[18] In this case, M_w/M_n values of 1.3–1.5 were obtained for G0–G2 arborescent poly(Z-lysine), as well as for the analogous poly(TFA-lysine) systems. Even with the improved procedure of Collet et al.,[21] a polydispersity index of 1.46 was obtained for a G3 polymer with $M_n = 1.72\times10^5$. The molecular weight of the arborescent polylysines obtained in both cases was also lower than in the current investigation. A significant advantage of these *grafting from* procedures is nonetheless the minimized formation of linear polylysine contaminant in the reaction. It is also clear that the NCA derived from the protected lysine and glutamic acid monomers are not sensitive to the same types of side reactions.

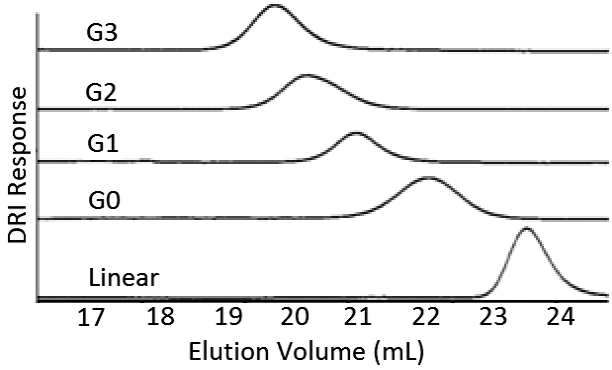

Figure 3.14 SEC traces for purified arborescent PBG samples up to G3.

The number-average branching functionality of the arborescent polypeptides, f_n, defined as the number of side chains added in the last grafting reaction, is also reported in Table 3.3. The branching functionality increases over successive generations, as more coupling sites are available after each grafting cycle. On the other hand it also becomes more difficult for the coupling sites to react in the upper generation substrates as a result of increased crowding. The branching functionality thus increased 4.2-, 4.4-, and 2.3-fold when grafting onto G0, G1, and G2 substrates, respectively. The modest increases in branching functionality and M_n observed for the G3 polymer are attributed to the dense structure of the G2 substrate, making it difficult for the linear side chains to diffuse to the coupling sites. Since the same batch of side chains was used to synthesize the G2 and G3 polymers, possible variations in coupling efficiency due to fluctuations in the fraction of active (primary amine-terminated) side chains can be excluded. Similar variations in branching functionality were observed in the synthesis of arborescent polystyrene by an analogous grafting onto scheme,[1,19] a significant decrease in coupling efficiency being observed for the G2 substrate.

The coupling efficiency and the branching functionality should be correlated to some extent, since they both depend on the accessibility of the reactive sites.

Table 3.3 Characteristics of Arborescent PBG Samples of Successive Generations

		DRI	MALLS				
	M_n side chains[a]	M_n^{app} [b]	M_n	M_w/M_n	G_y (%)[c]	C_y (%)[d]	f_n [e]
G0PBG	6600	1.80×10^4	5.3×10^4	1.04	62	58	6.6
G1PBG	4000	3.93×10^4	1.3×10^5	1.06	38	30	22
G2PBG	3900	8.31×10^4	4.9×10^5	1.03	46	50	96
G3PBG	3900	1.34×10^5	1.1×10^6	1.03	32	21	165

[a] From ^{1}H NMR analysis; [b] apparent M_n from a linear polystyrene standards calibration curve; [c] grafting yield from SEC analysis using a DRI detector; [d] fraction of coupling sites on the substrate consumed in the reaction, [e] branching functionality: number of branches added in the last grafting cycle.

3.4.4 Hydrodynamic Diameter

Dynamic light scattering (DLS) measurements were performed on arborescent PBG samples of successive generations, to compare their hydrodynamic diameter (d_h) in DMF and in DMSO. The results obtained are summarized in Table 3.4. First- and second-order analysis of the correlation function, $|g_1(\tau)|$ and $|g_2(\tau)|$, respectively, provides information on the size dispersity of the system. For a strictly monodispersed size distribution, the results from first- and second-order analysis of the DLS correlation function would be identical, since the correlation function can be represented by a single exponential decay.[39] The relatively small differences between the numbers reported in Table 3.4 for the first- vs. second-order analysis results is therefore consistent with a uniform molecular size distribution, as would be expected from the low M_w/M_n values reported in Table 3.3. It is clear that there is a significant difference in d_h between the DMF and DMSO solutions for all the generations. A

salt was added at low concentration (0.05% w/v LiCl) to both solvents used in the DLS measurements, as aggregation was otherwise apparent, particularly in DMF. ^{1}H NMR spectra were also compared before and after the addition of salt at the same concentration, to ensure that it had no influence on the α-helix vs. random coil conformations of the chains. The smaller d_h values obtained in DMF are attributed to the more compact α-helix conformation adopted by the PBG chains (as confirmed by ^{1}H NMR analysis, Figure 3.12) in comparison to the randomly coiled chains in DMSO. This result is quite surprising, as the change in conformation is observed even for the highly crowded G3 polymer structure, containing as many as 289 PBG side chains.

Table 3.4 Hydrodynamic Diameter of Arborescent PBG

	DMF[a]		DMSO[a]	
	d_{h1}	d_{h2}	d_{h1}	d_{h2}
G1PBG	10.7	8.4	15.7	14.1
G2PBG	13.1	12.1	21.3	20.1
G3PBG	24.5	23.5	34.5	32.5

[a] All values in nm; 0.05% LiCl added to suppress aggregation.

3.5 Conclusions

The results presented show that well-defined arborescent polypeptides, presumably more biocompatible than their arborescent analogues derived from vinyl monomers, can be synthesized in a controlled fashion over successive generations. Narrow MWD ($M_w/M_n \leq 1.06$) were maintained for molecular weights reaching ca. 10^6 over only four grafting cycles. The grafting yield (30–65%) and coupling efficiency (20–60%) attained in these reactions may require further optimization, as this would simplify the purification of the products. The

covalent attachment of hydrophilic chain segments forming a corona at the surface of the hydrophobic arborescent polypeptide core should yield water-soluble unimolecular micelles suitable for drug delivery applications.

Chapter 4

Arborescent Unimolecular Micelles: Poly(γ-benzyl L-glutamate) Core Randomly Grafted with Hydrophilic Chain Segments

4.1 Overview

Amphiphilic copolymers were obtained by randomly grafting arborescent poly(γ-benzyl L-glutamate) (PBG) cores of generations G1-G3 with polyglycidol, poly(ethylene oxide), or poly(L-glutamic acid) chain segments. This was achieved by first subjecting arborescent PBG samples with narrow molecular weight distributions (M_w/M_n < 1.1) to partial acidolysis of the benzyl ester protecting groups, to produce substrates with randomly distributed carboxylic acid functionalities. Linear polymers with narrow molecular weight distributions (M_w/M_n < 1.20) and containing a primary amine chain end were also synthesized. Poly(glycidol acetal) (PGlyAc) and poly(ethylene oxide) (PEO) were obtained by anionic polymerization, and poly(γ-*tert*-butyl L-glutamate) (PtBuGlu) by the ring-opening polymerization of γ-*tert*-butyl L-glutamate N-carboxyanhydride. Grafting was achieved for PGlyAc samples with M_n = 9100 and 32,400 in combination with the G1 and G2 PBG substrates. Samples of PEO with M_n = 5100 and PtBuGlu with M_n = 2200 were each grafted onto G1, G2, and G3 PBG substrates. All the arborescent copolymers generated were characterized by size exclusion chromatography and dynamic light scattering, to evaluate the success of the synthetic strategies used and their ability to provide unimolecular micelles in organic and aqueous solvents. The yields obtained in the grafting reactions were mostly similar to those observed in the synthesis of the arborescent PBG substrates described in Chapter 3. The solution properties of the arborescent copolymers were found to vary with the type of hydrophilic chain segments used, as well as the PBG substrate generation number.

4.2 Introduction

Block copolymers with amphiphilic properties have been studied extensively over the past 35 years.[1] When these block copolymers are dispersed in a solvent that is a thermodynamically good for one block and poor for the other, reversible self-assembly of the linear chains occurs to give what is commonly known as a micelle structure. Not only is the micelle formation process reversible but its structure is also dynamic, whereby an equilibrium exists between the chains aggregated within the micelles and free copolymer chains (unimers) in solution: A minimum concentration of unimers in solution (known as the critical micelle concentration or CMC) is necessary for the self-assembly to occur. In spite of their dynamic nature, block copolymer micelles derived from polysaccharides[2] or poly(ethylene oxide) in combination with polypeptides, lipids, or poly(lactic acid),[3] among others, have been successfully used in microencapsulation applications.

Due to the complexity of biological environments in which block copolymer systems can be employed, there is a desire to increase their thermodynamic stability, as characterized by the CMC, and the kinetic stability of micelles, i.e. the rate at which micelles disassemble at concentrations below the CMC. A method that can solve both micelle stability issues is to cross-link their core, to generate unimolecular micelles.[1,4] This concept was first introduced by Procházca et al.,[4] by cross-linking polystyrene-*b*-polybutadiene-*b*-polystyrene micelles having a polybutadiene core by UV radiation in the presence of a photoinitiator. Kakizawa et al. also demonstrated this technique for poly(ethylene glycol)-*b*-poly(L-lysine) containing thiol groups on a small fraction (10-20%) of the lysine repeat units.[5] Several other block copolymers have also been used to generate unimolecular micelles by cross-linking either the core or the shell of the micelles.[4,6,7]

Block copolymers are clearly useful to generate micelles; however a newer class of macromolecules, the dendritic polymers, may also be useful for that purpose. Dendritic polymers can be classified into three subcategories: dendrimers, hyperbranched polymers, and dendrigraft polymers, as discussed in Chapter 2. Unimolecular micelles have been derived from each of these dendritic polymer families, albeit characteristics such as the overall size, size distribution, core and shell densities, and surface functionality can vary widely in each case. Due to their nanometric dimensions and tailorable structure, these unimolecular micelles have shown potential for applications in microencapsulation.[8-11]

Dendrimers have the most perfect structure among the dendritic polymers families, being essentially monodispersed in many cases ($M_w/M_n < 1.01$). The first amphiphilic dendrimers were introduced in 1985 by Newkome et al.,[12] whereby a relatively non-polar "arborol" core structure was functionalized with a polyol surface making the dendrimer water-soluble. The first amphiphilic dendrimers produced by a convergent synthetic method were introduced in 1993 by Hawker et al.[13] In this case polyether macromolecules, derived from 3,5-dihydroxybenzyl alcohol, were functionalized with carboxylate end groups to enhance their solubility in basic aqueous media. Unfortunately the synthesis of dendrimers can be very tedious, requiring layer-by-layer additions to ensure complete reactions and well-defined structures. Their main limitation lies in steric crowding effects, since the number of branching points and end groups increases exponentially for each generation. For this reason micellar structures based on dendrimers are generally limited in their size (typically up to 15 nm in diameter) and their capacity to carry guest molecules.

A simpler method to build unimolecular micelles is using hyperbranched polymers. While these structures are not as well-defined as dendrimer micelles, they are easier to

synthesize and require fewer reaction steps to generate high molecular weight structures. A few groups have thus demonstrated the synthesis of water-soluble amphiphilic hyperbranched systems, but these micelles clearly have a strong tendency to aggregate.[14-19] Their tendency for self-assembly is likely linked to the structural imperfections arising from their synthesis, that does not allow the formation of a completely closed shell around the core to shield it efficiently from the aqueous environment. This promotes aggregation to generate larger, more stable micellar structures. The groups of Haag[20] and Yan[21] could confirm this self-assembly mechanism using transmission electron microscopy. Since unimolecular micelles are difficult to obtain for hyperbranched amphiphiles, it becomes difficult to compare them with other unimolecular micelle systems.

Arborescent (or dendrigraft) polymers are a class of dendritic macromolecules developed concurrently by Gauthier and Möller[22] and by Tomalia et al.[23] in 1991. Arborescent polymers have a degree of structural perfection intermediate between dendrimers and hyperbranched polymers. Arborescent polymers are generated from randomly functionalized substrates (thus producing randomly branched structures analogous to the hyperbranched systems), that allow the attachment of polymer chain segments with a narrow size distribution (in analogy to dendrimers, but using macromolecules as building blocks instead of monomer units). Figure 4.1 depicts the synthesis of an arborescent polymer of generation 1 (G1), but molecules of generations up to G4 have been produced in this fashion. These structures are characterized by a tree-like architecture and a narrow molecular weight distribution ($M_w/M_n \leq 1.1$).

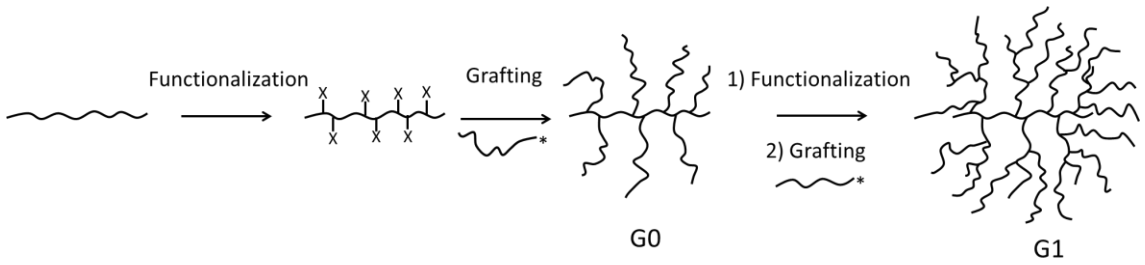

Figure 4.1 Schematic representation of the generation-based synthesis of arborescent polymers.

The synthetic strategy used for arborescent polymers also allows the construction of covalently bonded micellar structures, since polar chain segments may be added in the last grafting cycle. The first arborescent copolymers micelles, incorporating a polystyrene (PS) core and a poly(ethylene oxide) (PEO) shell, were reported by Gauthier et al. in 1996.[24] The PEO shell was terminally grafted from peripheral hydroxyl chain ends on the polystyrene chains attached to the core in the last grafting cycle. The resulting arborescent micelles, of generations up to G4, were unimolecular (non-aggregated) and water-soluble in most cases. Other arborescent copolymer micelles were synthesized by Kee and Gauthier using a shell of poly(2-vinylpyridine) (P2VP) chains,[25] and more recently, a shell of poly(*tert*-butyl methacrylate) (P*t*BMA) chains.[26] In this instance the P2VP or P*t*BMA chains were attached onto randomly functionalized G0, G1, and G2 PS cores. The arborescent PS-*g*-P2VP structures, with hydrodynamic diameters ranging from 30-160 nm, were non-aggregated in aqueous and methanolic solutions acidified with HCl.[27] The arborescent PS-*g*-P2VP unimolecular micelles were shown to have interesting solubilization properties[28] and release kinetics[29] for different types of small molecule hydrophobes. The copolymers containing P*t*BMA shells also yielded unimolecular water-soluble micelles once the *tert*-butyl protecting

groups was removed to produce a poly(methacrylic acid) (PMAA) shell. The arborescent micellar systems of PS-*g*-P2VP and PS-*g*-PMAA were useful to demonstrate the potential of arborescent copolymers in microencapsulation, but they lack the biocompatibility required for biomedical applications for both the shell and core components. To overcome this limitation, we report herein the synthesis of arborescent copolymers based on poly(γ-benzyl L-glutamate) (PBG) cores with different hydrophilic shell components. The synthesis of PBG by the ring opening polymerization of N-carboxyanhydrides has been reported as early as the 1950s,[30] but this methodology has recently regained interest due to the fact that this polymer is biocompatible, making it suitable for biomedical applications.[31] The synthesis of PBG cores of generations G0 to G3 was discussed in detail in Chapter 3. Using grafting techniques similar to those described in Chapter 3, chain segments of either PEO, poly(glycidol acetal) (PGlyAc), or poly(γ-*tert*-butyl L-glutamate) (PtBuGlu) were covalently attached to the PBG cores to form a shell as shown in Figure 4.2. Anionic polymerization techniques were used to generate linear PEO and PGlyAc with primary amine chain ends. Ring-opening polymerization was used to generate linear PtBuGlu in the same manner as linear PBG. Since PEO is water-soluble, no further modification is necessary to generate a hydrophilic shell. In the case of PGlyAc and PtBuGlu the acetal and *tert*-butyl ester protecting groups, respectively, must be removed to generate a hydrophilic shell. The focus of the current investigation is on synthetic aspects, but the solution properties of the micelles obtained are examined with dynamic light scattering (DLS) measurements.

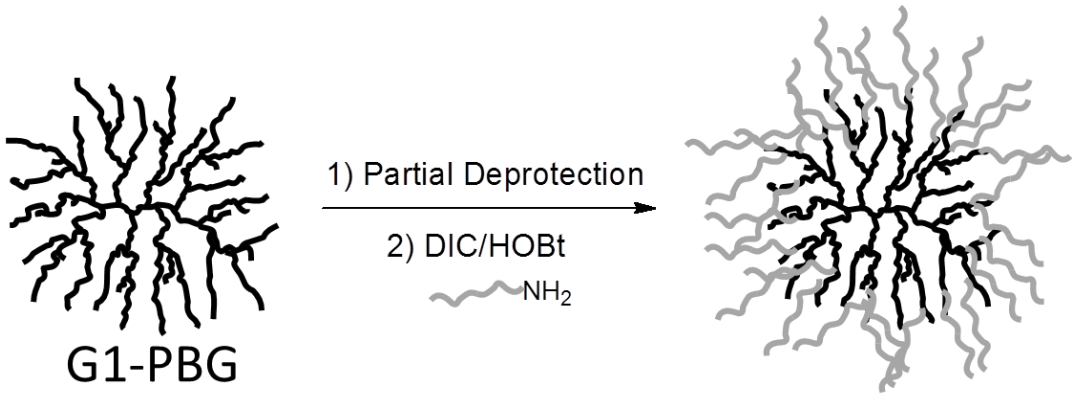

Figure 4.2 Schematic representation of the synthesis of an arborescent copolymer micelle.

4.3 Experimental Procedures

4.3.1 Characterization and Sample Preparation

Nuclear Magnetic Resonance (NMR) Spectroscopy. ^{1}H NMR spectroscopy served to quantify the deprotection level of the PBG substrate polymers and to ensure the purity of the linear polymers serving as side chains after their synthesis. It also served for the determination of the number-average degree of polymerization (X_n) of the PEO5 and PtBuGlu2 chains, as well as to estimate the molecular weight of the arborescent copolymers containing PtBuGlu, since SEC analysis could not be employed for that purpose. The instrument used was a Bruker 300 MHz spectrometer. The concentration of all the samples was 15-20 mg/mL and 16 scans were averaged.

^{19}F NMR spectroscopy was used to determine the chain end primary amine functionality level, f_{NH2}, of the polymers used in the grafting reactions. The procedure followed was adapted from Ji et al.[32] and was applied successfully in Chapter 3 to

demonstrate the living character of the linear PBG chains. The instrument used was a Bruker 300 MHz spectrometer. The concentration of all the samples was 30-35 mg/mL and 64 scans were averaged. A detailed experimental procedure is provided in Section 4.3.5.

Size Exclusion Chromatography (SEC) Analysis. Analysis of the PGlyAc linear chains was performed on a Viscotek GPCmax instrument equipped with a TDA 305 triple detector array and a Viscotek UV Detector 2600. Size exclusion was performed with three Polyanalytik Superes™ Series linear mixed bed columns in series having linear polystyrene molecular weight ranges of up to 400×10^3, 4×10^6, and 20×10^6, all columns having dimensions of 300 mm × 8 mm. A flow rate of 1.0 mL/min and a temperature of 35 ºC were used for the THF mobile phase.

The analysis of the PEO and PtBuGlu linear chains and all the arborescent copolymers was performed on a SEC instrument using DMF as the mobile phase. It consisted of a Waters 510 HPLC pump, a 50 μL injection loop, and a Waters 2410 differential refractometer (DRI) detector. A Wyatt MiniDAWN laser light scattering detector operating at a wavelength of 690 nm served to determine the absolute molecular weight of the graft polymers. The column used was a 500 mm × 10 mm Jordi Gel Xstream H_2O Mixed Bed model with a linear polystyrene molecular weight range of 10^2–10^7. The mobile phase was DMF with LiCl (1 g/L, added to minimize adsorption of the polymer onto the column) at a flow rate of 1.0 mL/min at room temperature.

Preparative SEC was carried out on a system consisting of a Waters M45 HPLC pump, a 2-mL sample injection loop, a Waters R401 differential refractometer detector, and either a Jordi Gel DVB 1000 Å 250 mm × 22 mm or a Jordi Gel DVB Mixed Bed 250 mm ×

22 mm preparative SEC column. DMF with 0.2 g/L LiCl served as the mobile phase at room temperature at a flow rate of 3.0 mL/min. The crude polymer samples were injected as 20-30 mg/mL solutions in DMF with 0.2 g/L LiCl.

Refractive Index Increment Determination. Measurement of the refractive index increment (dn/dc) of the linear polymers (PGlyAc, PEO) was necessary to determine the absolute molecular weight of the samples by SEC. These were determined on a Brookhaven Instruments BI-DNDC 620 Differential Refractometer with a wavelength of 620 nm, using five polymer solutions in DMF ranging from 1 to 5 mg/mL at 30 ºC.

Infrared Analysis. The qualitative analysis of the terminal azide functionality for PGlyAc32 was determined by infrared analysis as discussed in Section 4.4.1. The analysis was performed on a Bruker Vector 22 FT-IR spectrometer, with OPUS 6.0 software to acquire and manipulate the spectra. The analysis was performed with 64 scans from 400 to 4000 cm^{-1} at 1 cm^{-1} resolution. The PGlyAc32 sample was prepared by placing the viscous polymer directly between salt (NaCl) plates.

Dynamic Light Scattering. Batch-wise dynamic light scattering measurements were carried out on a Brookhaven BI-200SM light scattering goniometer equipped with a BI-APD (avalanche photodiode) detector and a Claire Lasers CLAS2-660-140C (120 mW) laser operating at 660 nm. All the samples were measured at 25 °C and a scattering angle of 90°. The samples were filtered twice with a 3 μm PTFE membrane filter before the analysis. The correlator was operated in the exponential sampling mode and hydrodynamic diameters were calculated from the z-average translational diffusion coefficients obtained from first- and second-order cumulant analysis of the correlation function, to better account for

polydispersity effects. Solutions were prepared at concentrations ranging from 0.1-2 % w/v, depending on the molecular weight (generation number) of the sample. If a solvent exchange was necessary, 3 mL of sample solution was placed in a 12,000-14,000 molecular weight cut-off regenerated cellulose dialysis bag overnight in at least 200 mL of the new solvent. The next day, the solvent was replaced and left stirring for at least 2 h longer to ensure complete removal of the original solvent.

4.3.2 Solvent and Reagent Purification

N,N'-Dimethylformamide (DMF; Aldrich, peptide synthesis grade) was purified by distillation under reduced pressure and was stored in the dark to prevent degradation due to photochemical reactions. Dimethylsulfoxide (DMSO, Caledon, 99.9%), and *n*-hexylamine were purified by stirring overnight with CaH_2 and distillation under reduced pressure. The DMF, DMSO, and *n*-hexylamine were stored under nitrogen in round-bottomed flasks (RBF) over 3 Å molecular sieves (EMD). Ethyl acetate (Caledon, 99+%) was dried by stirring overnight with $LiAlH_4$ under nitrogen and distilled immediately before use. Tetrahydrofuran (THF) used for anionic polymerization was distilled over sodium-benzophenone ketyl (Aldrich, 99%) under nitrogen. Toluene used for anionic polymerization was distilled over oligostyryllithium under nitrogen. Ethylene oxide (EO, Air Liquide) was purified using phenylmagnesium chloride as a drying agent under high vacuum described in Section 4.3.4. 2,3-Epoxy-1-(1-ethoxyethoxy)propane (glycidol, Aldrich, 95%), ethyl vinyl ether (Aldrich, 99%), *p*-toluenesulfonic acid monohydrate (Aldrich, ≥98.5%), sodium hydrogen carbonate ($NaHCO_3$, Aldrich, 99%), diphenylmethane (Aldrich, 99%), naphthalene (Aldrich, 99%), triisobutylaluminum (Aldrich, 1.0 M in hexanes), 3-aminopropanol (Aldrich, ≥99%),

tetrabutylammonium azide (Aldrich), phenylmagnesium chloride (Aldrich, 2.0 M in THF), N,N'-diisopropylcarbodiimide (DIC; Aldrich, 99%), γ-*tert*-butyl L-glutamic acid (Bachem, >99%), HBr solution (Aldrich, 33%w/w in acetic acid), 1-hydroxybenzotriazole (HOBt; Fluka, water content ca. 15% w/w), trifluroroacetic acid (TFA, Caledon), methanol (EMD), diethyl ether (EMD), triethylamine (TEA, EMD, Reagent grade), acetic anhydride (Caledon, >99%), tetrahydrofuran (THF, Aldrich, ≥99%), triphosgene (Aldrich, 98%), $LiAlH_4$ (Aldrich, 95%), magnesium sulfate ($MgSO_4$, anhydrous 97%, Fisher), deuterated DMSO (d_6-DMSO, Cambridge isotopes, 99.9% D), and deuterated chloroform ($CDCl_3$, Cambridge isotopes, 99.9% D) were used as received from the suppliers.

4.3.3 Synthesis of Arborescent PBG Cores

The synthesis of partially deprotected arborescent poly(γ-benzyl L-glutamate) (PBG) cores of generations G1, G2, and G3 was carried out according to the procedures described in Chapter 3. The target deprotection level for the arborescent substrates was 30 mol%, i.e. the same as for the arborescent PBG syntheses.

4.3.4 Synthesis of Linear Polymers

Synthesis of 2,3-Epoxy-1-(1-ethoxyethoxy)propane (Glycidol Acetal). The synthetic procedure used was as described by Fitton et al.[33] 2,3-Epoxypropanol (40.0 g, 0.54 mol) and ethyl vinyl ether (200 mL) were loaded in a 500 mL RBF with a magnetic stirring bar and immersed in an ice-water bath. A catalytic amount of *p*-toluenesulfonic acid monohydrate (1.0 g, 5.3 mmol) was then added slowly, to ensure that the reaction temperature did not exceed 40 ºC and avoid the evaporation of ethyl vinyl ether. The reaction was removed from

the ice bath and allowed to warm to room temperature and proceeded for 3 h. A solution of saturated sodium hydrogen carbonate was then added until the pH was slightly basic (approx. 100 mL). The organic layer was isolated, dried over $MgSO_4$, and concentrated under reduced pressure. Distillation of the residue under reduced pressure gave the monomer as a colorless liquid that was stored under nitrogen at 4º C. Yield: 61.5 g (78%); ^{1}H NMR: (300 MHz, $CDCl_3$) δ: 4.65 (q, 1H), 3.75-3.19 (m, 4H), 3.04 (m, 1H), 2.68 (m, 1H), 2.50 (m, 1H), 1.17 (d, 3H), 1.10 (t, 3H).

Synthesis of Diphenylmethylpotassium. The procedure used for the synthesis of diphenylmethylpotassium (DPMK) was adapted from Normant and Angelo.[34] A 3-neck RBF with a magnetic stirring bar was attached to a high-vacuum line, flame-dried, and purged with nitrogen. Dry THF (150 mL) was added to the flask, followed by potassium metal (4.26 g, 109.2 mmol, 2 eq) cut into small pieces and naphthalene (7.0 g, 54.6 mmol, 1 eq). The solution became dark green and was allowed to stir for 30 min. Diphenylmethane (18.3 mL, 108.7 mmol, 2 eq) was then added to the flask with a syringe. The reaction was allowed to proceed overnight to give a dark red DPMK solution that was stored at room temperature under nitrogen.

Titration of the DPMK solution was performed using acetanilide under nitrogen. A 3-neck RBF was attached to the high vacuum line, flame-dried, and purged with nitrogen. THF (30 mL) was added, followed by a few drops of DPMK solution, until the solution remained a pale yellow color. Acetanilide (53.0 mg, 0.39 mmol) was added to the RBF, at which point the color disappeared. The DPMK solution was slowly added (0.77 mL) to obtain the same pale yellow color present initially. This volume corresponded to a DPMK concentration of 0.51 M.

Synthesis of α-Amino Poly(glycidol acetal) (Amino-PGlyAc9). In a typical anionic polymerization procedure, the monomer is purified on the high-vacuum line and transferred to an ampoule immediately before use. The glycidol acetal monomer could not be purified by that technique due to its high boiling point of 152-154 ºC however.[33] It was rather distilled over triisobutylaluminum in a fractional vacuum distillation set-up directly before use. Glycidol acetal (40.0 g) was placed in a 100 mL RBF equipped with a stirring bar and was purged with nitrogen. Triisobutylaluminum (2 mL, 2 mmol) was added to the flask with stirring. The flask became warm within minutes of adding the triisobutylaluminum. After the flask had cooled to room temperature the glycidol acetal was distilled under reduced pressure into a RBF that was then sealed with a rubber septum and purged with nitrogen.

A 3-neck RBF with a stirring bar was attached to the vacuum line, flame-dried under high vacuum, and purged with nitrogen. Dry THF (25 mL) was added to the RBF, followed by DPMK drop-wise until a faint yellow color persisted in the solution. 3-Aminopropanol (0.19 mL, 2.53 mmol) was then added, followed by DPMK (5.1 mL, 0.51 M) to deprotonate the alcohol. The solution became milky, but DPMK was added further until the solution maintained a faint yellow/red color for one minute. Freshly distilled glycidol acetal (25.2 g, 0.173 mmol, target X_n = 68, M_n = 10,000) was added and the flask was sealed. The temperature was increased to 65 ºC using an oil bath and the reaction was left stirring overnight under nitrogen. Degassed acidified methanol was then added to terminate the reaction. The solution was transferred to a regenerated cellulose dialysis bag with a 1000 molecular weight cutoff (MWCO) and left to stir in THF. The THF bath was changed once after 3 h and left to stir overnight. The dialysis bag was then emptied into a RBF and the THF was evaporated under vacuum to give a reddish-brown viscous polymer. Yield: 16.4 g (65%).

SEC (THF): M_n = 9100, M_w/M_n= 1.08; ^{1}H NMR: (300 MHz, CDCl3) δ: 4.66 (q, 1H), 3.70-3.39 (m, 7H), 1.24 (d, 3H), 1.15 (t, 3H) (initiator fragment protons not visible).

Synthesis of α-Azido PGlyAc32. To obtain a high molecular weight poly(glycidol acetal) sample (target M_n = 30,000), a different polymerization method was necessary to avoid a high polydispersity due to chain transfer reactions.[35,36] The procedure was adapted from Gervais et al.[36] The initiator tetrabutylammonium azide (0.38 g, 1.33 mmol) was dried before use by three cycles of azeotropic distillation with dry toluene under vacuum, and stored under nitrogen after redissolution in 20 mL of toluene in a glass ampoule sealed with a Teflon stopcock. A 1-L, 5-neck RBF was evacuated under high-vacuum, flame-dried, and purged with nitrogen. Dry toluene (400 mL) was then added and the RBF was cooled to -30 ºC with dry ice in a 2-propanol/water bath. Glycidol acetal (40.0 g, 0.274 mol, target X_n = 206, M_n = 30,000, freshly distilled over triisobutylaluminum), the initiator solution, and triisobutylaluminum (5.9 mL of solution, 5.9 mmol) were added in succession, and the 2-propanol/water bath was removed to allow the temperature to increase to room temperature. The reaction was left to run overnight, and degassed acidified methanol was added to terminate the reaction. The toluene solution was concentrated to approximately 50 mL and transferred to a regenerated cellulose dialysis bag with a 1000 MWCO and left to stir in THF. The THF bath was changed once after 3 h and left to stir overnight. The dialysis bag was then emptied into a RBF and the THF was evaporated to give a clear viscous polymer. Yield: 34.5 g (86%). IR: -N_3 stretch at 2102 cm^{-1}. SEC (THF): M_n = 32,400, M_w/M_n= 1.19; ^{1}H NMR (300 MHz, CDCl3) δ: 4.66 (q, 1H), 3.67-3.35 (m, 7H), 1.24 (d, 3H), 1.15 (t, 3H).

Reduction of α-Azido PGlyAc32 to α-Amino PGlyAc32. Reduction of the α-azide to an α-amine group was done by loading α-azido PGlyAc32 (30.0 g) into a 1-L RBF with 300 mL

of THF under nitrogen, and adding a solution of lithium aluminum hydride ($LiAlH_4$, 6.0 g in 200 mL of THF). The reaction was refluxed for 3 h, and left at room temperature overnight. Water (10 mL) was finally added slowly to destroy the excess $LiAlH_4$. The solution was centrifuged to remove salts, and placed in a 1000 MWCO regenerated cellulose dialysis bag in THF overnight, producing a clear reddish brown viscous polymer. Yield: 24.0 g (80%). IR: disappearance of $-N_3$ stretch at 2102 cm^{-1}. ^1H NMR: (300 MHz, CDCl3) δ: 4.66 (q, 1H), 3.67-3.35 (m, 7H), 1.24 (d, 3H), 1.15 (t, 3H).

Ethylene Oxide Purification. **Caution**: EO is highly toxic and volatile (b.p. 10 ºC), so it should be manipulated with great care in a well-ventilated fume hood, and the pure monomer should be cooled as much as possible to avoid excessive pressure buildup. Ethylene oxide (EO) was purified on a high-vacuum line using a manifold with connections for the EO tank line, and an ampoule containing a Teflon stopcock, a magnetic stirring bar, and approximately 2 g of calcium hydride as a drying agent. The manifold and the ampoule were evacuated and flame-dried, and EO (approximately 100 g) was condensed under vacuum to the ampoule by cooling it in liquid nitrogen. The ampoule was then mounted on another vacuum manifold equipped with an RBF containing a magnetic stirring bar, and another ampoule with a Teflon stopcock. The EO was degassed with three successive freeze-pump-thaw cycles. After closing the ampoule containing the EO, the rest of the manifold was evacuated and flame-dried. After purging the apparatus with nitrogen, phenylmagnesium chloride solution (PhMgCl, 9 mL, 2.0 M in THF) was added to the RBF on the manifold with a syringe. The THF was removed under vacuum and ca. 15 g of EO was transferred to the RBF containing the PhMgCl. The monomer was stirred for 1 h in an ice bath before slowly transferring it over to the empty storage ampoule. The amount of EO transferred was 12.3 g.

Polymerization of EO. A 5-neck 500-mL RBF with a magnetic stirring bar was attached to the high-vacuum line with the sealed ampoule containing the EO monomer (cooled with dry ice). The RBF was evacuated, flame-dried, purged with nitrogen, and dry THF (120 mL) was added followed by DPMK solution drop-wise until a faint yellow color persisted in the solution. 3-Aminopropanol (0.19 mL, 2.53 mmol) was then added, followed by DPMK (5.1 mL, 0.51 M) to deprotonate the alcohol. The solution became milky, and DPMK was added further until a faint yellowish-red color persisted for 1 min in the solution. The EO monomer (12.3 g, 0.279 mol, target X_n = 110, M_n = 5000) was then transferred under vacuum and the reaction temperature was brought to 45 ºC with an oil bath. The reaction was allowed to proceed for 6 d, after which time a dark brown solution was obtained. Degassed acidified methanol was added to terminate the reaction. The solution was concentrated to approximately 50 mL under vacuum and precipitated in cold diethyl ether. A brown powder was recovered by suction filtration. It was redissolved in methanol and precipitated in cold diethyl ether, recovered by suction filtration, and dried under vacuum overnight to produce an off-white powder. Yield: 8.5 g (69%). SEC (DMF): M_n^{app} = 6200, M_w/M_n^{app} = 1.16. ^{1}H NMR: (300 MHz, CDCl3): X_n = 114, δ: 3.87-3.37(m, 456H), 2.88 (br, 1H), 1.96 (br, -OH).

Synthesis of γ-tert-Butyl L-Glutamic Acid N-Carboxyanhydride (tBuGlu-NCA). The procedure used was similar to the one reported for the synthesis of γ-benzyl L-glutamic acid N-carboxyanhydride in Section 3.3.3. γ-*tert*-Butyl L-glutamic acid (10.0 g; 49.2 mmol) was suspended in 300 mL of dry ethyl acetate in a 1-L RBF fitted with a refluxing condenser and a gas bubbler. The flask was purged with N_2 and heated to reflux. Triphosgene (5.6 g, 18.7 mmol) was then added and refluxing was continued for 3 h. The flask was removed, stoppered, and cooled in a freezer (–10 °C) for 1 h. The solution was transferred to a cold

separatory funnel and quickly washed successively with 100 mL of ice-cold water and 100 mL of chilled 0.5% aqueous $NaHCO_3$ solution. The organic phase was dried over anhydrous $MgSO_4$, filtered, and concentrated to ca. 100 mL on a rotary evaporator. An equal volume of cold (–10 °C) hexane was then added to induce crystallization of the product. The mixture was left in the freezer overnight and the solid product was recovered by filtration in a Schlenk funnel under N_2. It was then dried overnight under vacuum to yield a white powder, and stored under N_2 in a freezer (-20 °C).Yield = 8.6 g (76 %). ^{1}H NMR (300 MHz, $CDCl_3$) δ: 6.75 (s, 1H), 5.11 (s, 2H), 4.38–4.33 (t, 1H), 2.59–2.53 (t, 2H), 2.35–2.21 (m, 1H), 2.21–2.02 (m, 1H), 1.42-1.37 (s, 9H).

Polymerization of tBuGlu-NCA. The procedure used was similar to the one reported for the polymerization of γ-benzyl L-glutamic acid N-carboxyanhydride in Section 3.3.3. The tBuGlu-NCA monomer (1.87 g, 8.1 mmol) was dissolved in dry DMF (15 mL) in a 100-mL RBF at 0 °C and *n*-hexylamine (50 μL, 0.38 mmol, for a target X_n = 20) was added with rapid stirring. The reaction was allowed to proceed for 5 d at 0 °C. The linear polymer was recovered by precipitation in diethyl ether, suction filtration, and drying under vacuum overnight to give a white powder. Yield = 0.8 g (53%). SEC (DMF): M_w/M_n = 1.15. ^{1}H NMR(300 MHz, d_6-DMSO): X_n = 11.8, δ: 4.19 (br, 12H), 2.24-2.18 (br, 24H), 1.81-1.69 (m, 24H), 1.34 (s, 108H), 1.25-1.13 (b, 10H), 0.81–0.79 (t, 3H).

4.3.5 Quantification of Primary Amines by ^{19}F NMR Analysis

The terminal primary amines on the linear polymers were quantified by a procedure adapted from Ji et al.[32] using ^{19} F NMR analysis. For example, a linear PEO sample synthesized from 3-aminopropanol, α-amino PEO5 (0.115 g, 2.25×10^{-5} mol of chains) was dissolved in 3 mL

of deuterated DMSO (d_6-DMSO). A solution of trifluorobenzaldehyde (TFBA, 0.1191 g, 6.84×10^{-4} mol), and benzotrifluoride (BTF, 0.1014 g, 8.15×10^{-4} mol) in 2 g of d_6-DMSO was prepared (BTF served as an internal standard). The reagent solution (0.2306 g, 7.07×10^{-5} mol TFBA, 7.18×10^{-5} mol BTF) was added to the polymer solution and stirred for 2 h; a 0.5 mL sample was then transferred to an NMR tube for analysis. The integrated peak areas from the ^{19}F NMR spectra were used to determine the f_{NH2} values as described in Section 4.4.1.

4.3.6 Synthesis of Arborescent Copolymers

The coupling reaction to generate arborescent copolymers was similar to the coupling reaction used to generate arborescent PBG. A 25% excess of side chains was added in the reaction to account for any primary amine deactivation before or during the coupling reaction. The solvent serving in the coupling reactions depended on the side chains used. The preferred solvent for the coupling reactions was DMSO for reasons discussed in Chapter 3. The coupling reactions with PEO side chains were performed in DMSO. DMF served for the coupling reactions involving the PGlyAc and PtBuGlu side chains, since these had limited solubility in DMSO. An example of a coupling reaction is provided below for the PGlyAc32 side chains.

Synthesis of G1PBG-g-PGlyAc32. The partially deprotected polymer serving as substrate, G1PBG (0.012 g, 0.022 mmol $-CO_2H$, 1 eq) and the side chain polymer (PGlyAc32, 0.90 g, 0.028 mmol $-NH_2$, 1.25 eq) were dissolved in dry DMF (5 mL) in a 25-mL RBF. The peptide coupling reagents N,N'-diisopropylcarbodiimide (DIC, 14 μL, 0.090 mmol, 5 eq) and 1-hydroxybenzotriazole (HOBt, 12 mg, 0.090 mmol, 5 eq) were then added to the reaction followed by triethylamine (TEA, 19 μL, 0.140 mmol, 6.3 eq). The reaction was allowed to

proceed for 24 h at room temperature in the dark before adding *n*-hexylamine (9 μL, 0.090 mmol, 5 eq), to deactivate residual carboxylic acid sites. After 1 h the product was diluted with 25 mL of DMF and purified by preparative SEC. The purified arborescent copolymer was dialyzed against THF in a 1000 MWCO bag overnight and stored in solution at 4 ^{o}C until needed. SEC (DMF): Grafting yield = 15%, M_n = 3,080,000, M_w/M_n = 1.06 (MALLS).

The arborescent copolymers with PEO5 and PtBuGlu2 side chains were synthesized by the same procedure, but DMSO served as solvent in the PEO5 reactions. Both sample series were purified by preparative SEC in DMF and recovered by precipitation in cold diethyl ether, suction filtration, and drying under vacuum.

Deprotection of G1PBG-g-PGlyAc32. The acetal protecting group of the G1PBG-*g*-PGlyAc32 copolymer had to be removed to obtain water-soluble micelles. Different deprotection methods attempted and will be discussed briefly in the results and discussion section of this chapter. The most successful approach for the arborescent copolymers was adapted from a method reported by Mendrek et al.[37] The copolymer G1PBG-*g*-PGlyAc32 (0.130 g, 0.120 g GlyAc units, 0.82 mmol GlyAc) was placed in a 25-mL RBF equipped with a magnetic stirring bar and DMF (8 mL). A concentrated hydrochloric acid (HCl) solution (11.7 M, 0.32 mL, 3.72 mmol HCl) was then added and the reaction was stirred for 30 min at room temperature, at which point a saturated $NaHCO_3$ aqueous solution was added until the acid was neutralized (pH > 7, ca. 4 mL). The solvents were removed under reduced pressure and the polymer was redissolved in ethanol. Insoluble salt were removed by suction filtration, and the crude product was placed in a 12,000-14,000 MWCO dialysis bag in methanol to remove linear polyglycidol fragments that may have been cleaved during the deprotection step. The copolymer was stored in solution in a refrigerator at 4º C.

Deprotection of G1PBG-g-PtBuGlu2. The purified copolymer G1PBG-*g*-PtBuGlu2 (40 mg) was dissolved in trifluoroacetic acid and stirred for 5 min. The copolymer was then recovered by precipitation in diethyl ether, suction filtration, and drying under vacuum overnight to yield a white solid. Yield: 25 mg (78%).

4.4 Results and Discussion

4.4.1 Synthesis of α-Amino Linear Polymers

Several linear polymers containing a primary amine chain end functionality were used to demonstrate the synthesis of water-soluble arborescent copolymer micelles.

Synthesis of α-Amino Poly(glycidol acetal). Polyglycidol contains a poly(ethylene oxide) backbone with a $-CH_2OH$ side-group in every structural unit. This characteristic appears advantageous in comparison with PEO, as it hinders the formation of crystalline domains in polyglycidol. Polyglycidol otherwise displays low toxicity, similarly to PEO.[38] The additional hydroxyl groups in polyglycidol also allow further chemical modifications and make it appealing to target specific applications.

The procedure for the synthesis of α-amino-PGlyAc9 was adapted from Dworak et al.,[39] using the initiator 3-aminopropanol to produce poly(glycidol acetal) with a terminal primary amine functionality. 3-Aminopropanol was deprotonated with DPMK to produce an alcoholate capable of initiating the polymerization of glycidol acetal. The amine protons of the initiator molecule do not disrupt the polymerization reaction, as they are orders of magnitude less labile than the proton from the alcohol group on the initiator. For comparison,

1-propanol has a pK_a of 16, whereas primary amines have a pK_a of ca. 36. Therefore the abstraction of a proton from the amine group by the alcoholate functionality is impossible.

The anionic polymerization of unprotected glycidol leads to a branched polymer structure due to the fast exchange between the alcoholates and the hydroxyl groups present in the polymer chain. This causes significant branching, which has occasionally proven to be useful.[40] To obtain a linear polymer with a narrow molecular weight distribution, a protected form of glycidol must be used. The procedure developed by Fitton et al.[33] yields a protected glycidol monomer in the acetal form, suitable for anionic polymerization, in high yield and purity. The polymerization of glycidol acetal with the 3-aminopropanol/DPMK initiator system, to obtain linear PGlyAc with a primary amine terminal functionality, is depicted in Figure 4.3.

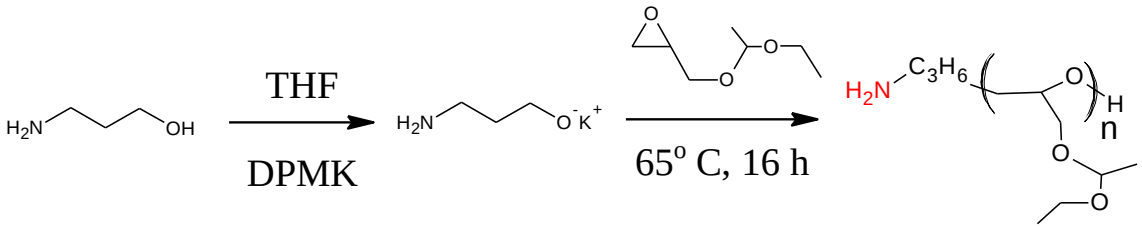

Figure 4.3 Polymerization of glycidol acetal with 3-aminopropanol and DPMK.

Due to the high boiling point of the glycidol acetal monomer (152-154 ºC),[33] it could not be dried using high-vacuum line purification techniques often employed for monomers in anionic polymerization. To achieve the high level of monomer purity required for anionic polymerization, purification was first attempted by simple distillation without additives immediately before the reaction, with a simple reduced pressure distillation setup.

Polymerization reactions using that monomer gave molecular weight distributions broader than typically expected for anionic procedures ($M_w/M_n \geq 1.20$). An additional attempt to distill the monomer from calcium hydride prior to use also had little influence on the polydispersity. Triisobutylaluminum was finally explored as a drying agent, as it is known to act as proton scavenger[41] and is safe to use with glycidol acetal since it has been employed in the activated monomer polymerization of glycidol acetal.[36] This monomer purification technique yielded much better results with respect to the polydispersity of poly(glycidol acetal), with $M_w/M_n \leq 1.10$.

Synthesis of α-Amino Poly(glycidol acetal). The synthesis of α-*azido* PGlyAc32 relied upon an activated oxirane monomer polymerization method introduced by Carlotti et al.,[35] using azide salt initiators along with glycidol acetal. [42] The activated monomer polymerization mechanism initiated by an azide salt is depicted in Figure 4.4. This polymerization technique allows the synthesis of poly(glycidol acetal) with M_n up to 30,000, while maintaining a relatively low polydispersity ($M_w/M_n \leq 1.30$).

The azide functionality of α-azido poly(glycidol acetal) was reduced to a primary amine using $LiAlH_4$ in THF. The reduction was easily monitored by infrared (IR) analysis, since azide stretching vibrations produce a strong absorption near 2100 cm^{-1}. The disappearance of this peak should therefore be indicative of the presence of a primary amine at the chain end, even if the molecular weight of the polymer is relatively high. This is seen in Figure 4.5, by comparing IR spectra obtained before and after the reduction reaction. To ensure that no degradation occurred during reduction SEC measurements were compared before and after the reaction, yielding M_w/M_n values of 1.19 and 1.20, respectively.

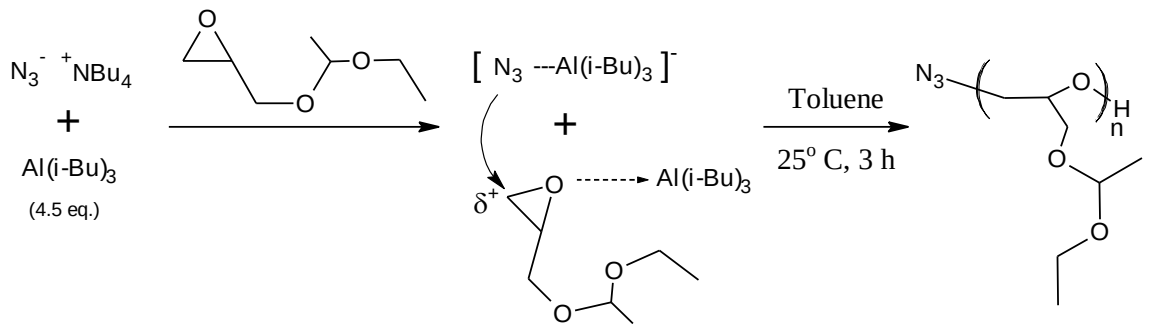

Figure 4.4 Activated monomer mechanism for the anionic polymerization of glycidol acetal initiated by tetrabutylammonium azide.

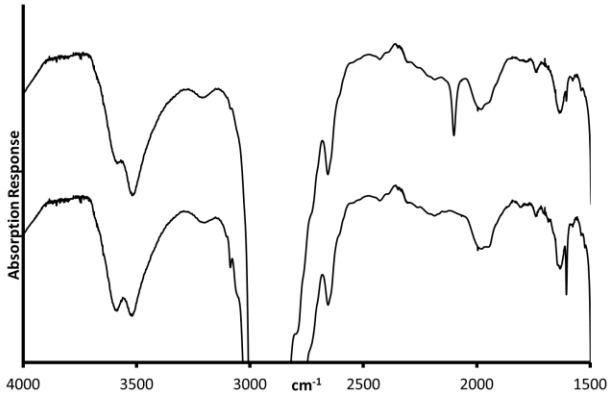

Figure 4.5 IR Spectra for α-azido PGlyAc32 (top) and α-amino PGlyAc32 (bottom).

^{1}H NMR analysis served to confirm that no deprotection occurred during the synthesis and the isolation of the PGlyAc samples. The initiator protons from 3-aminopropanol (for PGlyAc9) and the protons α to the azide or amine functionality (for PGlyAc32) were not resolved from the repeating units, and therefore no M_n values could be derived from ^{1}H NMR analysis. Table 4.1 provides the molecular weight and polydispersity of the poly(glycidol acetal) samples used in the grafting reactions with the PBG substrates, as determined by SEC analysis.

Table 4.1 Characteristics of the linear polymer chains used to generate the arborescent copolymer micelles

	SEC[a]		^{1}H NMR		^{19}F NMR
Polymer	M_n	M_w/M_n	X_n[b]	M_n[c]	f_{NH2}(%)[d]
PGlyAc9	9,100	1.08	-	-	64
PGlyAc32	32,400	1.19	-	-	-
	M_n^{app}	M_w/M_n			
PEO5	6,200	1.16	114	5,100	91
PtBuGlu2	3,200	1.20	11.8	2,300	99

[a] PGlyAc analyzed on a triple detection SEC system in THF using dn/dc = 0.045 mL/g.[37] PEO and PtBuGlu analyzed on a SEC system with a DRI detector, in DMF with 0.1 % LiCl, so only apparent molecular weights are reported; [b] number-average degree of polymerization; [c] M_n calculated from X_n; [d] terminal primary amine content determined from ^{19}F NMR analysis according to Ji et al.[32]

Synthesis of α-Amino Poly(ethylene oxide). Poly(ethylene oxide) is well-known for being biocompatible and water-soluble, so it is a natural choice as a hydrophilic shell material for the arborescent copolymers. There are different alternatives to obtaining primary amine-terminated poly(ethylene oxide). Commercially available PEO with a terminal hydroxyl group can be modified through either halogenation[43] or tosylation[44] of the hydroxyl group, which can then be converted to an azide functionality. Reduction of the azide yields a terminal primary amine functionality. Since this approach involves multiple reaction steps, the probability of incomplete or side reactions leading to lower levels of amine functionality is increased. It therefore seemed more practical to make use of the anionic polymerization of ethylene oxide with a bifunctional initiator to ensure a high level of amine functionality. Table 4.1 provides the molecular weight and polydispersity of the PEO5 sample used in the grafting reactions. ^{1}H NMR spectra for a commercial PEO monomethyl ether sample with M_n = 5000 and the α-amino PEO5 sample synthesized are compared in Figure 4.6. For α-amino PEO5, a number-average degree of polymerization (X_n) of 114 was calculated from

the integrated intensities for the -CH_2- protons next to the terminal amine (δ 2.9 ppm) relatively to the four protons in the repeat units. This corresponds to a M_n = 5100. The peak near δ 2.8 ppm is due to residual diethyl ether.

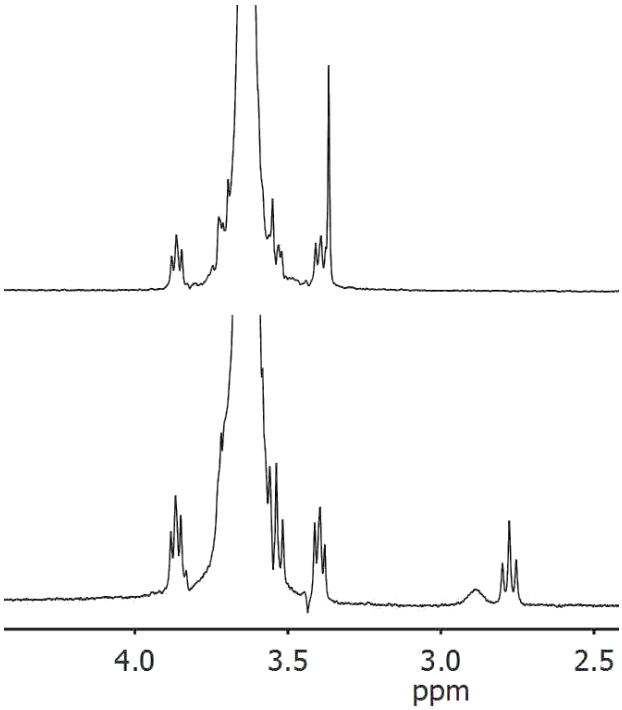

Figure 4.6 ^{1}H NMR Spectra for PEO5 monomethyl ether (top) and synthesized α-amino PEO5 (bottom) in $CDCl_3$.

The primary amine functionality level, f_{NH2}, is also reported in Table 4.1. Following a procedure developed by Ji et al.,[32] the terminal amine of α-amino PEO5 was reacted with trifluorobenzaldehyde (TFBA) to determine the fraction of polymer chains containing a primary amine functionality. The same procedure was applied in Chapter 3 to the analysis of linear PBG. The amine quantification reaction with TFBA is described in Figure 4.7. The reaction produces an imine that changes the environment of the fluorine atoms on the benzene ring of TFBA. A ^{19}F NMR spectrum obtained for the PEO5 amine quantification

reaction using TFBA and BTF is shown in Figure 4.8. Three molar equivalents of TFBA were used to ensure that the PEO5 chains reacted completely with TFBA. Three equivalents of BTF were also used as internal standard in the measurement.

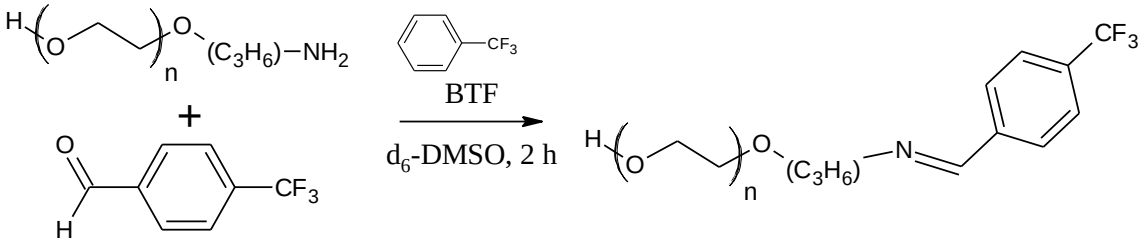

Figure 4.7 Reaction of α-amino PEO5 with trifluorobenzaldehyde to produce an imine quantified by ^{19}F NMR spectroscopy.

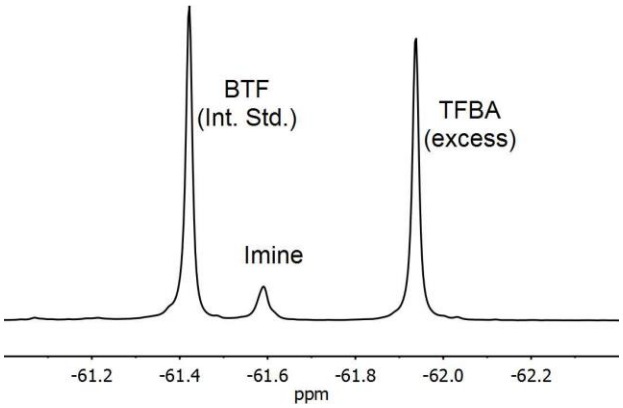

Figure 4.8 ^{19}F NMR spectrum for amine quantification in α-amino PEO5.

Equation 4.1 shows how f_{NH2} was determined by integration of the peaks in the ^{19}F NMR spectrum. Since the number-average molecular weight of the polymer is known (M_n = 5100), it is possible to determine the number of moles of chains present in the reaction. The integration value for the imine fluorides (0.287) was thus compared to the integration value for the BTF fluorides (internal standard, 1.000) to give f_{NH2} = 0.91. Since there are errors

involved in determining the exact M_n value for PEO5 by ^{1}H NMR analysis and in the amine quantification procedure, the f_{NH2} value also has an uncertainty associated with it. Fortunately, the accuracy of this value is not critical since an excess of side chains was used in the coupling reactions. It rather served to confirm that terminal primary amine functionalities were indeed present on the linear polymers, and therefore that the anionic polymerization reaction using 3-aminopropanol as bifunctional initiator was successful. The same amine quantification procedure was carried out for PGlyAc9 and PGlyAc32. Sample PGlyAc9 produced an f_{NH2} = 0.64; however, PGlyAc32 did not produce a detectable signal for the imine even with a reaction time of 4 h, likely due to the larger chain length of the polymer. The PGlyAc32 polymer was used in the grafting reactions, even though no primary amine quantification was possible for that sample.

$$\boldsymbol{f_{NH2} = \frac{mol\ imine}{mol\ polymer\ chains} = \frac{mol\ BTF \times \left(\frac{Imine\ integration}{BTF\ integration}\right)}{\left(\frac{g\ of\ polymer}{M_n\ of\ polymer}\right)} = \frac{6.40\times10^{-5} mol \times \left(\frac{0.287}{1.00}\right)}{\frac{0.1030\ g}{5100\ g/mol}} = 0.91} \qquad (4.1)$$

Synthesis of Poly(γ-tert-butyl L-glutamate). Cleavage of the *tert*-butyl ester protecting group from that polymer yields poly(L-glutamic acid) (PGA), known to be a biocompatible water-soluble material at neutral or basic pH, since the carboxylic acid units have a pK_a close to 5. PGA has been used in biomedical applications[45] and should also be useful as hydrophilic shell material for the PBG micelles.

The synthesis of PtBuGlu2 proved to be most difficult among the four linear polymer samples investigated. There is very little published work on the synthesis of PtBuGlu homopolymers. Ngyuen et al. reported the synthesis of PtBuGlu from the NCA monomer in

chloroform at 0º C for up to one week.[46] Polydispersities of 1.34 and 1.16 were reported for polymers with similar DP_n = 63 and 59, respectively, which points at reproducibility issues.

The synthesis of PtBuGlu was attempted by a procedure similar to the one described for linear PBG in Chapter 3; unfortunately, the polymerization did not proceed as expected under these conditions. The ring-opening polymerization of tBuGlu-NCA, shown in Figure 4.9, used *n*-hexylamine with the monomer in DMF at 0º C under nitrogen for 5 days. The polymer yield was low due to incomplete monomer conversion, even though the reaction was allowed to proceed for 2 days longer than for the corresponding linear PBG syntheses. Table 4.1 summarizes the characteristics of the PtBuGlu2 sample used in the grafting reactions. The target DP_n was 20, but an experimental DP_n = 12 was obtained. The polydispersity of the sample nevertheless remained low (M_w/M_n = 1.15), indicating that the polymerization was not affected by side reactions. It was also determined that f_{NH2} = 0.99 for PtBuGlu2. To produce a water-soluble polymer, the *tert*-butyl ester was removed by dissolving it in pure TFA for a few minutes. This reaction also served for the selective deprotection of the shell material once linear PtBuGlu was grafted onto the PBG substrates, to produce poly(L-glutamic acid) (PGA) segments soluble in physiological buffer (pH 7.4).

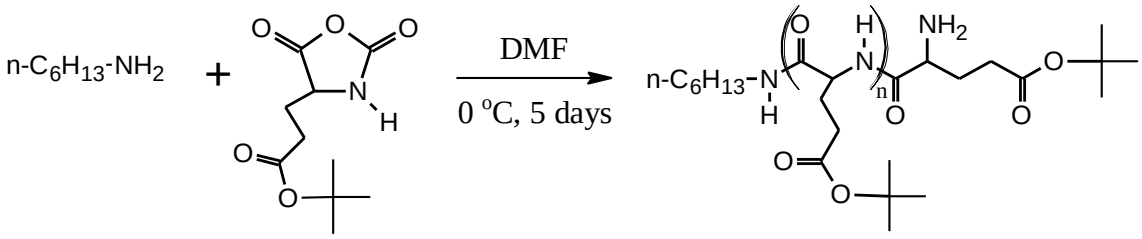

Figure 4.9 ROP of tBuGlu-NCA using *n*-hexylamine as initiator.

The SEC system using DMF was equipped with a MALLS detector, but unfortunately the light scattering signal for PEO5 and PtBuGlu2 was too weak to allow reliable absolute M_n value measurements. Consequently, only apparent M_n values are reported for these polymers. The different linear side chain samples were used for comparison of their grafting efficiency onto PBG substrates in the synthesis of arborescent copolymers, and to determine their ability to yield water-soluble unimolecular micelles.

4.4.2 Synthesis of Arborescent Copolymers: General Comments

Previous amphiphilic arborescent copolymer syntheses reported by Gauthier et al. included polystyrene (PS) substrates randomly chloromethylated[25] or acetylated[27] to generate coupling sites, grafted with poly(2-vinyl pyridine) (P2VP) side chains forming the shell. These systems provide a basis for comparison with arborescent copolymers derived from PBG substrates. The properties of arborescent copolymers can be tailored by adjusting structural parameters in their synthesis, such as the type of polymer side chains forming their shell or the length of the polymer chains attached. The branching density can be controlled through the functionalization level of the substrate, and the overall branching functionality by using different substrate generations. Three different polymer chain compositions were examined to generate randomly grafted arborescent copolymers in the current investigation, to allow a comparison of the grafting yields (defined as the fraction of linear chain segments becoming coupled to the substrate) when using randomly functionalized PBG substrates, and to determine their influence on the solubility of the micelles in aqueous environments. PBG substrates of generations G1-G3 were employed to observe any trends related to variations in the PBG core generation number.

The standard grafting procedure described for the PBG core synthesis in Section 3.3 was also adopted for the preparation of the arborescent copolymers. A 25 mol% excess of linear chain segments was used in all cases to ensure that a maximum number of linear chains could be attached to the PBG substrates, and to compensate for any side reactions that may have occurred to the terminal primary amine groups before or during the grafting reaction. A five-fold excess of coupling agents (DIC and HOBt) was also used with respect to the carboxylic acid functionalities on the substrate to ensure their complete activation. Finally, triethylamine was added to avoid protonation of the terminal primary amine groups on the side chains, known to decrease the reactivity of primary amines significantly.[47,48] Since PGlyAc and PtBuGlu were not very soluble in DMSO, DMF was selected as the solvent for these grafting reactions. While DMSO was the preferred solvent for the grafting reactions reported in Chapter 3, it was also determined that DMF, when properly purified and stored, can likewise serve for that purpose.

Furthermore it was determined that generation 0 arborescent polystyrene (G0PS) substrates have a more open structure as compared to G1-G3PS molecules, which also have a more spherical shape. This was shown to promote the formation of large aggregates by arborescent G0PS-*g*-P2VP copolymers, which were not observed for copolymers based on substrates of generations G1 and above.[27] Consequently, the G0PBG substrate was not considered for the preparation of the amphiphilic copolymer micelles.

4.4.3 Arborescent PBG-*graft*-PGly Copolymers

The results for the grafting reactions of randomly deprotected PBG substrates with the two different PGlyAc side chains are summarized in Table 4.2. Arborescent copolymers were

obtained for the G1PBG and G2PBG substrates, but the reactions failed with the G3PBG substrate and very little grafting (< 2%) took place. This may be due to the denser structure of the G3PBG substrate at the periphery of the molecules in comparison to G2PBG or G1PBG, and the ensuing steric effects hindering the grafting reaction. Gauthier et al. indeed observed enhanced chain crowding for upper generations of PS substrates grafted with linear deuterated PS side chains in small angle neutron scattering (SANS) experiments.[49]

Table 4.2 Characteristics of randomly grafted PBG-*g*-PGlyAc arborescent copolymers

	PBG Substrate			Graft Copolymer			
Copolymer[a]	M_n [b]	% Deprotected[c]	G_y [d]	M_n [b]	M_w/M_n [b]	f_n [e]	% GlyAc[f]
G1PBG-*g*-PGlyAc9	234,000	35	9	661,000	1.10	47	65
G2PBG-*g*-PGlyAc9	1.1×10^6	34	3	1.8×10^6	1.10	75	38
G3PBG-*g*-PGlyAc9	3.0×10^6	34	Failed reaction				
G1PBG-*g*-PGlyAc32	234,000	35	15	3.1×10^6	1.06	88	92
G2PBG-*g*-PGlyAc32	1.1×10^6	26	5	4.2×10^6	1.07	96	74
G3PBG-*g*-PGlyAc32	3.0×10^6	34	Failed reaction				

[a] All reactions done with 25 mol% excess of side chains; [b] absolute values from SEC-MALLS analysis in DMF; [c] deprotection level determined from ^{1}H NMR analysis; [d] grafting yield: fraction of side chains attached to the substrate; [e] branching functionality: number of side chains added in the last grafting cycle; [f] GlyAc weight fraction determined from the absolute molecular weight of the copolymer and the substrate.

The molecular weights of the copolymers in Table 4.2 increased relatively to the PBG substrates, while the polydispersity remained low ($M_w/M_n \leq 1.11$) in all cases. The absolute molecular weight of the substrates and the arborescent copolymers were determined by SEC-MALLS analysis in DMF. When comparing these results with the PS-*g*-P2VP systems reported by Gauthier et al.,[25,27] the grafting yields are lower for the PBG-*g*-PGlyAc systems

and the weight fraction of shell material is also lower. One reason for the lower grafting yields obtained in the present case certainly lies in the 25% molar excess of side chains used in the coupling reactions. The branching functionality, f_n, corresponding to the number of chains segments added in the last grafting reaction, was determined by dividing the molecular weight increase observed for the copolymer by the molecular weight of the linear side chains used. The weight fraction of glycidol acetal in the copolymers (last column in Table 4.2) corresponds to the molecular weight increase for the copolymers divided by their total molecular weight.

The grafting yield (G_y) in the synthesis of arborescent polymers is traditionally determined from the peak area ratio for the graft polymer and the unreacted side chains from the DRI detector in the SEC experiments, as it was done in Section 3.4.3. In the case of graft copolymers, however, the core and the shell components that may have significantly different dn/dc values, which in turn affects the magnitude of their DRI responses. In DMF, the dn/dc values for PBG, PGlyAc, PEO, and PtBuGlu are 0.099, 0.031, 0.044, and 0.097, respectively. The large difference in the dn/dc values for the PGlyAc and PEO versus PBG complicates the grafting yield determination from the DRI signal. To avoid this problem, a different method was developed to determine the grafting yield, based on the weight fraction of each component in the copolymers, along with the known amounts of the substrate and side chains used in each grafting reaction. An example of a grafting yield calculation by that method is provided in Equation 4.2 for sample G1PBG-*g*-PGlyAc32. In this case 0.012 g of PBG substrate and 0.900 g of PGlyAc32 side chains were used in the reaction, and a PGlyAc weight fraction of 0.92 was determined from the molecular weight difference between the copolymer and substrate. Multiplying the known mass of PBG used by the weight fraction

ratios corresponds to a mass of 0.138 g PGlyAc contained in the copolymer. Dividing this mass of PGlyAc by the total mass used in the grafting reaction (0.900 g PGlyAc), a grafting yield of 15% is obtained.

$$G_y = \frac{mass\ PBG\ (g) \times \frac{Wt.Fraction\ PGlyAc}{Wt.Fraction\ PBG}}{mass\ PGlyAc\ (g)} = \frac{0.012 \times \frac{0.92}{0.08}}{0.900} = 0.15 \quad \textbf{(4.2)}$$

Several factors should contribute to the relatively low grafting yield observed in these experiments such as core chain flexibility (mobility), the functionalization (deprotection) level of the substrate, and the reactivity of the functional groups. Beyond the use of a 25% excess of side chains mentioned earlier, the lack of core flexibility is presumably a dominant factor limiting the extent to which the linear chains can penetrate into the substrate and react with the randomly distributed coupling sites. The deprotection reaction for the PBG substrates is assumed to proceed randomly; based on that assumption, a significant fraction of the coupling sites must be located deeper inside the core of the PBG substrate and be less accessible in the grafting reaction. If the PBG core behaves like a rigid branched system, it will be difficult for the linear PGlyAc chains to access these coupling sites. In the PS-*g*-P2VP systems previously examined PS is known to maintain a random coil conformation in THF, the solvent used for the grafting reactions. Even though the arborescent PS substrates are highly branched, they should maintain a certain level of chain mobility. This allows linear chains to penetrate deeper into the core, and ultimately to better access to the coupling sites. In a previous study, in was shown that a grafting reaction of P2VP side chains with $M_n \approx$ 35,000 onto a G1PS substrate proceeded in 34% yield; this effect was explained by steric congestion within the arborescent structures, independently of the experimental conditions

used.[27] The situation can only be worse for PBG, as it is known to maintain a predominantly α-helix conformation in DMF for chain lengths significantly longer than 10 repeat units,[50] and more so in DMF than in DMSO.[51] To confirm this for arborescent PBG, dynamic light scattering measurements were performed and discussed in Section 3.3.4. It was clear from these measurements that PBG has a more compact structure in DMF relatively to DMSO for all three PBG generations (G1, G2, and G3). The dominant α-helix conformation of PBG should lead to enhanced chain segment rigidity, further restricting the mobility of the chains in addition to steric crowing in the highly branched arborescent polymer structures. In comparison to arborescent PS syntheses, lower grafting yields were also observed in Chapter 3 due to the compact structure of PBG, even when DMSO was used as solvent for the grafting reaction. Therefore it was likewise expected that lower grafting yields would be obtained in the synthesis of arborescent copolymers from PBG substrates.

Another factor that may have influenced the grafting yield in the PBG systems is the functionalization (deprotection) level of the substrates, which ranged from 26-35 mol%, whereas the functionalization level of the PS substrates used in the previous investigations was typically 15-25 mol%. In a specific grafting reaction there is a maximum chain density that can be achieved due to steric hindrance. Once this maximum density is reached, further coupling of linear chain segments with the substrate will be strongly hindered, regardless of the functionality level of the substrate or the number of linear chain segments present in the reaction.

The reactivity of the chemical species involved in the coupling reaction may also play a role in the success of the grafting process. Highly reactive living anionic P2VP chain segments were previously coupled with acetylated or chloromethylated PS substrates,

whereas peptide coupling chemistry served to graft onto the PBG substrates in the current case. Anionic grafting should therefore be much more effective than peptide coupling, and it was indeed shown that under appropriate conditions the grafting yield could reach up to 95% in anionic grafting.[27] This technique is also very sensitive to protic impurities however, and special care must be taken to avoid side reactions of the living P2VP side chains; in comparison, peptide coupling techniques are much less demanding. Furthermore, it is also worth pointing out that the low grafting yields observed for the PGlyAc side chains could be due to incomplete primary amine functionalization, since f_{NH2} = 0.64 was determined for PGlyAc9, and it could not even be determined for PGlyAc32 (f_{NH2} not determined); in any case, these were in all likelihood lower than for the PEO (f_{NH2} = 0.91) and PtBuGlu side chains (f_{NH2} = 0.99). Finally, as pointed out earlier, the excess of side chains used in the coupling reactions is another reason for the relatively low grafting yields achieved: The 25 mol% excess of linear chains segments used would allow for a maximum grafting yield of 80%, even in the event that all the carboxylic acid sites are consumed in the coupling reaction. The grafting yields reported were not corrected for the stoichiometry used.

The SEC traces obtained for the different arborescent PGlyAc copolymer samples after purification are compared in Figure 4.10. For convenience, purification was achieved by preparative SEC with DMF and LiCl. The DMF and salt components were then removed by dialysis against THF. The arborescent copolymers with PGlyAc32 side chains display a significant increase in apparent molecular weight in comparison with their PGlyAc9 counterparts.

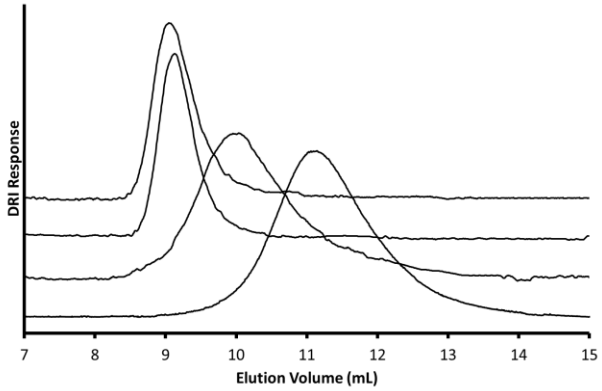

Figure 4.10 SEC traces in DMF with 0.1% LiCl for (from top to bottom) G2PBG-*g*-PGlyAc32, G1PBG-*g*-PGlyAc32, G2PBG-*g*-PGlyAc9, and G1PBG-*g*-PGlyAc9 arborescent copolymers.

Dynamic Light Scattering Measurements. The solution properties of arborescent PGlyAc copolymers were investigated with DLS measurements in THF, known to be a good solvent for the poly(glycidol acetal) shell and a poor solvent for PBG. First- and second-order analysis of the correlation function, $|g_1(\tau)|$ and $|g_2(\tau)|$, respectively, provides information on the size dispersity of the system. Monodispersed samples are expected to yield identical results for their first- and second-order analysis, since the correlation function can be represented by a single exponential decay under these conditions.[52] Therefore as the size distribution of a sample broadens, the difference between the first- and second-order measurement results will increase.The first- and second-order hydrodynamic diameters (d_{h1} and d_{h2}, respectively) obtained for the copolymers in THF are compared with the values obtained for the PBG substrates in DMF in Table 4.3. The uncertainties reported are either the standard deviation for a series of 5 measurements or 1 nm, whichever is larger.

Table 4.3 DLS measurements for PBG substrates and PGlyAc arborescent copolymers

	PBG Substrate (DMF)[a]		Graft Copolymer (THF)[b]	
Copolymer	d_{h1}[c]	d_{h2}[d]	d_{h1}[c]	d_{h2}[d]
G1PBG-*g*-PGlyAc9	$11._5 \pm 1$	$9._8 \pm 1$	$29._2 \pm 1$	$25._6 \pm 1$
G2PBG-*g*-PGlyAc9	$18._6 \pm 1$	$17._4 \pm 1$	$26._8 \pm 1$	$25._0 \pm 1$
G1PBG-*g*-PGlyAc32	$11._5 \pm 1$	$9._8 \pm 1$	$47._1 \pm 1$	$45._3 \pm 1$
G2PBG-*g*-PGlyAc32	$18._9 \pm 1$	$17._3 \pm 1$	$70._0 \pm 1$	$66._6 \pm 1$

[a] DMF with 0.05% LiCl to prevent aggregation; [b] pure THF; [c] hydrodynamic diameter from 1st order analysis of the correlation function (nm); [d] diameter from 2nd order analysis (nm).

The arborescent copolymers in Table 4.3 display good agreement between the first- and second-order analysis results, demonstrating that the molecules have a uniform size and exist in solution as unimolecular species. When comparing the hydrodynamic diameters to their respective PBG substrates, it is clear that the copolymers significantly increased in size. A larger increase is observed when grafting longer PGlyAc chains as expected. Interestingly, the two copolymer samples with the PGlyAc9 side chains have a similar size of ca. 25 nm in THF. This could be due to the collapse of the larger G2PBG core in THF, and/or to the decreased mobility of the PGlyAc chains in the more crowded G2 vs. G1 copolymers (with f_n = 75 vs. 47, respectively).

Deprotection of the Poly(glycidol acetal) Side Chains. To obtain water-soluble micelles, removal of the acetal protecting group on the poly(glycidol acetal) side chains forming the shell is necessary. The deprotection of glycidol acetal units has been reported in the literature for both linear homopolymers and copolymers.[37,39,53,54] For arborescent copolymers, special care is required to avoid degradation of the PBG cores. Consequently the deprotection of

G1PBG-*g*-PGlyAc32 was explored for several methods reported in the literature, to determine the best method applicable to these systems. A reaction scheme for the acidolysis of the acetal protecting group is displayed in Figure 4.11. SEC traces obtained for the crude products obtained by different deprotection protocols are compared in Figure 4.12 for sample G1PBG-*g*-PGlyAc32. The SEC trace for the purified copolymer before deprotection is also provided in Figure 4.12 for comparison, to help determine the extent of degradation occurring for the arborescent systems in each case.

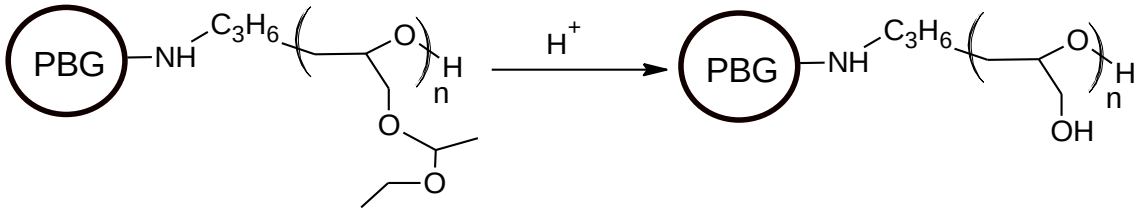

Figure 4.11 Acidolysis of the acetal groups in arborescent PBG-*g*-PGlyAc copolymers.

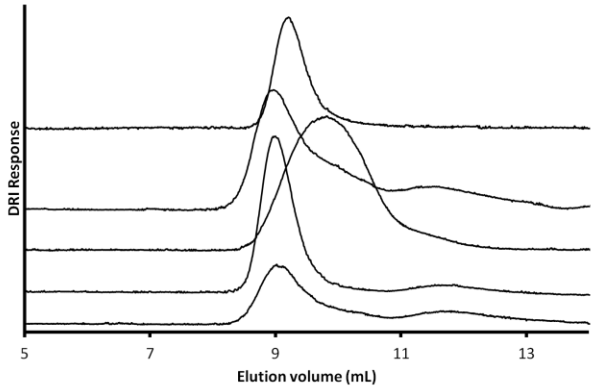

Figure 4.12 SEC traces in DMF with 0.1% LiCl for different deprotection reactions of G1PBG-*g*-PGlyAc32. From top to bottom, G1PBG-*g*-PGlyAc32 (reference trace), $AlCl_3$ deprotection, formic acid deprotection, HCl deprotection (30 min), HCl deprotection (90 min).

The first deprotection method, reported by Namboodri and Varma,[55] used a catalytic amount of aluminum chloride hexahydrate in methanol to remove the acetal protecting groups from small molecules, and was more recently applied by Dimitrov et al.[53] to copolymers containing glycidol acetal. The reaction, when allowed to proceed for 30 min, led to significant degradation according to the SEC trace in Figure 4.12. The second deprotection method, with neat formic acid, was proposed by Taton et al.[54] for the deprotection of a poly(glycidol acetal)-*b*-poly(ethylene oxide) copolymer. The first step involves dissolution of the polymer in neat formic acid to produce formate groups, which are then saponified with potassium hydroxide in a dioxane/methanol mixture to release the hydroxyl functionalities. This technique, when applied to the arborescent copolymer, also led to significant degradation, as seen for the third SEC trace in Figure 4.12. More recently, Mendrek et al. also investigated different techniques for the deprotection of poly(glycidol acetal).[37] They found that a concentrated HCl solution in DMF achieved 95% acetal group cleavage after only 30 min, and 100% removal after 45 min. The fourth and fifth SEC traces in Figure 4.12 are for the arborescent copolymers obtained under these conditions (also reported in the experimental section), where the arborescent copolymer was dissolved in a DMF solution containing 4.5 eq of HCl relatively to the acetal protecting groups. Complete removal of the acetal protecting groups was confirmed by ^{1}H NMR analysis after 30 min, although a small amount of side chain degradation was also observed as a broad peak at elution volumes around 11.5-12 mL. To confirm that this degradation did not affect the PBG substrate, the same experiment was run with the G1PBG substrate in the HCl/DMF solution. SEC samples removed after up to 120 min displayed no sign of degradation. It is therefore clear that a 30 min reaction time using HCl/DMF works best for the deprotection of the arborescent

copolymers. The small amount of degradation products observed is likely due to random cleavage of some polyglycidol (PGly) segments. These chain segments should not have a significant impact on the solution properties of the arborescent copolymers, but they were nevertheless removed by dialysis of the crude product against methanol in a 12,000-14,000 MWCO bag. The SEC elution curves obtained for the purified arborescent PBG-*g*-PGly copolymers, shown in Figure 4.13, follow a similar trend to the elution curves for the protected polymers displayed in Figure 4.10

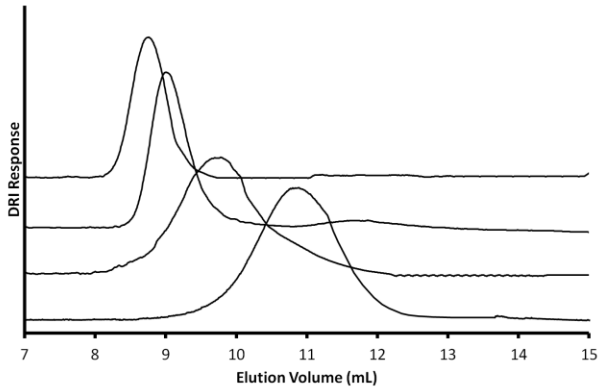

Figure 4.13 SEC traces in DMF with 0.1% LiCl for (from top to bottom) G2PBG-*g*-PGly16, G1PBG-*g*-PGly16, G2PBG-*g*-PGly5, and G1PBG-*g*-PGly5 arborescent copolymers.

Dynamic Light Scattering Measurements. The results of the DLS measurements for the (deprotected) PBG-*g*-PGly arborescent copolymers are provided in Table 4.4. These were performed in both DMF with 0.05% LiCl and in an aqueous phosphate buffer solution (PBS). No aggregation is expected in DMF, since it is a good solvent for both the core and the shell components. The first- and second-order hydrodynamic diameters in DMF show trends similar to the protected arborescent copolymers (Table 4.3). The small difference in the first-

and second-order hydrodynamic diameters further confirms that no significant molecular weight distribution broadening occurred during the deprotection step. In DMF the hydrodynamic diameters for G2PBG-*g*-PGly5 are slightly larger than for G1PBG-*g*-PGly5, which would be consistent with expansion of the G2PBG core, in contrast to the results obtained in THF (Table 4.3). It should be noted that the weight fraction of glycidol in the copolymer changes significantly once the acetal group is cleaved from the glycidol units, as it accounts for essentially half of their molecular weight. Thus the weight fraction of glycidol acetal before deprotection in G1PBG-*g*-PGly5 (65%), G2PBG-*g*-PGly5 (38%), G1PBG-*g*-PGly16 (92%), and G2PBG-*g*-PGly16 (74%) decreased to 48%, 23%, 85%, and 59% glycidol, respectively, after acidolysis. Gradual solvent exchange from DMF to PBS by dialysis was necessary to measure the hydrodynamic diameters in aqueous PBS, since significant aggregation occurred for all the samples. The baseline of the correlation function was unstable for G2PBG-*g*-PGly5 due to the presence of very large aggregates, which precluded DLS measurements on that sample. Both G1PBG-*g*-PGly5, G1PBG-*g*-PGly16, and G2PBG-*g*-PGly16 displayed relatively good agreement between the first- and second-order hydrodynamic diameters in PBS, but this is likely the result of self-assembly by a closed association mechanism (i.e. with a fixed number of molecules per aggregate), as indicated by their large hydrodynamic diameters in comparison to the DMF results. Self-assembly likely occurs to prevent exposure of the PBG cores to the unfavorable aqueous environment, which is an indication that the copolymers obtained by random grafting have a poorly defined core-shell morphology, even for the copolymers with high PGly contents.

Table 4.4 DLS measurements for the PBG and PGly arborescent copolymers

	PBG Substrate (DMF)[a]		Graft Copolymer (DMF)[a]		Graft Copolymer (PBS)[b]	
Copolymer	d_{h1}[c]	d_{h2}[d]	d_{h1}[c]	d_{h2}[d]	d_{h1}[c]	d_{h2}[d]
G1PBG-*g*-PGly5	$11._5 \pm 1$	$9._8 \pm 1$	$39._3 \pm 1$	$36._0 \pm 1$	196 ± 3	184 ± 2
G2PBG-*g*-PGly5	$18._6 \pm 1$	$17._4 \pm 1$	$43._1 \pm 1$	$42._3 \pm 1$	aggregation	
G1PBG-*g*-PGly16	$11._5 \pm 1$	$9._8 \pm 1$	$62._9 \pm 1$	$57._4 \pm 1$	166 ± 3	156 ± 3
G2PBG-*g*-PGly16	$18._6 \pm 1$	$17._4 \pm 1$	$73._2 \pm 1$	$68._6 \pm 1$	143 ± 3	131 ± 2

[a] DMF with 0.05% LiCl to prevent aggregation; [b] phosphate buffer solution (pH 7.4); [c] hydrodynamic diameter from 1st order analysis of the correlation function (nm); [d] diameter from 2nd order analysis (nm).

4.4.4 Arborescent PBG-*graft*-PEO Copolymers

The conditions used to synthesize the arborescent PBG-*g*-PEO copolymers were similar to the ones described for PBG-*g*-PGlyAc, except for employing DMSO rather than DMF as solvent in the grafting reactions. The results obtained with linear PEO5 side chains are summarized in Table 4.5. In analogy to PGlyAc grafting there was an increase in molecular weight for the copolymers relatively to the PBG substrates, while the molecular weight distribution remained narrow ($M_w/M_n \leq 1.07$). This is also seen in the SEC traces for the purified products provided in Figure 4.14, where a decrease in elution volume is clearly noticeable as the generation number increases. The grafting yields achieved for the PBG-*g*-PEO copolymers were higher than for the PBG-*g*-PGlyAc reactions. This is somewhat unexpected since the main limiting factor in the grafting reactions seems to be the rigidity of the PBG substrates. It is interesting that the grafting yields for G2PBG-*g*-PEO5 and G3PBG-g-PEO5 are significantly higher than for G1PBG-*g*-PEO5, while it would be expected to decrease as the PBG substrate generation increases, in analogy to other arborescent systems.[22,25,27] The G3PBG-*g*-PEO5 synthesis was also more successful than for the G3PBG-

g-PGlyAc9 and G3PBG-*g*-PGlyAc32 samples, so the success of the reactions with the PEO side chains may lie in the different nature of the linear PEO chains. Since the PEO chains contain no substituents, they are likely more flexible than PGlyAc carrying the bulky acetal protecting groups. This may allow linear PEO5 to penetrate deeper into the G3PBG substrate than linear PGlyAc9 or PGlyAc32. Differences in miscibility between PBG and PEO vs. PGlyAc could also potentially have contributed to the differences observed.

Table 4.5 Characteristics of arborescent PBG substrates and PEO copolymers

	PBG Substrate			Graft Copolymer			
Copolymer[a]	M_n[b]	% Deprotected[c]	G_y[d]	M_n[b]	M_w/M_n[b]	f_n[e]	% PEO[f]
G1PBG-*g*-PEO5	234,000	35	28	1.0×10^6	1.07	150	77
G2PBG-*g*-PEO5	1.1×10^6	26	62	6.9×10^6	1.05	1133	84
G3PBG-*g*-PEO5	3.0×10^6	34	58	2.3×10^7	1.04	3900	87

[a] All grafting reactions done with 25 mol% excess of side chains; [b] absolute values from SEC-MALLS analysis in DMF; [c] deprotection level from ^{1}H NMR analysis; [d] grafting yield: fraction of side chains becoming attached to the substrate; [e] branching functionality: number of side chains added in the last grafting cycle; [f] PEO weight fraction determined from the absolute molecular weights of the copolymer and the substrate.

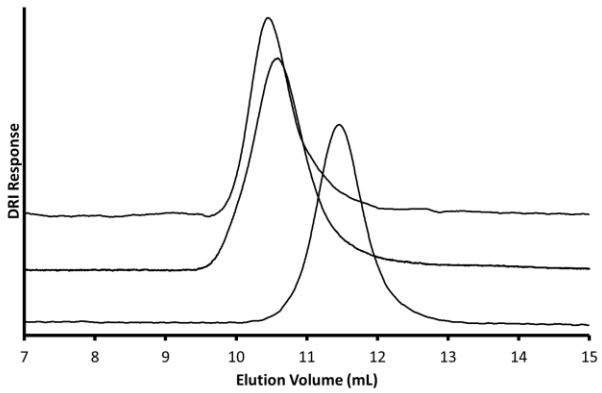

Figure 4.14 SEC traces in DMF with 0.1% LiCl for (from top to bottom) G3PBG-*g*-PEO5, G2PBG-*g*-PEO5, and G1PBG-*g*-PEO5 arborescent copolymers.

Dynamic Light Scattering Measurements. The DLS analysis results obtained for the PBG-*g*-PEO arborescent copolymers are summarized in Table 4.6. The measurements in DMF show size increases for the copolymers relatively to the PBG substrates. There is a larger than expected difference between the first- and second-order hydrodynamic diameters of the copolymers in DMF, since the molecular weight distribution of the samples is narrow according to the SEC measurements ($M_w/M_n \leq 1.07$). The PBG-*g*-PEO arborescent copolymers should not aggregate significantly in a DMF, since it is a good solvent for both the PBG and PEO components; however a small population of aggregates may still be present in the DMF solutions and give rise to the deviations observed.

To determine whether the PBG-*g*-PEO arborescent copolymers would form unimolecular micelles in aqueous solutions, the DLS samples in DMF were transferred to 1000 MWCO bags and dialyzed against PBS solution. The only arborescent copolymer sample that remained in solution under these conditions was G1PBG-*g*-PEO5, albeit it was still significantly aggregated: The first- and second-order hydrodynamic diameters differed by 32 nm, clearly indicating the formation of polydispersed aggregated species. Copolymer G1PBG-*g*-PEO5 had the lowest grafting yield, but it was nonetheless still soluble in aqueous media. Samples G2PBG-*g*-PEO5 and G3PBG-*g*-PEO5 slowly precipitated out of solution as the DMF was gradually replaced with the aqueous PBS solution. The insolubility of these arborescent copolymers is presumably due to exposure of the hydrophobic PBG core to the aqueous environment, which would occur if the PEO shell insufficiently shields the hydrophobic PBG core. Since G1PBG-*g*-PEO5 contains a low fraction of PEO, it should be less soluble in aqueous environments than G2PBG-*g*-PEO5 and G3PBG-*g*-PEO5. A possible explanation for this unexpected behavior may lie in the greater mobility of the core and shell

material in the lower branching functionality G1 molecules (f_n = 150), allowing them to rearrange and self-assemble into stable colloidal species more efficiently than the G2 and G3 copolymers.

Table 4.6 DLS measurements for arborescent PBG and PEO copolymers

	PBG Substrate (DMF)[a]		Graft Copolymer (DMF)[a]		Graft Copolymer (PBS)[b]	
Copolymer	d_{h1}[c]	d_{h2}[d]	d_{h1}[c]	d_{h2}[d]	d_{h1}[c]	d_{h2}[d]
G1PBG-*g*-PEO5	$11._5 \pm 1$	$9._8 \pm 1$	$22._5 \pm 1$	$13._3 \pm 1$	157 ± 3	125 ± 2
G2PBG-*g*-PEO5	$18._6 \pm 1$	$17._4 \pm 1$	$46._3 \pm 1$	$36._8 \pm 1$	insoluble	
G3PBG-*g*-PEO5	$28._8 \pm 1$	$27._1 \pm 1$	$76._2 \pm 1$	$56._8 \pm 1$	insoluble	

[a] DMF with 0.05% LiCl to prevent aggregation; [b] phosphate buffer solution (pH 7.4); [c] hydrodynamic diameter from 1st order analysis of the correlation function (nm); [d] diameter from 2nd order analysis (nm).

4.4.5 Arborescent PBG-*graft*-PGA Copolymers

The procedures used to generate the PBG-*g*-PtBuGlu arborescent copolymers were similar to those described for PBG-*g*-PGlyAc, using DMF as solvent for the grafting reactions due to the greater solubility of the PtBuGlu2 chains than in DMSO. The characteristics of the PBG-*g*-PtBuGlu arborescent copolymers obtained are summarized in Table 4.7. The absolute M_n of the arborescent copolymer could not be determined by SEC analysis for these samples, due to a noisy light scattering signal. The M_n of the copolymers was rather estimated from their known composition (determined by ^{1}H NMR analysis) along with the known M_n value of the PBG substrate. This approach has its limitations and may overestimate the M_n, since part of the signal from the core may be lost (due to its reduced mobility) in ^{1}H NMR analysis; this approach can still provide a rough M_n value for comparison with the other copolymer systems. Apparent polydispersity values could still be determined from the DRI detector

signal. The grafting yields followed the expected decreasing trends for increasing generation numbers. The SEC elution curves obtained for the different PBG-*g*-PtBuGlu2 arborescent copolymers are compared in Figure 4.15. The G2PBG-*g*-PtBuGlu2 and G3PBG-*g*-PtBuGlu2 samples have a small shoulder on the higher molecular weight side of the peak. Significant tailing is also present on the lower molecular weight side of the SEC trace for G3PBG-*g*-PtBuGlu2. These peak shape distortions could indicate that the grafting reaction did not proceed as smoothly in this case as for the grafting reactions using PGlyAc and PEO side chains, or else that these copolymers interact with the column packing.

Table 4.7 Characteristics of arborescent PBG and PtBuGlu copolymers

	PBG Substrate			Graft Copolymer			
Copolymer[a]	M_n[b]	% Deprotected[c]	G_y[d]	M_n[e]	M_w/M_n[f]	f_n[g]	% PtBuGlu[h]
G1PBG-*g*-PtBuGlu2	212,000	35	61	922,000	1.17	309	77
G2PBG-*g*-PtBuGlu2	1.1×10^6	26	27	2.2×10^6	1.22	478	51
G3PBG-*g*-PtBuGlu2	3.0×10^6	34	11	4.7×10^6	1.17	743	36

[a] Grafting reaction with 25% excess of side chains; [b] absolute values from SEC-MALLS in DMF; [c] deprotection level from ^{1}H NMR analysis; [d] grafting yield: fraction of side chains attached to the substrate; [e] M_n estimated using the weight fraction of PtBuGlu in copolymer and M_n from PBG substrate; [f] apparent M_w/M_n from the DRI detector; [g] branching functionality: number of branches added in the last grafting cycle; [h] PtBuGlu %weight fraction determined by ^{1}H NMR analysis.

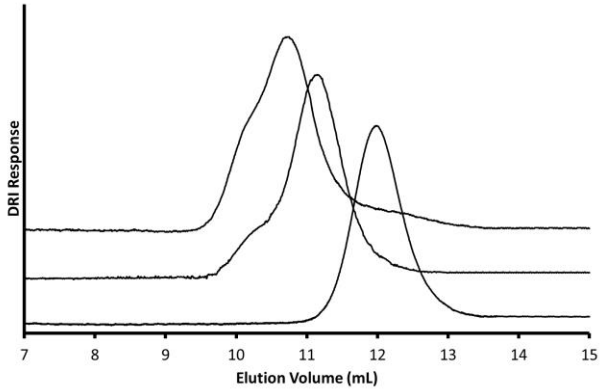

Figure 4.15 SEC traces in DMF with 0.1% LiCl for (from top to bottom) G3PBG-*g*-PtBuGlu2, G2PBG-*g*-PtBuGlu2, and G1PBG-*g*-PtBuGlu2 arborescent copolymers.

To obtain water-soluble arborescent micelles, the PBG-*g*-PtBuGlu copolymers were dissolved in TFA for a few minutes to selectively remove the *tert*-butyl ester groups, and then precipitated in diethyl ether. Due to the loss of the *tert*-butyl ester group, the composition of the corresponding PBG-*g*-PGA1.5 copolymers decreased to 70, 42, and 28 wt% PGA for the G1, G2, and G3 samples, respectively. The PBG-*g*-PGA copolymers were insoluble in DMF, so only DLS measurements in PBS were performed. Even in that case solubilization of the copolymers required sonication, and G3PBG-*g*-PGA1.5 was insoluble in PBS even after extended sonication (1 h) and heating to 50 ºC; consequently, that sample was not analyzed by DLS. The results of the measurements are summarized in Table 4.8. Sample G1PBG-*g*-PGA1.5 had large first- and second-order hydrodynamic diameters, indicative of self-assembly into large aggregates. The relatively small difference between the first- and second-order analyses nevertheless indicates that the aggregates are uniform in size, and therefore result from a closed association mechanism. Sample G2PBG-*g*-PGA1.5 displayed a larger difference between the first- and second-order diameters, consistent with an open association mechanism with a variable number of copolymer molecules among the

aggregates. The difference in aggregation behavior observed for sample G1PBG-*g*-PGA1.5 may again result from the more flexible and open structure of the G1PBG core facilitating the self-assembly process as compared to the G2PBG core.

Table 4.8 DLS measurements for arborescent PBG and PGA copolymers

	PBG Substrate (DMF)[a]		Graft Copolymer (PBS)[b]	
Copolymer	d_{h1}[c]	d_{h2}[d]	d_{h1}[c]	d_{h2}[d]
G1PBG-*g*-PGA1.5	$11._3 \pm 1$	$10._0 \pm 1$	221 ± 2	211 ± 2
G2PBG-*g*-PGA1.5	$18._6 \pm 1$	$17._4 \pm 1$	$59._5 \pm 1$	$44._6 \pm 1$
G3PBG-*g*-PGA1.5	$28._8 \pm 1$	$27._1 \pm 1$	insoluble	

[a] DMF with 0.05% LiCl to prevent aggregation; [b] phosphate buffer solution (pH 7.4); [c] hydrodynamic diameter from 1st order analysis of the correlation function (nm); [d] diameter from 2nd order analysis (nm).

4.5 Conclusions

Linear polymers of PGlyAc, PEO, and PtBuGlu with narrow molecular weight distributions ($M_w/M_n < 1.20$) were synthesized and covalently grafted onto randomly functionalized arborescent PBG substrates to generate arborescent copolymers.

The arborescent copolymers of PBG-*g*-PGlyAc were prepared using PGlyAc chains with M_n = 9100 and 32,400, to demonstrate that the composition and the hydrodynamic diameter of the copolymers can be controlled by varying the length of the side chains added in the shell. The G3PBG substrates were unreactive towards both of these PGlyAc chains. The grafting yields achieved were also lower for the G1PBG and G2PBG substrates in comparison with the analogous arborescent PS-*g*-P2VP copolymers previously synthesized. This result was tentatively rationalized in terms of the stiff and compact structure of the arborescent PBG substrates. The least damaging method examined for the removal of the

acetal protecting groups from the arborescent copolymers was acidolysis in HCl/DMF mixtures with short (30 min) contact times, to minimize polyglycidol degradation. Removal of the acetal groups produced arborescent PBG-*g*-PGly unimolecular micelles in DMF, but these self-assembled into aggregates in aqueous media.

Arborescent PBG-*g*-PEO copolymers were generated in higher yields relatively to the PBG-*g*-PGlyAc copolymers. The DLS results demonstrated an increase in hydrodynamic diameter in DMF, but aggregation and insolubility were observed in aqueous (PBS) solutions.

Arborescent copolymers of PBG-*g*-PtBuGlu were likewise synthesized, albeit in lower yields than the PBG-*g*-PGlyAc and PBG-*g*-PEO copolymers. Selective cleavage of the *tert*-butyl ester protecting groups was easily achieved with TFA to produce arborescent PBG-*g*-PGA copolymers. Dissolution of these copolymers in PBS produced aggregates of uniform size for G1PBG-*g*-PGA1.5, and polydispersed aggregates for G2PBG-*g*-PGA1.5, presumably due to the more flexible structure of the G1PBG core.

The arborescent copolymers generated by attaching hydrophilic chain segments to randomly functionalized PBG cores are useful to demonstrate the synthesis of biocompatible micellar compounds, in spite of the aggregated structures obtained. It will be shown in the following chapter that aggregation can be minimized or eliminated by terminal grafting (as opposed to random grafting) of the hydrophilic segments. These results will provide further support for the aggregation mechanism proposed herein, namely via interaction of the incompletely shielded hydrophobic cores in the randomly grafted structures.

Chapter 5

Arborescent Unimolecular Micelles: Poly(γ-benzyl L-glutamate) Core End Grafted with Hydrophilic Chain Segments

5.1 Overview

Arborescent poly(γ-benzyl L-glutamate)s (PBG) with carboxyl chain ends were synthesized by grafting linear PBG chain segments containing a di-*tert*-butyl ester-protected glutamic acid initiator fragment onto randomly functionalized generation 0 (G0), G1, and G2 arborescent PBG substrates. Selective cleavage of the *tert*-butyl ester protecting groups yielded arborescent PBG substrates of generations G1, G2, and G3, respectively, functionalized with carboxylic acid groups near their surface. Linear chain segments of poly(glycidol acetal), poly(ethylene oxide), and poly(γ-*tert*-butyl L-glutamate) containing a terminal primary amine were synthesized and coupled with the PBG substrates, to generate arborescent copolymers with a crew-cut core-shell morphology. The goal of this work was to evaluate the usefulness of the chain end grafting method versus random grafting demonstrated previously for the arborescent PBG substrates. Size exclusion chromatography was used to determine the grafting yield, molecular weight, polydispersity index, branching functionality, and composition of the arborescent copolymers. Narrow molecular weight distributions ($M_w/M_n \leq 1.15$) and moderate grafting yields (19-50%) were obtained for the arborescent copolymers. Dynamic light scattering measurements were used to investigate the solution properties of the arborescent copolymers. The grafting yields obtained were higher relatively to the random grafting method, and the copolymers had less tendency to aggregate in aqueous solutions when using either polyglycidol, poly(ethylene oxide), or poly(L-glutamic acid) as the shell components. This difference is attributed to a better-defined core-shell morphology for the end grafted than the randomly grafted copolymers.

5.2 Introduction

Dendrigraft (arborescent) polymers are a class of macromolecules that contain many polymer segments assembled in a dendritic (multi-level) highly branched architecture. This characteristic gives unique properties to these polymers. Ionic polymerization techniques are typically used for the synthesis of arborescent polymers, as they provide precise control over their structure. Arborescent systems were first introduced in 1991, concurrently by Tomalia et al.[1] and by Gauthier and Möller.[2] A schematic representation of the generation-based synthesis of arborescent polymers is shown in Figure 5.1. Cationic polymerization techniques were employed by Tomalia et al. to construct comb-burst polymers of polyethylenimine, whereas Gauthier and Möller relied upon anionic polymerization techniques to construct arborescent polystyrene (PS). Both schemes use a *grafting onto* approach, whereby well-defined linear chain segments synthesized in a separate step are coupled with a suitably functionalized substrate. This procedure allows for independent molecular weight analysis of the attached linear chain segments, the substrates, and the arborescent polymers. Further progress was made by Gauthier et al. to gain a better understanding of the morphology and solution properties of arborescent polystyrene, using techniques such as dynamic light scattering,[3,4] atomic force microscopy,[5] fluorescence spectroscopy,[6] and small-angle neutron scattering.[7] Understanding the structure-property relations for arborescent polymers can allow tailoring these systems for specific applications.

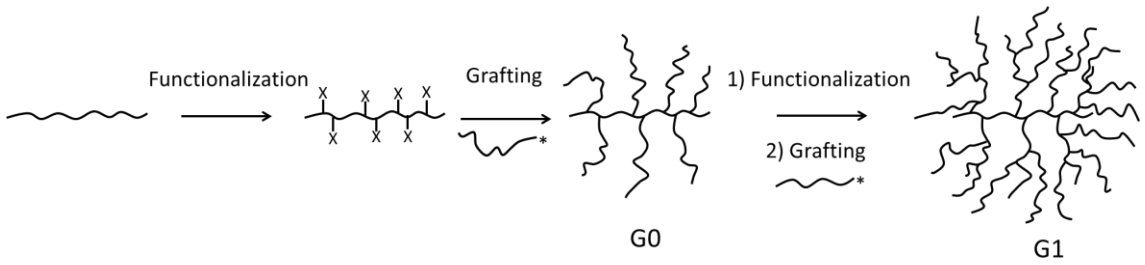

Figure 5.1 Schematic representation of the generation-based synthesis of arborescent polymers.

More recently, amphiphilic arborescent copolymers have been synthesized by the *grafting onto* approach from poly(2-vinyl pyridine) (P2VP) and randomly functionalized PS substrates.[8,9] Due to their amphiphilic nature, the polystyrene-*graft*-poly(2-vinyl pyridine) (PS-*g*-P2VP) arborescent copolymers were found to behave like unimolecular micelles in acidic aqueous solutions, and were capable to solubilize[10] and release[11] small molecule hydrophobic probes in a controlled manner in aqueous environments. While the PS-*g*-P2VP system was useful for the purpose of concept demonstration, it lacks biocompatibility for biomedical applications.

Previously to the PS-*g*-P2VP arborescent copolymers, amphiphilic arborescent copolymers incorporating a PS core and a biocompatible poly(ethylene oxide) (PEO) shell were synthesized. [12] A *grafting from* approach was used in this case, by polymerizing ethylene oxide from the chain ends of the PS core acting as polyfunctional macroinitiator. Unfortunately this approach relies upon anionic polymerization, which may lead to stability issues when applying it to substrates other than polystyrene.

Chain end (as opposed to random) coupling of the hydrophilic shell segments with the hydrophobic core should otherwise be advantageous, as shown in a schematic representation of the arborescent copolymer structures generated by the two different grafting

methods in Figure 5.2. The chain end functionalized cores are expected to produce a better-defined crew-cut core-shell morphology as compared to random grafting. The chain end grafted arborescent copolymers thus resemble more closely a block copolymer structure with spherical symmetry, and are more likely to remain as unimolecular species in solution due to enhanced shielding of the hydrophobic cores. Similarly to block copolymer (multimolecular) micelles, the characteristics of arborescent copolymers can be adjusted by varying the PS core generation number, the length of the PS chains, and the length of the PEO segments forming the shell. Not surprisingly, polystyrene-*chain-end-grafted*-poly(ethylene oxide) (PS-*eg*-PEO) arborescent copolymers produced transparent dispersions in water, but unfortunately it was not determined whether these species were aggregated or unimolecular. The PEO forming the shell is well-known to be biocompatible; however the PS core is not. It would be desirable to design a similar system containing all biocompatible components and to investigate its solution properties, more specifically to determine whether they behave like unimolecular micelles.

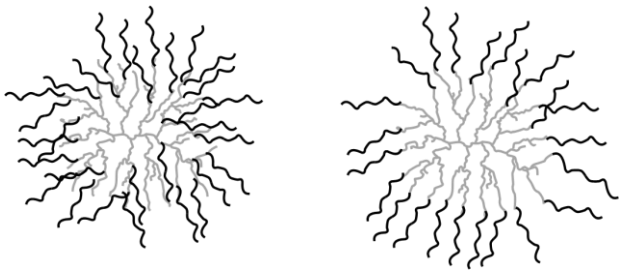

Figure 5.2 Schematic representation of randomly grafted (left) and chain end grafted (right) arborescent copolymers derived from a G1 core.

The new methodology reported herein provides a new grafting technique, wherein biocompatible polymers are coupled with chain end functionalized arborescent poly(γ-benzyl

L-glutamate) (PBG) substrates of different generations. The chain end grafted arborescent copolymers serve for comparison with the randomly grafted arborescent copolymers reported in Chapter 4. The same shell components and standard peptide coupling techniques were used as in Chapter 4, with either poly(glycidol acetal) (PGlyAc), poly(ethylene oxide) (PEO), or poly(γ-*tert*-butyl L-glutamate) (PtBuGlu) linear chains grafted onto chain end functionalized PBG cores. Dynamic light scattering (DLS) measurements were utilized to investigate their solution properties.

5.3 Experimental Procedures

5.3.1 Characterization and Sample Preparation

Nuclear Magnetic Resonance (NMR) Spectroscopy. ^{1}H NMR spectroscopy served to determine the deprotection level of the arborescent PBG substrate polymers, and to ensure the purity of the linear polymers used as shell materials. It also served for the determination of the number-average degree of polymerization X_n of the PEO and PtBuGlu linear chains, and the weight fraction of PtBuGlu in the arborescent copolymers containing PtBuGlu. The instrument used was a Bruker 300 MHz spectrometer. The concentration of all the samples was 15-20 mg/mL and 16 scans were averaged.

^{19}F NMR spectroscopy was served to determine the chain end primary amine functionality, f_{NH2}, of the polymers used in the grafting reactions. The procedure followed was adapted from Ji et al.[13] and was applied successfully in Section 3.4.3 to demonstrate the 'living' character of the linear PBG chains. The instrument used was a Bruker 300 MHz

spectrometer. The concentration of all the samples was 30-35 mg/mL and 64 scans were averaged.

Size Exclusion Chromatography (SEC) Analysis. Analysis of the PGlyAc linear chains was performed on a Viscotek GPCmax instrument equipped with a TDA 305 triple detector array and a Viscotek UV Detector 2600. Size exclusion was performed with three Polyanalytik Superes™ Series 300 mm × 8 mm linear mixed bed columns in series, having linear polystyrene molecular weight exclusion limits of 400×10^3, 4×10^6, and 20×10^6. A flow rate of 1.0 mL/min and a temperature of 35 ºC were used for the THF mobile phase.

The analysis of the PEO and the PtBuGlu linear chains, and of all the arborescent copolymers was performed on a SEC instrument using DMF as the mobile phase. It consisted of a Waters 510 HPLC pump, a 50 μL injection loop, and a Waters 2410 differential refractometer (DRI) detector. A Wyatt MiniDAWN laser light scattering detector operating at a wavelength of 690 nm served to determine the absolute molecular weight of the graft polymers. The column used was a 500 mm × 10 mm Jordi Gel Xstream H_2O Mixed Bed model with a linear polystyrene molecular weight range of 10^2–10^7. The mobile phase was DMF with LiCl (1 g/L, added to minimize adsorption of the polymers onto the column) at a flow rate of 1.0 mL/min at room temperature.

Preparative SEC work was carried out on a system consisting of a Waters M45 HPLC pump, a 2-mL sample injection loop, a Waters R401 differential refractometer detector, and either a Jordi Gel DVB 1000 Å 250 mm × 22 mm or a Jordi Gel DVB Mixed Bed 250 mm × 22 mm preparative SEC column. DMF with 0.2 g/L LiCl served as the mobile phase at room

temperature at a flow rate of 3.0 mL/min. The crude polymer samples were injected as 20-30 mg/mL solutions in DMF with 0.2 g/L LiCl.

Refractive Index Increment Determination. Measurement of the refractive index increment (dn/dc) of the linear polymers (PGlyAc, PEO) was necessary to determine their absolute molecular weight by SEC. These were determined at 30 ºC on a Brookhaven Instruments BI-DNDC 620 Differential Refractometer with a wavelength of 620 nm, using five polymer solutions in DMF ranging in concentration from 1 to 5 mg/mL.

Dynamic Light Scattering. Batch-wise dynamic light scattering measurements were carried out on a Brookhaven BI-200SM light scattering goniometer equipped with a BI-APD (Avalanche Photo Diode) detector and a Claire Lasers CLAS2-660-140C (120 mW) laser operating at 660 nm. All the samples were measured at 25 °C and a scattering angle of 90°. The samples were filtered twice with a 3 μm PTFE membrane filter before analysis. The correlator was operated in the exponential sampling mode and hydrodynamic diameters were calculated from the z-average translational diffusion coefficients obtained from first- and second-order cumulant analysis of the correlation function, to better account for polydispersity effects. Solutions were prepared at concentrations ranging from 0.1-2 % w/v, depending on the molecular weight (generation number) of the sample. If a solvent exchange was necessary, 3 mL of sample solution was placed in a 12,000-14,000 molecular weight cut-off regenerated cellulose dialysis bag overnight in at least 200 mL of the new solvent. The next day, the solvent was replaced and the sample was left stirring again for at least 2 h, to ensure complete removal of the original solvent.

5.3.2 Solvent and Reagent Purification

N,N-Dimethylformamide (DMF; Aldrich, peptide synthesis grade) was purified by distillation under reduced pressure and was stored in the dark to prevent degradation due to photochemical reactions. Dimethylsulfoxide (DMSO, Caledon, 99.9%) and *n*-hexylamine were purified by stirring overnight with CaH_2 and distillation under reduced pressure. The purified DMF, DMSO, and *n*-hexylamine samples were stored under nitrogen in round-bottomed flasks (RBF) over 3 Å molecular sieves (EMD). Ethyl acetate (Caledon, 99+%) was dried by stirring overnight with $LiAlH_4$ under nitrogen and distillation immediately before use. Tetrahydrofuran (THF) used for anionic polymerization was distilled over sodium-benzophenone ketyl under nitrogen. Toluene used for anionic polymerization was distilled over oligostyryllithium under nitrogen. Ethylene oxide (EO, Air Liquide) was purified with phenylmagnesium chloride as a drying agent under high vacuum as described in Section 5.3.4. H-Glu(OtBu)-OtBu·HCl (Bachem, >99%), 2,3-epoxy-1-(1-ethoxyethoxy)propane (glycidol, Aldrich, 95%), ethyl vinyl ether (Aldrich, 99%), *p*-toluenesulfonic acid monohydrate (Aldrich, ≥98.5%), sodium hydrogen carbonate ($NaHCO_3$, Aldrich, 99%), diphenylmethane (Aldrich, 99%), naphthalene (Aldrich, 99%), triisobutylaluminum (Aldrich, 1.0 M in hexanes), 3-aminopropanol (Aldrich, ≥99%), phenylmagnesium chloride (Aldrich, 2.0 M in THF), N,N'-diisopropylcarbodiimide (DIC; Aldrich, 99%), γ-*tert*-butyl L-glutamic acid (Bachem, >99%), HBr solution (Aldrich, 33%w/w in acetic acid), HCl solution (Aldrich, 37%w/v), 1-hydroxybenzotriazole (HOBt; Fluka, water content ca. 15% w/w), trifluroroacetic acid (TFA, Caledon), methanol (EMD), diethyl ether (EMD), triethylamine (TEA, EMD, Reagent grade), tetrahydrofuran (THF, Aldrich, ≥99%), triphosgene (Aldrich, 98%), $LiAlH_4$ (Aldrich, 95%), and magnesium sulfate

($MgSO_4$, anhydrous 97%, Fisher), deuterated DMSO (d_6-DMSO, Cambridge isotopes, D, 99.9%), and deuterated chloroform ($CDCl_3$, Cambridge isotopes, D, 99.9%) were used as received from the suppliers.

5.3.3 Synthesis of Arborescent PBG Cores

The synthesis of the partially deprotected arborescent poly(γ-benzyl L-glutamate) (PBG) cores from generation 0 (G0) to generation 2 (G2) was accomplished according to the procedures described in Sections 3.3.6 and 3.3.7. The chain end functionalized arborescent PBG substrates were generated by grafting glutamic acid-functionalized PBG chains in the last reaction cycle as described below.

Synthesis of Glu(OtBu)$_2$-Poly(γ-benzyl L-glutamate) [(tBuO)$_2$-PBG)]. The amino acid H-Glu(OtBu)-OtBu·HCl was used to initiate the polymerization of γ-benzyl L-glutamic acid N-carboxyanhydride (Bz-Glu-NCA, synthetic procedure described in Section 3.3.3) to produce linear PBG serving as side chains in the last cycle of the arborescent PBG core syntheses. To this end Bz-Glu-NCA (5.0 g, 19.0 mmol) was dissolved in dry DMF (10 mL) in a 25-mL round-bottomed flask (RBF) containing a magnetic stirring bar. The temperature was then increased to 40º C with an oil bath, and a solution of H-Glu(OtBu)-OtBu·HCl (0.243 g, 0.82 mmol, in 2 mL dry DMF) was added to the reaction for a target degree of polymerization X_n = 23. The reaction was allowed to proceed at 40º C for 7 d. The reaction was cooled to room temperature and triethylamine (0.1 mL, 1 mmol) was added to scavenge the HCl from the primary amine chain end of the polymer. After 5 min the solution was precipitated in methanol, and the polymer was recovered by suction filtration and drying under vacuum overnight. Yield = 3.0 g (72%). SEC (DMF): M_w/M_n = 1.18. ^{1}H NMR (300MHz, d_6-DMSO):

X_n = 24.0, δ: 8.2-7.8 (b, 24H), 7.28–7.21 (s, 120H), 5.03–4.89 (s, 48H), 4.33–3.89 (b, 24H), 2.33–1.70 (b, 96H), 1.32 (s, 18H).

Synthesis of chain end functionalized PBG substrates. The partially deprotected polymer serving as substrate [G0PBG, 0.173 g, 0.29 mmol $–CO_2H$] and the polymer serving as side chains $(OtBu)_2$-PBG (1.39 g, 0.29 mmol) were dissolved in dry DMSO (16 mL) in a 50-mL RBF. The peptide coupling agents N,N'-diisopropylcarbodiimide (DIC, 230 μL, 1.45 mmol) and 1-hydroxybenzotriazole (HOBt, 196 mg, 1.45 mmol) were then added to the reaction, followed by triethylamine (TEA, 202 μL, 1.45 mmol). The reaction was allowed to proceed for 24 h at room temperature before adding *n*-hexylamine (147 μL, 1.45 mmol), to deactivate residual carboxylic acid sites. After 1 h the product was diluted in DMF and purified by preparative SEC. The purified polymer solution was concentrated and precipitated in methanol; the polymer was recovered by suction filtration, and dried under vacuum overnight. Yield: 0.6 g. SEC (DMF): Grafting yield = 50% (DRI), M_n = 282,000, M_w/M_n = 1.05 (MALLS). ^{1}H NMR (300MHz, d_6-DMSO) δ: 8.2-7.8 (b, 1H), 7.28–7.20 (s, 5H), 5.03–4.89 (s, 2H), 4.33–3.89 (b, 1H), 2.33–1.70 (b, 4H), 1.31 (s, 18H).

To selectively remove the *tert*-butyl ester protecting groups at the chain ends, the arborescent G1PBG substrate (0.4 g) was dissolved in trifluoroacetic acid (4 mL). After 5 min the polymer was precipitated in methanol, recovered by suction filtration, and dried under vacuum overnight. ^{1}H NMR analysis was used to confirm the complete removal of the *tert*-butyl ester protecting groups, without loss of the benzyl ester protecting groups. Yield: 0.350 g (88%). ^{1}H NMR (300MHz, d_6-DMSO) δ: 8.2-7.8 (b, 1H), 7.28–7.20 (s, 5H), 5.03–4.89 (s, 2H), 4.33–3.89 (b, 1H), 2.33–1.70 (b, 4H).

5.3.4 Synthesis of Linear Polymers

Synthesis of 2,3-Epoxy-1-(1-ethoxyethoxy)propane (Glycidol Acetal). The synthetic procedure used was as described by Fitton et al.[14] 2,3-Epoxypropanol (40.0 g, 0.54 mol) and ethyl vinyl ether (200 mL) were loaded in a 500-mL RBF with a magnetic stirring bar and immersed in an ice-water bath. A catalytic amount of *p*-toluenesulfonic acid monohydrate (1.0 g, 5.3 mmol) was then added slowly, to ensure that the reaction temperature did not exceed 40 ºC and minimize the evaporation of ethyl vinyl ether. The reaction was removed from the ice bath to warm to room temperature and allowed to proceeded for 3 h. Enough saturated sodium hydrogen carbonate solution was then added until the pH of the solution was slightly basic (ca. 100 mL). The organic layer was isolated, dried over $MgSO_4$, and concentrated under reduced pressure. Distillation of the residue under reduced pressure gave the monomer as a colorless liquid that was stored under nitrogen at 4º C. Yield: 61.5 g (78%); ^{1}H NMR: (300 MHz, $CDCl_3$) δ: 4.65 (q, 1H), 3.75-3.19 (m, 4H), 3.04 (m, 1H), 2.68 (m, 1H), 2.50 (m, 1H), 1.17 (d, 3H), 1.10 (t, 3H).

Synthesis of Diphenylmethylpotassium. The procedure used for the synthesis of diphenylmethylpotassium (DPMK) was adapted from Normant and Angelo.[15] A 3-neck RBF with a magnetic stirring bar was attached to a high-vacuum line, flame-dried, and purged with nitrogen. Dry THF (150 mL) was added to the flask, followed by potassium metal (4.26 g, 109 mmol, 2 eq) cut into small pieces and naphthalene (7.0 g, 54.6 mmol, 1 eq). The solution became dark green and was allowed to stir for 30 min. Diphenylmethane (18.3 mL, 108 mmol, 2 eq) was then added to the flask with a syringe. The reaction was allowed to proceed overnight, giving a dark red solution. The DPMK solution was stored at room temperature under nitrogen.

Titration of the DPMK solution was performed with acetanilide under nitrogen. A 3-neck RBF was attached to the high vacuum line, flame-dried, and purged with nitrogen. THF (30 mL) was added, followed by a few drops of DPMK solution until the solution remained a pale yellow color. Acetanilide (53.0 mg, 0.39 mmol) was added to the RBF, at which point the color disappeared. A volume of 0.77 mL of the DPMK solution was necessary to reach the same pale yellow end point. This corresponded to a DPMK concentration of 0.51 M.

Synthesis of α-Amino Poly(glycidol acetal) (Amino-PGlyAc9). In a typical anionic polymerization procedure, the monomer is purified on a high-vacuum line and transferred to an ampoule immediately before use. Glycidol acetal could not be purified by that technique due to its high boiling point of 152-154 ºC however.[14] It was rather distilled over triisobutylaluminum in a fractional vacuum distillation setup immediately before use. The glycidol acetal (40.0 g) was loaded in a 100-mL RBF with a stirring bar and the flask was purged with nitrogen. Triisobutylaluminum solution (2 mL, 2 mmol) was added with stirring. The solution became warm within minutes of adding the triisobutylaluminum. After the flask had cooled to room temperature, the glycidol acetal was distilled under reduced pressure into a RBF that was then sealed with a rubber septum and purged with nitrogen.

A 3-neck RBF with a stirring bar was attached to the vacuum line, flame-dried under high vacuum, and purged with nitrogen. Dry THF (25 mL) was added to the RBF, followed by DPMK drop-wise until a faint yellow color persisted in the solution. 3-Aminopropanol (0.19 mL, 2.53 mmol) was then added, followed by DPMK (5.1 mL, 0.51 M) to deprotonate the alcohol. The solution became milky but DPMK was added further, until the solution maintained a faint yellow/red color for one minute. Freshly distilled glycidol acetal (25.2 g, 0.173 mmol, target X_n = 68, M_n = 10,000) was added and the flask was sealed. The

temperature was increased to 65 ºC with an oil bath and the reaction was left stirring overnight under nitrogen. Degassed acidified methanol was then added to terminate the reaction. The solution was transferred to a regenerated cellulose dialysis bag with a 1000 molecular weight cutoff (MWCO) and left to stir in THF. The THF bath was changed once after 3 h and left to stir overnight. The dialysis bag was then emptied into a RBF and the THF was removed under vacuum to give a reddish-brown viscous polymer. Yield: 16.4 g (65%). SEC (THF): M_n = 9100, M_w/M_n= 1.08; ^{1}H NMR: (300 MHz, CDCl3) δ: 4.66 (q, 1H), 3.70-3.39 (m, 7H), 1.24 (d, 3H), 1.15 (t, 3H) (initiator protons not visible).

Ethylene oxide purification. CAUTION: EO is highly toxic and volatile (b.p. 10 ºC), so it should be manipulated with great care in a well-ventilated fume hood, and the monomer should be cooled as much as possible to avoid excessive pressure buildup. Ethylene oxide (EO) was purified on a high-vacuum line using a manifold with connections for the EO tank line, and an ampoule with a Teflon stopcock containing a magnetic stirring bar and approximately 2 g of calcium hydride as a drying agent. The manifold and the ampoule were evacuated and flame-dried, and EO (approximately 100 g) was condensed under vacuum to the ampoule by cooling it in liquid nitrogen. The ampoule was then mounted onto another vacuum manifold having a RBF with a magnetic stirring bar, and another ampoule with a Teflon stopcock. The EO was degassed with three successive freeze-pump-thaw cycles. The ampoule containing the EO was closed, and the rest of the manifold was evacuated and flame-dried. After purging the apparatus with nitrogen, phenylmagnesium chloride solution (PhMgCl, 9 mL, 2.0 M in THF) was added to the RBF on the manifold with a syringe. The THF was removed under vacuum and ca. 15 g of EO was transferred to the RBF containing

the PhMgCl. The solution was stirred for 1 h in an ice bath before slowly recondensing the monomer over to the empty storage ampoule. The amount of EO transferred was 12.3 g.

Polymerization of EO. A 5-neck 500 mL RBF with a magnetic stirring bar was attached to the high-vacuum line with the sealed ampoule containing the EO monomer (cooled with dry ice). The RBF was evacuated, flame-dried, purged with nitrogen, and dry THF (120 mL) was added followed by DPMK solution drop-wise until a faint yellow color persisted in the solution. 3-Aminopropanol (0.19 mL, 2.53 mmol) was then added, followed by DPMK solution (5.1 mL, 0.51 M) to deprotonate the alcohol. The solution became milky and DPMK was added further until a faint yellowish-red color persisted for 1 min in the solution. The EO monomer (12.3 g, 0.279 mol, target X_n = 110, M_n = 5000) was then transferred under vacuum and the reaction temperature was brought to 45 ºC with an oil bath. The reaction was allowed to proceed for 6 d, after which time a dark brown solution was obtained. Degassed acidified methanol was added to terminate the reaction. The solution was concentrated to approximately 50 mL under vacuum and precipitated in cold diethyl ether. A brown powder was recovered by suction filtration. It was redissolved in methanol, precipitated in cold diethyl ether, recovered by suction filtration, and dried under vacuum overnight to produce an off-white powder. Yield: 8.5 g (69%). SEC (DMF): M_n^{app} = 6200, M_w/M_n^{app} = 1.16. ^{1}H NMR: (300 MHz, CDCl3): X_n = 114, δ: 3.87-3.37(m, 456H), 2.88 (br, 1H), 1.96 (br, -OH).

Synthesis of γ-tert-Butyl L-Glutamic Acid N-Carboxyanhydride (tBuGlu-NCA). The procedure used was similar to the one reported for the synthesis of γ-benzyl L-glutamic acid N-carboxyanhydride in Section 3.3.3. γ-*tert*-Butyl L-glutamic acid (10.0 g; 49.2 mmol) was suspended in 300 mL of dry ethyl acetate in a 1-L RBF fitted with a refluxing condenser and

a gas bubbler. The flask was purged with N_2 and heated to reflux. Triphosgene (5.6 g, 18.7 mmol) was added and refluxing was continued for 3 h. The flask was then removed, stoppered, and cooled in a freezer (–10 °C) for 1 h. The solution was transferred to a cold separatory funnel and quickly washed successively with 100 mL of ice-cold water and 100 mL of chilled 0.5% aqueous $NaHCO_3$ solution. The organic phase was dried over anhydrous $MgSO_4$, filtered, and concentrated to ca. 100 mL on a rotary evaporator. An equal volume of cold (–10 °C) hexane was added to induce crystallization of the product. The mixture was left in the freezer overnight and the solid product was recovered by filtration in a Schlenk funnel under N_2. It was dried overnight under vacuum to yield a white powder, and stored under N_2 in a freezer (-10 °C).Yield = 8.6 g (76 %). ^{1}H NMR (300 MHz, $CDCl_3$) δ: 6.75 (s, 1H), 5.11 (s, 2H), 4.38–4.33 (t, 1H), 2.59–2.53 (t, 2H), 2.35–2.21 (m, 1H), 2.21–2.02 (m, 1H), 1.42-1.37 (s, 9H).

Polymerization of tBuGlu-NCA. The procedure used was similar to the one reported for the polymerization of γ-benzyl L-glutamic acid N-carboxyanhydride in Section 3.3.3. The tBuGlu-NCA monomer (1.87 g, 8.1 mmol) was dissolved in dry DMF (15 mL) in a 100-mL RBF at 0 °C and *n*-hexylamine (50 μL, 0.38 mmol, for a target X_n = 20) was added with rapid stirring. The reaction was allowed to proceed for 5 d at 0 °C. The linear polymer was recovered by precipitation in diethyl ether, suction filtration, and drying under vacuum overnight to yield a white powder. Yield = 0.8 g (53%). SEC (DMF): M_w/M_n = 1.15. ^{1}H NMR(300 MHz, d_6-DMSO): X_n = 11.8, δ: 4.19 (br, 12H), 2.24-2.18 (br, 24H), 1.81-1.69 (m, 24H), 1.34 (s, 108H), 1.25-1.13 (b, 10H), 0.81–0.79 (t, 3H).

5.3.5 Quantification of Primary Amines by ^{19}F NMR Analysis

The terminal primary amines of the different linear polymers were quantified by ^{19} F NMR analysis. For example, a linear PBG sample synthesized from a bifunctional initiator, Glu(OtBu)$_2$-Poly(γ-benzyl L-glutamate) or (OtBu)$_2$-PBG (0.0951 g, 1.73×10^{-5} mol of chains) was dissolved in 3 mL of deuterated DMSO (d_6-DMSO). A solution of trifluorobenzaldehyde (TFBA, 0.1105 g, 6.35×10^{-4} mol), and benzotrifluoride (BTF, 0.0925 g, 7.56×10^{-4} mol) in 2 g d_6-DMSO was prepared (BTF served as an internal standard). The reagent solution (0.3088 g, 8.81×10^{-5} mol TFBA, 8.79×10^{-5} mol BTF) was added to the polymer solution and stirred for 2 h; a 0.5 mL sample was then transferred to an NMR tube for analysis. The integrated peak areas from the ^{19}F NMR spectra were used to determine the f_{NH2} values as described in detail in Section 4.4.1 for the linear side chains, and more briefly in Section 5.4.1 for (OtBu)$_2$-PBG.

5.3.6 Synthesis of Arborescent Copolymers

The reaction to generate the arborescent copolymers was similar to the coupling reaction described for the arborescent PBG syntheses. A 25% excess of side chains was used in the reactions, to compensate for any primary amine deactivation occurring before or during the coupling reaction. The solvent employed depended upon the side chains that were used. The preferred solvent was DMSO for reasons discussed in Section 3.4.3, and was used for the coupling reactions with the PEO side chains. DMF served for coupling reactions with the PGlyAc and PtBuGlu side chains, since these have limited solubility in DMSO. An example of a coupling reaction is provided below using the PEO5 side chains.

Synthesis of G1PBG-eg-PEO5. The partially deprotected substrate [G1PBG, 0.031 g, 0.010 mmol –CO_2H] and the polymer serving as side chains (PEO5, 0.066 g, 0.013 mmol chains)

were dissolved in dry DMSO (2 mL) in a 10-mL RBF. The peptide coupling reagents diisopropylcarbodiimide (DIC, 8 μL, 0.051 mmol) and 1-hydroxybenzotriazole (HOBt, 7 mg, 0.051 mmol) were then added to the reaction followed by triethylamine (TEA, 9 μL, 0.064 mmol). The reaction was allowed to proceed for 24 h at room temperature before adding *n*-hexylamine (5 μL, 0.050 mmol), to deactivate residual carboxylic acid sites. After 1 h the product was diluted with DMF and purified by preparative SEC. SEC (DMF): Grafting yield = 29%, M_n = 442,000, M_w/M_n = 1.05 (MALLS).

Deprotection of G1PBG-eg-PGlyAc9. The cleavage of the acetal protecting groups from the PGlyAc chains attached to arborescent PBG was investigated and discussed in Chapter 4. The most successful approach for the arborescent copolymers was adapted from a method reported by Mendrek et al.[22] The copolymer G1PBG-*eg*-PGlyAc9 (0.085 g, 0.060 g GlyAc units, 0.41 mmol GlyAc) was placed in a 25-mL RBF with a magnetic stirring bar and DMF (4 mL). A concentrated hydrochloric acid (HCl) solution (11.7 M, 0.16 mL, 1.86 mmol HCl) was added and the reaction was stirred for 30 min at room temperature, at which point a saturated $NaHCO_3$ aqueous solution was added until the acid was neutralized (pH > 7, ca. 2 mL). The solvents were removed under reduced pressure and the polymer was redissolved in ethanol. Insoluble salts were removed by suction filtration, and the crude product was placed in a 12,000-14,000 MWCO dialysis bag in methanol to remove any linear polyglycidol fragments that may have been cleaved off in the deprotection step. The copolymer obtained was stored in solution in a refrigerator at 4 ºC.

Deprotection of G2PBG-eg-PtBuGlu2. The purified copolymer G2PBG-*eg*-PtBuGlu2 (0.080 g) was dissolved in trifluoroacetic acid and stirred for 5 min. It was then precipitated in

diethyl ether, recovered by suction filtration, and dried under vacuum overnight. Yield: 0.045 g (70%).

5.4 Results and Discussion

5.4.1 Synthesis of Linear PBG Using a Glutamic Acid Derivative as Initiator

The ring-opening polymerization of α-amino acid N-carboxyanhydrides (NCA) has been studied extensively over the past 50 years.[16,17] Different initiator systems have been developed for that purpose and have been successful in generating well-defined linear polypeptides. The most commonly used method for generating short polypeptide chains (X_n <50) relies upon the normal amine (NA) polymerization mechanism displayed in Figure 5.3, that involves a primary amine initiator. A primary amine such as *n*-hexylamine attacks the carbonyl group of the NCA, followed by the loss of carbon dioxide to regenerate a primary amine capable of attacking another α-amino acid NCA. This NA mechanism leads to a polypeptide chain with a polyamide backbone and a primary amine chain end.

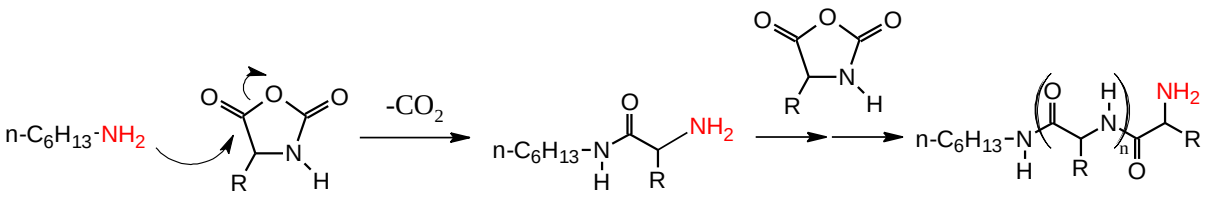

Figure 5.3 Normal amine mechanism for the primary amine-initiated polymerization of α-amino acid N-carboxyanhydrides.

The Glu(OtBu)$_2$·HCl initiator is in the hydrochloride salt form and therefore behaves differently from a typical primary amine initiator in the NCA polymerization, by having a

much lower nucleophilicity than primary amines. It was first pointed out by Knobler et al. in 1964 that the primary amine hydrochloride salt is at equilibrium with its non-protonated form, which is capable of initiation of an NCA through the NA mechanism.[18] The equilibrium for the *n*-hexylamine hydrochloride salt is shown in Figure 5.4. Primary amine hydrochloride salt initiators have been used previously at relatively high reaction temperatures, to produce block copolymers containing polypeptide chain segments.[19,20] In these cases, primary amine macroinitiators in the hydrochloride salt form were used to grow small polypeptide chain segments at temperatures between 40-80 ºC. The primary amine hydrochloride salt initiators were used to prevent the well-known activated monomer mechanism (AMM), first proposed by Ballard and Mamford, [21] from occurring in the ring-opening polymerization of NCAs as shown in Figure 5.5. In the AMM, the primary amine behaves like a base and abstracts a proton from an NCA monomer. This "activated" monomer has the potential to act as a nucleophile towards other NCA monomers and initiate their polymerization.

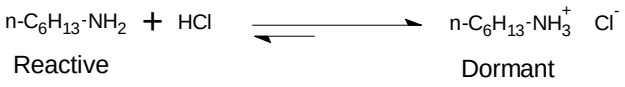

Figure 5.4 *n*-Hexylamine hydrochloride salt equilibrium.

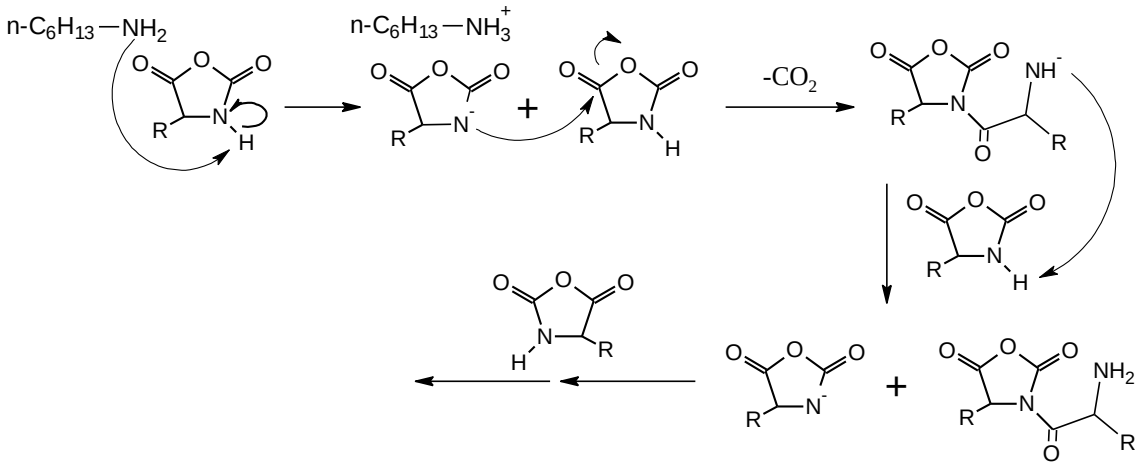

Figure 5.5 Activated monomer mechanism for the ring-opening polymerization of an NCA.

The success of these primary amine hydrochloride salt initiator systems led us to use the glutamic acid derivative, $Glu(OtBu)_2 \cdot HCl$, as initiator for the polymerization of Bz-Glu-NCA. This initiator should remain at equilibrium with its non-protonated (reactive) state as shown in Figure 5.6. Since the equilibrium strongly favors the protonated (dormant) state of the primary amine hydrochloride salt, it will be unreactive towards NCAs most of the time. When the hydrochloride dissociates to its non-protonated state, it can quickly react with an NCA monomer. After the loss of CO_2 following opening of the NCA ring, the primary amine will revert to its hydrochloride form. This equilibrium also comes into play for the primary amine chain end throughout the propagation stage of the polymerization. A higher temperature is necessary to increase the equilibrium exchange rate and allow the primary amine hydrochloride salts to react more efficiently.

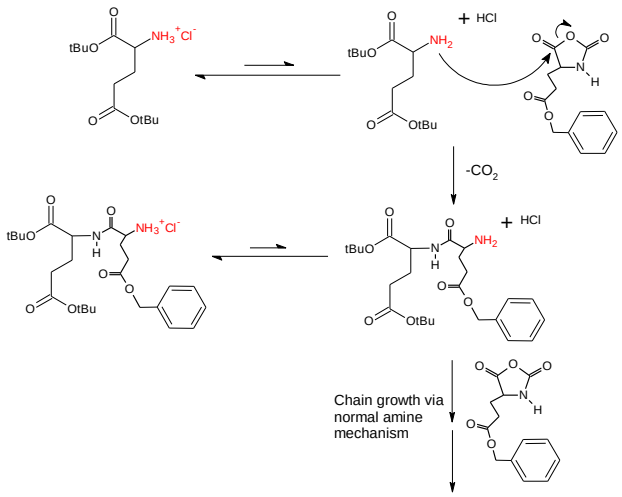

Figure 5.6 Initiation and propagation of Bz-Glu-NCA using Glu(OtBu)$_2$·HCl as initiator.

The initiator Glu(OtBu)$_2$·HCl was successful for the polymerization of γ-benzyl L-glutamic acid N-carboxyanhydride (Bz-Glu-NCA), but a reaction temperature of 40 ºC and a reaction time of 7 days were necessary to ensure a high monomer conversion. The molecular weight distribution remained relatively low (M_w/M_n = 1.18), albeit it was still broader than for the linear PBG polypeptide samples obtained in Chapter 3 (M_w/M_n < 1.11) using *n*-hexylamine at 0 ºC for 3 days. The broader molecular weight distribution obtained for the Glu(OtBu)$_2$·HCl initiator may be due to its slower initiation rate, even at higher reaction temperatures, relatively to *n*-hexylamine. A number-average degree of polymerization X_n = 24 was obtained by ^{1}H NMR analysis, as shown in Figure 5.7, very close to the theoretical value of 23. The integrated peak intensity for the 18 protons of the *tert*-butyl ester groups in the initiator fragment, found at 1.3 ppm, were compared with that for the two benzylic protons on each repeat unit at 5.0 ppm. Residual DMF from the polymerization reaction is

responsible for the peaks at 2.7, 2.9, and 7.9 ppm, and residual water from the precipitation in methanol also appears at 3.3 ppm.

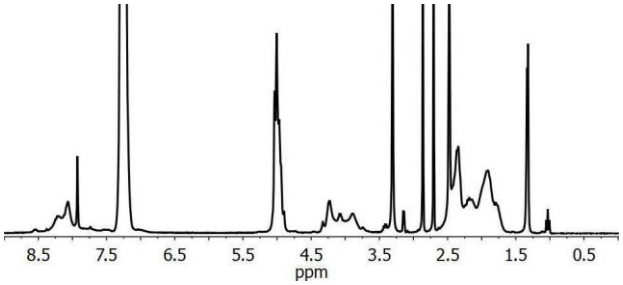

Figure 5.7 ^{1}H NMR spectrum for Glu(OtBu)$_2$·HCl-initiated linear PBG in d$_6$-DMSO.

Another measure of the success of the linear PBG synthesis initiated by Glu(OtBu)$_2$·HCl [(OtBu)$_2$-PBG] is the primary amine functionality content of the chains, f_{NH2}, obtained after isolation of the polypeptide. The f_{NH2} value corresponds to the number of primary amines present as chain ends relatively to the number of linear chains in a given polymer sample. A detailed discussion of the method for obtaining the f_{NH2} values by ^{19}F NMR analysis was provided in Chapter 4. A f_{NH2} value of 0.95 was obtained for (OtBu)$_2$-PBG. To further demonstrate that the hydrochloride salts are less reactive than free primary amines, a small sample of (tBuO)$_2$-PBG was precipitated prior to the addition of triethylamine, to preserve the primary amine hydrochloride salt form of the chain end. When the ^{19}F NMR analysis technique was used to determine the f_{NH2} for the (tBuO)$_2$-PBG·HCl sample, a f_{NH2} value of only 0.38 was obtained after the standard 2 h reaction time with the aldehyde. Triethylamine was then added (1 equiv) to the reaction, to displace HCl from the polymer chain end; after 2 h, the f_{NH2} value increased to 0.94. This confirms that the primary amine hydrochlorides have a much lower reactivity than the free primary amines as expected.

The ^{19}F NMR spectra for the f_{NH2} determination of $(tBuO)_2$-PBG·HCl are provided in Figure 5.8.

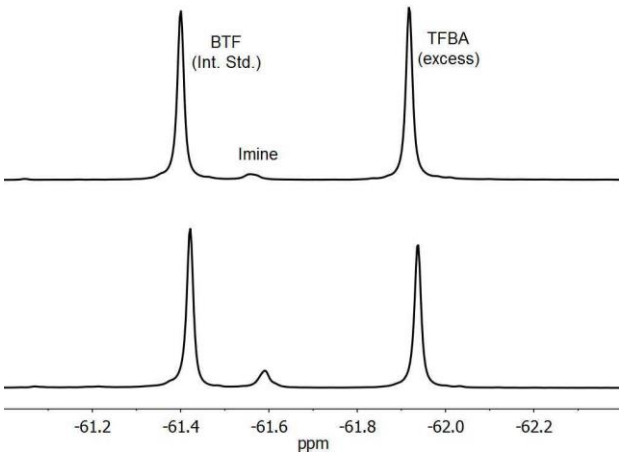

Figure 5.8 ^{19}F NMR spectra for $(tBuO)_2$-PBG·HCl primary amine functionality determination after 2 h of reaction (top), and 2 h after the addition of triethylamine (4 h total reaction time; bottom).

5.4.2 Synthesis of Chain End Functionalized PBG Substrates

To obtain chain end functionalized PBG substrates, the $(tBuO)_2$-PBG linear chains synthesized were grafted onto randomly deprotected arborescent PBG substrates of generations G0, G1, and G2 by standard peptide coupling techniques. This led to arborescent PBG polymers of generations G1, G2, and G3, respectively, containing *tert*-butyl ester-protected carboxylic acid groups near the periphery as shown in Figure 5.9. The *tert*-butyl ester protecting groups were selectively cleaved by dissolving the arborescent polymer samples in trifluoroacetic acid (TFA), thus releasing two carboxylic acid functional groups at each chain end. This functionalized arborescent PBG served as substrate in subsequent

grafting reactions with the linear chain segments acting as a shell component, as is also shown in Figure 5.9.

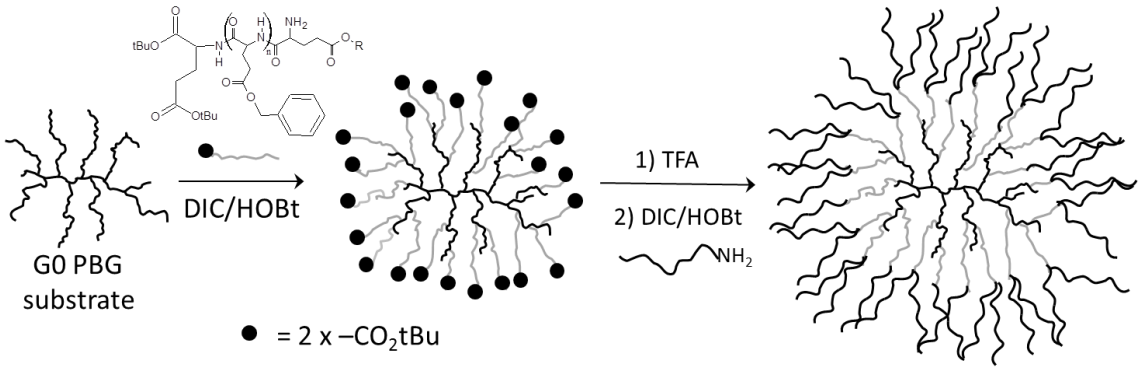

Figure 5.9 Schematic representation of the synthesis of double-functionalized chain end G1 PBG substrates, and the G1PBG *end-grafted* arborescent copolymers.

^{1}H NMR analysis was used to determine the mole fraction of *tert*-butyl ester groups relatively to the number of repeat monomer units in the molecule before and after deprotection. The corresponding ^{1}H NMR spectra obtained for a G1 sample are displayed in Figure 5.10. Each chain end corresponds to 18 protons for the two *tert*-butyl ester protecting groups per chain end. Equation 5.1 was used to determine the mole fraction of *tert*-butyl ester protecting groups in the arborescent substrates:

$$f_{tBu} = \frac{(\text{Integral } \textit{tert}\text{-butyl H})/18}{(\text{Integral methine H})/1} = \frac{0.633/18}{1/1} = 0.035 \times 2 = 0.07 \qquad (5.1)$$

It was confirmed by ^{1}H NMR spectroscopy that complete removal of the *tert*-butyl ester protecting groups was achieved, and that no significant amount of benzyl ester protecting groups, if any, had been cleaved. Complete disappearance of the *tert*-butyl protons at 1.3 ppm is observed, and the small peaks remaining near 1.3 ppm are from the *n*-

hexylamine residues attached to the PBG substrates in the previous grafting reactions. Comparison of the methine proton signal at 3.8-4.4 ppm to the benzyl ester protecting group protons at 5 ppm before and after acidolysis was performed to ensure there was no significant loss of the benzyl ester protecting groups during acidolysis. Similar procedures were used to generate the G2 and G3 chain end functionalized PBG substrates. The number-average molecular weight and functionalization level of these substrates will be provided together with their arborescent copolymer counterparts in the following section.

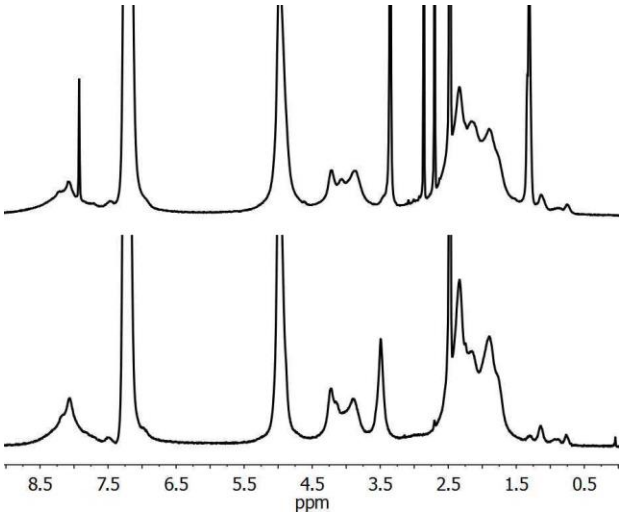

Figure 5.10 ^{1}H NMR spectra in d_6-DMSO for a G1 chain end functionalized PBG sample before (top) and after acidolysis (bottom) of the *tert*-butyl ester protecting groups.

5.4.3 Synthesis of Chain End Grafted Arborescent Copolymers

A detailed discussion of the synthesis of the linear polymer chain segments used as shell components can be found in Chapter 4, so this will not be discussed further here. The characterization data for the linear chain segments are provided in Table 5.1**.**

Table 5.1 Characteristics of linear chains for PBG grafting

	SEC[a]		^{1}H NMR		^{19}F NMR
Polymer	M_n	M_w/M_n	X_n[b]	M_n[c]	f_{NH2}(%)[d]
PGlyAc9	9,100	1.08	-	-	64
	M_n^{app}	M_w/M_n			
PEO5	6,200	1.16	114	5,100	91
PtBuGlu2	3,200	1.20	11.8	2,300	99

[a] PGlyAc analyzed on a SEC-triple detection system in THF with dn/dc = 0.045 mL/g.[22] PEO and PtBuGlu analyzed in DMF with 0.1 % LiCl on a SEC-DRI detector only, so only apparent molecular weights are reported; [b] number-average degree of polymerization; [c] M_n calculated from X_n; [d] terminal primary amine content determined by ^{19}F NMR analysis according to the procedure of Ji et al.[13]

The terminal primary amine group on the linear polymer chain segments was coupled with the carboxylic acid moieties at the chain ends of the arborescent PBG substrates. The peptide coupling reagents DIC and HOBt were used for that purpose, along with triethylamine as a proton scavenger. A 25% excess of linear chain segments was added in the reactions, to ensure maximized reaction of coupling sites on the arborescent PBG substrates, and to compensate for the potential loss of amine functionalities during coupling. Chain end functionalized arborescent substrates of generations G1, G2, and G3 were employed in the reactions. Similarly to Chapter 4, the G0 arborescent substrate was not investigated, as it was expected to have a more open structure relatively to the higher generations of PBG favoring the formation of multimolecular micelles in aqueous solutions.

5.4.4 PBG-*end-grafted*-PGly Arborescent Copolymers

The overall functionality level of the chain end functionalized PBG substrates (7-12 mole%) is considerably lower than for the randomly functionalized PBG substrates used in Chapter 4 (26-38 mole%). The accessibility of the coupling sites is expected to be higher for the chain end functionalized PBG substrates, however, since they are located closer to the periphery of the molecules. This should also provide arborescent copolymers with a better-defined crew-cut core-shell morphology, more suitable to shield the PBG cores in solvents selective for the shell component. As the grafting reaction proceeds the accessibility of the remaining coupling sites should decrease, irrespective of whether randomly or chain end functionalized arborescent PBG substrate are used, due to increased steric hindrance from the newly grafted linear chains in the shell. This may also become a problem for the chain end functionalized PBG substrates, since the coupling sites are paired up at each chain end as shown in Figure 5.9. Once the first coupling site at a given chain end reacts, the probability of the second coupling site at the same chain end is likely reduced, due to steric hindrance from the first chain grafted. However, even if only one coupling site per chain end of the PBG substrates can react, the result would be similar to the *grafting from* technique used by Gauthier et al. to generate arborescent PS-*eg*-PEO copolymers.[12] Since a 25% excess of linear chain segments was added in the reactions relatively to the coupling sites, the grafting yield (defined as the fraction of linear chain segments becoming coupled to the substrate) can only reach a maximum value of 80% if all coupling sites on the substrate are consumed. A grafting yield above 40% likewise indicates that, on average, at least one of the two coupling sites per PBG substrate chain has reacted.

The results obtained for the grafting reactions of arborescent PBG-*end-grafted*-PGlyAc (PBG-*eg*-PGlyAc) copolymers are provided in Table 5.2. The grafting yield, G_y, was determined from the known masses of the substrate and side chains used in the grafting reaction, along with the copolymer weight fractions (calculated from the M_n values of the PBG substrate and copolymer). An example of grafting yield determination is provided in Equation 5.2 for the G2PBG-eg-PGlyAc9 copolymer. In this case 0.020 g of PBG substrate was used, whereas a weight fraction of 0.55 for the PGlyAc component in the copolymer corresponded to a mass of 0.024 g PGlyAc. Dividing the mass of PGlyAc contained in the copolymer by the total mass used in the grafting reaction (0.131 g PGlyAc), a grafting yield of 19% is obtained.

Table 5.2 Characteristics of chain end grafted PBG-*eg*-PGlyAc arborescent copolymers

Copolymer[a]	PBG Substrate			Graft Copolymer			
	M_n (g/mol) [b]	% -CO_2H[c]	G_y[d]	M_n (g/mol) [b]	M_w/M_n [b]	f_n [e]	% GlyAc[f]
G1PBG-*eg*-PGlyAc9	238,000	9	50	824,000	1.08	64	71
G2PBG-*eg*-PGlyAc9	1.1×10^6	12	19	2.5×10^6	1.07	149	55
G3PBG-*eg*-PGlyAc9	3.0×10^6	11	21	6.6×10^6	1.04	396	55

[a] All grafting reactions done with 25% excess of side chains; [b] absolute values from SEC-MALLS in DMF, [c] deprotection level determined by ^{1}H NMR analysis; [d] grafting yield: fraction of side chains attached to the substrate (80% maximum); [e] branching functionality: number of branches added in the last grafting cycle; [f] GlyAc weight fraction from the difference in the absolute M_n of the copolymer and the substrate.

$$G_y = \frac{mass\ PBG\ (g) \times \frac{Wt.Fraction\ PGlyAc}{Wt.Fraction\ PBG}}{mass\ PGlyAc\ (g)} = \frac{0.02 \times \frac{0.55}{0.45}}{0.131} = 0.19 \quad (5.2)$$

Using the grafting yields for comparison, the syntheses of the chain end grafted arborescent copolymers G1PBG-*eg*-PGlyAc9 and G2PBG-*eg*-PGlyAc9 were more

successful than for the randomly functionalized PBG substrates under the same reaction conditions (Chapter 4), for which grafting yields of only 9 and 3% were obtained for G1PBG-*g*-PGlyAc9 and G2PBG-*g*-PGlyAc9, respectively. These results are provided in Table 5.3 for comparison. It is even more noteworthy that the grafting reaction for G3PBG-*eg*-PGlyAc9 was successful, while it essentially failed for G3PBG-*g*-PGlyAc9. The greater success of grafting reactions for chain end functionalized G3PBG substrates demonstrates the better accessibility of these coupling sites relatively to the randomly functionalized PBG substrates. The molecular weight distribution of the PBG-*eg*-PGlyAc arborescent copolymer samples is also slightly narrower ($M_w/M_n \leq 1.08$) than for the PBG-*g*-PGlyAc copolymers ($M_w/M_n \leq 1.11$), although the difference is small and may be insignificant. Both the G1 and G2 chain end grafting reactions produced higher molecular weight copolymers than the G1 and G2 random grafting reactions, respectively. As a result a larger number of PGlyAc linear chain segments were grafted in both cases, thus increasing the branching functionality f_n (i.e. the number of linear chain segments grafted onto the substrate). The f_n values were calculated by dividing the molecular weight difference of the arborescent copolymer and substrate by the molecular weight of the linear chains segments added. An example of this calculation for G1PBG-*eg*-PGlyAc9 is provided in Equation 5.3:

$$f_n = \frac{M_n(\text{G1PBG-eg-PEO5}) - M_n(\text{G1PBG})}{M_n(\text{PGlyAc9})} = \frac{824{,}000 - 238{,}000}{9{,}100} = 64.4 \qquad (5.3)$$

The weight fraction of poly(glycidol acetal) in the chain end grafted arborescent copolymers was calculated from the molecular weight difference for the arborescent copolymers and the substrates. Using G1PBG-*eg*-GlyAc9 as an example, the molecular

weight difference, 590,000, divided by the molecular weight of the arborescent copolymer, 824,000, yields a weight fraction of poly(glycidol acetal) of 71%. Not only are the PGlyAc linear chain segments more likely to be grafted close to the periphery of the PBG substrates relatively to the randomly grafted arborescent copolymers, but there are also more of them, which should provide enhanced shielding for the PBG cores. The SEC traces obtained for the purified PBG-*eg*-PGlyAc samples are provided in Figure 5.11. It is clear that there is a significant difference in elution volume over successive generations, corresponding to the differences in molecular weight and hydrodynamic volume for the arborescent copolymers.

Table 5.3 Characteristics of randomly grafted arborescent PBG-g-PGlyAc copolymers previously synthesized.

	PBG Substrate			Graft Copolymer			
Copolymer[a]	M_n[b]	% Deprotected[c]	G_y[d]	M_n[b]	M_w/M_n[b]	f_n[e]	% GlyAc[f]
G1PBG-*g*-PGlyAc9	234,000	35	9	661,000	1.10	47	65
G2PBG-*g*-PGlyAc9	1.1×10^6	34	3	1.8×10^6	1.10	75	38
G3PBG-*g*-PGlyAc9	3.0×10^6	34	Failed reaction				

[a] All grafting reactions done with 25% excess of side chains; [b] absolute values from SEC-MALLS in DMF; [c] deprotection level determined from ^{1}H NMR analysis; [d] grafting yield: fraction of side chains attached to the substrate (maximum yield 80%); [e] branching functionality: number of branches added in the last grafting cycle; [f] GlyAc weight fraction from the difference in the absolute molecular weights of the copolymer and the substrate.

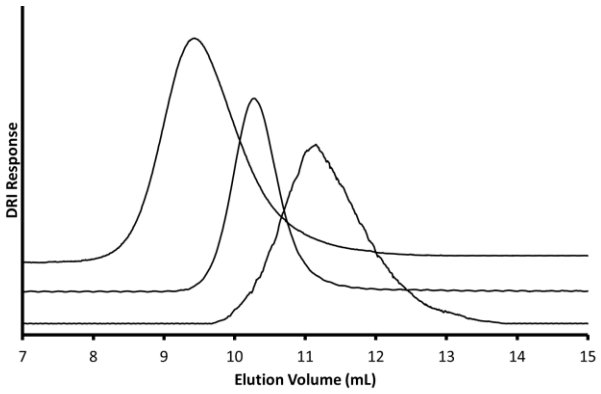

Figure 5.11 SEC traces in DMF with 0.1% LiCl for purified arborescent copolymers: (top to bottom) G3PBG-*eg*-PGlyAc9, G2PBG-*eg*-PGlyAc9, and G1PBG-*eg*-PGlyAc9.

Dynamic Light Scattering Measurements. The DLS measurements were initially performed on the PBG-*eg*-PGlyAc arborescent copolymers in THF, to evaluate their solution properties. The results obtained under these conditions are summarized in Table 5.4. The uncertainties reported in the table are either the standard deviation for a series of 5 measurements or 1 nm, whichever was larger. THF is a good solvent for the poly(glycidol acetal) shell, but a poor solvent for the PBG cores. First- and second-order analysis of the correlation function, $|g_1(\tau)|$ and $|g_2(\tau)|$, respectively, provides unbiased information on the size dispersity of the system. Strictly monodispersed samples yield identical results for their first- and second-order analysis, since the correlation function can be represented by a single exponential decay under these conditions.[23] Therefore, when the size distribution of a sample broadens, the difference between the first- and second-order analysis results will increase. The first- and second-order hydrodynamic diameters (d_{h1} and d_{h2}, respectively) obtained by this approach are compared to the values obtained for the PBG substrates in DMF in Table 5.4. THF and DMF being good solvents for the shell and the core components of the copolymers, an increase in hydrodynamic diameter is seen for the copolymers relatively to their

respective PBG substrates. To ensure that the hydrodynamic diameters observed in THF are not the result of aggregation, DLS measurements were also performed in DMF (with 0.05% LiCl) for sample G2PBG-*eg*-PGlyAc9, yielding d_{h1} and d_{h2} values of 30.3 and 27.7 nm, respectively, only slightly larger than the values obtained in THF. This confirms that the d_{h1} and d_{h2} values in Table 5.4 reflect the characteristics of the non-aggregated arborescent copolymers in THF, and that the slightly lower values observed in THF are likely due to the collapse of the PBG cores. The results obtained in THF for the PGlyAc copolymers show that this material is promising as a protective shell for the PBG cores in selective solvents, when using chain end functionalized PBG substrates.

Table 5.4 DLS measurements for PBG-*eg*-PGlyAc arborescent copolymers

	PBG Substrate (DMF)[a]		Graft Copolymer (THF)[b]	
Copolymer[a]	d_{h1}[c]	d_{h2}[d]	d_{h1}[c]	d_{h2}[d]
G1PBG-*eg*-PGlyAc9	$12._8 \pm 1$	$11._7 \pm 1$	$22._9 \pm 1$	$18._8 \pm 1$
G2PBG-*eg*-PGlyAc9	$18._9 \pm 1$	$17._3 \pm 1$	$29._1 \pm 1$	$24._9 \pm 1$
G3PBG-*eg*-PGlyAc9	$28._4 \pm 1$	$26._8 \pm 1$	$42._3 \pm 1$	$39._6 \pm 1$

[a] DMF with 0.05% LiCl to prevent aggregation; [b] Pure THF; [c] hydrodynamic diameter from 1st order analysis of the correlation function (nm); [d] diameter from 2nd order analysis (nm).

Similarly to the arborescent copolymers containing PGlyAc in Chapter 4, removal of the acetal protecting group on the poly(glycidol acetal) side chains was necessary to produce water-soluble micelles. The optimal approach for the removal of the acetal protecting groups was discussed in Section 4.4.2, and is based on a procedure adapted from Mendrek et al.[22] DLS analysis results for the arborescent PBG-*eg*-PGly (deprotected) copolymers are

provided in Table 5.5. In DMF the hydrodynamic diameter of the arborescent PBG-*eg*-PGly copolymers display a trend similar to their protected counterparts with respect to their increase in size as a function of their generation number, as well as a small difference between the d_{h1} and d_{h2} values. The arborescent PBG-*g*-PGly copolymers were all soluble in PBS, but there was a significant increase in hydrodynamic diameter observed for all three generations. The increased discrepancy between the d_{h1} and d_{h2} values is also indicative of the presence of aggregated species. Similarly to Chapter 4, these results suggest that self-assembly likely occurs in these systems, to minimize exposure of the PBG cores to the unfavorable aqueous environment. However the size of the aggregated species for G1PBG-*eg*-PGly5 (d_{h2} = 56 nm) is significantly smaller than for the randomly grafted G1PBG-*g*-PGly5 sample, which had d_{h2} = 184 nm. G2PBG-*eg*-PGly5 likewise forms much smaller aggregates than its randomly grafted analogue G2PBG-*g*-PGly5, which could not be analyzed due to extensive aggregation leading to an unstable baseline for the correlation function. In both cases, the G2PBG copolymers were more aggregated than the G1PBG copolymers. Interestingly, when G3PBG-eg-PGly5 was analyzed, lower d_{h1} and d_{h2} values were obtained than for G1PBG-*eg*-PGly5 and G2PBG-*eg*-PGly5, but a large difference remained between the d_{h1} and d_{h2} values for G3PBG-*eg*-PGly5. This suggests that aggregation was still present for the G3PBG copolymer, albeit it was less pronounced than for the lower generations since the hydrodynamic diameters were closer to the values obtained in DMF. It is possible that because the G3PBG core is denser than the G1PBG and G2PBG cores, intramolecular rearrangements are more difficult, thus forcing the PGly chains to shield the PBG cores more effectively.

Table 5.5 DLS measurements for PBG-*eg*-PGly arborescent copolymers

	PBG Substrate (DMF)[a]		Graft Copolymer (DMF)[a]		Graft Copolymer (PBS)[b]	
Copolymer[a]	d_{h1}[c]	d_{h2}[d]	d_{h1}[c]	d_{h2}[d]	d_{h1}[c]	d_{h2}[d]
G1PBG-*eg*-PGly5	$12._8 \pm 1$	$11._7 \pm 1$	$26._1 \pm 1$	$21._0 \pm 1$	$77._7 \pm 1$	$56._3 \pm 1$
G2PBG-*eg*-PGly5	$18._9 \pm 1$	$17._3 \pm 1$	$34._6 \pm 1$	$31._2 \pm 1$	$121._8 \pm 2$	$88._5 \pm 1$
G3PBG-*eg*-PGly5	$28._4 \pm 1$	$26._8 \pm 1$	$44._8 \pm 1$	$39._4 \pm 1$	$63._5 \pm 1$	$48._0 \pm 1$

[a] DMF with 0.05% LiCl to prevent aggregation; [b] phosphate buffer solution with pH 7.4; [c] Hydrodynamic diameter from 1st order analysis of the correlation function (nm); [d] diameter from 2nd order analysis (nm).

5.4.5 PBG-*end-grafted*-PEO Arborescent Copolymers

The arborescent copolymer syntheses using the PEO linear chain segments were performed under the same conditions as for PGlyAc, with the exception that DMSO served as the reaction solvent in place of DMF. The results obtained for the grafting reactions are provided in Table 5.6. The SEC traces for the PBG-*eg*-PEO arborescent copolymers, displayed in Figure 5.12, show a shift to lower elution volumes for the higher generation arborescent copolymers, while the molecular weight distributions remain narrow over successive generations. The molecular weight increases observed are not as significant as for the randomly functionalized PBG substrates in this case, as shown in Table 5.7. This can be explained by the lower functionality level of the chain end functionalized PBG substrates, as well as the greater ability of the flexible PEO chains to diffuse to coupling sites buried inside the substrate. The grafting yields, G_y, reported for the PBG-*eg*-PEO5 copolymers in Table 5.6 are similar to the grafting yields obtained for the PGlyAc chain segments (Table 5.2), with the exception of G1PBG-*eg*-PGlyAc9 being higher. This contrasts with the case when randomly functionalized PBG substrates were used with the PEO chain segments, were higher yields were obtained relatively to PGlyAc. The more consistent trends in the grafting

yield for the chain end functionalized PBG substrates suggest that the chain end grafting reactions were less restricted by steric hindrance. The placement of the coupling sites at the periphery of the substrate molecules, and the lower functionality level of the PBG substrates explain these higher grafting yields. The branching functionality, f_n, and the weight fraction of PEO are both related to the molecular weight increase for the arborescent copolymers relatively to the PBG substrates. The weight fraction of PEO in the chain end grafted copolymers was 37%, 48%, and 45%, for the G1, G2, and G3 samples respectively (Table 5.6), i.e. smaller than for the randomly grafted PEO segments (77%, 84%, and 87% for the G1, G2, and G3 samples, respectively; Table 5.7).

Table 5.6 Characteristics of the chain end grafted PBG-*eg*-PEO arborescent copolymers

	PBG Substrate			Graft Copolymer			
Copolymer[a]	M_n (g/mol) [b]	% -CO_2H[c]	G_y[d]	M_n (g/mol) [b]	M_w/M_n [b]	f_n [e]	% EO[f]
G1PBG-*eg*-PEO5	280,000	7	29	442,000	1.05	32	37
G2PBG-*eg*-PEO5	1.1×10^6	12	25	2.1×10^6	1.07	202	48
G3PBG-*eg*-PEO5	3.0×10^6	11	25	5.5×10^6	1.03	482	45

[a] All grafting reactions done with 25% excess of side chains; [b] Absolute values from SEC-MALLS in DMF; [c] Deprotection level from ^{1}H NMR analysis; [d] Grafting yield: fraction of side chains attached to the substrate; [e] Branching functionality: number of branches added in the last grafting cycle; [f] EO weight fraction determined from the absolute molecular weights of the copolymer and the substrate.

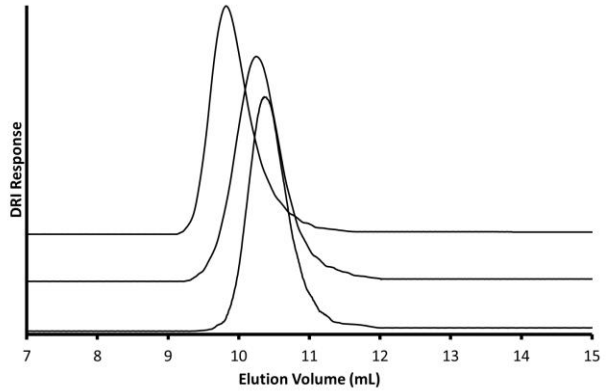

Figure 5.12 SEC traces in DMF with 0.1% LiCl for the purified arborescent copolymers: (top to bottom) G3PBG-*eg*-PEO5, G2PBG-*eg*-PEO5, and G1PBG-*eg*-PEO5.

Table 5.7 Characteristics of randomly grafted arborescent PBG-g-PEO copolymers previously synthesized.

	PBG Substrate			Graft Copolymer			
Copolymer[a]	M_n[b]	% Deprotected[c]	G_y[d]	M_n[b]	M_w/M_n[b]	f_n[e]	% PEO[f]
G1PBG-*g*-PEO5	234,000	35	28	1.0×10^6	1.07	150	77
G2PBG-*g*-PEO5	1.1×10^6	26	62	6.9×10^6	1.05	1133	84
G3PBG-*g*-PEO5	3.0×10^6	34	58	2.3×10^7	1.04	3900	87

[a] All grafting reactions done with 25% excess of side chains; [b] Absolute values from SEC-MALLS in DMF; [c] deprotection level from ^{1}H NMR analysis; [d] grafting yield: fraction of side chains attached to the substrate; [e] branching functionality: number of branches added in the last grafting cycle; [f] EO weight fraction determined from absolute molecular weights of copolymer and substrate.

Dynamic Light Scattering Measurements. The PBG-*eg*-PEO arborescent copolymers were characterized by DLS measurements in both DMF and PBS; the results obtained are provided in Table 5.8. In DMF, there is a good agreement between d_{h1} and d_{h2} values for all three generations. Both PBG and PEO are soluble in DMF, so there is no reason to observe aggregation under these conditions. Interestingly, the hydrodynamic diameters are very

similar for G3PBG-*eg*-PEO5 and G2PBG-*eg*-PEO5 in DMF; the reason for this is not clear. Prior to the DLS measurements in PBS, the arborescent copolymers in DMF were placed in a 1000 MWCO dialysis bag in a PBS solution overnight. The end-grafted samples display better solubilization than the randomly grafted PBG-*g*-PEO5 arborescent copolymers, which had large aggregated species for G1PBG-*g*-PEO5 and were insoluble for G2PBG-*g*-PEO5 and G3PBG-*g*-PEO5. In the PBS solution, both G1PBG-*eg*-PEO5 and G3PBG-*eg*-PEO5 have reasonably good agreement between the d_{h1} and d_{h2} values (~5 nm difference) with a moderate increase in hydrodynamic diameters with respect to the values measured in DMF. The G2PBG-*eg*-PEO5 copolymer behaved similarly to G2PBG-*eg*-PGly5 however, with a larger hydrodynamic diameter increase from DMF to PBS, as well as a larger difference between the d_{h1} and d_{h2} values (~14 nm). The solution properties observed for the PBG-*eg*-PEO copolymers in the PBS solutions demonstrate the advantage of chain end *grafting onto* method relatively to random *grafting onto* to generate optimal core-shell morphologies: The arborescent PBG-*eg*-PEO copolymers behave more clearly like unimolecular micelles in aqueous environments, even though the PEO weight fraction is these copolymers is lower than in their randomly grafted analogues.

Table 5.8 DLS measurements for PBG-*eg*-PEO arborescent copolymers

Copolymer[a]	PBG Substrate (DMF)[a]		Graft Copolymer (DMF)[a]		Graft Copolymer (PBS)[b]	
	d_{h1}[c]	d_{h2}[d]	d_{h1}[c]	d_{h2}[d]	d_{h1}[c]	d_{h2}[d]
G1PBG-*eg*-PEO5	$11._6 \pm 1$	$10._0 \pm 1$	$21._1 \pm 1$	$18._0 \pm 1$	$30._7 \pm 1$	$25._9 \pm 1$
G2PBG-*eg*-PEO5	$18._9 \pm 1$	$17._3 \pm 1$	$38._1 \pm 1$	$34._0 \pm 1$	$59._0 \pm 1$	$45._1 \pm 1$
G3PBG-*eg*-PEO5	$28._4 \pm 1$	$26._8 \pm 1$	$38._4 \pm 1$	$37._0 \pm 1$	$48._4 \pm 1$	$43._9 \pm 1$

[a] DMF with 0.05% LiCl to prevent aggregation; [b] phosphate buffer solution with pH 7.4; [c] hydrodynamic diameter from 1st order analysis of the correlation function (nm); [d] diameter from 2nd order analysis (nm).

5.4.6 PBG-*end-grafted*-PtBuGlu Arborescent Copolymers

PBG-end-grafted-PtBuGlu Arborescent Copolymers. In view of the success of the grafting reaction of chain end functionalized PBG substrates with PGlyAc and PEO chains, the synthesis of a G2PBG-*eg*-PtBuGlu2 arborescent copolymer was also briefly explored to determine whether the chain end grafting method could also work for bulkier PtBuGlu chains as well. The characteristics for the arborescent G2PBG-*eg*-PtBuGlu2 copolymer obtained are provided in Table 5.9. The absolute M_n of the arborescent copolymer was not determined by SEC, due to unreliable light scattering measurements for that sample related to a high molecular weight shoulder present in the copolymer peak for the light scattering signal, possibly due to aggregation of the copolymers within the SEC column. The M_n was rather estimated from the known composition of the copolymer (by ^{1}H NMR analysis) along with the known M_n value of the PBG substrate. As discussed in Chapter 4, this approach has its limitations and may overestimate the M_n, since part of the signal for the core may be lost (due to its reduced mobility) in the ^{1}H NMR analysis, but this method still provides a rough M_n estimate for comparison to the other copolymer systems. The polydispersity was estimated from the differential refractometer detector signal. The grafting yield obtained, G_y

= 50%, corresponds to an average of more than one PtBuGlu chain for every doubly functionalized chain end on the PBG substrates. In comparison to the randomly grafted G2PBG-*g*-PtBuGlu copolymer synthesized in Chapter 4 a higher grafting yield was obtained, but the overall weight fraction of PtBuGlu in the copolymers was lower due to the lower substrate functionality level.

Table 5.9 Characteristics of G2PBG-*eg*-PtBuGlu2 arborescent copolymer

	PBG Substrate			Graft Copolymer			
Copolymer[a]	M_n (g/mol) [b]	% -CO_2H[c]	G_y [d]	M_n (g/mol) [e]	M_w/M_n [f]	f_n [g]	% PtBuGlu[h]
G2PBG-*eg*-PtBuGlu2	960,000	10	50	1.6×10^6	1.15	290	41

[a] Grafting reaction with 25% excess of side chains; [b] absolute values from SEC-MALLS in DMF; [c] deprotection level from ^{1}H NMR analysis; [d] grafting yield: fraction of side chains attached to the substrate; [e] M_n estimated using the weight fraction of PtBuGlu in copolymer and M_n from PBG substrate; [f] apparent M_w/M_n from the DRI detector; [g] branching functionality: number of branches added in the last grafting cycle; [h] PtBuGlu %weight fraction determined by ^{1}H NMR analysis.

Dynamic Light Scattering Measurements. Selective cleavage of the *tert*-butyl ester protecting groups from the PtBuGlu side chains was achieved by dissolving the arborescent copolymer in TFA, to produce chain segments of poly(L-glutamic acid) (PGA) at the periphery of the arborescent copolymer. The purified sample was dissolved in PBS by sonication for the DLS measurements (Table 5.10). There is a significant increase in the hydrodynamic diameter for the deprotected arborescent copolymer that is similar to the trends observed for arborescent PBG-*eg*-PGly and PBG-*eg*-PEO. As well, the good agreement between the d_{h1} and d_{h2} values in PBS demonstrates the lack of aggregation, i.e. that these arborescent copolymers behave like unimolecular micelles in an aqueous environment. For comparison, the randomly grafted G2PBG-*g*-PGA1.5 copolymer of Chapter 4 had d_{h1} and d_{h2} values of 60 and 45 nm,

respectively. This again suggests that the end-grafted copolymers with PGA have a better-defined core-shell morphology leading to non-aggregated species than their randomly grafted counterparts.

Table 5.10 DLS Measurements for the G2PBG-*eg*-PGA arborescent copolymer

	PBG Substrate (DMF)[a]		Graft Copolymer (PBS)[b]	
Copolymer[a]	d_{h1}[c]	d_{h2}[d]	d_{h1}[c]	d_{h2}[d]
G2PBG-*eg*-PGA1.5	$17._6 \pm 1$	$16._7 \pm 1$	$47._0 \pm 1$	$43._0 \pm 1$

[a] DMF with 0.05% LiCl to prevent aggregation; [b] phosphate buffer solution with pH 7.4; [c] hydrodynamic diameter from 1st order analysis of the correlation function (nm); [d] diameter from 2nd order analysis (nm).

5.5 Conclusions

The synthesis of amphiphilic copolymers by terminal grafting onto the chains of arborescent PBG substrates was successfully demonstrated for different generations, and for polar polymers of different compositions forming the shell.

The synthesis of the PBG substrates with carboxyl chain ends started with the ring-opening polymerization of Bz-Glu-NCA initiated with the hydrochloride salt of di-*tert*-butyl ester-protected glutamic acid. These linear PBG chains were grafted onto randomly functionalized G0, G1 and G2 PBG substrates, and the *tert*-butyl ester protecting groups at the chain ends were selectively cleaved to produce two carboxyl groups per chain end on the branched PBG substrates.

Arborescent copolymers were derived from the chain end functionalized PBG substrates by adding a shell of PGly, PEO, or PGA chains; these compounds were characterized by SEC and DLS measurements. The grafting yields obtained for the chain end

functionalized PBG substrates were higher relatively to the grafting yields for the randomly functionalized substrates. Narrow molecular weight distributions ($M_w/M_n \leq 1.15$) were maintained for the chain end grafted arborescent copolymers.

The solution properties of the arborescent PBG-*eg*-PGly, PBG-*eg*-PEO, and PBG-*eg*-PGA copolymers were investigated in organic and aqueous media. All the copolymers were soluble, but PBG-*eg*-PGly displayed self-assembly. The resulting degree of association was much lower than for the analogous randomly grafted PBG-*g*-PGly copolymers described in Chapter 4 however. Arborescent PBG-*eg*-PEO produced essentially non-aggregated species in aqueous solutions for all three generations of copolymers investigated. An arborescent G2PBG-*eg*-PGA copolymer likewise produced non-aggregated species in aqueous PBS.

These results provide evidence that hydrophobic arborescent PBG cores can serve in the design of water-soluble unimolecular micelles. A well-defined core-shell morphology appears to be a key factor enhancing the water solubility of these arborescent PBG copolymer micelles.

Chapter 6

Arborescent Unimolecular Micelles: Poly(γ-benzyl L-glutamate) Core Grafted with a Hydrophilic Shell by "Click" Chemistry

6.1 Overview

Amphiphilic copolymers were obtained by grafting arborescent poly(γ-benzyl L-glutamate) (PBG) cores of generations G1-G3 with polyglycidol, poly(ethylene oxide), or poly(2-hydroxyethyl acrylate) chain segments via copper(I)-catalyzed azide-alkyne Huisgen cycloaddition (CuAAC) "click" chemistry. Biocompatible shell materials are highly desirable for these systems to find uses in biomedical applications such as microencapsulation. Azide-terminated linear chain segments of polyglycidol, poly(ethylene oxide), and poly(2-hydroxyethyl acrylate) were grafted onto alkyne-functionalized arborescent PBG cores. The alkyne functional groups on the arborescent PBG substrates were either randomly distributed on the substrates or exclusively at the end of the chains added in the last grafting cycle of the core synthesis. The location of these coupling sites was found to influence the ability of the arborescent copolymers to form unimolecular micelles in aqueous environments. The aqueous solubility properties were also dependent on the type of material used for the shell side chains. The chain end *grafting onto* approach was more efficient at producing unimolecular micelles in solution than random grafting. This difference is attributed to the better core-shell morphology of arborescent copolymers with end-grafted shell segments, as demonstrated for other related systems. Click chemistry is comparable to the peptide coupling techniques in terms of grafting yield, but opens up possibilities for grafting a broader range of polymers under mild conditions to generate arborescent copolymers.

6.2 Introduction

Dendrigraft (arborescent) polymers are a class of dendritic polymers built using a synthetic strategy similar to dendrimers, with the notable exception of using polymeric building blocks instead of low molecular weight monomer units. Among the first examples of arborescent polymers were the arborescent polystyrenes synthesized by Gauthier and Möller in 1991.[1] These polymers are obtained by a *grafting onto* scheme, whereby well-defined linear side chains are first coupled with a randomly functionalized linear polymer substrate. This yields a generation zero (G0) arborescent polymer; through repetitive cycles of substrate functionalization and grafting, the subsequent generations of arborescent polymers are produced as shown in Figure 6.1. Using this *grafting onto* approach, arborescent polymers with high molecular weights ($M_n > 10^6$) and narrow molecular weight distributions ($M_w/M_n \approx 1.1$) can be obtained in only a few grafting cycles.[2] This has been achieved most commonly by coupling living anionic polymers with suitably functionalized substrates.[1-4] The advantage of this method lies in the high reactivity of the living anionic polymers, which allows fast and efficient coupling. Unfortunately, anionic polymer species are highly unstable and the grafting reactions must be performed in situ under inert conditions, which limits the scope of these *grafting onto* methods. In Chapter 3, the synthesis of arborescent poly(γ-benzyl L-glutamate) (PBG) was achieved by the ring-opening polymerization of benzyl L-glutamic acid N-carboxyanhydride in combination with carbodiimide peptide coupling techniques. Both the substrates and the side chains can be isolated and stored prior to use, and the tolerance to impurities is higher for carbodiimide-mediated coupling than for anionic grafting, albeit this reaction still remains sensitive to different side reactions. It would be beneficial to achieve the synthesis of arborescent polymers by a *grafting onto* scheme

providing access to synthetic polymers with reactive functionalities that can tolerate a wider range of reaction conditions and side chain compositions.

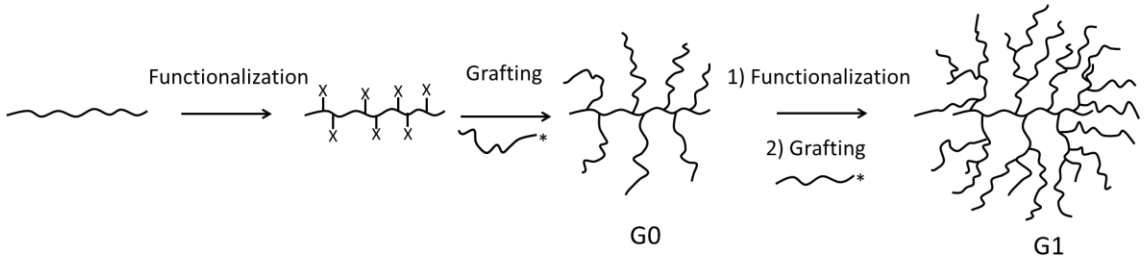

Figure 6.1 Schematic representation of the generation-based synthesis of arborescent polymers.

The term "click" chemistry was first coined in 2001 by Sharpless et al., to describe reactions that are among others *modular, wide in scope, give very high yields*, and generate only *inoffensive by-products*.[5] These criteria are met by the copper(I)-catalyzed azide-alkyne Huisgen cycloaddition (CuAAC) reaction, that was developed concurrently by the groups of Meldal[6] and Sharpless[7] in 2002. A general scheme for the copper(I)-catalyzed azide-alkyne reaction is provided in Figure 6.2. Meldal et al. used the CuAAC reaction to synthesize peptidotriazoles on a solid support, but they were unaware of its connection to "click" chemistry. Sharpless et al. more clearly realized the potential of this reaction and described it as having an "unprecedented level of selectivity, reliability, and scope for those organic synthesis endeavors which depend on the creation of covalent links between diverse building blocks". Since the application of the CuAAC reaction to polymer synthesis by Wu and coworkers[8] in 2004, various macromolecular architectures have been constructed by that method. [9,10] Due to the selectivity of the CuAAC reactions a broader range of solvents,

functional groups, and impurities can be tolerated, enabling different pathways to build well-defined macromolecules.

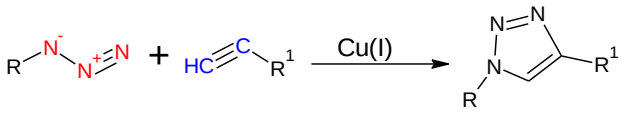

Figure 6.2 Copper(I)-catalyzed azide-alkyne Huisgen cycloaddition (CuAAC).

More recently, the CuAAC reaction has been used in conjunction with the ring-opening polymerization of α-amino acid N-carboxyanhydrides to synthesize amphiphilic block copolymers containing poly(γ-benzyl L-glutamate) (PBG) components. Lecommandoux and coworkers thus used click chemistry to link previously synthesized homopolymers of PBG with poly[2-(dimethylamino)ethyl methacrylate] (PDMAEMA),[11] poly(trifluoroacetyl L-lysine) (PTFALys),[12] or dextran[13] to generate well-defined block copolymers (M_w/M_n < 1.20). These amphiphilic block copolymers self-assemble to yield micellar structures, but can be limited in applicability range by their critical micelle concentrations. Engler et al. also used CuAAC to generate comb-branched polymers from a linear poly(γ-propargyl L-glutamate) (PPLG) backbone and azide-terminated poly(ethylene oxide) side chains, to demonstrate the high efficiency of the *grafting onto* approach.[14] Grafting yields > 95% were achieved for the linear PPLG substrates. It was shown that PPLG maintained a predominantly α-helix conformation in DMF during the grafting reaction, which provided better access to the grafting sites on the linear substrates. The solubility characteristics of the graft copolymers were not investigated.

In Chapters 4 and 5, it was demonstrated that well-defined ($M_w/M_n \leq 1.22$) amphiphilic arborescent copolymers could be synthesized by coupling PBG substrates with

linear side chains using carbodiimide-mediated peptide coupling techniques. Reported herein is a new synthetic strategy for producing amphiphilic arborescent copolymers with CuAAC grafting reactions. Alkyne-functionalized arborescent PBG substrates were prepared by reacting propargylamine with the carboxylic acid functionalities of partially deprotected PBG substrates. These alkyne-functionalized substrates were subsequently coupled with either α-azido polyglycidol (PGly), ω-azido poly(ethylene oxide) (PEO), or ω-azido poly(2-trimethylsilylethyl acrylate) [P(HEA-TMS)] linear chain segments by the CuAAC reaction to generate amphiphilic arborescent copolymers capable of forming water-soluble unimolecular micelles. The synthesis of these arborescent copolymers by the CuAAC method is illustrated in Figure 6.3. The focus of the current investigation was on the synthetic aspects, but the solution properties of the micelles obtained were also examined using dynamic light scattering (DLS) measurements.

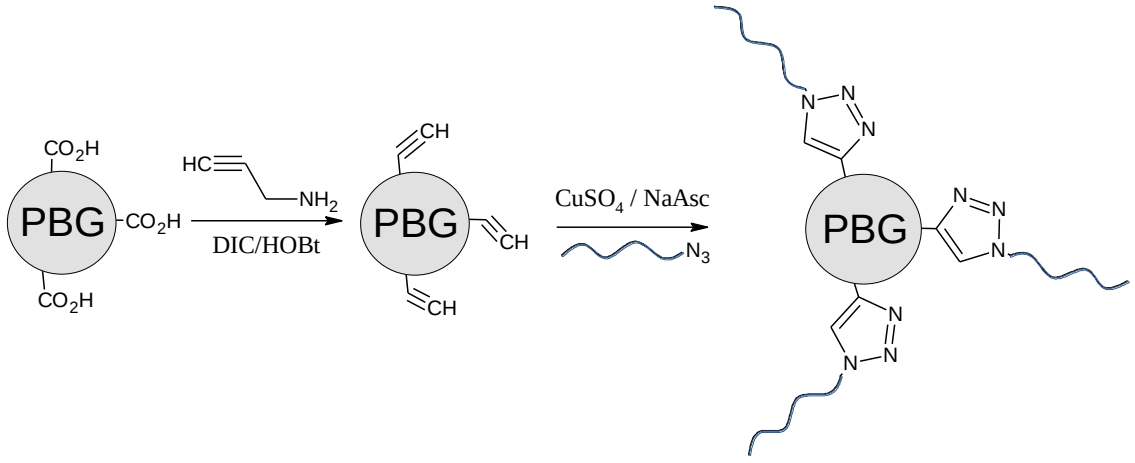

Figure 6.3 Schematic representation of the synthesis of arborescent copolymers by the CuAAC reaction.

6.3 Experimental Procedures

6.3.1 Characterization and Sample Preparation

Nuclear Magnetic Resonance (NMR) Spectroscopy. ^{1}H NMR spectroscopy served to determine the deprotection level of the arborescent PBG substrate polymers, and to monitor the purity of the linear polymers serving as side chains after their synthesis. It also served for the determination of the number-average degree of polymerization (X_n) of P(HEA-TMS). The instrument used was a Bruker 300 MHz spectrometer. The concentration of all the samples was 15-20 mg/mL and 16 scans were averaged in the measurements.

Size Exclusion Chromatography (SEC) Analysis. Analysis of the α-azido poly(glycidol acetal) (PGlyAc) linear chains was performed on a Viscotek GPCmax instrument equipped with a TDA 305 triple detector array and a Viscotek UV Detector 2600. Size exclusion was performed with three Polyanalytik Superes™ Series linear mixed bed columns of 300 mm × 8 mm in series, having linear polystyrene molecular weight exclusion limits of 400×10^3, 4×10^6, and 20×10^6. A flow rate of 1.0 mL/min and a temperature of 35 ºC were used for the THF mobile phase.

Analysis of the PEO and P(HEA-TMS) linear chains, and all the arborescent copolymers was performed on a SEC instrument consisting of a Waters 510 HPLC pump, a 50 μL injection loop, and a Waters 2410 differential refractometer (DRI) detector. A Wyatt MiniDAWN laser light scattering detector operating at a wavelength of 690 nm served to determine the absolute molecular weight of the graft polymers. The column used was a 500 mm × 10 mm Jordi Gel Xstream H2O Mixed Bed model with a linear polystyrene molecular weight range of 10^2–10^7. DMF with LiCl (1 g/L, added to minimize adsorption of the

polymer onto the column) was used at a flow rate of 1.0 mL/min as the mobile phase at room temperature.

Preparative SEC was carried out on a system consisting of a Waters M45 HPLC pump, a 2-mL sample injection loop, a Waters R401 differential refractometer detector, and a Jordi Gel DVB 1000 Å or Mixed Bed 250 mm × 22 mm preparative SEC column. DMF with 0.2 g/L LiCl served as the mobile phase at room temperature and a flow rate of 3.0 mL/min. The crude polymer was injected as a 20-30 mg/mL solution in DMF with 0.2 g/L LiCl.

Refractive Index Increment Determination. Knowledge of the refractive index increment (dn/dc) of linear α-azido polyglycidol, ω-azido poly(ethylene oxide), and ω-azido poly(2-trimethylsilylethyl acrylate) was necessary to determine the absolute molecular weight of the arborescent copolymers by SEC. The dn/dc values were determined on a Brookhaven Instruments BI-DNDC 620 Differential Refractometer. The analysis of each linear polymer required five solutions in DMF ranging from 1-5 mg/mL at 30 ºC.

Infrared Analysis. Qualitative analysis of the terminal azide functionalities of α-azido polyglycidol, ω-azido poly(ethylene oxide) and ω-azido poly(2-trimethylsilylethyl acrylate) was performed by infrared analysis on a Bruker Vector 22 FT-IR spectrometer, with the OPUS 6.0 software package to acquire and manipulate the spectra. The analysis was performed with 64 scans from 400 to 4000 cm^{-1} at 1 cm^{-1} resolution.

Dynamic Light Scattering Measurements. Batch-wise dynamic light scattering measurements were carried out on a Brookhaven BI-200SM light scattering goniometer equipped with a BI-APD (Avalanche Photo Diode) detector and a Claire Lasers CLAS2-660-140C (120 mW) laser operating at 660 nm. All the samples were measured at 25 °C and a scattering angle of

90°. The samples were filtered twice with 3.0 μm PTFE membrane filters before analysis. The correlator was operated in the exponential sampling mode and the hydrodynamic diameters were calculated from the z-average translational diffusion coefficients obtained from first- and second-order cumulant analysis of the correlation function, to better account for polydispersity effects. Solutions were prepared at concentrations ranging from 0.1-2 % w/v, depending on the molecular weight (generation number) of the sample. If a solvent exchange was necessary, 3 mL of sample solution was placed in a 12,000-14,000 molecular weight cut-off regenerated cellulose dialysis bag overnight in at least 200 mL of the new solvent. The next day, the solvent was replaced and the sample was left stirring for at least 2 h further to ensure complete removal of the original solvent.

6.3.2 Solvent and Reagent Purification

N,N'-Dimethylformamide (DMF; Aldrich, peptide synthesis grade) was purified by distillation under reduced pressure and was stored in the dark to prevent degradation due to photochemical reactions. *n*-Hexylamine was purified by stirring overnight with CaH_2 and distillation under reduced pressure. The DMF and *n*-hexylamine were stored under nitrogen in round-bottomed flasks (RBF) over 3 Å molecular sieves (EMD). The toluene used for anionic polymerization was distilled over oligostyryllithium under nitrogen. 2,3-Epoxy-1-propanol (glycidol, Aldrich, 95%), ethyl vinyl ether (Aldrich, 99%), concentrated hydrogen chloride (HCl, Aldrich, 37 w/w%), poly(ethylene glycol) monomethyl ether (Polysciences Inc., M_n = 5000), dichloromethane (DCM, Aldrich, ≥ 99%), *p*-toluenesulfonyl chloride (Aldrich, ≥ 98%), pyridine (Aldrich, ≥ 99%), sodium azide (NaN_3, Aldrich, ≥ 99%), 2-hydroxyethyl acrylate (HEA, Aldrich, 96%), chlorotrimethylsilane (TMSCl, Aldrich, 98%),

ethyl acetate (Caledon, >99%), anhydrous magnesium sulfate ($MgSO_4$, Fisher, 97%), copper(I) bromide (CuBr, Aldrich, 99.999%), *N*,*N*′,*N*″,*N*″-pentamethyldiethylenetriamine (PMDETA, Aldrich, 99%), methyl 2-bromopropanionate (Aldrich, 98%), propargylamine (Aldrich, 98%), cupric sulfate pentahydrate ($CuSO_4$, VWR International), sodium ascorbate (NaAsc, Aldrich, ≥ 98%), sodium hydrogen carbonate ($NaHCO_3$, Aldrich, 99%), triisobutylaluminum (Aldrich, 1.0 M in hexanes), tetrabutylammonium azide (Aldrich), N,N'-diisopropylcarbodiimide (DIC; Aldrich, 99%), 1-hydroxybenzotriazole (HOBt; Fluka, water content ca. 15% w/w), methanol (EMD), diethyl ether (EMD), triethylamine (TEA, EMD Reagent grade), tetrahydrofuran (THF, Aldrich, ≥ 99%), deuterated DMSO (d_6-DMSO, Cambridge Isotopes, 99.9% D), deuterated chloroform ($CDCl_3$, Cambridge Isotopes, 99.9% D), and regenerated cellulose dialysis bags (Spectra Por, 1000 MWCO and 12,000-14,000 MWCO) were used as received from the suppliers.

6.3.3 Synthesis of Linear Polymers with a Terminal Azide Functionality

Synthesis of 2,3-Epoxy-1-(1-ethoxyethoxy)propane (Glycidol Acetal). The synthetic procedure used was as described by Fitton et al.[15] 2,3-Epoxy-1-propanol (40.0 g, 0.54 mol) and ethyl vinyl ether (200 mL) were loaded in a 500-mL round-bottomed flask (RBF) with a magnetic stirring bar and immersed in an ice-water bath. A catalytic amount of *p*-toluenesulfonic acid monohydrate (1.0 g, 5.3 mmol) was then added slowly, to ensure that the reaction temperature did not exceed 40 ºC and avoid the evaporation of ethyl vinyl ether. The reaction was removed from the ice bath to warm to room temperature and allowed to proceed for 3 h. Saturated $NaHCO_3$ solution was then added until the pH of the reaction mixture was slightly basic (approx. 100 mL). The organic layer was isolated, dried over

$MgSO_4$, and concentrated under reduced pressure. Distillation of the residue under reduced pressure gave the monomer as a colorless liquid that was stored under nitrogen at 4° C. Yield: 61.5 g (78%); ^{1}H NMR: (300 MHz, $CDCl_3$) δ: 4.65 (q, 1H), 3.75-3.19 (m, 4H), 3.04 (m, 1H), 2.68 (m, 1H), 2.50 (m, 1H), 1.17 (d, 3H), 1.10 (t, 3H).

Synthesis of α-Azido PGlyAc14. The procedure used to obtain an α-azido poly(glycidol acetal) sample (target M_n = 10,000 g/mol) was adapted from Gervais et al.[16] The initiator, tetrabutylammonium azide (0.57 g, 2.00 mmol), was dried before use by three cycles of azeotropic distillation with dry toluene under vacuum and stored under nitrogen after redissolution in 30 mL of toluene in a glass ampoule sealed with a Teflon stopcock. A 1-L, 5-neck RBF was evacuated under high-vacuum, flame-dried, and purged with nitrogen. Dry toluene (240 mL) was then added and the RBF was cooled to -30 ºC with dry ice in a 2-propanol/water bath. Glycidol acetal (20.0 g, 0.135 mol, target X_n = 68.5, M_n = 10,000, freshly distilled over triisobutylaluminum), the initiator solution, and triisobutylaluminum (2.0 mL of solution, 2.0 mmol) were then added in succession, and the 2-propanol/water bath was removed to allow the reaction to proceed at room temperature overnight. Degassed ethanol was added to terminate the reaction. The toluene was removed, and the polymer was redissolved in 100 mL of diethyl ether and left in the fridge overnight to precipitate salts formed in the reaction. These were removed by filtration with a 0.45 μm PTFE filter, and the diethyl ether was removed under vacuum to achieve a constant sample weight. Yield: 17.9 g (90%). IR: sharp N_3 stretch at 2102 cm^{-1}. SEC (THF): M_n = 14,100, M_w/M_n= 1.06; ^{1}H NMR (300 MHz, $CDCl_3$) δ: 4.66 (q, 1H), 3.67-3.35 (m, 7H), 1.24 (d, 3H), 1.15 (t, 3H).

Synthesis of α-Azido PGly7. Removal of the acetal protecting group from α-azide poly(glycidol acetal) is necessary to produce hydrophilic linear chain segments. Among

different methods investigated for that purpose, an approach leading to minimal degradation of the polymer was adapted from Mendrek et al.[17] α-Azide PGlyAc14 (7.0 g, 0.048 mol acetal, 1 eq) was dissolved in 350 mL of DMF and placed in a 1-L RBF with a magnetic stirring bar. A concentrated HCl solution (20 mL, 11.65 M, 0.24 mol of HCl, 5 eq) was then added to the RBF with rapid stirring. The reaction was allowed to proceed for 30 min at room temperature before adding enough saturated $NaHCO_3$ solution to neutralize the HCl (approximately 40 mL). The DMF and water were removed under high vacuum, the polymer was redissolved in 30 mL of ethanol, and insoluble salts were removed by filtration. The polymer solution was transferred to a 1000 molecular weight cut off (MWCO) dialysis bag and left in an ethanol bath (500 mL) overnight. The ethanol in the dialysis bath was then replaced with methanol and allowed to stir for 2 h longer. The methanol was finally evaporated and the polymer was dried in a vacuum oven at 50 ºC overnight. Yield: 2.6 g (74%). SEC (DMF): M_n^{app} = 10,200, M_w/M_n^{app} = 1.14 (DRI), IR: sharp N_3 stretch at 2102 cm^{-1}. ^1H NMR (300 MHz, d_6-DMSO) δ: 4.66 (q, 1H), 3.67-3.35 (m, 5H).

Synthesis of ω-Tosyl PEO5. To synthesize α-azide PEO5, a commercially available linear PEO monomethyl ether sample with M_n = 5000 (X_n = 113), containing a terminal hydroxyl group, served as starting material. ω-Hydroxy PEO5 (10.0 g, 0.002 mol –OH, 1 eq) was added to 100 mL of dichloromethane (DCM) in a 250-mL RBF. *p*-Toluenesulfonyl chloride (7.63 g, 0.04 mol, 20 eq) and pyridine (3.2 mL, 0.04 mol, 20 eq) were dissolved in 40 mL of DCM in a 250-mL RBF with a magnetic stirring bar. The ω-hydroxy PEO5 solution was added to the *p*-toluenesulfonyl chloride solution and allowed to stir overnight at room temperature under nitrogen. The polymer was then precipitated in cold diethyl ether, recovered by suction filtration, and dried under vacuum to yield a light pink powder. The

polymer was redissolved in methanol and precipitated in cold diethyl ether, recovered, and dried under vacuum overnight to yield a white powder. According to ^{1}H NMR analysis only 85% conversion was obtained, so the tosylation reaction was repeated on the same polymer sample to achieve 100% conversion, as confirmed by ^{1}H NMR analysis. Yield: 9.6 g (96%). ^{1}H NMR (300 MHz, $CDCl_3$) δ: 9.29 (d, 1H), 8.88 (q, 4H), 8.45 (m, 3H), 7.99-7.94 (m, 6H), 7.80 (d, 4H), 7.32 (d, 2H), 7.25-7.15 (d, 4H), 4.15-4.10 (t, 2H), 3.85-3.35 (b, 444H), 2.43 (s, 1H), 2.34 (s, 2H).

Synthesis of ω-Azido PEO5. ω-Tosyl PEO5 (9.6 g, 1.92 mmol ω-tosyl, 1 eq) was added to 50 mL of DMF in a 100-mL RBF with a magnetic stirring bar. Once the polymer had dissolved sodium azide (NaN_3, 2.5 g, 38.4 mmol, 20 eq) was added, and the RBF was purged with nitrogen and stirred for 48 h at room temperature. The solution became cloudy since NaN_3 is not completely soluble in DMF. Deionized water was added until the solution became clear, and the reaction was allowed to stir for 30 min in a well-ventilated fume hood, to allow any hydrazoic acid vapours potentially present to escape. The polymer was precipitated in cold diethyl ether, recovered by suction filtration, and dried under vacuum for 1 h. The polymer was then redissolved in 40-50 mL of methanol, precipitated in diethyl ether, recovered, and dried under vacuum overnight. Yield: 7.5 g (78%). IR: azide stretch at 2115 cm^{-1}. ^{1}H NMR (300 MHz, $CDCl_3$) δ: 3.85-3.35 (b, 4H).

Synthesis of 2-(Trimethylsilyloxy)ethyl Acrylate (HEA-TMS). Attempts were made to synthesize unprotected 2-hydroxyethyl acrylate (HEA) in a bulk polymerization via atom transfer radical polymerization (ATRP), but these produced broad molecular weight distributions ($M_w/M_n \geq 1.3$) and in some cases cross-linking. To achieve the controlled polymerization of HEA via ATRP, the hydroxyl group was protected to avoid cross-linking

and produce narrow molecular weight distributions. The procedure used was adapted from Mühlebach et al.[18] Freshly distilled HEA (50 mL, 0.435 mol, 1 eq), dichloromethane (500 mL), and triethylamine (73 mL) were loaded in a 1-L RBF with a magnetic stirring bar. While stirring under nitrogen at 0 ºC, trimethylsilyl chloride (61 mL, 0.479 mol, 1.1 eq) was added over 20 min. The reaction was allowed to warm to room temperature and the triethylamine hydrochloride salts formed were removed by suction filtration. The dichloromethane was evaporated off and the solution was filtered again, diluted with ethyl acetate (300 mL), and washed 3 times with 300 mL of deionized water. The organic solution was dried over $MgSO_4$, the ethyl acetate was evaporated, and the product was distilled under vacuum to give a colorless liquid. Yield: 61.2 g (74%). ^{1}H NMR (300 MHz, $CDCl_3$) δ: 6.43-6.37 (d, 1H), 6.17-6.07 (q, 1H), 5.82-5.79 (d, 1H), 4.22-4.19 (t, 2H), 3.81-3.78 (t, 2H), 0.10 (s, 9H).

Synthesis of ω-Bromo P(HEA-TMS)11. The polymerization was conducted in a pre-dried Schlenk flask with a magnetic stir bar. Copper(I) bromide (CuBr, 0.155 g, 1.08 mmol, 1 eq) was loaded in the flask and purged with nitrogen. *N*,*N*,*N*′,*N*″,*N*″-Pentamethyldiethylenetriamine (PMDETA, 0.450 mL, 2.16 mmol, 2 eq) was added, followed by HEA-TMS (16.2 g, 86.2 mmol, 80 eq) and methyl 2-bromopropionate (0.120 mL, 1.08 mmol, 1 eq). The target degree of polymerization (X_n) was 50, corresponding to M_n = 9400 and 63% monomer conversion. Three freeze-pump-thaw cycles were performed on the bulk solution to remove dissolved oxygen. The Schlenk flask was then purged with nitrogen and placed in a 90 ºC oil bath with rapid stirring. The polymerization reaction was monitored by ^{1}H NMR analysis based on monomer conversion. The color of the mixture was light green before it was placed in the oil bath, but it slowly became darker green as the reaction

proceeded. A small sample for ^{1}H NMR analysis was removed with a syringe after 20 min, taking care to maintain the reaction under nitrogen. The sample was quickly transferred to a vial and cooled in liquid nitrogen for a few seconds to stop the polymerization. On the basis of the ^{1}H NMR analysis result after 20 min, the polymerization was stopped after 35 min by opening the Schlenk flask to the air and cooling in a liquid nitrogen bath. Water was added to precipitate the polymer which was isolated by centrifugation, redissolved in 50 mL of ethyl acetate, and dried over $MgSO_4$. The ethyl acetate was evaporated and the polymer was dried under vacuum overnight. After the yield was determined, the polymer was dissolved in diethyl ether (100 mL) and stored in a refrigerator (4 ºC). Yield: 9.2 g (78%), SEC (DMF): M_n^{app} = 9500, M_w/M_n^{app} = 1.21 (DRI), ^{1}H NMR (300 MHz, $CDCl_3$): X_n = 57.3, M_n = 10,800, δ: 6.45-6.39 (m, 4H), 6.19-6.09 (m, 4H), 5.84-5.80 (m, 4H), 4.07 (b, 115H), 3.73 (b, 115H), 2.33 (b, 57H), 1.90-1.40 (b, 115H), 1.13 (b, 3H), 0.10 (s, 516H).

Synthesis of ω-Azido P(HEA-TMS)11. ω-Bromo P(HEA-TMS)11 (5.0 g, 0.463 mmol, 1 eq) was loaded in a dry 100-mL RBF with a magnetic stirring bar and purged with nitrogen. DMF (50 mL) was added followed by sodium azide (NaN_3, 0.60 g, 9.26 mmol, 20 eq). The reaction was stirred overnight at room temperature. To minimize cleavage of the labile TMS protecting groups by hydrazoic acid produced when sodium azide is exposed to water, the DMF solution was decanted to remove any insoluble NaN_3, poured into 200 mL of water, and centrifuged. The polymer was then redissolved in 50 mL of ethyl acetate and dried over $MgSO_4$. The ethyl acetate was evaporated and the polymer was dried under vacuum overnight. After the yield was determined, the polymer was redissolved in diethyl ether and stored in a refrigerator (4 ºC). Yield: 3.5 g (70%). IR: azide stretch at 2117 cm^{-1}. ^{1}H NMR

(300 MHz, $CDCl_3$) δ: 6.45-6.39 (m, 4H), 6.19-6.09 (m, 4H), 5.84-5.80 (m, 4H), 4.07 (b, 115H), 3.73 (b, 115H), 2.33 (b, 57H), 1.90-1.40 (b, 115H), 1.13 (b, 3H), 0.10 (s, 464H).

6.3.4 Synthesis of *Click-grafted* Arborescent Copolymers

Synthesis of Alkyne-functionalized Arborescent PBG Cores. The synthesis of arborescent PBG samples randomly and chain end-functionalized with carboxylic acid groups was described in Chapters 4 and 5, respectively. To obtain alkyne-functionalized arborescent PBG substrates, propargylamine was coupled with the carboxylic acid moieties with the peptide coupling reagents DIC and HOBt. For example, chain end carboxylic acid-functionalized G1PBG (0.202 g, 6.64×10^{-5} mol CO_2H, 1 eq) was placed in a 10-mL RBF with 4 mL of dry DMF. N,N'-Diisopropylcarbodiimide (DIC, 52 μL, 3.32×10^{-4} mol, 5 eq) and 1-hydroxybenzotriazole (HOBt, 45 mg, 3.32×10^{-4} mol, 5 eq) were then added to the reaction, followed by propargylamine (8 μL, 1.33×10^{-4} mol, 2 eq). The reaction was left stirring overnight under nitrogen at room temperature. The crude product was purified by preparative SEC in DMF, to ensure the complete removal of excess propargylamine. The purified product was concentrated to 4-6 mL, precipitated in methanol, centrifuged, and dried overnight in a vacuum oven. Yield: 0.153 g (76%). SEC (DMF): M_n = 280,000, M_w/M_n = 1.05 (MALLS). ^{1}H NMR (300MHz, d_6-DMSO) δ: 8.2-7.8 (b, 1H), 7.28–7.20 (s, 5H), 5.03–4.89 (s, 2H), 4.35–3.80 (b, 1H), 3.80-3.70 (b, 2H), 3.10-2.90 (b, 1H), 2.33–1.70 (b, 4H), 1.35-1.10 (b, 10H), 0.80-0.70 (b, 3H).

Synthesis of Click-grafted Arborescent Copolymers. The azide-alkyne Huisgen cycloaddition reaction can be catalyzed by numerous copper(I) compounds, but it was found that a combination of copper(II) sulfate pentahydrate ($CuSO_4$) and sodium L-ascorbate (NaAsc)

worked best with the alkyne-functionalized PBG substrates. For example, chain end alkyne-functionalized G1PBG (30.1 mg, 9.78×10^{-6} mol alkyne, 1 eq), α-azido PGly7 (69 mg, 9.78×10^{-6} mol N_3, 1 eq), and $CuSO_4$ (4.9 mg, 1.96×10^{-5} mol, 2 eq) were dissolved in 3 mL of DMF and placed in a dry Schlenk flask with a magnetic stirring bar. One freeze-pump-thaw (FPT) cycle was performed, and NaAsc (7.7 mg, 3.91×10^{-5} mol, 4 eq) was added while the flask was purged with nitrogen. One more FPT cycle was performed to remove any oxygen present, and the flask was purged with nitrogen before stirring at room temperature. The color of the reaction turned from light green to light yellow after 5 min. After 24 h of reaction the solution was diluted with DMF containing 0.2 g/L LiCl and the arborescent copolymer was purified by preparative SEC. SEC (DMF): Grafting yield = 60% (DRI), M_n = 906,000, M_w/M_n = 1.09 (MALLS).

6.4 Results and Discussion

6.4.1 Synthesis of Linear Polymers with a Terminal Azide Functionality

Three types of linear polymers were synthesized to couple with the hydrophobic arborescent PBG cores and generate a hydrophilic shell. The characterization data obtained for the linear polymers are provided in Table 6.1.

Table 6.1 Characteristics of the linear polymers with terminal azide functionalities

	SEC[a]		^{1}H NMR	
Polymer	M_n	M_w/M_n	X_n[b]	M_n[c]
PGlyAc14	14,100	1.06	-	-
	M_n^{app}	M_w/M_n^{app}		
PGly7	10,200	1.14	-	-
PEO5	5,900	1.08	113	5,000
P(HEA-TMS)11	9,500	1.21	57.3	10,800

[a] PGlyAc analyzed with a triple detection SEC system in THF using dn/dc = 0.045 mL/g;[17] PEO and P(HEA-TMS) analyzed with a DRI detection SEC system in DMF with 0.1 % LiCl, so only apparent molecular weights are reported; [b] number-average degree of polymerization; [c] M_n calculated from X_n.

Synthesis of α-Azido Polyglycidol. In Chapter 4, α-azido poly(glycidol acetal) with a molecular weight of 32,000 was synthesized by a procedure adapted from Gervais et al.[16] The same procedure was applied here to synthesize α-azido poly(glycidol acetal) with a target M_n = 10,000. The actual M_n determined by size exclusion chromatography was 14,100. The higher than expected molecular weight is attributed to tetrabutylammonium azide losses during azeotropic drying of the initiator prior to the polymerization; the molecular weight distribution of the polymer nevertheless remained narrow (M_w/M_n = 1.06). Due to the presence of overlapping proton peaks in the spectrum, an accurate estimate of the degree of polymerization could not be obtained from ^{1}H NMR analysis. One advantage of CuAAC coupling is that many functional groups other than azides or alkynes do not interfere with the reaction. This allowed removal of the acetal protecting groups prior to the coupling reaction, which was not possible when using the standard peptide coupling techniques described in Chapters 4 and 5. After removal of the acetal protecting groups the α-azido polyglycidol7 sample (α-azido PGly7, M_n = 7100) was characterized by SEC in DMF to ensure that no

significant degradation had occurred, and also by IR spectroscopy to verify that the azide functionality was still present. The IR spectra obtained before and after the removal of the acetal protecting groups are provided in Figure 6.4. The sharp azide stretch near 2100 cm^{-1} remains strong in the α-azido PGly7 spectrum, whereas the broad peak between 3500-3000 cm^{-1} is due to the free hydroxyl groups present in each repeating unit of α-azido PGly7. The characterization data from the SEC and ^{1}H NMR analyses are summarized in Table 6.1.

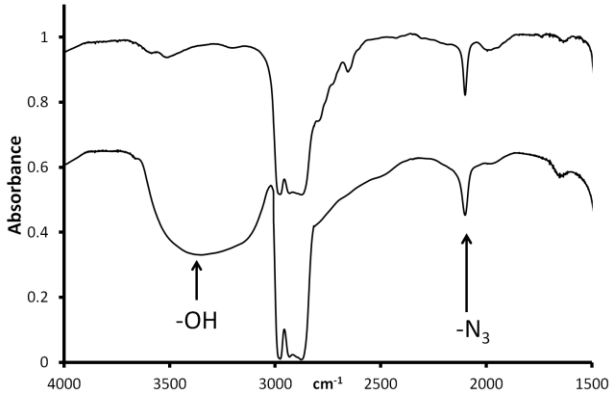

Figure 6.4 IR spectra for α-azido PGlyAc14 (top) α-azido PGly7 (bottom).

Synthesis of ω-Azido Poly(ethylene oxide). Commercially available poly(ethylene oxide) (PEO) monomethyl ether with M_n = 5000, containing one ω-hydroxyl group, was converted to ω-azido PEO via an ω-tosyl PEO intermediate. Anhydrous conditions are important to ensure full conversion of ω-hydroxyl PEO to ω-tosyl PEO. A large excess of *p*-toluenesulfonyl chloride (20 equivalents) and allowing the reaction to proceed overnight are also helpful to obtain full conversion. Unfortunately even under these conditions only 85% conversion was achieved, so a second reaction step under the same conditions was necessary to achieve full conversion. The ^{1}H NMR spectra obtained for ω-hydroxyl PEO5 and ω-tosyl

PEO5 are shown as the top and middle spectra in Figure 6.5, respectively. The peak at 4.15 ppm in the ω-tosyl PEO5 spectrum corresponds to the -CH_2- protons adjacent to the ω-tosyl functional group. The conversion level calculated by integration of the signal at 4.15 ppm and the peak for the backbone protons at 3.6 ppm yielded a ratio of 1:113, corresponding to 100% conversion of ω-hydroxyl PEO5 to ω-tosyl PEO5. Sodium azide was then used to convert the tosylated polymer to ω-azido PEO5. The reaction was allowed to proceed for 48 h to ensure complete conversion. The ^{1}H NMR spectrum obtained for ω-azido PEO5 is displayed at the bottom of Figure 6.5. The protons adjacent to the tosyl group (4.15 ppm) disappeared after the reaction, confirming that the group had been displaced. No signals were visible for the protons adjacent to the azido group due to overlapping signals from the protons in the polymer backbone near 3.6 ppm. To qualitatively confirm that the azide functionality was present on the PEO chains, IR analysis was performed before and after the azidation reaction; the spectra obtained are compared in Figure 6.6. An azide stretch is clearly present at 2116 cm^{-1} after azidation, however quantification of the azide functionality could not be achieved by IR analysis. The characterization data for ω-azido PEO5 are provided in Table 6.1.

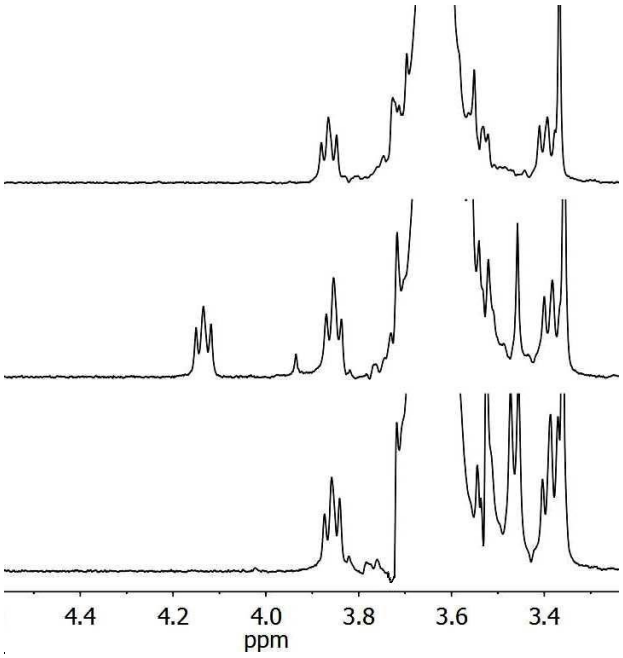

Figure 6.5 ^{1}H NMR spectra for ω-hydroxy PEO5 (top), ω-tosyl PEO5 (middle), and ω-azido PEO5 (bottom) in $CDCl_3$.

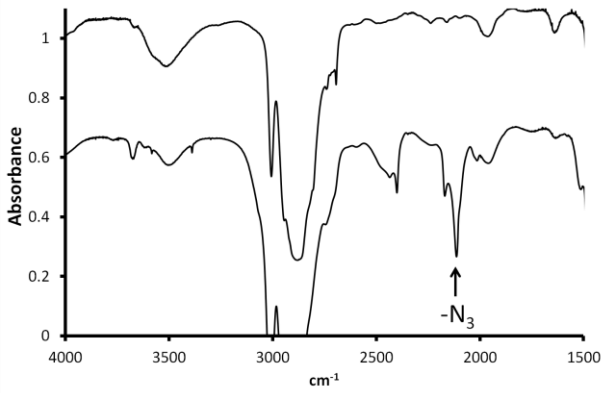

Figure 6.6 IR Spectra for ω-tosyl PEO5 (top) and ω-azido PEO (bottom).

Synthesis of ω-Azido Poly(2-trimethylsilylethyl acrylate). Ionic polymerization is an established method to produce well-defined polymers, but it suffers from its extreme sensitivity to impurities requiring stringent reaction conditions. ATRP is a controlled radical

polymerization method introduced concurrently by the groups of Sawamoto[19] and Matyjaszewski[20] in 1995; the latter described an ATRP reaction as "a multicomponent system consisting of the monomer, initiator with a transferable (pseudo) halogen, and a catalyst (composed of a transition metal and any suitable ligand)".[21] The ATRP mechanism proposed by Wang and Matyjaszewski is provided in Figure 6.7.

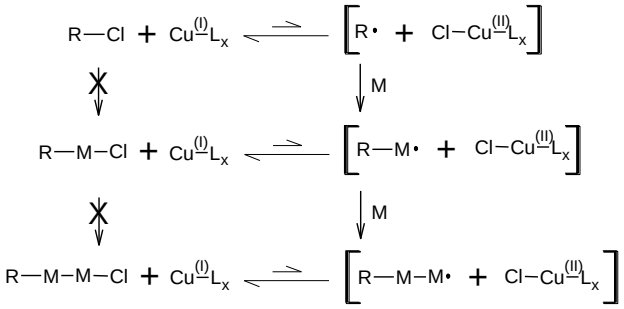

Figure 6.7 Reaction scheme for ATRP proposed by Wang and Matyjaszewski.[20]

The ATRP of 2-hydroxyethyl acrylate (HEA) in its unprotected form has been reported; however it was proposed that better control over the polymerization reaction and higher conversions could be achieved if the hydroxyl group were protected.[18] The HEA monomer was therefore protected with a labile trimethylsilyl (TMS) group. The reaction scheme for a CuBr/*N*,*N*,*N*′,*N*″,*N*″-pentamethyldiethylenetriamine (PMDETA) catalyst system, in combination with a halogen initiator derived from methyl 2-bromopropanionate, as used in the current investigation, is shown in Figure 6.8. The polymerization of HEA-TMS was monitored by ^{1}H NMR analysis on the basis of monomer conversion. The ^{1}H NMR spectra obtained for the HEA-TMS monomer, the polymerization of HEA-TMS after 20 and 35 min, as well as for purified P(HEA-TMS)11 are compared in Figure 6.9. The

polymerization was stopped after 35 min based on the results from the t = 20 min sample. The monomer conversion was calculated from the peak integration ratio for the alkene protons of the monomer (6.5-5.7 ppm) and the trimethylsilyl protons present on both the monomer and the polymer at 0.1 ppm. At t = 20 min, 49% monomer conversion had been reached. Based on a monomer to initiator ratio (M/I) of 80, 49% monomer conversion should correspond to a degree of polymerization X_n = 39. The ratio of the polymer backbone -CH_2- protons (2.0-1.3 ppm) to the methyl initiator protons (1.1 ppm) provided an X_n value of 35. At t = 35 min the monomer conversion (74%) corresponded to X_n = 59, whereas NMR analysis yielded X_n = 57. After sample purification X_n = 57.3 was obtained, corresponding to M_n = 10,800. A summary of the monomer conversion and calculated X_n values is provided in Table 6.2.

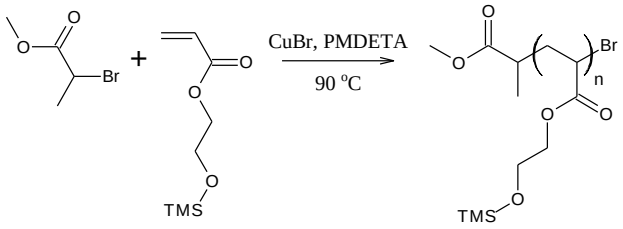

Figure 6.8 Polymerization of HEA-TMS by ATRP initiated by methyl 2-bromopropionate.

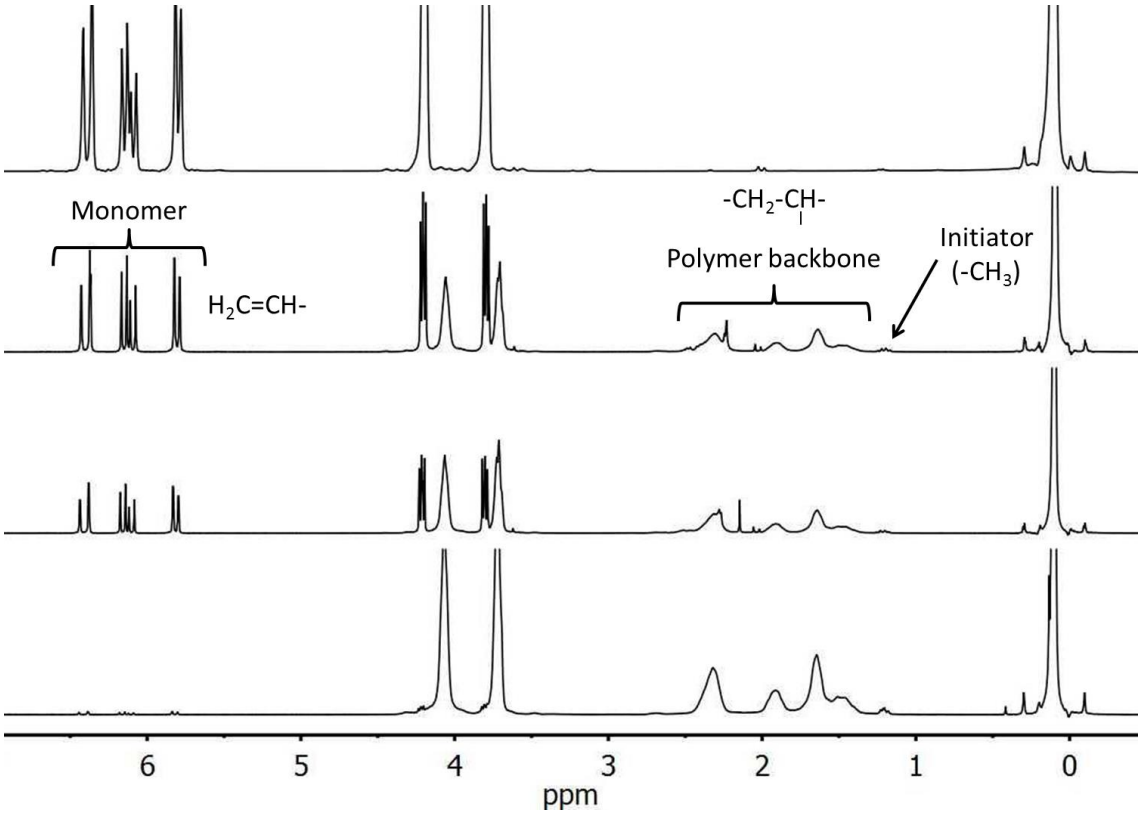

Figure 6.9 ^{1}H NMR spectra for (top to bottom) HEA-TMS monomer, P(HEA-TMS)11 at t =20 min, t =35 min, and purified P(HEA-TMS)11.

Table 6.2 Characterization of the ATRP of HEA-TMS.

	Monomer		Initiator
t (min)	% conversion[a]	X_n [b]	X_n [c]
0	0	-	-
20	49	39.2	35.8
35	74	59.5	57.1
35[d]	-	-	57.3

[a] From the monomer and trimethylsilyl proton peaks; [b] from the % monomer conversion; [c] calculated from the initiator proton peaks; [d] purified polymer.

The conversion of ω-bromo P(HEA-TMS)11 to ω-azido P(HEA-TMS)11 was performed with NaN_3 in DMF over 48 h. Confirmation for the presence of the azide functionality could not be obtained by ^1H NMR analysis due to overlapping peaks from the polymer that interfered with the protons adjacent to the ω-bromo and ω-azido functionalities. IR analysis was used to confirm the presence of an azide group on the polymer, albeit not quantitatively. The IR spectrum for ω-azido P(HEA-TMS)11 displayed in Figure 6.10 has a small peak for the azide stretch at 2117 cm^{-1}. Characterization data for ω-azido P(HEA-TMS)11 are provided in Table 6.1. The ^1H NMR spectrum for ω-azido P(HEA-TMS)11 revealed that approximately 7% of the TMS protecting groups were cleaved during the azidation reaction. This is attributed to the presence of hydrazoic acid, produced by trace amounts of water in the DMF used for the reaction. ω-Azido P(HEA-TMS)11 was stored in diethyl ether until it was used in the coupling reaction, to avoid potential cross-linking of the unprotected 2-hydroxyethyl acrylate repeating units.

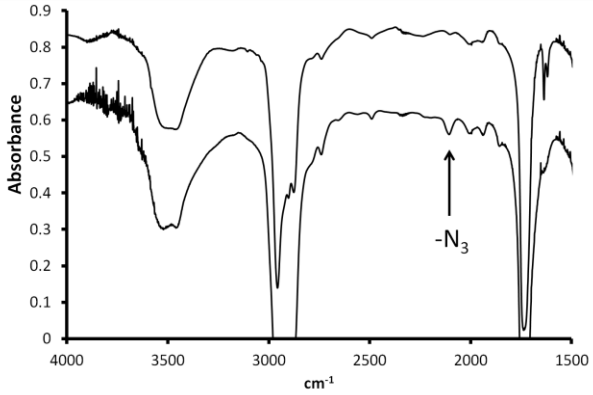

Figure 6.10 IR spectra for ω-bromo P(HEA-TMS)11 (top) and ω-azido P(HEA-TMS)11 (bottom).

6.4.2 Synthesis of Alkyne-functionalized Arborescent PBG Cores

Alkyne-functionalized PBG substrates were obtained by reacting the carboxylic acid functionalities of partially deprotected arborescent PBG substrates with propargylamine using standard peptide coupling techniques. The synthesis of arborescent PBG, either randomly or chain end functionalized with carboxylic acids, has been discussed in detail in Chapters 4 and 5, respectively. A schematic representation of the preparation of the two types of alkyne-functionalized G1 PBG substrates is provided in Figure 6.11 as an example. Both syntheses started from a randomly carboxylic acid-functionalized G0 PBG substrate. In Figure 6.11A, a G1 PBG substrate with randomly distributed carboxylic acid groups is generated as described in Chapters 3 and 4. In Figure 6.11B, PBG side chains derived from an initiator with two *tert*-butyl ester-protected carboxylic acid functionalities were used to generate the G1 PBG substrate. This allowed selective deprotection of the *tert*-butyl ester protecting groups at the chain ends with TFA. A 1-fold excess of propargylamine was added in the reaction to ensure complete conversion of the carboxylic acid groups to alkyne amide functionalities. The carboxylic acid functionalities on the substrates were easily accessible to the small molecule propargylamine, so that complete conversion was expected. For convenience, a preparative SEC instrument was used to isolate the alkyne-functionalized PBG substrates from excess propargylamine prior to ^{1}H NMR analysis.

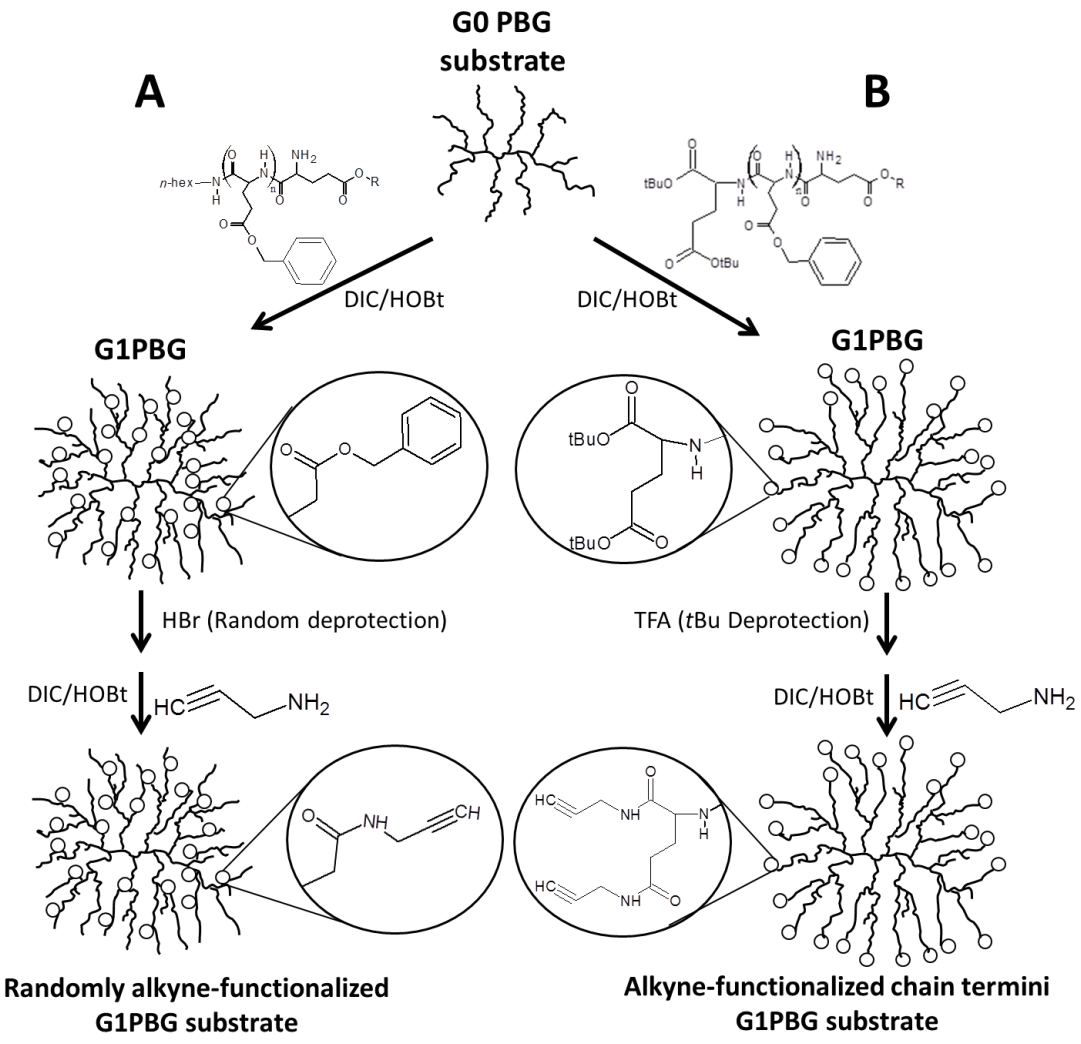

Figure 6.11 Schematic representation of the synthesis of (A) random alkyne-functionalized and (B) chain termini alkyne-functionalized G1PBG substrates from randomly carboxylic acid-functionalized G0PBG.

^{1}H NMR spectra illustrating the synthesis of a randomly alkyne-functionalized G1PBG substrate are provided in Figure 6.12. The spectrum for G1PBG before removal of a portion of the benzyl ester protecting groups is displayed at the top, whereas the spectrum for partially (19 mol%) deprotected G1PBG is shown in the middle. The benzyl ester protons at

5.0 and 7.2 ppm have a decreased intensity relatively to the methine proton at 4.4-3.7 ppm after partial deprotection. The spectrum for randomly alkyne-functionalized G1PBG, provided at the bottom of the figure, has an alkyne proton resonance appearing at 3.0 ppm, and a signal for the protons adjacent to the alkyne group near 3.8 ppm. The alkyne substitution level was determined by integration of the signal at 3.0 ppm and the methine proton peak from 4.4-3.7 ppm. An overlapping peak at 3.0 ppm is from *n*-hexylamine, the initiator serving in the ring-opening polymerization of benzyl glutamate to synthesize the PBG substrates. This signal was present before the propargylamine reaction and was therefore subtracted from the integration value. The overlapping peaks at 3.8 ppm from the propargylamine protons were likewise subtracted from the peak integral for the methine proton at 4.4-3.7 ppm. The carboxylic acid and alkyne functionality levels determined by that method were both 19 mol%, indicating 100% conversion.

The ^{1}H NMR spectra referring to the synthesis of G1PBG functionalized with alkyne groups at the chain ends are provided in Figure 6.13. The top spectrum is for the G1 polymer with *tert*-butyl group-protected chain ends, which can be selectively deprotected by dissolution in neat TFA (to provide free carboxylic acid functionalities) while leaving the benzyl ester substituents along the chains unaffected (middle spectrum on Figure 6.13). The spectrum at the bottom is for G1PBG modified with alkyne chain termini. The same alkyne proton and α-protons appear as in Figure 6.12, albeit at a lower intensity. An alkyne functionality level of 7 mol% was determined for the chain end-functionalized G1PBG, which also corresponds to 100% conversion.

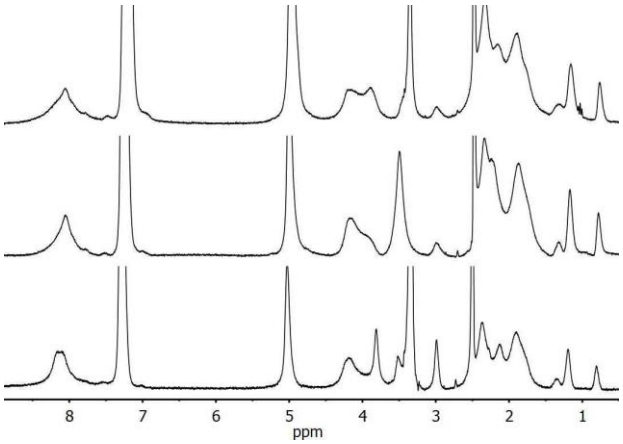

Figure 6.12 ^{1}H NMR spectra for (top to bottom) G1PBG substrate, randomly deprotected (19 mol% CO_2H), and randomly alkyne-functionalized (19 mol% alkyne) in d_6-DMSO.

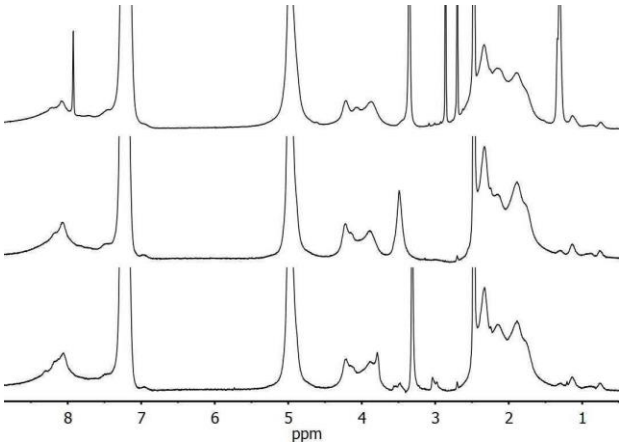

Figure 6.13 ^{1}H NMR spectra for (top to bottom) G1PBG with *tert*-butyl-protected chain ends, deprotected chain ends (7 mol% CO_2H), and alkyne-functionalized chain ends (7 mol% alkyne) in d_6-DMSO.

6.4.3 Optimization of CuAAC Reactions with PBG and Synthesis of G0 copolymers

The solubility characteristics of the PBG substrates limited the solvents to either DMF or DMSO in the CuAAC reactions, and also influenced the selection of the catalyst system. Due

to its solubility in DMF a combination of CuBr with PMDETA was first explored, as it is the most widely used catalyst system for polymer-related CuAAC reactions.[22] Regioselectivity between the 1,4- and 1,5-disubstituted triazoles was not a main concern here, since the main focus was on increasing the grafting yield in the reaction. Oxygen was always removed from the reactions by three freeze-pump-thaw cycles and purging with nitrogen. All the grafting reactions reported herein used a 1:1 ratio of azide:alkyne functionalities.

For investigative purposes, ω-azido P(HEA-TMS)11 was initially coupled with a linear PBG substrate randomly functionalized with 31 mol% of alkyne functionalities. The color of the solution at the beginning of the reaction was green but turned bright yellow within 5 min. The color then slowly turned darker over the 24 h reaction period until the solution was exposed to air, when it reverted back to green. The grafting yield (fraction of side chains grafted onto the substrate) was determined from the weight fraction of each component in the copolymers, along with the known amounts of the substrate and side chains used in each grafting reaction, where a detailed explanation is given in Section 4.4.3. A grafting yield of 74% was achieved after a 24 h of reaction under the conditions described above, without signs of degradation or cross-linking. The SEC trace obtained for the (linear) PBG-*click*-P(HEA-TMS)11 [PBG-*c*-P(HEA-TMS)11] crude product is provided in Figure 6.14 (top). This test reaction was followed by P(HEA-TMS)11 grafting onto a randomly functionalized arborescent G0PBG substrate containing 33 mol% of alkyne functionalities. The three other traces in Figure 6.14 correspond to the crude products for G0PBG-*c*-P(HEA-TMS)11 at reaction time intervals of (from top to bottom) 24 h, 48 h, and 7 d. After 24 h tailing was observed on the low molecular weight (right) side of the graft copolymer peak and when the reaction was allowed to proceed further, no increase in grafting yield was

observed. Tailing was more pronounced after 48 h, and even more so after 7 d, however. Degradation is also obvious from the decrease in the height of the arborescent copolymer peak as compared to the non-grafted P(HEA-TMS)11 chains over time. To verify that the degradation was not related to the presence of P(HEA-TMS) in the reaction, an α-azido polystyrene sample with M_n = 5100 was used in place of ω-azido P(HEA-TMS)11, producing similar results. A test involving only the G0PBG substrate with CuBr and PMDETA was also performed under the same reaction conditions, except for the absence of linear chains. SEC traces obtained for the G0PBG substrate before and after the addition of CuBr and PMDETA are compared in Figure 6.15. It is clear that substrate degradation and a minor amount of cross-linking occurred over the 24 h reaction period, as peak broadening occurred on both the high and low molecular weight sides of the peak.

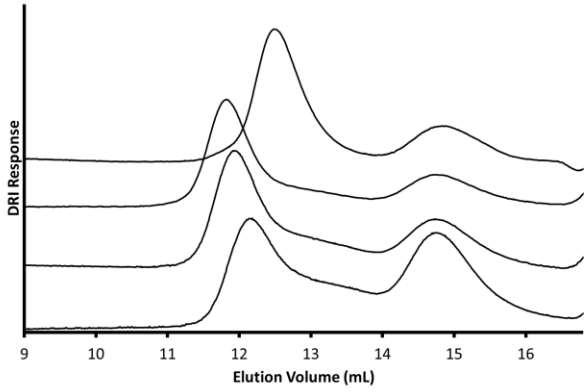

Figure 6.14 SEC traces in DMF with 0.1% LiCl for (top to bottom) PBG-*c*-P(HEA-TMS)11, and G0PBG-*c*-P(HEA-TMS)11 after 24 h, 48 h, and 7 d.

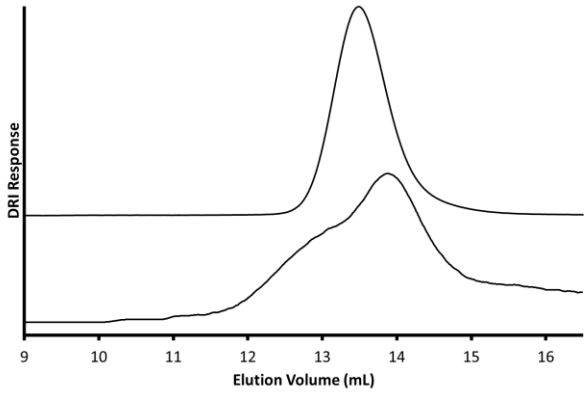

Figure 6.15 SEC traces in DMF with 0.1% LiCl for the G0PBG substrate initially (top), and 24 h after the addition of CuBr/PMDETA.

Alternate catalyst systems were therefore considered to avoid the degradation of arborescent PBG. This included bromotris(triphenylphosphine) copper(I) bromide [$(TPP)_3$-CuBr)], in the hope that the triphenylphosphine groups would lower the reactivity of CuBr sufficiently to circumvent the degradation of arborescent PBG while still allowing the CuAAC reaction to proceed at a reasonable rate. Under the same reaction conditions for the previous arborescent G0PBG-*c*-P(HEA-TMS)11 copolymer syntheses, $(TPP)_3$-CuBr resulted in a very low grafting yield (< 5%) after 24 h, as seen in Figure 6.16. The low yield could be explained either by the lower reactivity of the catalyst system, or by the influence of a Staudinger reaction occurring between triphenylphosphine and the azide group on ω-azido P(HEA-TMS)11, deactivating the azide functionality. A lower amount of $(TPP)_3$-CuBr could help to avoid this deactivation, but would also decrease the rate of the grafting reaction.

Another attempt was made using copper(II)sulfate pentahydrate ($CuSO_4$) with sodium ascorbate (NaAsc), since this method is also a widely used source of Cu(I).[23] The $CuSO_4$/NaAsc catalyst system is generally used in aqueous or aqueous/alcoholic mixtures,

due to the limited solubility of NaAsc in organic solvents. The benefit of this approach is that reactions can still proceed in the presence of oxygen, since NaAsc acts as a reducing agent for copper(II) and can regenerate copper(I) from copper(II) continuously during the reaction. Since NaAsc has limited solubility in DMF, two cycles of freeze-pump-thaw were used to remove dissolved oxygen prior to the addition of NaAsc to ensure the presence of a maximum amount of copper(I) catalyst in the reaction. The color of the reaction started as a greenish blue before the NaAsc addition but turned bright yellow only minutes after adding NaAsc and persisted over the 24 h reaction period. Removal of the copper catalyst was efficiently achieved by preparative SEC, as indicated by the absence of color in the purified arborescent copolymer solutions. This synthetic protocol was applied to the preparation of the G0PBG copolymers with the different α-azido side chain materials.

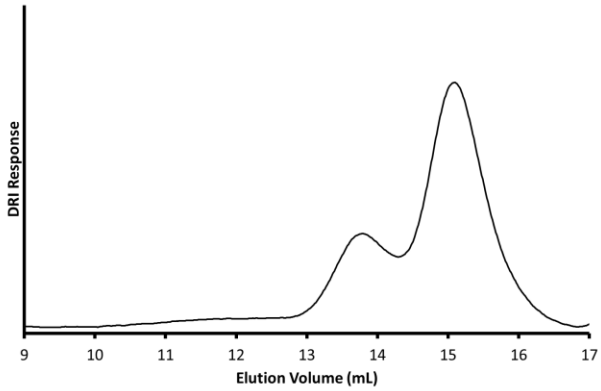

Figure 6.16 SEC chromatogram in DMF with 0.1% LiCl for G0PBG-*c*-P(HEA-TMS)11 after 24 h using CuBr-TPP.

The characteristics of the purified arborescent copolymers derived from randomly alkyne-functionalized G0PBG substrates coupled with ω-azido P(HEA-TMS)11, α-azido PGly7, and ω-azido PEO5 are provided in Table 6.3. The SEC traces obtained for the

corresponding crude arborescent copolymers are provided in Figure 6.17. It is clear from the SEC traces that symmetrical arborescent copolymer peaks, without signs of degradation, were produced over 24 h for all three grafting reactions, demonstrating that the $CuSO_4$/NaAsc catalyst was useful under these conditions. The range of grafting yields listed in Table 6.3 (54-93%) suggests that the nature of the side chains influences the grafting yield. Given the limited amount of data available, it is unclear whether this variation is related to characteristics such as the chemical composition or the bulkiness of the side chains. While the G0PBG substrate was useful to optimize the CuAAC reactions applied to the synthesis of arborescent copolymers, coupling reactions of the higher generation substrates of arborescent PBG (G1-G3) with $CuSO_4$/NaAsc may provide further insight into these reactions. The upper generations of arborescent PBG substrates are also potentially more interesting to generate stable water-soluble unimolecular micelles due to their increased branching functionalities.

Table 6.3 Characteristics of randomly alkyne-functionalized G0PBG substrates click-grafted with various α-azide side chains using the $CuSO_4$/NaAsc catalyst system

	PBG Substrate			Graft Copolymer			
Copolymer [a]	M_n (g/mol) [b]	% Alkyne [c]	G_y [d]	M_n (g/mol) [b]	M_w/M_n [b]	f_w [e]	% Shell [f]
G0PBG-*c*-P(HEA-TMS)11	51,000	18	57	324,000	1.17	25	84
G0PBG-*c*-PGly7	51,000	18	93	331,000	1.02	40	85
G0PBG-*c*-PEO5	51,000	18	54	172,000	1.09	24	70

[a] All reactions done with 1:1 azide:alkyne ratio; [b] absolute values from SEC-MALLS analysis in DMF; [c] functionalization level from ^{1}H NMR analysis; [d] grafting yield: fraction of side chains attached to the substrate; [e] branching functionality: number of side chains added in the last grafting cycle; [f] weight fraction of shell material, calculated from the difference in absolute molecular weights of the copolymer and the substrate.

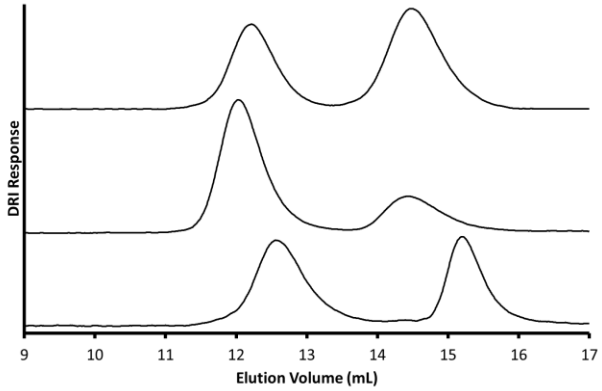

Figure 6.17 SEC traces in DMF with 0.1% LiCl for (top to bottom) G0PBG-*c*-P(HEA-TMS)11, G0PBG-*c*-PGly7, and G0PBG-*c*-PEO5 after 24 h using $CuSO_4$/NaAsc.

6.4.4 Randomly Click-grafted Arborescent Copolymers from G1 and G2 Substrates

The linear side chains with terminal azide functionalities were also click-grafted onto arborescent G1PBG and G2PBG substrates randomly functionalized with alkyne groups using the $CuSO_4$/NaAsc catalyst system. Grafting onto G3PBG was not attempted, since the results obtained in Chapter 4 showed that random grafting on the G3PBG substrates was unsuccessful. The characteristics of the random click-grafted arborescent copolymers derived from the G1 and G2 substrates are summarized in Table 6.4. The grafting yield varied between 8-27% in most cases, except for G1PBG-*c*-PEO5 which had a yield of 57%, while the synthesis of G2PBG-*c*-P(HEA-TMS)11 was unsuccessful. These relatively low grafting yields were expected due to steric hindrance arising from the compact structure of the arborescent PBG substrates, as previously observed for the other random grafting reactions performed in Chapter 4. The higher grafting yield observed for G1PBG-*c*-PEO5 may be linked to the more open structure of G1PBG, together with the high flexibility of the PEO chains. A similar effect was observed previously (Chapter 4), in that the only successful grafting reaction with the randomly functionalized G3PBG substrate was for the PEO5 side

chains, with a grafting yield of 58%. The molecular weight distribution of all the arborescent copolymers obtained was relatively narrow ($M_w/M_n \leq 1.14$). The SEC traces for the purified copolymers with P(HEA-TMS)11, PGly7, and PEO5 side chains are compared in Figure 6.18 with the exception of the G2PBG-*c*-P(HEA-TMS)11 sample where only the crude product was obtained due to the failed reaction. Symmetrical peaks are observed for all the purified arborescent copolymers, indicating that no degradation occurred during the click-grafting reactions.

Table 6.4 Characteristics of arborescent G1 and G2 copolymers obtained by random click-grafting

	PBG Substrate			Graft Copolymer			
Copolymer[a]	M_n (g/mol) [b]	% Alkyne[c]	G_y[d]	M_n (g/mol) [b]	M_w/M_n [b]	f_n [e]	% Shell[f]
G1PBG-*c*-P(HEA-TMS)11	322,000	19	27	1.2×10^6	1.14	80	73
G2PBG-*c*-P(HEA-TMS)11	1.1×10^6	32		Reaction failed			
G1PBG-*c*-PGly7	322,000	19	20	734,000	1.09	58	56
G2PBG-*c*-PGly7	1.1×10^6	32	13	2.8×10^6	1.03	234	60
G1PBG-*c*-PEO5	322,000	19	57	1.2×10^6	1.13	166	72
G2PBG-*c*-PEO5	1.1×10^6	32	8	1.8×10^6	1.08	140	38

[a] All reactions done with a 1:1 azide:alkyne ratio; [b] absolute values from SEC-MALLS in DMF; [c] functionalization level determined from ^{1}H NMR analysis; [d] grafting yield: fraction of side chains attached to the substrate; [e] branching functionality: number of side chains added in the last grafting cycle; [f] weight fraction of shell material, from the difference in absolute molecular weights of the copolymer and the substrate.

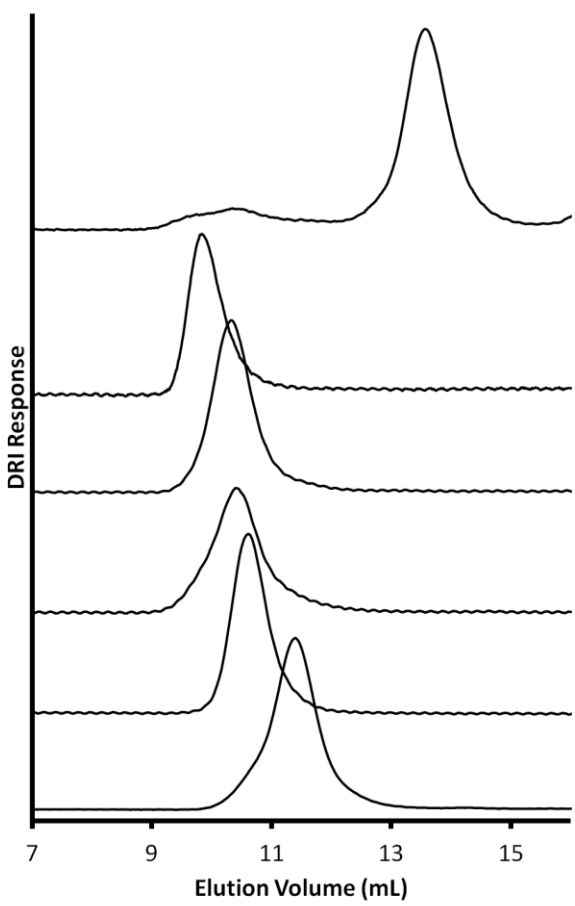

Figure 6.18 SEC traces in DMF with 0.1% LiCl for (top to bottom) G2PBG-*c*-P(HEA-TMS)11 crude, G2PBG-*c*-PGly7, G2PBG-*c*-PEO5, G1PBG-*c*-P(HEA-TMS)11, G1PBG-*c*-PGly7, G1PBG-*c*-PEO5.

Dynamic Light Scattering Measurements. DLS measurements were performed on the arborescent copolymers in DMF and in aqueous phosphate buffer solution (PBS) to characterize their solution properties. To obtain a water-soluble PHEA shell, removal of the labile TMS protecting group was achieved by simply adding a few drops of a dilute HCl solution into the DMF solution containing the G1PBG-*c*-P(HEA-TMS)11 sample and stirring for a few minutes. Both the PGly and PEO shell components are water-soluble and required no further modifications. First- and second-order analysis of the correlation function,

$|g_1(\tau)|$ and $|g_2(\tau)|$, respectively, provides information on the size dispersity of the system. Monodispersed samples are expected to yield identical results for their first- and second-order analysis, since the correlation function can be represented by a single exponential decay under these conditions.[24] Therefore as the size distribution of a sample broadens, the difference between the first- and second-order hydrodynamic diameters (d_{h1} and d_{h2}, respectively) obtained are compared with their respective PBG cores in DMF in Table 6.5. The uncertainties reported are either the standard deviation for a series of 5 measurements or 1 nm, whichever is larger.

Table 6.5 DLS measurements for randomly click-grafted arborescent copolymers

	PBG Core (DMF)[a]		Graft Copolymer (DMF)[a]		Graft Copolymer (PBS)[b]	
Copolymer	d_{h1}[c]	d_{h2}[d]	d_{h1}[c]	d_{h2}[d]	d_{h1}[c]	d_{h2}[d]
G1PBG-*c*-PHEA7	$11._7 \pm 1$	$10._4 \pm 1$	$61._8 \pm 1$	$47._6 \pm 1$	128 ± 1	104 ± 1
G1PBG-*c*-PGly7	$11._7 \pm 1$	$10._4 \pm 1$	$78._5 \pm 1$	$65._8 \pm 1$	221 ± 2	199 ± 2
G2PBG-*c*-PGly7	$18._7 \pm 1$	$17._5 \pm 1$	$39._0 \pm 1$	$35._1 \pm 1$	$94._9 \pm 1$	$67._4 \pm 1$
G1PBG-*c*-PEO5	$11._7 \pm 1$	$10._4 \pm 1$	$24._2 \pm 1$	$20._5 \pm 1$	insoluble	
G2PBG-*c*-PEO5	$18._7 \pm 1$	$17._5 \pm 1$	$30._4 \pm 1$	$27._8 \pm 1$	insoluble	

[a] DMF with 0.05% LiCl to prevent aggregation; [b] phosphate buffer solution (pH 7.4); [c] hydrodynamic diameter from 1st order analysis of the correlation function (nm); [d] diameter from 2nd order analysis (nm).

The relatively narrow molecular weight distributions observed in the SEC measurements ($M_w/M_n \leq 1.14$) suggest that the first- and second-order hydrodynamic diameters of the arborescent copolymers should be in close agreement. This is indeed the case for most samples characterized in DMF, since this solvent is good for both the core and

the shell components of the molecules. One notable exception is for the d_{h1} and d_{h2} values of G1PBG-*c*-PHEA7 in DMF, which are much larger than expected based on the size of the PBG cores in DMF and the previous investigations of similar systems (Chapters 4 and 5), suggesting that aggregated species were present in that sample. The d_{h1} and d_{h2} values also vary by 14 nm, which is likewise consistent with an open aggregation process. A similar result is observed for G1PBG-*c*-PGly7, with significantly larger d_{h1} and d_{h2} values and a 13 nm difference. Aggregation is not expected for arborescent PBG in DMF, but once it has been partly deprotected (through loss of the benzyl ester protecting group) its solubility in DMF is decreased. The aggregation is therefore attributed to the fact that the G1PBG copolymers have a rather open structure relatively to the G2PBG copolymers, which favors aggregation of PBG cores in DMF. Indeed, the denser G2PBG-*c*-PGly7 and the arborescent copolymers containing PEO had d_{h1} and d_{h2} values in much closer agreement in DMF. The larger and more variable hydrodynamic diameters observed in PBS solutions for the arborescent copolymers containing PHEA and PGly were expected based on previous results obtained for randomly grafted shell components (Chapter 4). The insolubility of the G1PBG-*c*-PEO5 and G2PBG-*c*-PEO5 samples was likewise expected. The aggregation observed in PBS solutions is attributed to the PBG core not being completely shielded from its surrounding environment, due to poorly defined core-shell morphology obtained when the shell components are attached randomly to the PBG substrates.

6.4.5 Chain end Click-grafted Arborescent Copolymers

Chain end grafted copolymers derived from arborescent PBG substrates were previously synthesized using peptide coupling techniques (Chapter 5). It was shown that chain end

grafting provided improved yields and solution properties relatively to random grafting described in Chapter 4. A similar trend was therefore expected for the CuAAC approach.

Click-grafting reactions of P(HEA-TMS)11 with both the G1PBG and G2PBG chain end functionalized substrates were attempted but failed, as less than a 3% grafting yield was observed in both cases. The reactions worked for the α-azido PGly7 and ω-azido PEO5 chains, however, and the characteristics of the copolymers obtained are provided in Table 6.6. The grafting yields observed for the arborescent copolymers using PGly follow the expected trend, with yields decreasing as the substrate generation number increases. The copolymers with PEO had lower grafting yields than those containing PGly. The G1PBG-*ec*-PEO5 and G2PBG-*ec*-PEO5 samples also had significantly larger polydispersities of 1.30 and 1.23, respectively, that may lead to inaccurate absolute molecular weight determinations by the SEC-MALLS detector. The SEC traces obtained for the arborescent copolymers are provided in Figure 6.19. Repeat SEC measurements and syntheses for both G1PBG-ec-PEO5 and G2PBG-ec-PEO5 yielded results similar to those in Table 6.6. It is obvious that the elution volumes for G1PBG-*ec*-PEO5 and G2PBG-*ec*-PEO5 are smaller than expected, suggesting that either cross-linking has taken place or that aggregation is present in the SEC measurements. Since no reliable molecular weight values could be obtained by SEC analysis of the G1PBG-*ec*-PEO5 and G2PBG-*ec*-PEO5 samples, the grafting yields were not obtained. The M_n and the weight fraction of the copolymers was attempted to be estimated from their known composition (determined by ^{1}H NMR analysis) along with the known M_n value of the PBG substrate as described in Section 4.4.5, however, in this case the signal from the PBG core was lost (due to its reduced mobility) in the ^{1}H NMR analysis. Therefore the grafting yields were determined from the area ratio of the peaks obtained with the DRI

detector. In this approach the graft copolymer peak area is divided by the total peak area for the graft copolymer and the unreacted side chain peaks. The grafting yields thus obtained are unfortunately overestimated, since a fraction of the graft copolymer peak response is due to the PBG core, which has a much higher dn/dc value than PEO (PBG dn/dc = 0.099 versus PEO dn/dc = 0.044 in DMF).

Table 6.6 Characteristics of arborescent copolymers obtained by chain end click-grafting

	PBG Substrate			Graft Copolymer			
Copolymer[a]	M_n (g/mol) [b]	% Alkyne[c]	G_y [d]	M_n (g/mol) [b]	M_w/M_n [b]	f_n [e]	% Shell[f]
G1PBG-*ec*-PGly7	280,000	7	98	906,000	1.09	89	69
G2PBG-*ec*-PGly7	1.1×10^6	12	47	3.2×10^6	1.02	294	65
G3PBG-*ec*-PGly7	3.0×10^6	11	30	6.3×10^6	1.01	467	52
G1PBG-*ec*-PEO5	280,000	7	50 [g]	-[h]	1.30	-	-
G2PBG-*ec*-PEO5	1.1×10^6	12	36 [g]	-[h]	1.23	-	-
G3PBG-*ec*-PEO5	3.0×10^6	11	24	4.8×10^6	1.04	738	38

[a] All reactions done with a 1:1 azide:alkyne ratio; [b] absolute values from SEC-MALLS in DMF; [c] functionalization level from ^{1}H NMR analysis; [d] grafting yield: fraction of side chains attached to the substrate; [e] branching functionality: number of side chains added in the last grafting cycle; [f] weight fraction of shell material, from the difference in absolute molecular weight of copolymer and substrate; [g] grafting yield from the peak area ratio in the DRI response; [h] absolute molecular weight not determined.

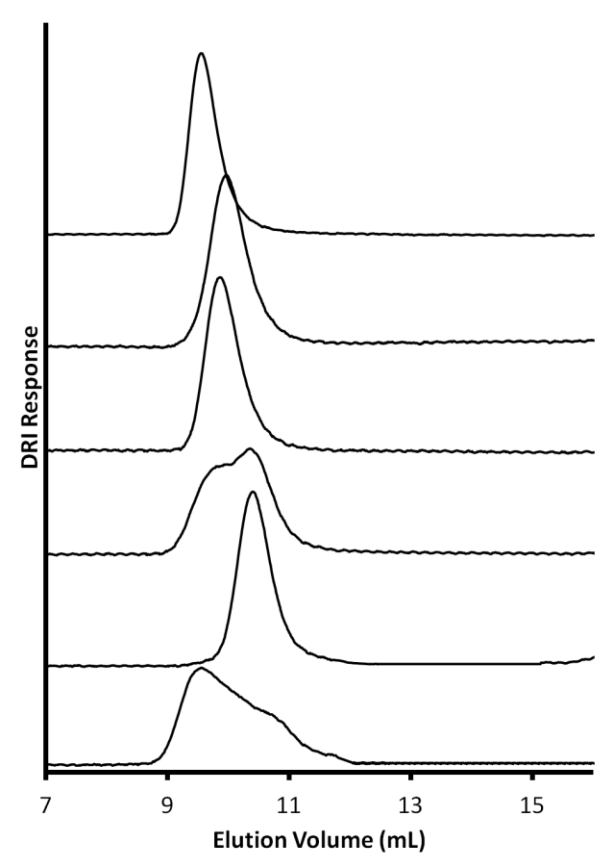

Figure 6.19 SEC traces in DMF with 0.1% LiCl for (top to bottom) G3PBG-*ec*-PGly7, G3PBG-*ec*-PEO5, G2PBG-*ec*-PGly7, G2PBG-*ec*-PEO5, G1PBG-*ec*-PGly7 and G1PBG-*ec*-PEO5.

Dynamic Light Scattering Measurements. DLS measurements were performed on the chain end click-grafted arborescent copolymers in DMF and in PBS to characterize their solution properties. The first- and second-order hydrodynamic diameters obtained are provided in Table 6.7. There is good agreement between the d_{h1} and d_{h2} values for all the samples in DMF. The G3PBG-*ec*-PGly7 sample has similar d_{h1} and d_{h2} values to G2PBG-*ec*-PGly7 in DMF, as observed previously for a series of arborescent copolymers with a randomly grafted PGlyAc shell (Chapter 4). The smaller than expected d_{h1} and d_{h2} values for G3PBG-*ec*-PGly7

could be due to the lower weight fraction of polyglycidol in that sample (last column in Table 6.6), which may force the PGly chains into a more collapsed conformation to shield the PBG core from the surrounding environment. The arborescent copolymers containing PEO display decreasing d_{h1} and d_{h2} values for increasing generation numbers. This trend was also observed when comparing the SEC traces for these samples, where G1PBG-*ec*-PEO5 was eluted at a smaller volume than both G2PBG-*ec*-PEO5 and G3PBG-*ec*-PEO5. Despite this unusual trend, the differences between the d_{h1} and d_{h2} values for each sample remain small (≤ 4 nm), indicating that these structures have a uniform size in DMF.

Table 6.7 DLS measurements for chain end click-grafted arborescent copolymers

	PBG Core (DMF)[a]		Graft Copolymer (DMF)[a]		Graft Copolymer (PBS)[b]	
Copolymer	d_{h1}[c]	d_{h2}[d]	d_{h1}[c]	d_{h2}[d]	d_{h1}[c]	d_{h2}[d]
G1PBG-*ec*-PGly7	11.$_6$ ± 1	10.$_0$ ± 1	30.$_3$ ± 1	26.$_3$ ± 1	78.$_9$ ± 2	54.$_6$ ± 1
G2PBG-*ec*-PGly7	18.$_9$ ± 1	17.$_3$ ± 1	39.$_7$ ± 1	35.$_5$ ± 1	72.$_5$ ± 1	53.$_0$ ± 1
G3PBG-*ec*-PGly7	28.$_4$ ± 1	26.$_8$ ± 1	39.$_9$ ± 1	38.$_9$ ± 1	43.$_5$ ± 1	39.$_8$ ± 1
G1PBG-*ec*-PEO5	11.$_6$ ± 1	10.$_0$ ± 1	46.$_8$ ± 1	42.$_1$ ± 1	61.$_7$ ± 1	54.$_4$ ± 1
G2PBG-*ec*-PEO5	18.$_9$ ± 1	17.$_3$ ± 1	43.$_9$ ± 1	39.$_4$ ± 1	45.$_8$ ± 1	41.$_7$ ± 1
G3PBG-*ec*-PEO5	28.$_4$ ± 1	26.$_8$ ± 1	38.$_3$ ± 1	35.$_4$ ± 1	56.$_9$ ± 1	50.$_5$ ± 1

[a] DMF with 0.05% LiCl to prevent aggregation; [b] phosphate buffer solution (pH 7.4); [c] hydrodynamic diameter from 1st order analysis of the correlation function (nm); [d] diameter from 2nd order analysis (nm).

The DLS results in PBS for the chain end click-grafted arborescent copolymer samples are again more promising than for the random click-grafted samples: G1PBG-*ec*-PGly7 and G2PBG-*ec*-PGly7 have much smaller d_{h2} values (54 and 53 nm, respectively) than their randomly click-grafted counterparts (d_{h2} values of 199 and 67 nm for G1PBG-*c*-PGly7

and G2PBG-*c*-PGly7, respectively). Sample G1PBG-*ec*-PGly7 has larger diameters than expected in PBS, and a large (24 nm) difference between d_{h1} and d_{h2}, consistent with the presence of aggregated species in the PBS solution. Interestingly, sample G3PBG-*ec*-PGly7 has similar d_{h1} and d_{h2} values in PBS and in DMF, confirming that these arborescent copolymers behave like unimolecular micelles in PBS.

It is clear from the DLS data in PBS that the chain end click-grafting technique is useful for the synthesis of arborescent copolymers containing PEO: Not only are all the arborescent copolymers soluble, but there is also good agreement between the d_{h1} and d_{h2} values for each generation. This trend was also observed when comparing the random versus chain end peptide coupling techniques employed in Chapters 4 and 5, respectively: The randomly grafted arborescent copolymers containing PEO were either insoluble or displayed extensive aggregation (Chapter 4), whereas the chain end grafted copolymers yielded unimolecular micelles (Chapter 5). Similarly to DMF, the DLS results for G1PBG-*ec*-PEO5 yielded the largest d_{h1} and d_{h2} values in PBS, as well as the largest discrepancy, suggesting that aggregated species were present in these copolymer solutions. The G2PBG-*ec*-PEO5 and G3PBG-*ec*-PEO5 both display good agreement between the d_{h1} and d_{h2} values in PBS. Given the good agreement between the d_{h1} and d_{h2} values in the DLS results for G1PBG-*ec*-PEO5 and G2PBG-*ec*-PEO5 in both DMF and PBS, it is evident that artifacts occurred in the SEC measurements of these copolymers (Figure 6.19), and although their exact nature is not clear, they could be related to aggregation and/or column adsorption during the SEC measurements.

6.5 Conclusions

The synthesis of well-defined arborescent copolymers consisting of linear chain segments grafted onto PBG cores by click chemistry was investigated. Well-defined linear polyglycidol (PGly), poly(ethylene oxide) (PEO), and poly(2-trimethylsilylethyl acrylate) [P(HEA-TMS)] with terminal azide functionalities were synthesized by different polymerization techniques and chain end modification. Arborescent PBG with alkyne functionalities either randomly distributed or at the chain ends of the were derived from the corresponding carboxylic acid-functionalized substrates and propargylamine by standard peptide coupling techniques.

The arborescent copolymers were synthesized by grafting either the PGly, PEO, or P(HEA-TMS) chains onto the PBG cores through the copper-catalyzed azide-alkyne Huisgen cycloaddition (CuAAC) reaction. Successful CuAAC reactions were achieved with copper(II) sulfate and sodium ascorbate as catalyst. The grafting yield varied from 29-65%, depending on the PBG substrate and linear chain segments employed. Well-defined arborescent copolymers ($M_w/M_n \leq 1.14$) were obtained with the exception of two samples, G1PBG-*ec*-PEO5 and G2PBG-*ec*-PEO5, characterized by M_w/M_n values of 1.30 and 1.23, respectively.

Dynamic light scattering measurements in PBS revealed that the randomly click-grafted arborescent copolymers with PHEA and PGly shells were soluble but formed aggregates, while the copolymers with a PEO shell were insoluble. Similar measurements for the chain end click-grafted copolymers provided evidence that most of these behaved like unimolecular micelles, although a low level of aggregation was present in some cases.

Chapter 7

Concluding Remarks and Recommendations for Future Work

7.1 Concluding Remarks

The research described in this Thesis focused on the synthesis of arborescent poly(γ-benzyl L-glutamate) (PBG) homopolymers and copolymers, and the investigation of the solution properties of the arborescent copolymers. Previously, anionic polymerization and grafting techniques have been employed to produce arborescent homopolymers and copolymers, but these require stringent procedures that limit the range of monomeric building blocks that can be used in the reactions. The synthesis of arborescent PBG relied upon successive grafting reactions of linear PBG containing a terminal primary amine onto carboxylic acid-functionalized PBG substrates by standard peptide coupling techniques. Branched polypeptides have been previously synthesized, but these were more limited in terms of the maximum molecular weight, branching functionality, and molecular weight distribution that could be achieved. This work was aimed at producing highly branched polypeptides potentially useful for biomedical applications. The resulting arborescent PBG (up to G3) have narrow molecular weight distributions ($M_w/M_n < 1.10$) and molecular weights reaching above 10^6.

Amphiphilic arborescent copolymers using PBG as the hydrophobic core component were first synthesized by the same peptide grafting technique used to generate arborescent PBG. Different amine chain end-functionalized linear polymers were thus grafted onto carboxylic acid-functionalized PBG substrates to generate a hydrophilic shell surrounding the PBG core. The ability for these amphiphilic arborescent copolymers to behave like unimolecular micelles was found to depend on whether the hydrophilic shell components were randomly or terminally grafted on the chains of the PBG cores. The chain end grafted arborescent copolymers displayed enhanced solubility and reduced aggregation in aqueous

solutions, consistent with a well-defined core-shell morphology expected to be advantageous in producing water-soluble unimolecular micelles.

Amphiphilic arborescent copolymers containing PBG were also synthesized by "click" coupling techniques, using the copper-catalyzed azide-alkyne Huisgen cycloaddition (CuAAC) reaction. In that case hydrophilic linear polymers with terminal azide functionalities were grafted onto either randomly or chain end alkyne-functionalized PBG substrates. The CuAAC reaction is highly selective and can be performed in the presence of many types of other functional groups, allowing the use of a wider range of polymer components. Similar grafting yields were observed for the CuAAC grafting reactions relatively to the peptide coupling approach, indicating that the success of the grafting reactions was more related to diffusion limitations than the experimental conditions used. The CuAAC technique allowed the linking of unprotected polyglycidol and poly(2-trimethylsilylethyl acrylate) side chains to the PBG substrates, which was not possible for the peptide coupling techniques. CuAAC grafting also led to enhanced water-solubility and reduced aggregation when compared to random grafting, which again confirmed that a well-defined core-shell morphology is preferable to generate unimolecular micelles in aqueous solutions.

7.2 Recommendations for Future Work

The work presented herein is the first investigation into the synthesis of arborescent PBG homopolymers and copolymers. The purpose of this work was to produce biocompatible versions of previously synthesized arborescent structures that demonstrated potential usefulness as microencapsulation vesicles with controlled release capability for small

molecules. Biocompatibility testing will be necessary to ensure that these new PBG-based arborescent copolymers are suitable for biomedical applications. Improvements or modifications in the synthetic protocols, as well as further characterization of these new arborescent structures will be necessary to tailor these arborescent copolymers to specific applications.

7.2.1 Optimization of the Arborescent PBG Homopolymer and Copolymer Syntheses

The synthesis of well-defined arborescent PBG homopolymers of generations up to G3 has been achieved, but the grafting reaction could be further optimized with respect to the grafting yield and coupling efficiency to reduce the amount of unreacted side chains and simplify the purification of the crude products. Depending on the solvent used, the PBG chains may contain predominantly α-helix conformations leading to stiffer arborescent polymer structures than previously synthesized. This reduced chain mobility may decrease the number of side chains that can react with a given PBG substrate due to steric crowding. In the current work, the functionality level of the randomly functionalized PBG substrates was maintained at 25-35%. Decreasing the substrate functionality level to 20% or less would likely increase the grafting yield and the coupling efficiency, since it is known that the grafting reactions are diffusion-controlled.[1] It is also important to confirm that the substrates do in fact contain randomly distributed functionalities. The partial deprotection of PBG to obtain carboxylic acid functionalities was assumed to produce randomly distributed carboxylic acid moieties within the substrates, but neighbouring group effects are possible in the acidolysis reaction and may have produced a blocky microstructure for the PBG substrates. This would decrease the grafting yield due to increased steric crowding near

unreacted coupling sites. Fluorescence spectroscopy studies can help to determine whether the coupling sites are randomly distributed or preferentially grouped. Fluorescent probes can be attached to linear and arborescent PBG with low carboxylic acid moiety contents (< 10%) to monitor the distribution of the coupling sites, similarly to previous experiments performed by Duhamel et al.[2]

The arborescent PBG homopolymers can also be synthesized by "click" chemistry techniques, similarly to the work performed in Chapter 6. Due to the high selectivity and efficiency of these reactions, this should provide further evidence that the grafting reactions using PBG substrates are by limited diffusion rather than by the side reactions occurring during grafting. The synthesis of alkyne-functionalized PBG substrates has been established in this work, and the synthesis of linear PBG with terminal azide functionality could be achieved with a bifunctional initiator containing both azide and primary amine functionalities for the ring-opening polymerizations of the γ-benzyl L-glutamate N-carboxyanhydride. The initiator 1-azido-3-aminopropane was first introduced by Carboni et al.,[3] and was subsequently successfully used for the initiation of γ-benzyl L-glutamate N-carboxyanhydride to yield well-defined α-azide PBG.[4,5]

Arborescent copolymers derived from PBG cores were synthesized using a *grafting onto* approach with either randomly or chain end functionalized PBG substrates. The copolymers generated using coupling sites located exclusively at the chain ends had clearly enhanced water-solubility and behaved more like unimolecular micelles relatively to the copolymers generated using randomly functionalized PBG substrates. It is recommended that these chain end grafted arborescent copolymers be used for future investigations, and the

optimization of the reaction conditions for either the peptide coupling or the CuAAC grafting methods is recommended.

7.2.2 Characterization of Arborescent Copolymers

Arborescent copolymers were generated from different generations of PBG hydrophobic cores (G1, G2, and G3) along with either polyglycidol, poly(ethylene oxide), poly(L-glutamic acid), or poly(2-hydroxyethyl acrylate) as hydrophilic shells. To determine the advantages and disadvantages of using PBG cores of specific generation numbers and of incorporating specific shell components, the detailed morphological characterization of these copolymers must be achieved. Variations in the chain length of the polymers used as hydrophilic shell may also be necessary to enhance the water solubility of the copolymers.

Previous solubilization studies for polycyclic aromatic hydrocarbon (PAH) probes have been performed on arborescent polystyrene-*graft*-poly(2-vinylpyridine) (PS-*g*-P2VP) copolymers. These copolymers behaved like unimolecular micelles in acidic aqueous solutions and were capable of solubilizing the different PAH probes. Investigations to determine the solubilization capacity and rate of the copolymers were performed while varying copolymer parameters such as the composition, poly(2-vinylpyridine) chain lengths, and branching functionality (i.e. generation number).[6] Additional studies were performed regarding their release kinetics for small molecules.[7] In vitro studies with either lidocaine or indomethacin were performed by loading the arborescent PS-*g*-P2VP copolymers with the compound, and it was determined that their release was based mainly upon a diffusion-controlled mechanism. Using these results and performing similar experiments on the

arborescent copolymers derived from PBG would provide evidence for unimolecular micelle systems more directly useful for biomedical applications including drug delivery.

References

Chapter 1

1. Gauthier, M.; Möller, M. *Macromolecules* **1991**, *24*, 4548-4553.
2. Hempenius, M. A.; Michelberger, W.; Möller, M. *Macromolecules* **1997**, *30*, 5602-5605.
3. Yuan, Z.; Gauthier, M. *Macromolecules* **2005**, *38*, 4124-4132.
4. Gauthier, M.; Tichagwa, L.; Downey, J. S.; Gao, S. *Macromolecules* **1996**, *29*, 519-527.
5. Gauthier, M.; Li, J.; Dockendorff, J. *Macromolecules* **2003**, *36*, 2642-2648.
6. Teertstra, S. J.; Gauthier, M. *Prog. Polym. Sci.* **2004**, *29*, 277-327.
7. Njikang, G.; Gauthier, M.; Li, J. *Polymer* **2008**, *49*, 1276-1284.
8. Njikang, G.; Gauthier, M.; Li, J. *Polymer.* **2008**, *49*, 5474-5481.

Chapter 2

1. Deming, T. J. *Adv. Polym. Sci.* **2006**, *202*, 1-18.
2. Hadjichristidis, N.; Iatrou, H.; Pitsikalis, M.; Sakellariou, G. *Chem. Rev.* **2009**, *109*, 5528-5578.
3. Kricheldorf, H. R. *Angew. Chem. Int. Ed.* **2006**, *45*, 5752-5784.
4. Chécot, F.; Rodríguez-Hernández, J.; Gnanou, Y.; Lecommandoux, S. *Polym. Adv. Technol.* **2006**, *17*, 782-785.
5. Sela, M.; Katchalski, E. *Adv. Protein Chem.* **1959**, *14*, 391-478.
6. Sun, H.; Meng, F.; Dias, A. A.; Hendricks, M.; Feijen, J.; Zhong, Z. *Biomacromolecules* **2011**, *12*, 1937-1955.
7. Scholl, M.; Kadlecova, Z.; Klok, H.-A. *Prog. Polym. Sci.* **2009**, *34*, 24-61.
8. Aliferis, T.; Iatrou, H.; Hadjichristidis, N. *J. Polym. Sci., Polym. Chem. Ed.* **2005**, *43*, 4670-4673.
9. van Nostrum, C. F. *Soft Matter* **2011**, *7*, 3246-3259.
10. Gaucher, G.; Dufresne, M.-H.; Sant, V. P.; Kang, N.; Maysinger, D.; Leroux, J. C. *J. Controlled Release* **2005**, *109*, 169-188.
11. Irfan, M.; Seiler, M. *Ind. Eng. Chem. Res.* **2010**, *49*, 1169-1196.
12. Medina, S. H.; El-Sayed, M. E. H. *Chem. Rev.* **2009**, *109*, 3141-3157.
13. Njikang, G.; Gauthier, M.; Li, J. *Polymer* **2008**, *49*, 1276-1284.
14. Njikang, G.; Gauthier, M.; Li, J. *Polymer* **2008**, *49*, 5474-5481.
15. Merrifield, R. B. *J. Am. Chem. Soc.* **1963**, *85*, 2149-2154.
16. (a) Leuchs, H. *Ber.* **1906**, *39*, 857-861 (b) Leuchs, H., Geiger, W. *Ber.* **1908**, *41*, 1721-1726.

17. El-Faham, A.; Albericio, F. *Chem. Rev.* **2011**, *111*, 6557-6602.

18. Hachmann, J.; Lebl, M. *Biopolymers* **2006**, *84*, 340-347.

19. Han, S.-Y.; Kim, Y.-A. *Tetrahedron 60* **2004**, 2447-2467.

20. Poché, D. S.; Moore, M. J.; Bowles, J. L. *Synth. Commun.* **1999**, *29*, 843-854.

21. Oya, M.; Katakai, R.; Nakai, H. *Chem. Lett.* **1973**, 1143-1144.

22. Fujita, Y.; Koga, K.; Kim, H.-K.; Wang, X.-S.; Sudo, A.; Nishida, H.; Endo, T. *J. Polym. Sci. Polym. Chem*. **2007**, *45*, 5365-5369.

23. Koga, K.; Sudo, A.; Endo, T. *J. Polym. Sci., Polym. Chem. Ed.* **2010**, *48*, 4351-4355.

24. Deming, T. J. *Nature* **1997**, *390*, 386-389.

25. Deming, T. J. *Macromolecules* **1999**, *32*, 4500-4502.

26. Dimitrov, I.; Schlaad, H. *Chem. Commun.* **2003**, 2944-2945.

27. Aliferis, T.; Iatrou, H.; Hadjichristidis, N. *Biomacromolecules* **2004**, *5*, 1653-1656.

28. Vayaboury, W.; Giani, O.; Cottet, H.; Deratani, A.; Schue, F. *Macromol. Rapid Commun.* **2004**, *25*, 1221-1224.

29. Lutz, J.-F.; Schütt, D.; Kubowicz, S. *Macromol. Rapid Commun.* **2005**, *26*, 23-28.

30. Kricheldorf, H. In *Models of Biopolymers in Ring Opening Polymerization*, CRC Press, Boca Raton, FL, **1990**, pp 160-225.

31. Tomalia, D. A.; Fréchet, J. M. J. In *Dendrimers and other Dendritic Polymers.* Fréchet, J., M., J.; Tomalia, D., A. Eds.; Wiley: New York, **2001**, p xxvii.

32. Tomalia, D. A.; Baker, H.; Dewald, J.; Hall, M.; Kallos, G.; Martin, S.; Roeck, J.; Ryder, J.; Smith, P. *Polym. J.* **1985**, *17*, 117-132.

33. Newkome, G. R.; Yao, Z.-q.; Baker, G. R.; Gupta, V. K. *J. Org. Chem.* **1985**, *50*, 2003-2004.

34. Hawker, C.; Fréchet, J. M. J. *J. Am. Chem. Soc.* **1990**, 1010-1013.

35. Denkewalter, R. G.; Kole, J. F.; Lukasavage, W. J. "Preparation of Lysine-Based Macromolecular Highly Branched Homogeneous Compound", **1979**, *U.S. Pat.,* 4,360,646.

36. Denkewalter, R. G.; Kole, J. F.; Lukasavage, W. J. "Macromolecular Highly Branched Homogeneous Compound Based on Lysine Units", **1981**, *U.S. Pat.,* 4,289,872.

37. Miller, T. M.; Neenan, T. X. *Chem. Mater.* **1990**, *2*, 346-349.

38. Wooley, K. L.; Hawker, C. J.; Fréchet, J. M. J. *J. Am. Chem. Soc.***1993**, *115*, 11496-11505.

39. Gunatillake, P. A.; Odian, G.; Tomalia, D. A. *Macromolecules* **1988**, *21*, 1556-1562.

40. Kim, Y. H.; Webster, O. W. *J. Am. Chem. Soc.* **1990**, *112*, 4592-4593.

41. Hawker, C. J.; Lee, R.; Fréchet, J. M. J. *J. Am. Chem. Soc*. **1991**, *113*, 4583-4593.

42. Flory, P. J. *J. Am. Chem. Soc*. **1952**, *74*, 2718-2723.

43. Yan, D.; Müller, A. H. E.; Matyjaszewski, K. *Macromolecules* **1997**, *30*, 7024-7033.

44. Hölter, D.; Burgath, A.; Frey, H. *Acta Polym.* **1997**, *48*, 30-35.

45. Hanselmann, R.; Hölter, D.; Frey, H. *Macromolecules* **1998**, *31*, 3790-3801.

46. Hölter, D.; Frey, H. *Acta Polym.* **1997**, *48*, 298-309.

47. Radke, W.; Litvinenko, G.; Müller, A. H. E. *Macromolecules* **1998**, *31*, 239-248.

48. Litvinenko, G.; Müller, A. H. E. *Macromolecules* **2002**, *35*, 4577-4583.

49. Cheng, K.-C.; Chuang, T.-H.; Chang,J.-S.; Guo, W.; Su, W.-F. *Macromolecules*, **2005**, *38*, 8252-8257.

50. Yan, D.; Gao, C. *Macromolecules* **2000**, *33*, 7693-7699.

51. Gao, C.; Yan, D. *Chem. Commun*. **2001**, *1*, 107-108.

52. Hawker, C. J.; Chu, F. *Macromolecules* **1996**, *29*, 4370-4380.

53. Miravet, J. F.; Fréchet, J. M. J. *Macromolecules* **1998**, *31*, 3461-3468.

54. Fréchet, J. M. J.; Henmi, M.; Gitsov, I.; Aoshima, S.; Leduc, M. R.; Grubbs, R. B. *Science* **1995**, *269*, 1080-1083.

55. Hawker, C. J.; Fréchet, J. M. J.; Grubbs, R. B.; Dao, J. *J. Am. Chem. Soc.* **1995**, *117*, 10763-10764.

56. Matyjaszewski, K.; Gaynor, S. G.; Kulfan, A.; Podwika, M. *Macromolecules* **1997**, *30*, 5192-5194.

57. Georgi, U.; Erber, M.; Stadermann, J.; Abulikemu, M.; Komber, H. Lederer, A.; Voit, B. *J. Polym. Sci., Polym. Chem*. *Ed.* **2010**, *48*, 2224-2235.

58. Simon, P. F. W.; Radke, W.; Müller, A. H. E. *Macromol. Rapid. Commun.* **1997**, *18*, 865-873.

59. Simon, P. F. W.; Müller, A. H. E. *Macromolecules* **2001**, *34*, 6206-6213.

60. (a) Suzuki, M.; Ii, A.; Saegusa, T. *Macromolecules* **1992**, *25*, 7071-7072. (b) Suzuki, M.; Yoshida, S.; Shiraga, K.; Saegusa, T. *Marcromolecules* **1998**, *31*, 1716-1719.

61. (a) Tokar, R.; Kubisa, P.; Penczek, S.; Dworak, A. *Macromolecules* **1994**, *27*, 320-322. (b) Dworak, A.; Walach, W.; Trzbicka, B. *Macromol. Chem. Phys*. **1995**, *196*, 1963-1970.

62. Sunder, A.; Hanselmann, R.; Frey, H.; Mülhaupt, R. *Macromolecules* **1999**, *32*, 4240-4246.

63. Vandenberg, E. J. *J. Polym. Sci., Polym. Chem. Ed.* **1985**, *23*, 915-949.

64. Chang, H.-T.; Fréchet, J. M. J. *J. Am. Chem. Soc.* **1999**, *121*, 2313-2314.

65. Gao, C.; Yan, D. *Prog. Polym. Sci.* **2004**, *29*, 183-275.

66. Kee., R. A.; Gauthier, M.; Tomalia, D. A. In *Dendrimers and other Dendritic Polymers.* Fréchet, J. M. J.; Tomalia, D. A. Eds.; Wiley: New York, **2001**, pp 209-236.

67. Tomalia, D. A.; Hedstrand, D. M.; Ferritto, M. S. *Macromolecules* **1991**, *24*, 1435-1438.

68. Gauthier, M.; Möller, M. *Macromolecules* **1991**, *24*, 4548-4553.

69. Li, J.; Gauthier, M. *Macromolecules* **2001**, *34*, 8918-8924.

70. Hempenius, M. A.; Michelberger, W.; Möller, M. *Macromolecules* **1997**, *30*, 5602-5605.

71. Zhang, H.; Li, Y.; Zhang, C.; Li, Z.; Li, X.; Wang, Y. *Macromolecules* **2009**, *42*, 5073-5079.

72. Yuan, Z.; Gauthier, M. *Macromolecules* **2005**, *38*, 4124-4132.

73. Teertstra, S. J.; Gauthier, M. *Prog. Polym. Sci.* **2004**, *29*, 277-327.

74. Six, J.-L.; Gnanou, Y. *Macromol. Symp.* **1995**, *95*, 137-150.

75. Rodriguez-Hernández, J.; Gatti, M.; Klok, H.-A. *Biomacromolecules* **2003**, *4*, 249-258.

76. Walach, W.; Kowalczuk, A.; Trzebicka, B.; Dworak, A. *Macromol. Rapid Commun.* **2001**, *22*, 1272-1277.

77. Collet, H.; Souaid, E.; Cottet, H.; Deratani, A.; Boiteau, L.; Dessalces, G.; Rossi, J.-C.; Commeyras, A.; Pascal, R. *Chem. Eur. J.* **2010**, *16*, 2309-2316.

78. Cheng, J.; Ling, X.; Zhong, Z.; Zhuo, R. *Macromol. Rapid. Commun.* **2011**, *32*, 1839-1845.

79. Yuan, Z.; Gauthier, M. *Macromolecules* **2006**, *39*, 2063-2071.

80. Knauss, D. M.; Al-Muallem, H. A.; Huang, T.; Wu, D. T. *Macromolecules* **2000**, *33*, 3557-3568.

81. Knauss, D. M.; Al-Muallem, H. A. *J. Polym. Sci., Polym. Chem. Ed.* **2000**, *38*, 4289-4298.

82. Asami, R.; Takaki, M.; Hanahata, H. *Macromolecules* **1983**, *16*, 628-631.

83. Ma, J.-J.; Bronn, W. R.; Silver, S. F. *Polym. Prepr., Am. Chem. Soc. Div. Polym. Chem.* **1994**, *35*, 572-573.

84. Riess, G. *Prog. Polym. Sci.* **2003**, *28*, 1107-1170.

85. Quémener, D.; Deratani, A.; Lecommandoux, S. *Top. Curr. Chem.* **2012**, *322*, 165-192.

86. Zhulina, E. B.; Borisov, O. V. *Macromolecules* **2012**, *45*, 4429-4440.

87. Moorefield, C. N.; Newkome, G., R. *C. R. Chimie* **2003**, *6*, 715-724.

88. Ambade, A. V.; Savariar, E. N.; Thayumanavan, S. *Mol. Pharmaceutics* **2005**, *2*, 264-272.

89. Radowski, M. R.; Shukla, A.; von Berlepsch, H.; Böttcher, H.; Pickaert, G.; Rehage, H.; Haag, R. *Angew. Chem. Int. Ed*. **2007**, *46*, 1265-1269.

90. Hong, H. Y.; Mai, Y. Y.; Zhou, Y. F.; Yan, D. Y.; Cui, J. *Macromol. Rapid Commun*. **2007**, *28*, 591-596.

91. Kee, R. A.; Gauthier, M. *Macromolecules* **2002**, *35*, 6526-6532.

92. Gauthier, M.; Li, J.; Dockendorff, J. *Macromolecules* **2003**, *36*, 2642-2648.

93. Yun, S. I.; Briber, R. M.; Kee, R. A.; Gauthier, M. *Polymer* **2003**, *44*, 6579-6587.

94. Yun, S. I.; Lai, K.-C.; Briber, R. M.; Teertstra, S., J.; Gauthier, M.; Bauer, D., J. *Macromolecules* **2008**, *41*, 175-183.

95. Gauthier, M.; Tichagwa, L.; Downey, J. S.; Gao, S. *Macromolecules* **1996**, *29*, 519-527.

96. Yun, S. I.; Cao, L.; Kang, T.-B.; Huh, M.; Gauthier, M. *J. Macromol. Sci., Phys. Ed.* **2011**, *50*, 2318-2333.

97. Kee, R. A.; Gauthier, M. *J. Polym. Sci., Polym. Chem. Ed.* **2008**, *46*, 2335-2346.

98. Deming, T. J. *Prog. Polym. Sci.* **2007**, *32*, 858-875.

99. Floudas, G.; Spiess, H., W. *Macromol. Rapid Commun.* **2009**, *30*, 278-298.

100. Habraken, G. J. M.; Heise, A.; Thornton, P. D. *Macromol. Rapid Commun.* **2011**, *33*, 272-286.

Chapter 3

1. Teerstra, S. J.; Gauthier, M. *Prog. Polym. Sci*. **2004**, *29*, 277-327.
2. Gauthier, M. *J. Polym. Sci., Polym. Chem. Ed.* **2007**, *45*, 3803-3810.
3. Carlmark, A; Hawker, C.; Hult, A.; Malkoch, M. *Chem. Soc. Rev.* **2009**, *38*, 352-362.
4. Scholl, M.; Kadlecova, Z.; Klok, H.-A. *Prog. Polym. Sci.* **2009**, *34*, 24-61.
5. Voit, B. I.; Lederer, A. *Chem. Rev*. **2009**, *109*, 5924-5973.
6. Esfand, R.; Tomalia, D. A. *Drug Discovery Today* **2001**, *6*, 427-436.
7. Sadler, K.; Tam, J. P. *Rev. Molec. Biotechnology* **2002**, *90*, 195-229.
8. Tomalia, D. A.; Reyna, L. A.; Svenson, S. *Biochem. Soc. Trans.* **2007**, *35*, 61-67.
9. Denkewalter, R. G.; Kolc, J. F.; Lukasavage, W. J. US Pat. 4,289,872, **1981**.
10. Aharoni, S. M.; Crosby III, C. R.; Walsh, E. K. *Macromolecules* **1982**, *15*, 1093-1098.
11. Denkewalter, R. G.; Kolc, J. F.; Lukasavage, W. J. US Pat. 4,410,688, **1983**.
12. Simanek, E. E.; Abdou, H.; Lalwani, S.; Lim, J.; Mintzer, M.; Venditto, V. J.; Vittur, B. *Proc. Royal Soc. A* **2010**, *466*, 1445-1468.
13. Baigude, H.; Katsuraya, K.; Okuyama, K.; Tokunaga, S.; Uryu, T. *Macromolecules* **2003**, *36*, 7100-7106.
14. Boysen, M. M. K.; Elsner, K.; Sperling, O.; Lindhorst, T. K. *Eur. J. Org. Chem.* **2003**, 4376-4386.
15. Tansey, W.; Ke, S.; Cao, X.-Y.; Pasuelo, M. J.; Wallace, S.; Li, C. *J. Controlled Release* **2004**, *94*, 39-51.
16. Wilms, D.; Stiriba, S.-E.; Frey, H. *Acc. Chem. Res.* **2010**, *43*, 129-141.

17. Xia, W.; Jiang, G.; Chen, W. *J. Appl. Polym. Sci*. **2008**, *109*, 2089-2094.

18. Klok, H.-A.; Rodríguez-Hernández, J. *Macromolecules* **2002**, *35*, 8718-8723.

19. Gauthier, M.; Möller, M. *Macromolecules* **1991**, *24*, 4548-4553.

20. Rodríguez-Hernández, J.; Klok, H.-A. *J. Polym. Sci., Polym. Chem. Ed.* **2003**, *41*, 1167-1187.

21. Collet, H.; Souaid, E.; Cottet, H.; Deratani, A.; Boiteau, L.; Dessalces, G.; Rossi, J.-C.; Commeyras, A.; Pascal, R. *Chem. Eur. J.* **2010**, *16*, 2309-2316.

22. Aliferis, T.; Iatrou, H.; Hadjichristidis, N. *J. Polym. Sci., Polym. Chem. Ed.* **2005**, *43*, 4670-4673.

23. Poché, D. S.; Moore, M. J.; Bowles, J. L. *Synth. Commun.* **1999**, *29*, 843-854.

24. Mitchell, J. C.; Woodward, A. E.; Doty, P. *J. Am. Chem. Soc.* **1957**, *79*, 3955-3960.

25. Kricherdorf, H. R. In *α-Amino acid-N-carboxyanhydrides and related heterocycles*, Springer: Berlin, **1987**, pp 88-93.

26. Dimitrov, I.; Schlaad, H. *Chem. Commun.* **2003**, 2944-2945.

27. Lutz, J.-F.; Schütt, D.; Kubowicz, S. *Macromol. Rapid Commun.* **2005**, *26*, 23-28.

28. Aliferis, T.; Iatrou, H.; Hadjichristidis, N. *Biomacromolecules* **2004**, *5*, 1653-1656.

29. Vayaboury, W.; Giani, O.; Cottet, H.; Deratani, A.; Schué, F. *Macromol. Rapid Commun.* **2004**, *25*, 1221-1224.

30. Blout, E. R., Idelson, M. *J. Am. Chem. Soc*. **1956**, *78*, 497-498.

31. Maeda, K.; Kamiya, N.; Yashima, E. *Chem. Eur. J.* **2004**, *10*, 4000-4010.

32. Yamaoka, K.; Ueda, K. *J. Phys. Chem.* **1982**, *86*, 406-413.

33. Duhamel, J.; Kanagalingam, S.; O'Brien, T. J.; Ingratta, M. W. *J. Am. Chem. Soc*. **2003**, *125*, 12810-12822.

34. Bradbury, E. M.; Crane-Robinson, C.; Goldman, H.; Rattle, H. W. E. *Nature* **1968**, *217*, 812-816.

35. Newkome, G., R. Personal communication.

36. Trisler, J. C.; Freasier, B. F.; Wu, S.-M. *Tetrahedron Lett.* **1974**, *9*, 687-690.

37. Newkome, G. R.; Robinson, J. M. *Tetrahedron Lett.* **1974**, *9*, 691-694.

38. Ji, S.; Hoye, T. R.; Macosko, C. W. *Macromolecules* **2005**, 38, 4679-4686.

39. Schmidt, M.; Burchard, W.; Ford, N. C. *Macromolecules* **1978**, *11*, 452-454.

Chapter 4

1. Gohy, J.-F. *Adv. Polym. Sci.* **2005**, *190*, 65-136.
2. Schatz, C.; Lecommandoux, S. *Macromol. Rapid Commun*. **2010**, *31*, 1664-1684.
3. Kwon, G. S.; Okano, T. *Adv. Drug Delivery Rev*. **1996**, *21*, 107-116.
4. Procházka, K.; Baloch, M. K.; Tuzar, Z. *Makromol Chem.* **1979**, *180*, 2521-2523.
5. Kakizawa, Y.; Harada, A.; Kakaoka, K. *J. Am. Chem. Soc*. **1999**, *121*, 11247-11248.
6. O'Reilly, R. K.; Hawker, C. J.; Wooley, K. L. *Chem. Soc. Rev*. **2006**, *35*, 1068-1083.
7. van Nostrum, C. F. *Soft Matter* **2011**, *7*, 3246-3259.
8. Newkome, G. R.; Moorefield, C. N. *C. R. Chimie* **2003**, *6*, 715-724.
9. Gauthier, M. *J. Polym. Sci., Part A: Polym. Chem*. **2007**, *45*, 3803-3810.
10. Satoh, T. *Soft Matter* **2009**, *5*, 1972-1982.
11. Wang, Y.; Grayson, S. M.; *Adv. Drug Del. Rev*. **2012**, *64*, 852-865.
12. Newkome, G. R.; Yao, Z.; Baker, G. R.; Gupta, V. K. *J. Org. Chem*. **1985**, *50*, 2003-2004.
13. Hawker, C. J.; Wooley, K. L.; Fréchet, J. M. J. *J. Chem. Soc*. **1993**, *1*, 1287-1297.
14. Tziveleka, L.-A.; Kontoyianni, C.; Sideratou, Z.; Tsiourvas, D.; Paleos, C. M. *Macromol. Biosci*. **2006**, *6*, 161-169.
15. Türk, H.; Shukla, A.; Rodrigues, P. C. A.; Rehage, H.; Haag, R. *Chem. Eur. J*. **2007**, *13*, 4187-4196.
16. Fieber, W.; Herrmann, A.; Ouali, L.; Velazco, M. I.; Kreutzer, G.; Klok, H.-A.; Ternat, C.; Plummer, C. J. G.; Månson, J.-A. E.; Sommer, H. *Macromolecules* **2007**, *40*, 5372-5378.

17. Chen, S.; Zhang, X.-Z.; Cheng, S.-X.; Zhuo, R.-X.; Gu, Z.-W. *Biomacromolecules* **2008**, *9*, 2578-2585.

18. Du,W.; Nyström, A. M.; Zhang, L.; Powell, K. T.; Li, Y.; Cheng, C.; Wickline, S. A.; Wooley, K. L. *Biomacromolecules* **2008**, *9*, 2826-2833.

19. Du,W.; Xu, Z.; Nyström, A. M.; Zhang, K.; Leonard, J. R.; Wooley, K. L. *Bioconjugate Chem*. **2008**, *19*, 2492-2498.

20. Radowski, M. R.; Shukla, A.; von Berlepsch, H.; Böttcher, H.; Pickaert, G.; Rehage, H.; Haag, R. *Angew. Chem. Int. Ed*. **2007**, *46*, 1265-1269.

21. Hong, H. Y.; Mai, Y. Y.; Zhou, Y. F.; Yan, D. Y.; Cui, J. *Macromol. Rapid Commun*. **2007**, *28*, 591-596.

22. Gauthier, M.; Möller, M. *Macromolecules* **1991**, *24*, 4548-4553.

23. Tomalia, D. A.; Hedstrand, D. M.; Ferritto, M. S. *Macromolecules* **1991**, *24*, 1435-1438.

24. Gauthier, M.; Tishagwa, L., Downey, J. S.; Gao, S. *Macromolecules* **1996**, *29*, 519-527.

25. Kee, R. A.; Gauthier, M. *Macromolecules* **2002**, *35*, 6526-6532.

26. Kee, R. A.; Gauthier, M. *J. Polym. Sci., Polym. Chem. Ed.* **2008**, *46*, 2335-2346.

27. Gauthier, M.; Li, J.; Dockendorff, J. *Macromolecules* **2003**, *36*, 2642-2648.

28. Njikang, G.; Gauthier, M.; Li, J. *Polymer* **2008**, *49*, 1276-1284.

29. Njikang, G.; Gauthier, M.; Li, J. *Polymer* **2008**, *49*, 5474-5481.

30. Blout, E. R.; Karlson, R. H.; Doty, P.; Hargitay, B. *J. Am. Chem. Soc.* **1954**, *76*, 4492-4493.

31. Yoda, R.; Komatsuzaki, S.; Hayashi, T. *Biomaterials* **1995**, *16*, 1203-1209.

32. Ji, S.; Hoye, T. R.; Macosko, C. W. *Macromolecules* **2005**, *38*, 4679-4686.

33. Fitton, A. O.; Hill, J.; Jane, D. E.; Millar, R. *Synthesis* **1987**, *12*, 1140-1142.

34. Normant, H.; Angelo, B. *Bull. Soc. Chim. France* **1960**, 354-359.

35. Billouard, C.; Carlotti, S.; Despois, P.; Deffieux, A. *Macromolecules* **2004**, *37*, 4038-4043.

36. Gervais, M.; Labbé, M.; Carlotti, S.; Deffieux, A. *Macromolecules* **2009**, *42*, 2395-2400.

37. Mendrek, S.; Mendrek, A.; Adler, H.-J.; Walach, W.; Dworak, A.; Kuckling, D. *J. Polym. Sci., Polym. Chem. Ed*. **2008**, *46*, 2488-2499.

38. Kainthan, R. K.; Janzen, J.; Levin, E.; Devine, D. V.; Brooks, D. E. *Biomacromolecules* **2006**, *7*, 703-709.

39. Dworak, A.; Panchev, I.; Trzebicka, B.; Walach, W. *Macromol. Symp*. **2000**, *153*, 233-242.

40. Sunder, A.; Hanselmann, R.; Frey, H.; Mülhaupt, R. *Macromolecules* **1999**, *32*, 4240-4246.

41. Wang. S. *US Pat. 20050070675*, **2005**.

42. Rejsek, V.; Sauvanier, D.; Billouard, C.; Desbois, P.;Deffieux, A.; Carlotti, S. *Macromolecules* **2007**, *40*, 6510-6514.

43. Gehrhardt, H.; Mutter, M. *Polym. Bull.* **1987**, *18*, 487-493.

44. Yaniç, C.; Bredenkamp, M. W.; Jacobs, E. P.; Spies, S. C.; Swart, P. *J. App. Polym. Sci.* **2000**, *78*, 109-117.

45. Li, Chun. *Adv. Drug. Delivery Rev*. **2002**, *54*, 695-713.

46. Nguyen, L.-T. T.; Vorenkamp, E. J.; Daumont, C. J. M.; ten Brinke, G.; Schouten, A. J. *Polymer* **2010**, *51*, 1042-1055.

47. Dimitrov, I.; Schlaad, H. *Chem. Commun*. **2003**, *23*, 2944-2945.

48. Lutz, J.-F.; Schütt, D.; Kubowicz, S. *Macromol. Rapid Commun*. **2005**, *26*, 23-28.

49. Yun, S. I.; Lai, K.-C.; Briber, R. M.; Teertstra, S. J.; Gauthier, M.; Bauer, B. J. *Macromolecules* **2008**, *41*, 175-183.

50. Mitchell, J. C.; Woodward, A. E.; Doty, P. *J. Am. Chem. Soc*. **1957**, *79*, 3955-3960.

51. Maeda, K.; Kamiya, N.; Yashima, E. *Chem. Eur. J.* **2004**, *10*, 4000-4010.

52. Schmidt, M.; Burchard, W.; Ford, N. C. *Macromolecules* **1978**, *11*, 452-454.

53. Dimitrov. P.; Porjazoska, A.; Novakov, C. P.; Cvetkovska, M.; Tsvetanov, C., B. Polymer **2005**, *46*, 6820-6828.

54. Taton, D.; Le Borgne, A.; Sepulchre, M.; Spassky, N. *Macromol. Chem. Phys*. **1994**, *195*, 139-148.

55. Namboodri, V. V.; Varma, R. S. *Tetrahedron Lett.* **2002**, *43*, 1143-1146.

Chapter 5

1. Tomalia, D. A.; Hedstrand, D. M.; Ferritto, M. S. *Macromolecules* **1991**, *24*, 1435-1438.
2. Gauthier, M.; Möller, M. *Macromolecules* **1991**, *24*, 4548-4553.
3. Gauthier, M.; Möller, M.; Burchard, W. *Macromol. Symp.* **1994**, *77*, 43-49.
4. Gauthier, M.; Chung, J.; Choi, L.; Nguyen, T., T. *J. Phys. Chem. B.* **1998**, *102*, 3138-3142.
5. Sheiko, S. S.; Gauthier, M.; Möller, M. *Macromolecules* **1997**, *30*, 2343-2349.
6. Frank, R. S.; Merkle, G.; Gauthier, M. *Macromolecules* **1997**, *30*, 5397-5402.
7. Yun, S. I.; Lai, K.-C.; Briber, R. M.; Teertstra, S. J.; Gauthier, M.; Bauer, B. J. *Macromolecules* **2008**, *41*, 175-183.
8. Kee, R. A.; Gauthier, M. *Macromolecules* **2002**, *35*, 6526-6532.
9. Gauthier, M.; Li, J.; Dockendorff, J. *Macromolecules* **2003**, *36*, 2642-2648.
10. Njikang, G.; Gauthier, M.; Li, J. *Polymer* **2008**, *49*, 1276-1284.
11. Njikang, G.; Gauthier, M.; Li, J. *Polymer* **2008**, *49*, 5474-5481.
12. Gauthier, M.; Tishagwa, L., Downey, J. S.; Gao, S. *Macromolecules* **1996**, *29*, 519-527.
13. Ji, S.; Hoye, T. R.; Macosko, C. W. *Macromolecules* **2005**, *38*, 4679-4686.
14. Fitton, A. O.; Hill, J.; Jane, D. E.; Millar, R. *Synthesis* **1987**, *12*, 1140-1142.
15. Normant, H.; Angelo, B. *Bull. Soc. Chim. France* **1960**, 354-359.
16. Kricheldorf, H. Angew. *Chem. Int. Ed.* **2006**, *45*, 5752-5784.
17. Hadjichristidis, N.; Iatrou, H.; Pitsikalis, M.; Sakellariou, G. *Chem. Rev.* **2009**, *109*, 5528-5578.

18. Knobler, Y.; Bittner, S.; Frankel, M. *J. Chem. Soc.* **1964**, 3941-3951.

19. Dimitrov, I.; Schlaad, H. *Chem. Commun.* **2003**, 2944-2945.

20. Lutz, J.-F.; Schütt, D.; Kubowicz, S. *Macromol. Rapid. Commun*. **2005**, *26*, 23-28.

21. Ballard, D.; Bamford, C. J. *J. Chem. Soc*. **1956**, 381-387.

22. Mendrek, S.; Mendrek, A.; Adler, H.-J.; Walach, W.; Dworak, A.; Kuckling, D. *J. Polym. Sci., Polym. Chem. Ed*. **2008**, *46*, 2488-2499.

23. Schmidt, M.; Burchard, W.; Ford, N. C. *Macromolecules* **1978**, *11*, 452-454.

Chapter 6

1. Gauthier, M.; Möller, M. *Macromolecules* **1991**, *24*, 4548-4553.
2. Li, J.; Gauthier, M. *Macromolecules* **2001**, *34*, 8918-8924.
3. Li, J.; Gauthier, M.; Teertstra, S. J. *Macromolecules* **2004**, *37*, 795-802.
4. Yuan, Z.; Gauthier, M. *Macromolecules* **2005**, *38*, 4124-4132.
5. Hartmuth, K. C.; Finn, M. G.; Sharpless, H. B.; *Angew. Chem. Int. Ed.* **2001**, *40*, 2004-2021.
6. Tornøe, C. W.; Christensen, C.; Meldal, M. *J. Org. Chem*. **2002**, *67*, 3057-3064.
7. Rostovtsev, V. V.; Green, L. G.; Fokin, V. V.; Sharpless, K. B. *Angew. Chem. Int. Ed.* **2002**, *41*, 2596-2599.
8. Wu, P.; Feldman, A. K.; Nugent, A. K.; Hawker, C. J.; Sheel, A.; Voit, B.; Pyun, J.; Fréchet, J. M. J.; Sharpless, K. B.; Fokin, V. V. *Angew. Chem. Int. Ed.* **2004**, *43*, 3928-3932.
9. Fournier, D.; Hoogenboom, R.; Schubert, U. S. *Chem. Soc. Rev.* **2007**, *36*, 1369-1380.
10. Kempe, K.; Krieg, A.; Becer, C. R.; Schubert, U. *Chem. Soc. Rev.* **2012**, *41*, 176-191.
11. Agut, W.; Taton, D.; Lecommandoux, S. *Macromolecules* **2007**, *40*, 5653-5661.
12. Agut, W.; Agnaou, R.; Taton, D.; Lecommandoux, S. *Macromol. Rapid Commun*. **2008**, *29*, 1147-1155.
13. Schatz, C.; Louguet, S.; Le Meins, J.-F.; Lecommandoux, S. *Angew. Chem. Int. Ed.* **2009**, *48*, 2572 -2575.
14. Engler, A. C.; Lee, H.-i.; Hammond, P. T. *Angew. Chem. Int. Ed.* **2009**, *48*, 9334-9338.

15. Fitton, A. O.; Hill, J.; Jane, D. E.; Millar, R. *Synthesis* **1987**, *12*, 1140-1142.

16. Gervais, M.; Labbé, M.; Carlotti, S.; Deffieux, A. *Macromolecules* **2009**, *42*, 2395-2400.

17. Mendrek, S.; Mendrek, A.; Adler, H.-J.; Walach, W.; Dworak, A.; Kuckling, D. *J. Polym. Sci., Polym. Chem. Ed*. **2008**, *46*, 2488-2499.

18. Müehlebach, A.; Gaynor, S. G.; Matyjaszewski, K. *Macromolecules* **1998**, *31*, 6046-6052.

19. Kato, M.; Kamigaito, M.; Sawamoto, M.; Higashimura, T. *Macromolecules* **1995**, *28*, 1721-1723.

20. Wang, J.-S.; Matyjaszewski, K. *J. Am. Chem. Soc.* **1995**, *117*, 5614-5615.

21. Matyjaszewski, K.; Xia, J. *Chem. Rev.* **2001**, *101*, 2921-2190.

22. Meldal, M.; *Macromol. Rapid Commun*. **2008**, *29*, 1016-1051.

23. Meldal, M.; Tornoe, C. W. *Chem. Rev*. **2008**, *108*, 2952-3015.

24. Schmidt, M.; Burchard, W.; Ford, N. C. *Macromolecules* **1978**, *11*, 452-454.

Chapter 7

1. Li, J.; Gauthier, M. *Macromolecules* **2001**, *34*, 8918-8924.
2. Duhamel, J.; Kanagalingam, S.; O'Brien, T., J.; Ingratta, M., W. *J. Am. Chem. Soc.* **2003**, *125*, 12810-12822.
3. Carboni, B.; Benalil, A.; Vaultier, M. *J. Org. Chem.* **1993**, *58*, 3736-3741.
4. Agut, W.; Taton, D.; Lecommandoux, S. *Macromolecules* **2007**, *40*, 5653-5661.
5. Zhou, Q.-H.; Zheng, J.-K.; Shen, Z.; Fan, X.-H.; Chen, X.-F.; Zhou, Q.-F. *Macromolecules* **2010**, *43*, 5637-5646.
6. Njikang, G.; Gauthier, M.; Li, J. *Polymer* **2008**, *49*, 1276-1284.
7. Njikang, G.; Gauthier, M.; Li, J. *Polymer* **2008**, *49*, 5474-5481.